Biopharmaceutics and Pharmacokinetics Characterization of Bioactive Flavones in *Scutellariae baicalensis* Georgi

LI, Chenrui

A Thesis Submitted in Partial Fulfillment
of the Requirement for the Degree of
Doctor of Philosophy
in
Pharmacy

September 2010

The Chinese University of Hong Kong

Thesis/Assessment Committee

Professor Lawrence William BAUM (Chair)

Professor ZUO Zhong (Thesis Supervisor)

Professor LIN Ge (Thesis Co-supervisor)

Professor HSIAO Wendy Wen-luan (External Examiner)

Professor KANFER Isadore (External Examiner)

Professor LEE Vincent HonLeung (Other Examiner/s)

論文評審委員會

Lawrence William BAUM 教授 (主席)

ZUO Zhong 教授 (論文導師)

LIN Ge 教授 (論文導師)

HSIAO Wendy Wen-luan 教授 (校外委員)

KANFER Isadore 教授 (校外委員)

LEE Vincent HonLeung 教授 (委員)

Abstract

Purpose: *Scutellariae baicalensis* Georgi is a medicinal plant widely distributed in Asia. Its dried root, *Radix Scutellariae* (RS), has been extensively used in Chinese and Japanese medicine. Six flavones including baicalein (B), wogonin (W), oroxylin A (OA) and their corresponding glucuronic acid conjugates (BG, WG, OAG) are the major bioactive components in RS. Our previous studies on B revealed an extensive first-pass metabolism during its absorption. Hence, it is expected that W and OA which have the similar structures as B, may share similar absorption and metabolic pathways as B. The present project aims to 1) establish an assay method for better quality control of RS; 2) provide further biopharmaceutic characterizations of W and OA in RS; 3) investigate the potential pharmacokinetic interactions among B, W and OA.

Methods: The intestinal absorption and metabolism of W and OA as well as the potential interactions among B, W and OA were investigated at *in vitro*, *in situ* and *in vivo* levels. Various models were employed including Caco-2 cell monolayer model, *in vitro* enzymatic kinetics study, rat *in situ* single-pass intestinal perfusion model and *in vivo* pharmacokinetic study in rats.

Results: Similar to B, W and OA showed favorable permeability in both the Caco-2 cell and the rat *in situ* single-pass perfusion models. However, they experienced extensive first-pass metabolism, mainly in the form of glucuronidation. Intracellularly formed WG and OAG could be effluxed to both the apical side (lumen side) and basolateral side (mesenteric blood side) mainly by MRPs, which was confirmed by inhibition transport studies in Caco-2 cells and transfected MDCK cells. The glucuronidation rate of OA was higher than that of W, which was observed by enzymatic kinetics studies by sub-cellular fractions with intrinsic clearances (V_{max}/K_m,

μl/min/mg) of 456 to 4170 for W and 509~5038 for OA. UGT 1A9 was the most potent metabolic enzyme for hepatic glucuronidation, while UGTs 1A8 and 1A10 were responsible for the intestinal glucuronidation of W and OA. The *in vivo* rat pharmacokinetics studies showed that W and OA may be readily absorbed and extensively metabolized with no parent compound detectable in blood after oral administration of W and OA. A new metabolite of W was identified to be the glucuronic acid conjugate at 5-OH of W. After co-administration of B, W and OA, decreased formation of BG, WG and OAG was observed in *in vitro* enzymatic kinetics study. Further studies in absorption models of Caco-2 cell monolayer and rat *in situ* single-pass intestinal perfusion demonstrated the enhancement in absorption of B, W and OA and decrease of BG, WG and OAG after the co-administration of B, W and OA. The ultimate pharmacokinetics interaction study revealed that glucuronides were the predominant form in systemic circulation and the AUC of OAG significantly increased after co-administration of B, W and OA.

Conclusion: Similar to B, W and OA may be well absorbed followed by extensive first-pass metabolism, which was mediated by various UGT isozymes. During absorption, the intracellularly formed WG and OAG were mainly effluxed by MRPs to both the lumen and mesenteric blood side of the intestine. Both *in vitro* and *in situ* models indicated that interactions among B, W and OA would lead to decreased glucuronidation and increased absorption of parent flavones. Due to extensive metabolism *in vivo*, only glucuronides appeared in systemic circulation after co-administration of B, W and OA in rats. The resulted increased systemic exposure of OAG indicated that the co-administration might lead to the enhancement of bioavailability for the studied flavones in the form of glucuronides.

摘要

研究目的: 黃芩是一種廣泛分佈于亞洲的藥用植物。其乾燥根廣泛應用于中國及日本的傳統醫藥治療。黃芩素，漢黃芩素，千層紙素及其相對應的葡萄糖醛酸結合物（黃芩苷，漢黃芩苷，千層紙素苷）是黃芩的主要生物活性物質。我們之前對於黃芩素的研究表明，黃芩素在其腸道吸收過程中發生顯著的首過效應。基於相似的化學結構，我們認為漢黃芩素及千層紙素可能與黃芩素具有相同的吸收和代謝途徑。 本研究的目的其一在於建立黃芩活性物質的含量測定方法以對其進行更好的質量控制，其二在於揭示漢黃芩素及千層紙素的生物藥劑學及藥物動力學特徵，其三在於研究黃芩苷，漢黃芩素及千層紙素的藥物動力學方面的相互作用。

研究方法: 本課題于體外，在體以及體內水平上對漢黃芩素及千層紙素的腸道吸收和代謝及黃芩中各類有效成分之間的藥物動力學相互作用進行了研究。研究利用如 Caco-2 單層細胞模型，大鼠腸道單相灌流模型，體外代謝模型及大鼠體內動力學等多種模型。

研究結果: 漢黃芩素及千層紙素在 Caco-2 單層細胞模型和大鼠腸道單相灌流模型上顯示良好的透過性。然而，兩者在吸收的同時也伴隨顯著的腸道首過代謝，

並主要生成相應的葡萄糖醛酸結合物。Caco-2 單層細胞以及 MDCK 上的轉運實驗表明細胞內生成的漢黃芩苷及千層紙素苷經多藥耐藥相關蛋白主動外排至腸道側及血流側。千層紙素的萄糖醛酸代謝強于漢黃芩素。且經 UGT1A9 主要負責黃芩素，千層紙素和漢黃芩素在肝臟的葡萄糖醛酸，而 UGT1A8 及 1A10 則主要參與三者在腸道的葡萄糖醛酸化。大鼠體內藥動學結果表明，口服后漢黃芩素和千層紙素被迅速吸收並葡萄糖醛酸化。5 位羟基葡萄糖醛酸結合物是漢黃芩素的另一种代謝物。三者合併給葯后，体外酶動力學研究表明三者生成的葡萄糖醛酸結合物均減少；Caco-2 單層細胞模型和大鼠腸道單相灌流模型的研究結果表明三者合併給葯后透過的原型藥物量增加的同時生成的代謝物減少。大鼠體內藥動學研究結果表明，葡萄糖醛酸結合物是黃芩素，漢黃芩素及千層紙素在血中的主要存在方式， 合併給葯后， 僅千層紙素苷的藥時曲綫下面積與單獨給葯相比有顯著性增加。

結論：漢黃芩素及千層紙素與黃芩素的吸收與代謝方式類似。雖然其腸道吸收較好，但在葡萄糖醛酸轉移酶作用下發生顯著的首過代謝。多藥耐藥相關蛋白參與其代謝產物的清除。体外及在体模型證實，黃芩素，漢黃芩素及千層紙素三者間的相互作用會導致原型藥物的吸收增加且代謝物的生成減少。然而由於體內強烈的代謝，三者合併給葯后生物利用度的增加僅表現于千層紙素苷在血中的總量增加。

ACKNOWLEDGEMENTS

I would like to greatly thank my supervisors, Prof. Zhong Zuo and Prof. Ge Lin for their guidance, consistent support, and invaluable encouragement throughout the course of my study.

I would also like to thank Dr. Li Zhang for his kind help and suggestion on my project. My heartiest thanks also go to the professors and technicians in our department for their helpful advice and technical support on my project. All other postgraduate students and research staff in school of pharmacy are thanked for their friendship and encouragement during my study.

Publications

Research papers

Li CR, Zhang L, Lin G, Zuo Z. Identification and quantification of baicalein, wogonin, oroxylin A and their major glucuronide conjugated metabolites in rat plasma after oral admnistration of *Radix Scutellariea* product. *J Pharm Biomed Anal*. Submitted and under revision.

Li CR, Zhou LM, Lin G, Zuo Z. Contents of major bioactie flavones in proprietary traditional Chinese medicine products and reference herb of *Radix Scutellariae*. *J Pharm Biomed Anal*. 50(2009): 298-306

Conference abstracts

Li CR, Lin G, Zuo Z. Pharmacokinetic interactions between three major bioactive flavoens in *Radix Scutellariae*. The 9th International ISSX Metting, Istanbul, Turkey, 2010/09/04-2010/09/08

Li CR, Lin G, Zuo Z. Metabolic interactions among the major bioactive flavones in *Radix Scutellariae*. 2010 AAPS Annual Meeting and Exposition, New Orleans, United States of America, 2010/11/14-2010/11/18

Li CR, Zhang L, Lin G, Zuo Z. Competition on the intestinal absorption and disposition of baicalein by wogonin and oroxylin A, the co-existing flavones in Radix Scutellariae. 2009 AAPS Annual Meeting and Exposition, Los Angeles, United States of America, 2009/11/08-2009/11/12

Li CR, Zhou LM, Lin G, Zuo Z. Contents of major bioactive flavones in proprietary products of Radix Scutellariae and its reference herb. 2009 AAPS Annual Meeting and Exposition, Los Angeles, United States of America, 2009/11/08-2009/11/12

List of Tables

List of Figures

List of Abbreviations

ABC	ATP-binding cassette
AUC	Area under the plasma concentration versus time curve
B	Baicalein
BG	Baicalin
BS	Sulfate of baicalein
C_{lint}	Intrinsic clearance
ER	Extraction ratio
HIM	Human intestinal microsome
HLC	Human liver cytosol
HLM	Human liver microsome
HPLC	High-performance liquid chromatogram
IS	Internal standard
LOD	Limit of detection
LOQ	Limit of quantification
MRP	Multi-drug resistant associated proteins
OATP	Organic anion transporter peptide
OA	Oroxylin A
OAG	Oroxylin A-7-*O*-glucuronide
OAS	Sulfate of OA
Papp	Apparent permeability coefficient
P-gp	P-glycoprotein
p.o.	Per os
PTCM	Proprietary traditional Chinese medicine
RE	Relative error
RIM	Rat intestinal microsome
RLC	Rat liver cytosol
RLM	Rat liver microsome
RS	*Radix Scutellariae*
RSD	Relative standard deviation
SD	Standard deviation
SULT	Sulfotransferases
TEER	Transepithelial electrical resistance
UGT	UDP-glucuronosyltransferase
W	Wogonin
WG	Wogonoside
WS	Sulfate of W

Table of Contents

Chapter One

Introduction

1.1　Background of *Radix Scutellariae*

1.1.1　Origin of *Radix Scutellariae*

Scutellariae baicalensis Georgi (Fig. 1.1) is a Labiatae plant. In addition to *Scutellariae baicalensis* Georgi, there are about 350 species belonging to the genus of *Scutellaria* and this genus has wide distribution in temperate regions and tropical mountains in Europe, North America and East Asia (Bruno et al., 2002). The common species in China include *S. viscidula* Bunge, *S. rehderiana* Diels, *S. amoena* C.H. Wright, *S. likiangensis* Diels, S. *hyperifolia* Level and *S. tenax* W.W. Smith var P.G.Y. (Liu et al., 2002). *Scutellariae baicalensis* Georgi is often medicinally chosen to treat inflammation, cardiovascular diseases, respiratory and gastrointestinal infections (Cui et al., 2010). *Radix Scutellariae* (RS, Fig. 1.1), which is also called Huangqin in Chinese, is the dried root of *Scutellariae baicalensis* Georgi. RS has been used extensively in Chinese and Japanese medicine and is officially listed in Chinese Pharmacopoeia with broad therapeutic effects such as purging fire, cleaning away heat, moinstening aridity, detoxifying toxicosis, stopping bleeding, preventing miscarriage, etc. (The Pharmacopoeia Commission of PRC, 2005, Li et al., 2004).
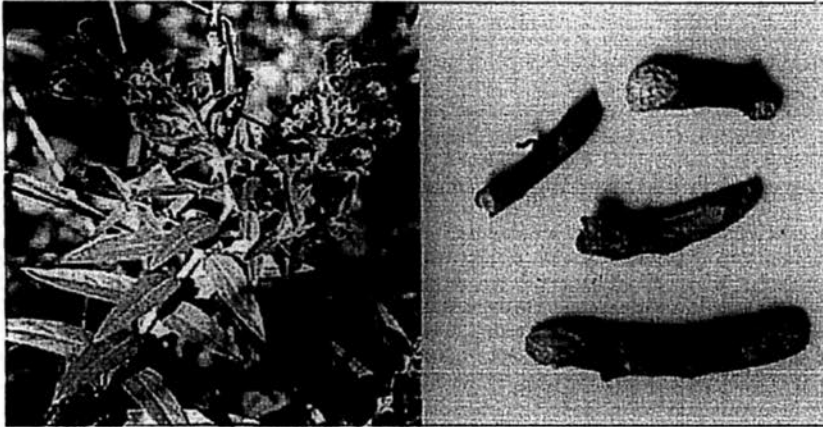
Fig. 1.1   **Photographs of *Scutellariae baicalensis* Georgi (left) and its dried root *Radix Scutellariae* (RS, right) (Shang et al., 2010)**

1.1.2   Pharmacological effects of RS

The pharmacological effects of RS have been extensively studied, mainly in the form of water and organic solvent extract. As one of the most well reported pharmacological effects, its anti-inflammatory effect is believed to be related with its inhibition of NO, cytokine, chemokine and growth factor production in macrophages (Yoon et al., 2009). A number of *in vitro* and *in vivo* studies confirmed the anti-inflammatory and anti-oxidative effect of RS (Kang et al., 2005, Chen et al., 2006, Shao et al., 1999, Choi et al., 2002, Schinella et al., 2002) and demonstrated its potential to treat colitis (Chung et al., 2007), stroke (Tang et al., 2004), colon cancer (Fukutake et al., 1998). In addition, the water decoction of RS exerted promising immunomodulatory activities on the immune function and the cell cycle distribution of mice and human immune cells (Li et al., 2010).

Moreover, the anti cancer effect of RS extract is a hot topic recently. The methanol extract of RS was found to be able to inhibit the proliferation of human monocytic leukemia cell line THP-1 and human osteogenic sarcoma cell line HOS (Himeji et al.,

2007). In an *in vivo* experiment, antitumor effects of RS on C3H/HeN mice implanted with a murine bladder cancer cell line (MBT-2) were confirmed (Ikemoto et al., 2000). The RS extract after pressurized liquid extraction also showed inhibitory effect on liver cancer cell lines (HepG2) (Ong et al., 2005).

In addition, RS exhibits other pharmacological effects. The water extract of RS showed anticonvulsant effect via the prevention of seizure spread in mice (Wang et al., 2000). Ethanol extract of RS inhibited high glucose-induced endothelial cell apoptosis, indicating its beneficial effect in preventing diabetes-associated microvascular complications (Suh et al., 2003). Furthermore, the extract of RS can induce interferon and inhibit the replication of influenza virus in mice (Chu et al., 2007).

1.1.3 Major chemicals isolated from RS

There have been 295 compounds isolated from the genus *Scutellaria*, including flavonoids, phenylethanoid glycosides, iridoid glycosides, diterpenes, triterpenoids, alkaloids, phytosterols and polysaccharides (Shang et al., 2010). It has been reported that flavonoids, frequently in the form of glycosides, constituted the most abundant ingredients and over 40 flavonoids have been found in RS (Ishimaru et al., 1995). Baicalein (B), baicalin (baicalein-7-glucuronide, BG), wogonin (W), wogonoside (wogonin-7-glucuronide, WG), oroxylin A (OA) and oroxylin A-7-glucuronide (OAG) are usually considered to be the main bioactive components in RS (Li et al., 1995). Their chemical structures are shown in Fig. 1.2. Besides, other flavonoids have been identified in RS including viscidulin III-2'-O-β-D-glucoside, 5,7,2',5'-tetrahydroxyflavone, (-)-

eriodictyol and rivularin (Zhang et al., 1994), chrysin 8-C-β-D-glucopyranoside (Zhang et al., 1997), and 5,2'-dihydroxy-6,7,8,3'-tetramethoxyflavone, skullcapflavone 1 (Nishikawa et al., 1999).

Baicalin (R_1=OH, R_2=H)   Baicalein (R_1=OH, R_2=H)

Wogonoside (R_1=H, R_2=OMe)   Wogonin (R_1=H, R_2=OMe)

Oroxylin A 7-O-glucuronide (R_1=OMe, R_2=H)   Oroxylin A (R_1=OMe, R_2=H)
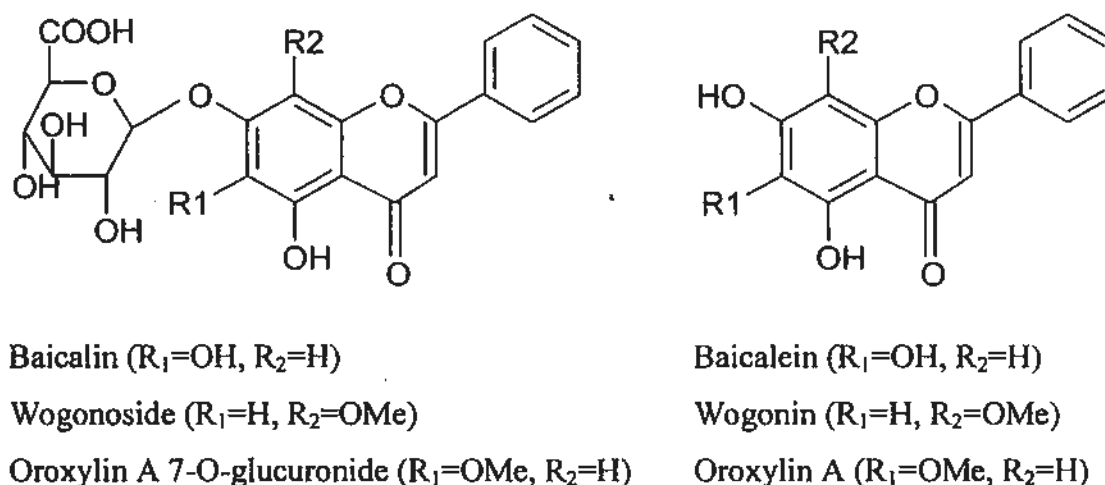
Fig. 1.2   Chemical structures of major bioactive flavones in RS

1.2   Preparations of RS herbal material and products

1.2.1   Preparations of crude herbal material of RS

In the traditional medicine pharmaceutical industry, the selection of raw material is significantly important, because it is the first step for the quality control of the preparations. For the raw material of RS, various studies about the extraction and quantification method of the major components revealed the contents vary in different tissues of RS and the whole plant from different sources. Table 1.1 summarized the reported extraction and quantification methods and the corresponding contents of the major components.

Generally, extraction by methanol or ethanol is frequently used because of the relatively high solubility of flavonoids in those solvents. The primary extraction is often conducted with the process of sonication or reflux. After evaporation to dryness, the crude powder is further processed by the techniques such as high-speed counter-current chromatography (Wu et al., 2005) or solid phase extraction (Zgórka et al., 2003) to produce specific ingredients with higher purity. Because of the variation in the polarity among ingredients, different extraction methods may produce different results. Compared with ethanol extraction, enzyme extraction produced highest extraction ratio for B and W (Wang et al., 2007). However, we should consider the possibility that the glycosides of BG, WG and OAG could be changed to the corresponding aglycones after the enzyme treatment. The extraction method should be carefully chosen in order to optimize the content of desired components.

In the current Chinese Pharmacopeia, BG is chosen as the marker for quality control of RS and it is authorized that the content of BG should not be less than 9% in dried RS (The Pharmacopoeia Commission of PRC, 2005). Due to the wide distribution of *Scutellariae baicalensis* Georgi on earth, the content of the major components may be influenced by the environmental factors. A series of studies have detected the contents of flavonoid constituents in RS cultivated in different areas, especially in China (Zhou et al., 2006, You et al., 2010, Song et al., 2006). The results showed the content had significant fluctuation and the content of baicalin was even below 9% in some area like Heihe in Heilongjian, Duolun in Inner Mongolia, Baikal in Russia (Yang et al., 2002). Particularly,

the content of BG and WG vary in different species of *Scutellaria* with *S. likiangensis* Diels containing the lowest amount of BG and *S. amoena* C.H. Wright containing the lowest amount of WG (Liu et al., 2002). In addition to BG, the other five bioactive flavones are also reported to exist in relatively high amount (Li et al., 1995, Li et al., 2005) which is also confirmed by our study (Li et al., 2009). Due to the abundance of the other co-existing bioactive flavones, it may not be accurate enough to only monitor the content of BG. As a result, more marker component in addition to BG should be involved for better quality control of RS.

Table 1.1   Summary of assay methods and content of major flavones in crude herbal material of RS

Raw material	Extraction method	Quantification method	Contents of major bioactive flavones (mg/g, w/w)						References
			BG	B	WG	W	OAG	OA	
Coptidis Rhizoma: RS 1:1	Extraction by 70% methanol	Micellar electrokinetic capillary electrophoresis	84.82±3.02	18.28±0.06	78.69±0.69	9.32±0.19	40.57±0.65	4.01±0.07	Li, 1995
Scutellariae planipes	Reflux by 50% ethanol for four times	HPLC-UV	127.7	35.6	35.3	9.3	N.A.	N.A.	Zhang, 1998
RS			144.0	29.9	30.8	9.7	N.A.	N.A.	
RS	SPE by supercritical carbon dioxide-MeOH-water	HPLC-UV	137.6±5.13	8.6±0.54	N.A.	2.2±0.09	N.A.	N.A.	Lin, 1999
RS from seventeen areas	Reflux by 70% ethanol for 3 h	HPLC-UV	60-190	1-16	20-80	0.1-3	Trace amount	N.A.	Yang, 2002
RS cultured in Europe	Extraction by methanol	HPLC-UV	81.2	N.A.	25.2	N.A	N.A.	N.A.	Bochořáková, 2003
RS	Solid phase extraction	HPLC-UV	19.33±0.72	0.41±0.016	N.A.	N.A.	N.A.	N.A.	Zgórka, 2003
RS	High-speed counter-current chromatography	HPLC-UV	116.23	N.A.	33.94	N.A.	N.A.	N.A.	Wu, 2005
RS	High-speed counter-current chromatography	HPLC-UV	N.A.	34.23	N.A.	12.21	N.A.	2.85	Li, 2005
Five batches of RS	Extraction by 70% ethanol	HPLC-UV	99.9-131.4	11.9-18.2	25.8-29.4	N.A.	N.A.	N.A.	Liu, 2005

Table 1.1　Summary of assay methods and content of major flavones in crude herbal material of RS (continued)

Raw material	Extraction method	Quantification method	Contents of major bioactive flavones (mg/g, w/w)						References
			BG	B	WG	W	OAG	OA	
RS root	Extraction by methanol: water:formic acid	HPLC-DAD-MS	150	4.7	N.A.	0.07	N.A.	N.A.	Horvath, 2005
RS shoot			N.A.	0.5	N.A.	0.03	N.A.	N.A.	
RS from sixteen areas	Reflux by 75% ethanol for 1 h	HPLC-UV	74.1-165	1.25-34.2	4.36-49.5	0-8.33	N.A	0.64-3.48	Zhang, 2005
RS (raw)	Extraction by methanol for three times	Microemulsion electrokinetic chromatography	14.6±4.2	3.20±2.8	4.02±2.3	N.A.	N.A.	N.A.	Zhang, 2006
RS (cooked)			25.8±2.4	0.21±2.9	0.85±2.2	N.A.	N.A.	N.A.	
RS from nine areas	Extraction by 70% ethanol	HPLC-ECD	141-325	0.48-8.65	N.A.	0.40-2.45	N.A.	N.A.	Zhou, 2006
RS from seventeen areas	Reflux by 70%ethanol or chloroform	HPLC-UV	84.9-135	0.4-2.8	N.A.	0.3-2.2	N.A.	N.A.	Song, 2006
RS	Dynamic microwave-assisted extraction	HPLC-UV	202.95±0.52	16.81±5.46	N.A.	4.18±3.46	N.A.	N.A.	You, 2007
RS	Extraction by 70% ethanol	Capillary electrophoresis	24.74~143.56	1.53~15.12	N.A.	0.36~4.80	N.A.	N.A.	Yu, 2007
RS from five areas	On-line continuous flow ultrasonic extraction	HPLC-UV	73.8-131.5	6.8-159	N.A.	4.4-14.3	N.A.	N.A.	You, 2010

N.A.: not available

1.2.2 Preparation of proprietary traditional Chinese medicine products of RS

Because of its extensive pharmacological effects, RS has been extensively employed in a number of traditional formulations in China and Japan for a long history including Huangqin Tang, Huangqin Shegan Tang (Shang et al., 2010) and Xiao-Chai-Hu-Tang (Sho-Saiko-To) (Kang et al., 2009, Chang et al., 2007). In addition, RS has been commonly involved in various proprietary traditional Chinese medicine (PTCM) products as major ingredient such as Huangqin Tablet, Yinhuang Tablet, Shuanghuanglian capsule, Shuanghuanglian oral liquid, Yiqing capsule, Angong Niuhuang Pill, Qingfeiyihuowan, etc. Comparing with single herb, the ingredients in the traditional formulation and PTCM products containing RS are more complicated. There are influences from the excipients to prepare the herbal formula as well as the ingredients from other co-existing herbs in the PTCM products in addition to RS itself. Therefore, these ingredients may interfere with the major bioactive components in their quantification assay. As a result, the techniques with high separation efficiency are frequently used in the quantification of components in the traditional formulations and PTCM products containing RS, especially the chromatography methods such as high-performance liquid chromatography, capillary electrophoresis, micellar electrokinetic capillary chromatography etc. Table 1.2 summarized the analytical methods that have been used for the quantification of major components in the traditional formulations and PTCM products containing RS.

Table 1.2   Summary of assay methods and detected components in the herbal preparation containing RS

Formulation	Sample preparation	Assay method	Detected components (Bold: RS components)	References
Yiqing capsule	Extracted by methanol	HPLC/DAD	Berberine, aloe-amodin, rhein, emodin, chrysophanol, baicalin, **baicalein, wogonoside and wogonin**	Li Y, 2010
Yiqing capsule	Extracted by methanol	HPLC/UV	rhein, emodin, chrysophanol, **baicalin, baicalein, wogonin** berberine, aloeemodin,	Qu, 2007
Qingfeiyihuowan	Extracted by methanol	Microemulsion electrokinetic chromatography (MEEKC)	**Baicalein, baicalin and wogonin**	Zhang, 2006
Compound Puqin tablet	Extracted by methanol	HPLC/UV	**Baicalin**	Li BL, 2010
Niuhuangjiedu Tablet	Extracted by methanol	HPLC/UV	**Baicalin**	Sun, 2009
Angong Niuhuang Pill	Extracted by methanol	HPLC/UV	Geniposide, **baicalin,** berberine hydrochloride	Han, 2007
Niu Huang Jie Du Pill	Extracted by 70% ethanol	Ultra performance liquid chromatography coupled with tunable UV detector (UPLC-TUV)	**Baicalin, baicalein, wogonoside, wogonin,** glycyrrhizic acid, liquiritin, rhein, emodin, chrysophanol and physcion	Liang, 2010
Fuzhisan	Extracted by methanol	HPLC-DAD-ELSD	**Baicalin** and ginsenoside Rb1	Zhao, 2009
Shuang-Huang-Lian oral liquid	Direct injection after dilution	Capillary electrophoresis with electrochemical detection (CE-ED)	**Baicalein, baicalin** and quercetin	Chen, 2000
Shuang-Huang-Lian oral liquid	Direct injection after dilution	HPLC/UV	**Baicalin** and chlorogenic acid	Cao, 2006
Sann-Joong-Kuey-Jian-Tang	Extracted by water	HPLC/UV	Gentiopicroside, mangiferin, palmatine, berberine, **baicalin, wogonin,** glycyrrhizin	Lin, 1996
Xiaochaihu Tang	Extracted by water	HPLC/UV	**Baicalin, wogonoside, baicalein, wogonin** glycyrrhizic acid	Liu, 2010

1.3   Pharmacological effects of major bioactive flavones

Among the isolated components in RS, six flavones, namely baicalein (B), baicalin (baicalein-7-glucuronide, BG), wogonin (W), wogonoside (wogonin-7-glucuronide, WG), oroxylin A (OA) and oroxylin A-7-glucuronide (OAG) are identified as the main bioactive components in RS (Li et al., 1995).

1.3.1   Pharmacological effects of B and BG

Both B and BG are bioactive. B prevented lipolysaccharide-induced production of nitric oxide in RAW264.7 mouse macrophages (Wakabayashi et al., 1999) and protected the inflammatory stimulated cell death of brain microglia by suppressing cytotoxic nitric oxide production (Suk et al., 2003). BG inhibited the binding of a number of chemokines to human leukocytes or cells transfected to express specific chemokine receptors, demonstrating its anti-inflammation effect (Li et al., 2000). The mechanism for anti-inflammation of B and BG were studied to be different on COX-2 gene expression in LPS-induced Raw 264.7 cells, which might be mediated through inhibition of C/EBPβ DNA binding activity (Woo et al., 2006). Anti-oxidation effect was observed in B and BG (Hamada et al., 1993; Gao et al., 1999). Anticancer effects of B were studied extensively *in vitro* and *in vivo*. B could inhibit the growth of mouse leukemia cells (L1210) (Ciesielska et al., 2002); human breast carcinoma cell line (MDA-MB-435) (So et al., 1996); human lung squamous carcinoma CH27 cells (Lee et al., 2005). The anticancer effect of B was confirmed by *in vivo* studies (Bonham et al., 2005; Ikemoto et al., 2004). For antivirus effect, B and BG could inhibit human immunodeficiency virus type 1 (Ahn et al., 2001; Kitamura et al., 1998). Besides, B could block DNA synthesis of

human cytomegalovirus (Evers et al., 2005) and BG had a moderate ability to reduce the production of hepatitis B virus and had no effect on host cells (Romero et al., 2005). Furthermore, B significantly attenuated oxidative cell death *in vitro* using a mouse hippocampal HT22 cell assay and could be used to develop as novel treatments for acute ischemic stroke (Lapchak et al., 2007). B attenuated ischemic-like injury in the neurons, which partly related to the inhibition of NMDA receptor-mediated 5-LOX activation (Ge et al. , 2007) and B could protect against cerebrovascular dysfunction and brain inflammation in heatstroke (Chang et al., 2007).

1.3.2 Pharmacological effects of W and WG

With respect to anti-oxidation and anti-virus effects, both W and WG are bioactive. W showed significant anti-inflammation effect (Chi et al., 2001; Park et al., 2001; Shen et al., 2002). Since nitric oxide (NO) produced by inducible nitric oxide synthase (iNOS) is one of the inflammatory mediators, the effects of 26 naturally occurring flavonoids on NO production were evaluated by LPS-activated RAW 264.7 cells *in vitro*. Wogonin was one of the most active flavonoids, having IC_{50} values of 17 μM (Kim et al., 1999). Wogonin at 0.5 mM directly attenuated enzymatic activity of COX-2. The protein expression of COX-2 was depressed by wogonin at concentrations of 10 mM and more. These results suggest that wogonin decreases inducible prostaglandin E2 production in macrophages by inhibiting both COX-2 activity and COX-2 expression (Wakabayashi et al., 2000). W and WG showed significant effects on NADPH-induced lipid peroxidation (Gao et al., 1999). W, B and BG inhibited cell proliferation on human bladder cancer cell lines (KU-1 and EJ-1) and murine bladder cancer cell line (MBT-2) in a dose-dependent

manner and RS showed anticancer effects on C3H/HeN Mice implanted with MBT-2 at a dose of 10 mg/mouse (Ikemoto et al., 2000). In a study to evaluate the biological activities on the human leukemia cell line (HL-60) by MTT assay, wogonin and fisetin were the most potent apoptotic inducers among seven structurally related flavonoids (luteolin, nobiletin, wogoin, baicalein, apigenin, myricetin and fisetin). The cytotoxic effects of wogonin and fisetin were accompanied by the dose- and time-dependent appearance of characteristics of apoptosis including DNA fragmentation, apoptotic bodies and the sub-GI ratio (Lee et al., 2002). In addition, wogonin exhibited central nervous effect. Wogonin was shown to inhibit the excitotoxicity induced by glutamate or N-methyl-D-aspartic acid and lipid peroxidation initiated by Fe^{2+} and L-ascorbic acid in rat brain homogenates (Cho et al., 2004). It also had a protective effect on neuronal cells damaged by oxygen and glucose deprivation in rat hipocampal slices in culture (Son et al., 2004). Wogonin significantly blocked convulsion induced by pentylenetetrazole and electroshock and reduced the electrogenic response score, which indicated that the anticonvulsive effects produced by wogonin were mediated by the GABAergic neuron (Park et al., 2007). Sho-saiko-to, a traditional herbal medicine to treat chronic hepatitis might modulate the CD4/CD8 ratio via the selective inhibition of $CD8^{+}$ T-cell proliferation by W and WG to exhibit this antihepatic effect (Ohtake et al., 2005). *In vitro* and *in vivo* studies demonstrated that wogonin possessed potent anti-hepatitis B virus activity and is under early development as an anti-HBV drug candidate (Guo et al., 2007).

1.3.3 Pharmacological effects of OA and OAG

OA showed the potential of anti-inflammation. Among eight polyphenols isolated from Chinese herbs, namely myricitrin, oroxylin A, penta-O-galloyl-β-glucopyranose, woodfordin C, oenothein B and cuphiin D1, only OA and myricitrin exhibited the effect of anti-inflammation. The mechanistic study revealed that OA inhibited LPS-induced iNOS and COX-2 gene expression by blocking NF-κB activation (Chen et al., 2000). *In vitro* and *in vivo* studies showed OA had central nervous effects. It inhibited [^{3}H]flunitrazepam binding to rat cerebral cortical membrane, interacted as an antagonist at the recognition site of GABA receptor, and abolished the anxiolytic myorelaxant and motor incoordination, which added OA to the list of CNS active flavonoids (Huen et al., 2003). Besides, OA could dramatically attenuate the memory impairment induced by 2VO and this effect might be mediated by the neuroprotective effects of OA as supported OA induced reductions in activated microglia and increases in BDNF expression and CREB phosphorylation (Kim et al., 2006). The results in another study suggested that OA may be useful for the treatment of cognitive impairments induced by cholinergic dysfunction via the GABAergic nervous system (Kim et al., 2007). After alkylation and condensation, a series of OA were produced and screened for antibacterial activity against a panel of susceptible and resistant Gram-positive and Gram-negative organisms. It was observed that acylation of 7-OH group in OA significantly enhanced the activity than the parent compound (Suresh et al., 2005). In addition, OA exhibited strong anti-tumor effect, which indicated that OA could be a promising antitumor drug. OA inhibited human hepatocellular carcinoma cell line HepG$_2$ in a concentration-and time-dependent manner by MTT-assay (Hu et al., 2006). The OA induced apoptosis in HepG2 cells was achieved through mitochondrial pathway (Liu et al., 2009). OA could decrease the tumor

volumes and weight of human cervical cancer HeLa cell line *in vitro* and *in vivo*, in which apoptosis induction might be involved (Li et al., 2009). OA was identified as the potent compound against respiratory syncytial virus (Ma et al., 2002). However, the study about the pharmacological effect of OAG was relatively less in comparison with the other five bioactive flavones in RS. OAG showed neuronal protective effect by binding to the PDZ domains of postsynaptic density protein and preventing the combination of this domain with neuronal nitric oxide synthase (Tang et al., 2004). OAG exhibited higher inhibition activity of prolyl oligopeptidase than OA, which could be used as a potential therapeutic agent for the treatment of neurological disorders (Marques et al., 2010).

1.4 Biopharmaceutic and pharmacokinetic studies of the major bioactive flavones in RS

1.4.1 Biopharmaceutics characteristics of bioactive flavones in RS

The studies about the biopharmaceutics profiles of the bioactive flavones in RS were also carried out by various models on *in vitro* and *in situ* scale. The results on Caco-2 cell monolayer model were consistent with the findings in rats. The aglycones of B easily passed through the monolayer from the apical side (lumen side) to the basolateral side (mesenteric blood side) due to its high lipophilicity and low molecular weight. During the absorption of B, it underwent extensive glucuronidation and sulfation. BG was found to have limited permeability possibly due to its high polarity and large molecule (Zhang et al., 2007a; Dai et al., 2008). Zhang et al. confirmed the involvement of MRPs and MXR in the efflux of BG (Zhang et al., 2007a). The transport and metabolism of flavonoids

from a Chinese herbal remedy Xiaochaihu-tang was studied on Caco-2 cell monolayer model. The results demonstrated that W and OA also had favorable permeability and the transport of OAG was mediated by efflux transporters (Dai et al., 2008). The rat *in situ* single-pass perfusion model revealed that the permeability of B was favorable for absorption and BG was not detected in the mesenteric blood after perfusion of BG at a dose of 200 μM (Zhang et al., 2005, Akao et al., 2004). B, rather than BG could be absorbed in the intestine (Liu et al., 2006). By *in vitro* enzyme incubation method, UGT 1A9 was in charge of the formation of BG and other isoforms of UGT also mediated its formation with different kinetic profiles (Zhang et al., 2007b).

1.4.2 Pharmacokinetics profiles of bioactive flavones in RS

Several studies have investigated the pharmacokinetics of the major ingredients in RS. Most of them concerned the pharmacokinetic profiles in rat. The studies in human were limited and they all just studied the urinary metabolism and excretion. There is no report about the pharmacokinetic characteristics of the major ingredients in the systematic circulation of human. Based on the results from animal and human studies so far, the pharmacokinetic profiles are expected to comply with the general pharmacokinetic characteristics of flavonoids. Major findings and the pharmacokinetic parameters of pharmacokinetic studies of major bioactive flavones in RS are summarized in the Table 1.3.

Among the six bioactive flavones in RS, B and BG were studied relatively more than the other four. The absorption of B was fast and good. However, it also underwent fast and

extensive metabolism either after its p.o. or i.v. administration. As a result, the bioavailability of B was quite low (Lai et al., 2003). The multi-peak phenomenon of the plasma concentration-time curve revealed the enterohepatic circulation of BG and it was confirmed by the study on germ-free rat (Xing et al., 2005). BG itself cannot be absorbed directly across the intestine and was firstly hydrolyzed into B, its aglycone, by intestinal bacteria (Akao et al., 2000). The involvement of enzymes in GI tract such as β-glycosidase or lactase phlorizin hydrolase (LPH) in the hydrolysis of BG has also been reported (Day et al., 2000, Day et al., 2003). Conjugated metabolism is the major route of metabolism for B in plasma and urine (Lai et al., 2003, Li et al., 2005). In addition to systemic exposure of RS, the distribution of BG in the cerebral nuclei was found to provide therapeutic effects of RS on the central nervous system (Zhang et al., 2006).

Table 1.3 Summary of pharmacokinetic parameters of the major bioactive ingredients in RS

Species	Administration	Main PK parameters	Findings	References
SD rat	• i.v. 37 μmol/kg B • p.o. 224 μmol/kg B and BG	i.v. B (B) AUC $_{0-t}$ (μmol·min/ml): 297.6±142.2 (BG) AUC $_{0-t}$ (μmol·min/ml): 927.2±462.8 p.o. B 　B: C_{max} (nmol/ml):13.6±9.0 　　t_{max} (min): 10.0±0.0 　　MRT (min): 651.7±262.9 　　AUC $_{0-t}$ (μmol·min/ml): 2980.5±1751.2 p.o. BG 　BG: C_{max} (nmol/ml):2.9±1.3 　　t_{max} (min): 395.6±438.8 　　MRT (min): 696.9±320.8 　　AUC $_{0-t}$ (μmol·min/ml): 1943.7±810.6	• Fast and extensive metabolism of B; • Absolute bioavailability of B: zero; • BG need to be hydrolyzed by bacterial in GI tract prior to absorption	Lai, 2003
SD rat	• p.o. 200 mg/kg BG; • p.o. RS extract (188 mg/kg BG, 47 mg/kg WG) ; • p.o. Huang-Lian-Jie-Du-Tang decoction (193 mg/kg BG, 43 mg/kg WG)	AUC $_{0-t}$ (μg·h/ml) Pure BG: 52.39±4.23 BG in extract 51.27±4.14 BG in decoction: 32.49±1.26 WG in extract: 13.94±1.93 WG in decoction: 7.35±0.86 $t_{1/2}$ (h): pure BG: 3.71±0.73 BG in extract:4.32±1.1 BG in decoction: 4.92±2.1 WG in extract: 5.14±0.55 WG in decoction: 5.19±3.28	• Bimodal phenomenon; • Pharmacokinetic interaction between ingredients in herbs in Huang-Lian-Jie-Du-Tang decoction in AUC of BG and WG	Lu, 2007
SD rat	• p.o. different herbal extract (0.4 g/kg BG): - SR; - SR+ LJF; - SR+ FF; - SR+LJF+FF	AUC $_{0-t}$ (ng·h/ml) SR:3360.00±1884.11 SR+LJF:5345.44±2468.32 SR+FF:7957.04±9621.10 SR+LJF+FF:2727.03±2178.21 t_{max} (h) SR: 4.42±4.01 SR+LJF: 4.50±2.32 SR+FF: 2.47±3.03 SR+LJF+FF: 4.53±4.62	• Co-existing herbs affected the elimination and bioavailability of BG	Di, 2006

Table 1.3   Summary of pharmacokinetic parameters of the major bioactive ingredients in RS (continued)

Species	Administration	Main PK parameters	Findings	References
SD rat	p.o. 12g/kg Xiexin decoction (BG 302.02, WG 55.61, B 30.94, W 11.96 mg/kg)	$t_{1/2}$ (h) BG: 7±3 WG: 6.4±2.1 CL/F (L/h/kg) BG 5.5±1.2 WG: 3.9±0.9	AUC_{0-t} (mg·h/L) BG: 48±8 WG:14±3	▪ B and W were not detectable in blood; ▪ Double peak phenomenon for BG and WG; ▪ B, W, BG, WG could be excreted into urine	Yan, 2007
SD rat	p.o. 10, 20, 40 mg/kg PF-2405 (equivalent to 4.5, 9.0, 18 mg/kg pure B) and 18 mg/kg B	*PF-2405 at 40mg/kg* t_{max} (min) B:214±227 BG:15.0±8.7 C_{max} (pmol/ml) B:515±278 BG: 8841±3154 AUC_{0-t} (pmol·h/ml) B: 4606±4630 BG: 39875±15395	*Pure B* t_{max} (min) B: 65.6±120 BG: 20.6±7.8 C_{max} (pmol/ml) B:374±218 BG: 6366±3728 AUC_{0-t} (pmol·h/ml) B:548±260 BG: 21067±10306	▪ Dose-linear pharmacokinetics for B and BG; ▪ Multiple peaks phenomenon for B and BG; ▪ Extract could increase the absorption of B	Kim, 2007
SD rat	i.v. 10 mg/kg RS ectract (4.4 mg/kg B, 1.15 mg/kg OA, 0.3 mg/kg W)	AUC_{0-t} (μg·min/ml) B: 32.1±4.9 OA: 0.54±0.10 W: 14.3±2.2	$t_{1/2}$ (min) B:316±77.1 OA:9.8±5.6 W:5.0±1.8		Kim, 2006
SD rat	i.v. 10 mg/kg B			▪ Major metabolite was BG; ▪ B could not be detected after 20 min	Zhang, 2004
Wistar rat	i.v. 37 μmol/kg BG p.o. 224 μmol/kg BG	*p.o. BG* t_{max}:5.0 h; $t_{1/2}$:12.06±5.46 h; CL:847.25±70.30 ml/min/kg F(%): 2.2±0.2	*i.v. BG* $t_{1/2}$:9.74±1.60h; CL:18.4±0.99 ml/min/kg	▪ Low oral bioavailability of BG; ▪ Enterohepatic circulation; ▪ Four metabolites of B were identified in bile	Xing, 2005

Table 1.3   Summary of pharmacokinetic parameters of the major bioactive ingredients in RS (continued)

Species	Administration	Main PK parameters	Findings	References
Wistar rat and germ-free rat	• p.o. 20 mg/kg BG • p.o. 12.1 mg/kg B	*Normal rat* t_{max} (h) BG: 2.4±0.89 B: 1.5±1.34 C_{max} (µg/ml) BG: 1.34±0.51 B: 1.69±0.65 AUC_{0-t} (µg·h/ml) BG: 9.10±2.91 B: 5.76±1.63 *Germ-free rat* t_{max} (h) BG: 0.38±0.14 C_{max} (µg/ml) BG: 0.34±0.10 AUC_{0-t} (µg·h/ml) BG: 1.09±0.37	• Absorption of BG was low; • BG appeared in the plasma quickly after p.o. B; • BG was hydrolyzed by the intestinal bacteria into B followed by absorption of B	Akao, 2000
Wistar rat	i.v. 111 mg/kg RS extract (90 mg/kg BG)	MRT(min) blood: 64.177±2.139 min cortex: 190.384±2.959 min striatum: 230.792±4.587 min $AUC_{0-\infty}$ (mg·min/L) blood: 580.612±39.395 cortex: 115.005±5.538 striatum: 483.715±42.681	• BG could pass through BBB; • Main distribution in striatum, thalamus and hippocampus area; • Different PK profile between blood and cerebral nuclei	Zhang, 2006
Wistar rat	• p.o. 10 g/kg Huangqin-Tang decoction • p.o. 10 g/kg RS decoction	*RS decoction* t_{max} (h) BG: 3.74±1.58 WG: 3.70±0.17 OG: 7.41±2.32 AUC_{0-t} (ng·ml/h) BG: 1875.33±449.68 WG: 10162.23±4351.27 OAG: 11442.73±4871.38 *Huangqin-Tang decoction* t_{max} (h) BG: 3.13±1.10 WG: 11.90±6.37 OG: 12.95±3.91 AUC_{0-t} (ng·ml/h) BG: 4044.98±2201.36 WG: 41984.69±3369.82 OAG: 13692.44±6352.11	• One-compartment model; • Other constituents in Huangqin-Tang could delay absorption and elimination of BG, WG and OAG	Zuo, 2003

Table 1.3   Summary of pharmacokinetic parameters of the major bioactive ingredients in RS (continued)

Species	Administration	Main PK parameters	Findings	References
Wistar rat	▪ p.o. pure BG ▪ Xiexin decoction ▪ RS extract (equivalent to 350 mg/kg BG)	Total urine excretion of BG 0–48 h (μg): BG: 251.91±15.80 Xiexin decoction: 543.56±29.21 RS Extract: 457.00±139.58	▪ Absorption of BG in decoction > RS extract and pure BG; ▪ WG and 7-O-glucuronide chrysin were metabolites of B in urine	Li, 2005
Wistar rat	▪ p.o. 5 mg/kg W		▪ Major metabolite was WG	Chen, 2002
Beagle dog	▪ i.v. 20 mg/kg W	$AUC_{0-\infty}$ (ng·h/ml): 2137.9±231.4 CL(1/h/kg): 9.45±1.09 Vd(1/h): 0.68±0.14 $t_{1/2}$(h): 1.51±0.43	▪ No gender difference in the pharmacokinetics of W; ▪ No subchronic toxicity was observed in heart, liver, spleen, lung, kidney, brain etc. after long time intravenous administration of W	Peng, 2009
Human	▪ p.o. 5.2 g/man RS extract (BG 616.0 g, B 52.5 g, WG 117.2 g, W 32.0 g)	Total urine excretion 0–48 h (μmol): BG: 43.1±4.5 BS: 64.8±6.3 WG: 21.6±2.0 WS: 20.7±1.7 $t_{1/2}$ (h) BG: 8.5±0.1 BS: 7.7±0.2 WG: 10.5±0.5 WS: 10.4±0.3	▪ No free form of B or W were found in urine; ▪ W was absorbed in a greater extent than B; ▪ Urinary excretion of BS was larger than BG and WS was comparable to WG	Lai, 2003
Human	p.o. 1.0 g/man BG		▪ Two metabolites of B were identified	Che, 2001

1.5   Interactions among the multiple ingredients in herbal medicines

Herbal medicines are attracting more and more attentions these days due to their beneficial effects and relatively low toxicities. In clinical practice, poly-pharmacy is common. Nowadays, it is not unusual that patients would administer various over-the-counter medications, vitamins, herbal medicines, together with their prescribed medications (Fugh-Berman A, 2000]. There have been a number of studies on the herb-drug and herb-herb interactions. Nevertheless, since the ingredients of herbal medicines are complicated and they often contain multiple components, the interaction among co-existing components in herbal medicines or herb extract is also a major concern for their safe application. As a matter of fact, there has been s numerous reports on the pharmacokinetics as well as pharmacodynamics interactions among the co-existing components in a medicinal herb in the form of herb extract or herb decoction or herb preparation, which will be summarized as follows.

1.5.1   Pharmacokinetic interactions

In most of the investigations on pharmacokinetic interactions, the marker components in a specific herb for the quality control were often chosen as the tested ingredients to investigate the changes of their pharmacokinetic profile by other co-existing components. Only a few studies clearly identify the potential ingredients that cause the interaction and their related mechanisms. Table 1.4 provides the examples of the pharmacokinetics interactions of multiple ingredients in herbal medicines. All the listed herbs are commonly used in traditional Chinese formulations or as herbal supplements such as Hawthorn fruits, *Salvia miltiorrhiza* (Dan Shen), Kava and RS. The studies usually used

area under the plasma concentration versus time profile (AUC) as the index to evaluate the extent of pharmacokinetic interactions. It has been reported that the co-existing ingredients could enhance the AUC of the tested ingredients (Chang et al., 2005, Song et al., 2007) as well as reduce the AUC of tested ingredients (Liu et al., 2008, Lu et al, 2007). After *in vitro* incubation with total rhubarb anthraquinoses in *Rheum officinale* Baill and its components including rhein, aloe-amodin, chrysophanol and physcion, the cellular absorption of emodin was significantly reduced in Caco-2 cell monolayer model (Liu et al., 2008). In summary, the pharmacokinetic interactions have been proved *in vitro* and *in vivo*. However, report on the pharmacokinetics interactions among the major bioactive flavones in RS is limited.

Table 1.4   Summary of pharmacokinetics interactions between multiple ingredients in herbal medicines

Herb	Administration	Marker component	Findings	References
Hawthorn fruits	i.v. and p.o. ■ Hawthorn fruit extract (HPE) ■ Four single compounds	(−)-epicatechin, chlorogenic acid, hyperoside, and isoquercitrin	■ After i.v., plasma concentration of four components were higher in HPE; ■ After p.o., only (−)-epicatechin was absorbed in parent form; its plasma concentration was similar in HPE and single compound group	Chang, 2005
Kava	p.o. (single dose) ■ Kawain ■ Kava extract p.o. (repeated dose) ■ Kava extract for 7 days ■ Single Kawain on the 8th day	Kawain	■ Co-administration with kava extract caused a tripling of kawain AUC_{0-8} h and a doubling of C_{max}. ■ 7-day pretreatment with kava extract (256 mg /kg/day) had no effect on the pharmacokinetics of kawain administered on day 8	Mathews, 2005
Cortex Moutan (CM)	p.o. ■ Paeoniflorin ■ CM extract ■ Suang-Dan (SD) decoction	Paeoniflorin	■ A bimodel phenomenon was observed after p.o. SD decoction; ■ Statistically significant increase in pharmacokinetic parameters of paeoniflorin including AUC_{0-t}, $AUC_{0-\infty}$ and MRT after p.o. CM extract and SD decoction comparing with pure paeoniflorin; ■ The ingredients resulting in the increase has not been identified	Wu, 2009
Radix Scutellariae	p.o. ■ Baicalin ■ RS extract ■ Huang-Lian-Jie-Du-Tang (HLJDT) ■ Baicalin+three other herb extract in HLJDT	Baicalin and wogonoside	■ Baicalin and wogonoside demonstrated bimodel phenomenon in the plasma profile; ■ C_{max} and AUC of baicalin were significantly reduced in HLJDT and co-administration with three other herbs; ■ Some ingredients in the other three herbs of HLJDT, not in *Radix scutellariae* itself, resulted in the reduction	Lu, 2007

Table 1.4   Pharmacokinetics interactions between multiple ingredients in herbal medicines (continued)

Herb	Administration	Marker component	Findings	References
Salvia miltiorrhiza BUNGE	i.v. • Tanshinone IIA • Cryptotanshinone • *Salvia miltiorrhiza* BUNGE extract	Tanshinone IIA and cryptotanshinone	▪ C_{max} and AUC of cryptotanshinone and tanshinone IIA increased after administration of the tanshinones extract in comparison with the equivalent dose of single component administration; ▪ Co-existing tanshinones in *Salvia miltiorrhiza* BUNGE extract resulted in the pharmacokinetics interactions	Song, 2007
Salvia miltiorrhiza BUNGE	i.v. • TSIIA extract loaded emulsion • Sal extract loaded emulsion • Mixture of TSIIA and Sal B loaded emulsion	Tanshinone IIA (TSIIA) and salvianolic acid B (Sal B)	▪ AUC and C_{max} of TSIIA and Sal B were increased after i.v. of mixed extracts-loaded emulsion in comparison with the equivalent dose of the corresponding single extract administration; ▪ $t_{1/2}$ showed no significant different between mixed extract group and single extract group	Guo, 2008
Fructus Schisandrae	p.o. • Schizandrin • Fructus Schisandrae aqueous extrac • Sheng-Mai-San	Schizandrin	▪ AUC_{0-t} and $T_{1/2}$ of schizandrin in *Fructus Schisandrae* aqueous extract and in SMS decoction were increased significantly than that when single Schizandrin was administrated; ▪ The ingredients in Sheng-Mai-San may delay its elimination and enhance its bioavailability in rat	Xu, 2008

1.5.2 Pharmacodynamic interactions

As for the pharmacodynamics interactions among the multiple components of herbal medicines, it could also result in synergic effects or antagonistic effect. As one of the major components in *Salvia miltiorrhiza* Bunge, salvianolic acid B exhibited higher efficacy (17 times) than the *Salvia miltiorrhiza* Bunge extract on the free radical-scavenging activity in DPPH assay and on preventing Cu^{2+}-induced LDL oxidation (Wu et al., 1998). Furthermore, Ren et al. used modified Ellman method to determine the inhibition effect of the major components in the acetone extract of *Salvia miltiorrhiza* to acetylcholinesterase. This spectrophotometric method based on the reaction of released thiocholine to give a coloured product, in which the IC_{50} of physostigmine was employed as a marker of acetylcholinesterase inhibitor. Also as two major components in *Salvia miltiorrhiza* Bunge, dihydrotanshinone and cryptotanshinone exhibited a reduced inhibitory effect on acetylcholinesterase in the form of compound mixture in comparison to their pure compounds (Ren et al., 2004). There has been no study about the pharmacodynamics interactions among the major bioactive flavones in RS.

1.6 Herb-drug and herb-herb interactions related to RS

Due to its broad application and relatively high intake in our daily diets, it is of great chance that RS might be consumed with other synthetic drugs. As a result, the herb-drug interactions between RS and other synthetic drugs should be paid attention to. In fact, co-administration of RS decoction with cyclosporine has been reported to significantly decrease the C_{max} and AUC $_{0 \to 540min}$ of cyclosporine by over 50% in rats via oral route. However, the pharmacokinetics parameters of cyclosporine were not altered after

intravenous administration. It was suggested that oral administration of RS decoction or its related preparations with cyclosporine should be avoided (Lai et al., 2004). It has been summarized that the mechanism of the flavonoids-drug interactions might be conducted from three aspects:1) Phase I metabolism; 2) Phase II metabolism and 3) Phase III metabolism, which is the efflux by membrane transporters (Lamber et al., 2007). Although there is no mechanistic study about the interaction between RS or its major bioactive flavones with other synthetic drugs, we believe that the second and third aspect might be involved based on our previous study on B and BG. Besides, it was reported that B showed inhibitory effect on MRP1 and MRP2 (van Zanden et al., 2005). B could increase the cell uptake of mitoxantrone on human breast cancer MCF-7 selected with mitoxantrone (Zhang et al., 2005). Therefore, if the synthetic drug is the substrate of MRP1, MRP2 or BCRP and consumed with drug preparations containing RS, there is great chance of drug-herb interactions.

For the reason that herbal medicines are usually consumed in the form of herbal extract, the effects of other co-administrated herbs on the pharmacokinetics of BG were also studied. In previous studies, the pharmacokinetic parameters of BG in rats after oral administration of pure BG, RS extract as well as herbal formulas containing RS such as Shuang-Huang-Lian, Huang-Lian-Jie-Du-Tang, Huangqin Tang and Xiexin decoction were obtained and compared. It was observed that some ingredients in the extract or formulas might interact with these bioactive flavones. *Rhizoma coptidis* and *Cortex phellodendri* in Huang-Lian-Jie-Du-Tang could inhibit the activity of β-glycosidase and thus decreased the systemic exposure of BG and WG (Lu et al., 2007). Co-existing

ingredients in Huangqin Tang could delay the absorption and prolong the circulation time as well as increase the absorption of BG and WG in rat, but the possible ingredients and mechanism are not clear (Zuo et al., 2003). Furthermore, Co-existing ingredients in Xiexin decoction could also delay the peak of BG in urine (Li et al., 2005). The RS extract could increase the absorption of B comparing with pure B (Kim et al., 2007). In summary, although the herb-herb interactions are mostly observation, there is lack of corresponding explanations. Due to the abundant existence and frequent utilization, the exploration of the herb-herb or interactions among the bioactive flavones in RS is essential.

1.7 Rationale of current study

Due to their effectiveness and relatively low toxicity, herbal medicines have drawn more and more attention during the past decades. With the growing use of herbal products, its quality becomes especially important to guarantee the safety and efficacy of the utilization of herbal medicines. Unlike the synthetic drugs, herbal medicines have complex compositions. The effectiveness of herbal medicines may be attributed to the overall effect of all the components rather than a single component.

Although BG is identified as the marker compound for quality control of RS and its content is requested to be not less than 9% (*w/w*) in dried RS in Pharmacopeia of PRC 2005 (The Pharmacopoeia Commission of PRC, 2005), there are other bioactive ingredients such as WG, OAG, W and OA existing in RS. Thus, the quality control of herbal medicine should contain the information of bioactive components as much as

possible. Nevertheless, most studies about the content of bioactive components in RS concentrated on B or BG and the information about the content of bioactive components in PTCM products of RS are limited.

The major obstacle for the further pharmacokinetic characterization of herbal medicines is their complicated multiple co-existing components. In the case when these components share the same absorption and metabolism pathway, there is great chance that they might compete with each other. Besides, the onset of pharmacodynamic effects and toxicity is closely related to the drug concentration *in vivo*. The interaction in pharmacokinetics might lead to the interaction in pharmacodynamics. There have been several reports about the pharmacokinetic and pharmacodynamic interactions between the co-existing components in a herb. As a result, the pharmacokinetic study about a single component in an herbal medicine is far from enough. The interaction in pharmacokinetics and pharmacodynamics of the multiple components in a herbal medicine is also of importance.

Despite their broad therapeutic values, low bioavailability of flavonoids has always been a serious problem which has limited their clinical application. Three reasons were proposed to contribute to the low oral bioavailability including 1) extensive Phase II intestinal first-pass metabolism; 2) involvement of efflux transporters; 3) interplay between metabolic enzymes and membrane transporters during their absorption. Our previous studies on B found that B underwent extensive intestinal and hepatic first-pass metabolism of glucuronidation which resulted in the low concentration of parent drug entering into the blood stream. UGT isoenzymes were responsible for the glucuronidation.

Besides, membrane transporters such as MRPs mediated the apical and basolateral efflux of formed metabolites (Zhang et al., 2005, Zhang et al., 2007a, Zhang et al., 2007b). Kim et al. found that the plasma concentration of W and OA were very low after oral administration of a standardized extract of RS in rat, indicating that W and OA might share the same problem of low bioavailability (Kim et al., 2007). Due to the similarity in chemical structure, it is proposed that W and OA might share the similar absorptive and dispositive pathways as B. Nevertheless, there is no literature systematically investigating the biopharmaceutic and pharmacokinetic characteristics of W and OA.

1.8   Objectives of the current study

The overall objective of the current study is to investigate the biopharmaceutic and pharmacokinetic interactions among the major bioactive flavones in RS. In order to achieve this, three specific objective need to be fulfilled:

(1) To verify the contents of the major bioactive components in the Proprietary Traditional Chinese Medicine products and the reference herb of RS;

(2) To investigate the absorptive and disposition characteristics of pure compounds of W and OA;

(3) To investigate the biopharmaceutic and pharmacokinetic interactions among B, W and OA.

In order to achieve objective (1), a simple and reliable HPLC/UV method has been established and validated to simultaneously quantify the content of six bioactive flavones in the reference herb and PTCM products containing RS.

In order to achiever objective (2), the following aspects have been conducted.

- An HPLC/UV method has been established and validated to quantify six bioactive flavones in plasma samples;

- The intestinal absorption and disposition of W and OA have been conducted in Caco-2 cell monolayer model and rat *in situ* single-pass intestinal perfusion model;

- The intestinal and hepatic metabolism of W and OA has been investigated by in vitro enzymatic kinetics study.

In order to achieve objective (3), the interactions among B, W and OA have been studied on *in vitro*, *in situ* and *in vivo* levels.

1.9 Study scheme

To better elucidate the flow of the investigations, the scheme of current study is summarized in Fig. 1.3.
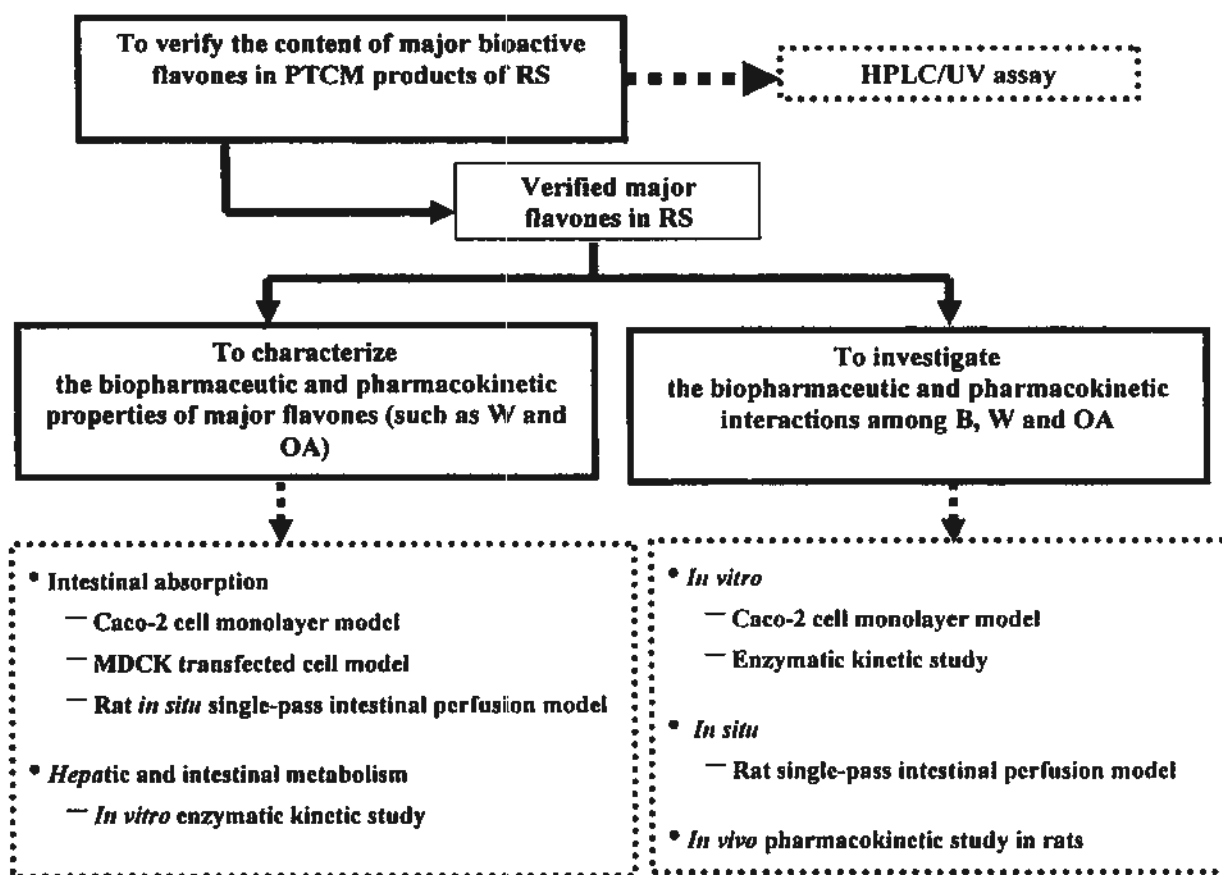
Figure 1.3   Proposed study scheme of the current project

Solid box demonstrate the objectives of this study;

Dotted box demonstrates the methods used in the study

Chapter Two

Content of major bioactive flavones in proprietary Traditional Chinese Medicine products and reference herb of *Radix Scutellariae*

2.1 Introduction

Scutellaria baicalensis Georgi is a medicinal plant widely distributed in Asia. Its dried root, *Radix Scutellariae* (RS, Huangqin in Chinese), is officially listed in the Chinese Pharmacopeia and recognized as bioactive ingredients in a number of proprietary traditional Chinese medicines. Flavonoids are the most abundant ingredients and six flavones, namely baicalein (B), baicalin (baicalein-7-glucuronide, BG), wogonin (W), wogonoside (wogonin-7-glucuronide, WG), oroxylin A (OA) and oroxylin A-7-glucuronide (OAG) were reported to be the major bioactive components in RS (Li et al., 1995). The chemical structures of the six major flavones are shown in Fig. 2.1.

Due to their effectiveness and relatively low toxicity, herbal medicines have drawn more and more attention during the past decades. With the growing use of herbal products, its quality becomes especially important to guarantee the safety and efficacy of the utilization of herbal medicines. BG is identified as the marker compound for quality control of RS and its content is requested to be not less than 9% (*w/w*) in dried RS in Pharmacopeia of PRC 2005 (The Pharmacopoeia Commission of PRC, 2005). There are a number of studies concerning the content determination of the bioactive components in RS using various assay methods, in which chromatography methods are frequently employed. These detection methods include

high-performance liquid chromatography (Zhang et al., 1998, Lin et al., 1999, Bochořáková et al., 2003, Wu et al., 2005, Horvath et al., 2005), capillary electrophoresis (Yu et al., 2007), microemulsion electrokinetic chromatography (Zhang et al., 2006) and micellar electrokinetic capillary electrophoresis (Li et al., 1995). Most studies just chose baicalin and/or baicalein as the marker compounds for quality control. However, there is evidence that the other components, including WG, OAG, W and OA, also exist in relatively high amount. It has been reported that a herb couple (*Coptidis Rhizoma: Radix Scutellariae*, 1:1) was extracted by 70% methanol and the contents of BG, WG, OAG, B, W and OA were determined to be 84.82±3.02, 78.69±0.69, 40.57±0.65, 18.28±0.06, 9.32±0.19, 4.01±0.07 mg/g (*w/w*) by micellar electrokinetic capillary electrophoresis (Li et al., 1995). In another study, RS was extracted by high-speed counter-current chromatography and the content of B, W and OA were 3.58%, 1.23% and 0.31% (*w/w*) using HPLC/UV analysis (Li et al., 2005). Unlike the synthetic drugs, herbal medicines have more complicated compositions. The effectiveness of herbal medicines may be attributed to the overall effect of all the components rather than a single component. Besides, the interactions among different components in different herbs are always a concern. Thus, the quality evaluation of herbal medicine should contain the information of as much bioactive components as possible.

The present study aims to develop a simple HPLC/UV method for the simultaneous determination of six bioactive flavones (baicalein, baicalin, wogonin, wogonoside, oroxylin A and oroxylin A-7-*O*-glucuronide) in the reference herb and commercial PTCM of RS, which could provide a more suitable method and significantly improve the quality evaluation of the raw material and commercial PTCM of RS.

Baicalein (B)

Wogonin (W)

Oroxylin A (OA)

3, 7-dihydroxyflavone (IS)

Baicalin (BG)

Wogonoside (WG)

Oroxylin A-7-O-glucuronide (OAG)
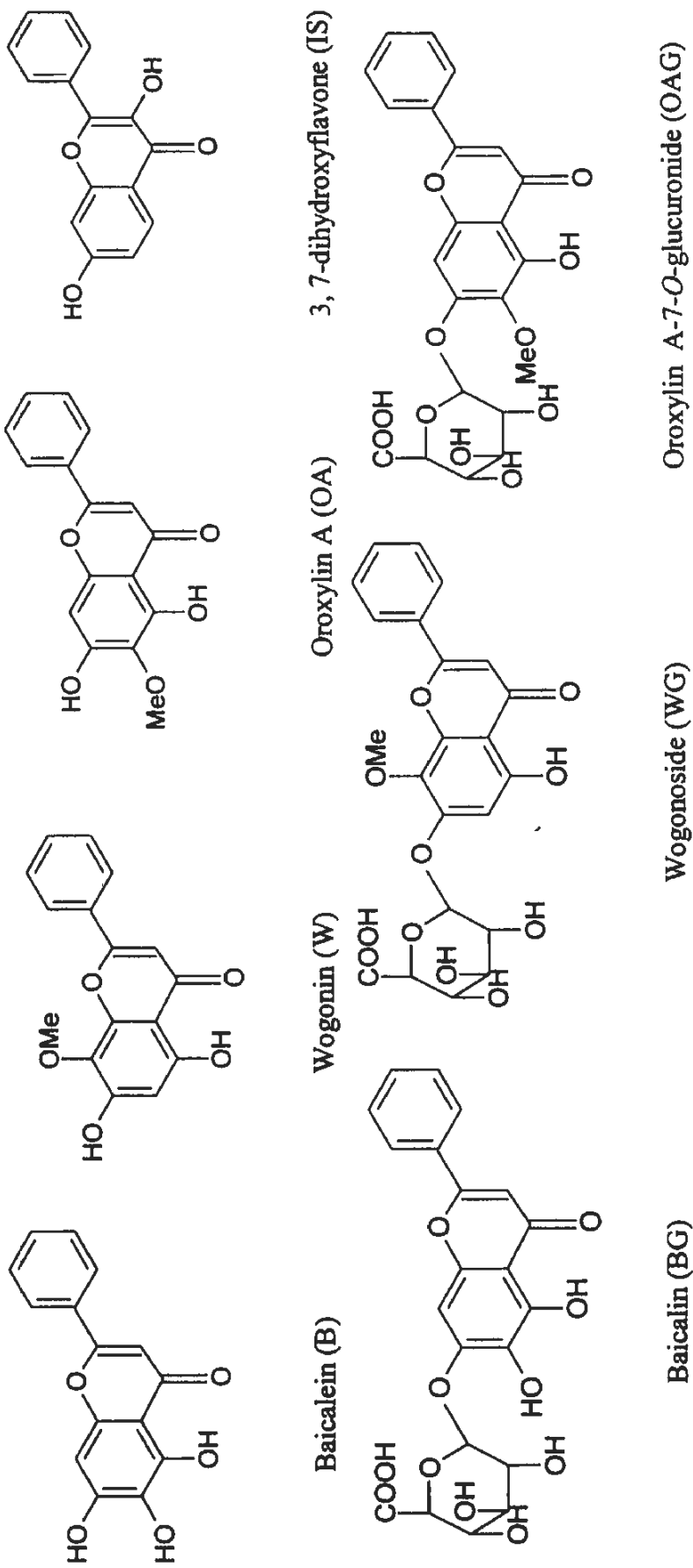
Fig. 2.1   Chemical structures of studied bioactive flavones in RS and

3,7-dihydroxyflavone (internal standard)

2.2 Experimental

2.2.1 Chemicals and reagents

Baicalein (B) and baicalin (BG) with purity over 98% were purchased from Sigma-Aldrich Chem. Co. (Milwaukee, WI, USA). Wogonin (W) and wogonoside (WG) with purity over 98% were purchased from AvaChem Scientific LLC (San Antonio, TX, USA). Oroxylin A (OA, purity over 98%) and Oroxylin A-7-O-glucuronide (OAG, purity over 95%) were supplied by Shanghai u-sea biotech co., Ltd (Shanghai China). 3, 7-dihydroxyflavone with purity of 97% was purchased from Indofine Chemical Company (Hillsborough, NJ, USA). Reference herb of *Radix Scutellariae* was purchased from the National Institute for Control of Pharmaceutical and Biological Products (Beijing, China). HQ-Tab, C-HQ-Tab, YH-Cap, YH-DP, SHL-Cap, SHL-S-Cap were purchased from pharmacy stores in mainland China. Acetonitrile (Labscan Asia, Thailand) and methanol (TEDIA company, Inc., USA) were HPLC grade and used without further purification. All other reagents were of at least analytical grade. Distilled and deionized water was prepared from Millipore water purification system (Millipore, Milford, USA).

2.2.2 Instrumentations

The HPLC system consists of Waters 600 controller (pump), Waters 717 auto sampler and Waters 996 Photodiode Array UV detector. The separation of all the analytes was performed by using a Thermo BDS Hypersil column (250 × 4.6 mm; 5 μm particle size) connected to a guard column (Delta-Pak C18 Guard-Pak, Waters). Data were collected by Waters Millennium software (version 3).

2.2.3 Chromatographic conditions

The mobile phase consisting of eluent A (20 mM sodium dihydrogen phosphate buffer, pH 4.6) and B (acetonitrile) was run at 1 ml/min. The linear gradient elution program was set as follows: eluent A decrease from 90 to 70% in the first 10 min, decrease from 70 to 40% in the next 2 min, maintained at 40 % for 4 min, then eluent A increased from 40 to 90% from 16 to 20 min and equilibrated for 5 min before the next injection. The injection volume was 100 µl and the detection wavelength was set at 270 nm.

2.2.4 Preparation of standard solutions and calibration curves

The stock solution of B, BG, W, WG, OA and OAG (1 mg/ml) as well as the internal standard (2 mg/ml) were prepared by dissolving appropriate amount of each authentic compound in DMSO separately. The working solutions were prepared by mixing and diluting the stock solutions of each compound with methanol and phosphate buffer (20 mM, pH 2.5) comprising 1% ascorbic acid (50: 50, v/v) to yield concentrations of 0.02, 0.05, 0.1, 0.2, 0.5, 1.0, 2.0, 5.0, 10.0 µg/ml, respectively and the internal standard was diluted to the final concentration of 100 µg/ml.

Working solutions for calibration curves were prepared by mixing 0.7 ml of various working standard solutions with 20 µl of internal standard solution. The calibration curves were plotted by the peak-area ratio of each analyte /internal standard versus the concentrations of each analyte. To avoid the bias to low concentrations caused by the high concentrations of the standard curve, the calibration curves of each analyte was separated into two ranges: 0.02-0.5 and 0.5-10.0 µg/ml.

2.2.5 Sample preparation

To prepare samples from solid dosage forms, 10 tablets (0.3 g/tablet), or dripping pills from 3 packaged bags (2.5 g/package), or 10 hard gelatin capsules (0.3 g /capsule) were put into a mortar and grinded to powder. To prepare samples from soft capsule, its content was obtained followed by mixing well into uniform semisolid. About 10 mg of the prepared powder or semisolid samples was accurately weighed and then extracted by 10 ml methanol: water mixture (80:20 v/v, containing 1 mM HCl). After sonication in water bath for 30 min, the mixture was centrifuged at 10,000 g for 5 min. The supernatant was obtained followed by filtration with 0.45 μm syringe filter and dilution prior to injection into HPLC system for analysis.

2.2.6 Method validation

The linearity, intra-day and inter-day precision and accuracy were investigated for method validation. The intra-day precision was determined within one day by analyzing five replicates control samples at concentrations of 0.05, 0.2, 1.0, 5.0 μg/ml. The inter-day precision was determined on five separate days for the control samples. The intra-day and inter-day precision were defined as the relative standard deviation (R.S.D.) and the accuracy was determined by calculating the relative error (R.E.). The limit of detection (LOD) was defined as the lowest concentration of the drug resulting in a signal-to-noise ratio of 3:1. The limit of quantification (LOQ) was defined as the lowest concentration of the drug resulting in a signal-to-noise ratio of 10:1 with precision below 20% and accuracy below ±20% (FDA, 2001).

2.2.7 Extraction recovery

Samples of the *Radix Scutellariae* reference herb and PTCM products (HQ-Tab, C-HQ-Tab, YH-Cap, YH-DP, SHL-Cap, SHL-S-Cap) were obtained and divided into two equal parts. One part was spiked with three different concentrations of standard solutions (low, medium and high) followed by thorough mixing and extraction as described in section 2.2.5, whereas the other part of the sample was directly extracted as described in section 2.2.5. The extraction recoveries of each compound were calculated as the percentage of the net amount of each compound obtained (determined amount in spiked samples – determined amount in un-spiked sample) after extraction versus actual amount added.

2.2.8 Application

The developed assay was applied to simultaneously determine the contents of baicalein, baicalin, wogonin, wogonoside, oroxylin A and oroxylin A-7-*O*-glucuronide in the reference herb and the commercial PTCM of RS in forms of tablet, capsule, dripping pill and soft capsule. All the samples were treated as described in section 2.2.5 followed by HPLC analysis. Since the contents of each analyte may vary in different products, the extracted solutions were appropriately diluted in order to fit the concentration range of the calibration curve.

2.3 Results and discussions

2.3.1 Chromatography

A simple HPLC/UV method has been developed and validated for simultaneous determination of the content of six representative flavones in the RS. Due to the difference in

the polarity between the glycosides and aglycones, it was difficult to separate them using isocratic elution. Thus, a linear gradient elution program has been employed.

Fig.2.2 exhibits the UV spectra of the six bioactive flavones. Fig.2.3 shows the representative HPLC chromatograms of the standard solution of six analytes at 1 μg/ml, reference herb of RS and the six PTCM products containing RS. Under the current chromatographic condition, the six components were satisfactorily separated. It was demonstrated that the co-existing ingredients in RS did not interfere in the determination of the six analytes and the internal standard. The peak of each analyte was identified by the comparison of the retention time and UV spectra with the authentic standards and confirmed by LC/MS/MS.
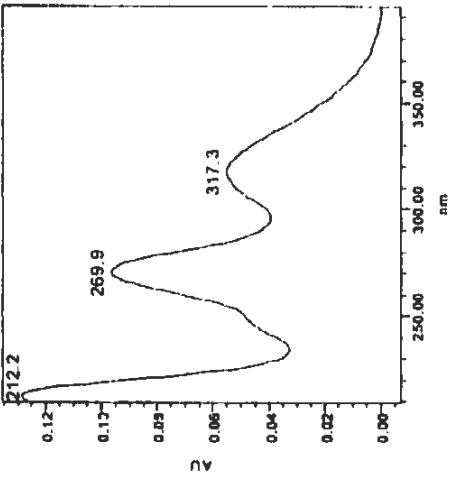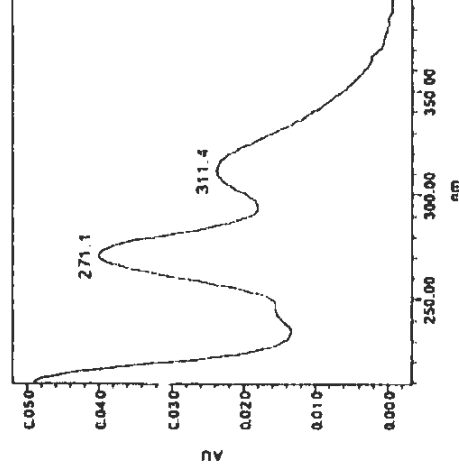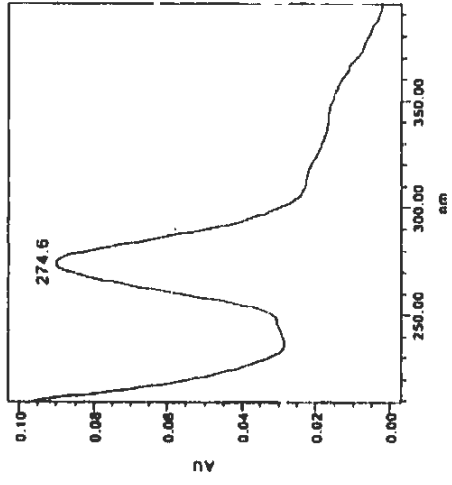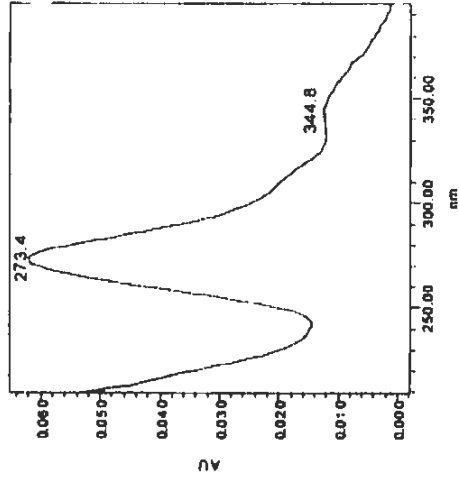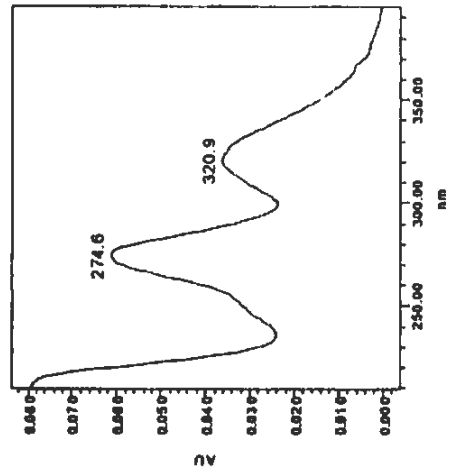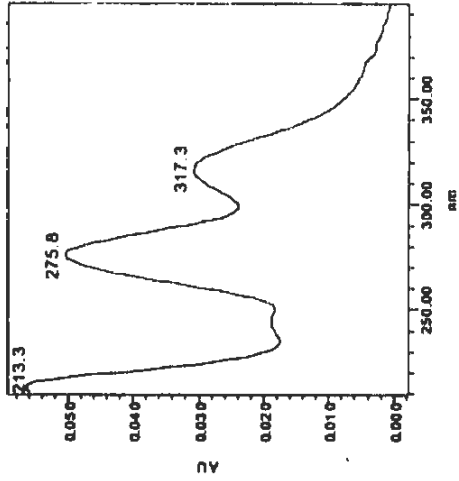
Fig. 2.2   UV spectra of major bioactive flavones in RS
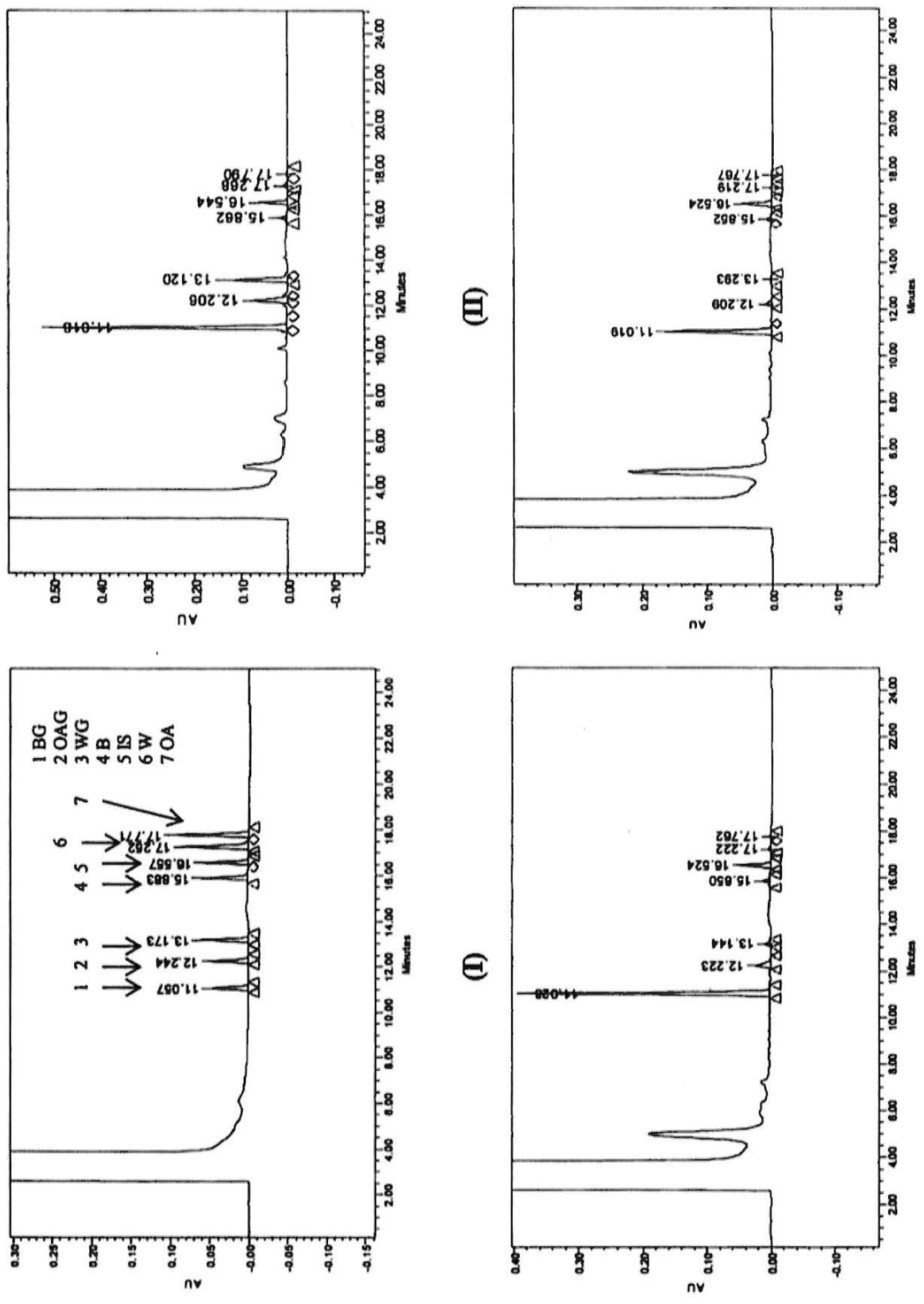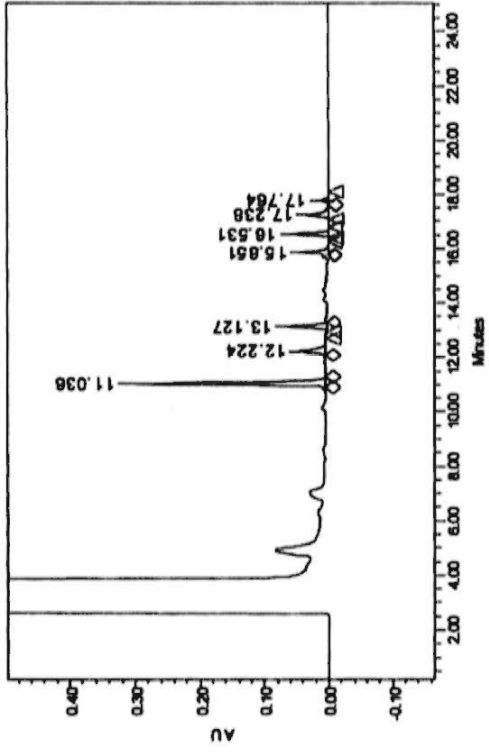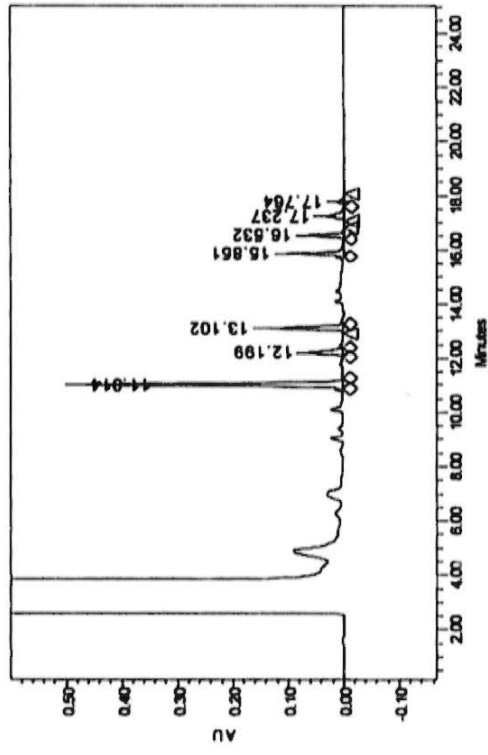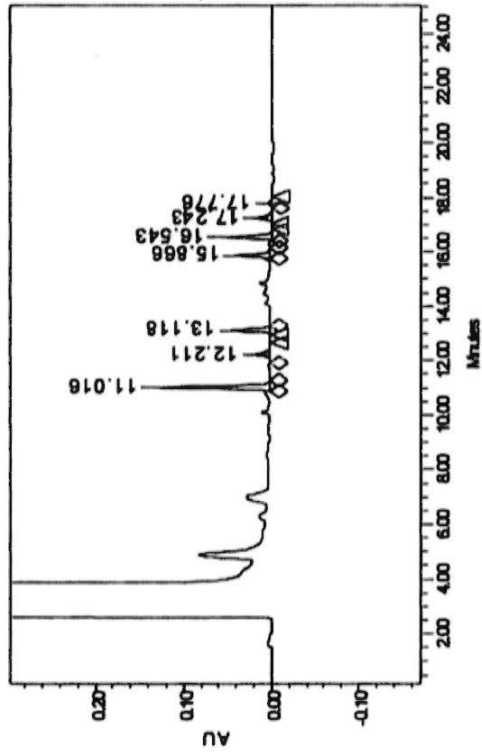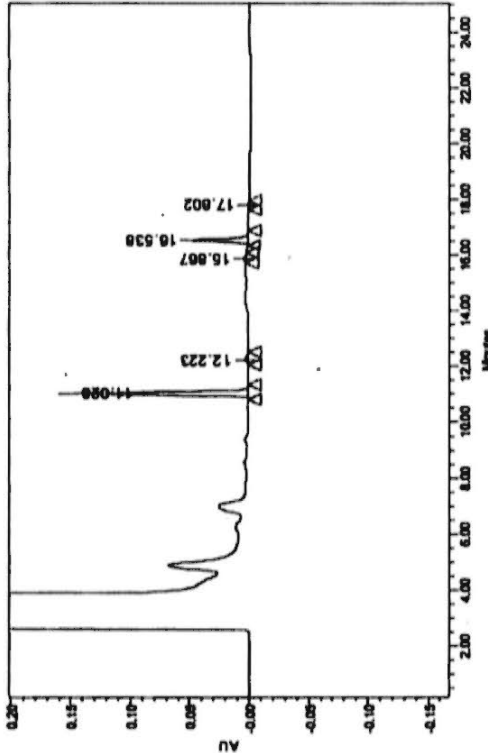
Fig. 2.3   Representative HPLC chromatograms of standard solution at 1 μg/ml (I) and extract of reference herb of RS (II); SHL-Cap (III); SHL-S-Cap (IV); C-HQ-Tab (V); HQ-Tab (VI); YH-DP (VII); YH-Cap (VIII)

Fig. 2.3 Representative HPLC chromatograms of standard solution at 1 µg/ml (I) and extract of reference herb of RS (II); SHL-Cap (III); SHL-S-Cap (IV); C-HQ-Tab (V); HQ-Tab (VI); YH-DP (VII); YH-Cap (VIII) (continued)

2.3.2 Method validation

The results of linear range and regression equations for the calibration curves are shown in Table 2.1. The calibration curves were plotted by the peak-area ratio of each analyte to the internal standard versus the concentration of each analyte. To avoid the bias to the low concentrations of the standard curve by the high concentrations, the calibration curves were separated into two ranges, 0.02-0.5 and 0.5-10.0 µg/ml. Within the linear range, the calibration curve had good linearity (R^2>0.99) for each analyte. For all the six bioactive flavones, LOD was 0.01µg/ml and the LOQ was 0.02 µg/ml. The intra-day and inter-day precision and accuracy of the assay method are also shown in Table 2.1. The R.S.D. of both the intra-day and inter-day precision for all the six compounds were below 10.14 %. The accuracy at four different concentrations was within the range of -7.83 to 4.06 %.

2.3.3 Extraction efficiency

The 2005 edition of Chinese pharmacopeia provides a method for the quality control of RS by determining the content of baicalin and 9% is the lowest content requirement in which 70% ethanol was employed as extraction solvent (The Pharmacopoeia Commission of PRC, 2005). For the current study, considering the higher solubility of the flavones in methanol and the convenience of operation, methanol was used as extraction solvent and sonication was employed to do the extraction.

Four different extraction solvents including methanol, methanol: water (80:20), methanol: water (50:50), methanol: water (20:80) were tried to extract the bioactive flavones from the reference herb and C-HQ-Tab, the representative PTCM product of *Radix Scutellariae*. The

extraction solvent of methanol: water (80:20) produced the highest extraction efficiency for the reference herb of RS. It was found that the extraction solvent system have less impact on the extraction efficiency of the PTCM product than that in the reference herb, which may be due to that the commercial products are produced by diluting the prepared RS extract with other excepients and are generally in low content of each component. Subsequently, the solvent of methanol: water (80:20) containing 1 mM HCl was employed throughout the experiment in order to optimize the unionized portion of the studied weak acidic components for their extraction by methanol. Then the efficiency of extraction method was tested in different dosage forms of the commercial products, i.e. HQ-Tab, C-HQ-Tab, YH-Cap, YH-DP, SHL-Cap, SHL-S-Cap and the reference herb of RS. The result of extraction recovery is listed in Tables 2.2a and 2.2b. The mean extraction recovery for the six bioactive flavones in five commercial products was within the range of 89.22-107.33 %.

Table 2.1   Regression equation, intra-day and inter-day precision and accuracy of six bioactive flavones

Flavones	Linear range (µg/ml)	Regression equation	R^2	Nominal conc. (µg/ml)	Intra-day (n=5) Determined conc. (µg/ml)	Precision (%R.S.D.)	Accuracy (%R.E.)	Inter-day (n=5) Determined conc. (µg/ml)	Precision (%R.S.D.)	Accuracy (%R.E.)
BG	0.02-0.50	y=0.8354X-0.0019	0.9998	0.05	0.05±0.00	2.62	-1.84	0.05±0.00	1.28	-2.51
				0.2	0.20±0.00	1.33	-2.32	0.20±0.00	2.01	-0.17
	0.50-10.0	y=0.7982X-0.0025	1	1.0	1.00±0.01	0.59	0.11	0.99±0.04	3.63	-0.98
				5.0	5.11±0.07	1.43	2.11	5.11±0.17	3.36	2.12
WG	0.02-0.50	y=1.0562X-0.0036	0.9998	0.05	0.05±0.00	3.73	-2.12	0.05±0.00	1.41	-1.40
				0.2	0.20±0.00	0.44	-1.62	0.20±0.00	1.93	0.53
	0.50-10.0	y=1.0290X-0.0180	0.9999	1.0	0.98±0.01	0.62	-2.36	0.97±0.04	3.80	-3.52
				5.0	5.11±0.08	1.53	2.13	5.11±0.17	3.31	4.06
OAG	0.02-0.50	y=0.7811X-0.0009	0.9998	0.05	0.05±0.00	3.86	-0.64	0.05±0.00	0.47	-0.42
				0.2	0.20±0.00	0.79	-2.30	0.20±0.01	3.60	1.09
	0.50-10.0	y=0.7579X-0.0059	0.9999	1.0	0.98±0.01	1.41	-1.79	0.98±0.04	4.27	-1.66
				5.0	5.19±0.13	2.51	3.85	5.20±0.18	3.45	4.06
B	0.02-0.50	y=1.1092X+0.002	0.9975	0.05	0.05±0.00	4.17	-6.14	0.05±0.00	4.71	-2.74
				0.2	0.19±0.00	0.49	-3.30	0.20±0.00	2.09	-0.58
	0.50-10.0	y=1.1866X-0.0308	0.9999	1.0	0.97±0.01	0.85	-3.41	0.95±0.04	4.42	-5.52
				5.0	5.17±0.06	1.13	3.41	5.20±0.17	3.24	3.97
W	0.02-0.50	y=1.3771X-0.002	0.9994	0.05	0.05±0.00	2.71	-1.73	0.05±0.00	5.89	-2.49
				0.2	0.19±0.00	0.74	-3.26	0.20±0.01	4.76	0.54
	0.50-10.0	y=1.3615X-0.0895	0.9982	1.0	1.03±0.01	1.10	3.25	0.92±0.09	9.79	-7.83
				5.0	5.17±0.06	1.13	3.43	5.19±0.20	3.86	3.81
OA	0.02-0.50	y=1.7977X+0.0125	0.9998	0.05	0.05±0.00	4.98	-3.04	0.05±0.01	10.14	3.24
				0.2	0.20±0.00	1.78	-1.35	0.20±0.00	1.86	1.19
	0.50-10.0	y=1.7787X+0.0256	0.9999	1.0	0.97±0.01	1.06	-3.19	0.95±0.06	3.74	-5.54
				5.0	5.08±0.06	1.14	1.50	5.11±0.16	3.20	2.11

Table 2.2a Extraction recoveries of BG, WG, OAG in various products of RS (n=3)

Products	BG Conc. (μg/ml) Spiked	Detected	Recovery (%)	WG Conc. (μg/ml) Spiked	Detected	Recovery (%)	OAG Conc. (μg/ml) Spiked	Detected	Recovery (%)
RH	2.0	1.79±0.03	89.43±1.72	2.0	1.88±0.03	94.07±1.56	2.0	1.87±0.06	93.28±2.78
	5.0	4.36±0.07	102.25±1.49	5.0	4.88±0.07	97.61±0.36	5.0	4.75±0.15	94.98±2.96
	10.0	9.54±0.20	95.42±1.95	10.0	9.51±0.10	95.12±0.98	10.0	9.42±0.13	94.16±1.33
HQ-Tab	2.0	1.94±0.06	96.78±2.83	1.0	1.00±0.01	100.41±0.71	1.0	1.01±0.01	101.15±1.15
	5.0	4.96±0.16	99.17±3.21	2.0	2.06±0.03	102.87±1.46	2.0	2.06±0.02	103.07±1.22
	10.0	9.54±0.01	95.42±0.11	5.0	5.33±0.01	106.57±0.13	5.0	5.26±0.02	105.26±0.34
YH-DP	2.0	1.97±0.07	98.60±3.61	0.20	0.21±0.00	104.42±0.30	0.20	0.21±0.00	107.33±1.67
	5.0	4.66±0.02	93.19±0.33	0.50	0.52±0.01	104.23±2.75	0.50	0.49±0.03	97.26±5.55
	10.0	9.80±0.07	97.99±0.69	1.00	1.04±0.00	103.90±0.09	1.00	1.02±0.02	102.30±1.68
YH-Cap	2.0	2.05±0.02	102.68±1.03	1.0	0.99±0.01	98.73±0.61	1.0	1.03±0.04	103.04±4.07
	5.0	4.87±0.02	97.39±0.44	2.0	1.96±0.08	98.12±4.14	2.0	2.11±0.05	105.36±2.34
	10.0	9.94±0.02	99.39±0.23	5.0	4.59±0.04	91.80±0.75	5.0	5.03±0.01	100.57±0.15
SHL-S-Cap	2.0	1.92±0.07	95.80±3.58	0.1	0.09±0.00	90.15±3.35	0.2	0.20±0.00	101.12±2.19
	5.0	4.60±0.04	92.07±0.79	0.2	0.19±0.00	96.24±1.04	0.5	0.50±0.01	100.75±1.16
	10.0	9.41±0.05	94.09±0.55	1.0	0.92±0.00	91.83±0.33	1.0	0.94±0.01	94.46±1.20

Table 2.2b   Extraction recoveries of B, W, OA in various products of RS (n=3)

Product	B Conc. (µg/ml)			W Conc. (µg/ml)			OA Conc. (µg/ml)		
	Spiked	Detected	Recovery (%)	Spiked	Detected	Recovery (%)	Spiked	Detected	Recovery (%)
RH	0.5	0.53±0.01	105.69±1.11	0.5	0.48±0.02	95.94±4.00	0.50	0.47±0.02	93.59±3.09
	1.0	1.01±0.02	101.18±2.49	1.0	0.93±0.04	93.05±4.18	1.00	0.97±0.04	97.26±3.59
	2.0	2.01±0.08	100.32±4.22	2.0	2.15±0.01	107.30±0.56	2.00	2.02±0.02	101.24±1.23
HQ-Tab	1.0	0.97±0.01	97.40±0.68	1.0	0.97±0.03	97.10±2.89	0.50	0.52±0.01	104.15±2.82
	2.0	2.06±0.03	102.96±1.68	2.0	1.99±0.03	99.27±1.45	1.00	0.97±0.01	97.09±0.90
	5.0	4.71±0.20	94.14±4.07	5.0	5.00±0.17	100.08±3.44	2.00	2.06±0.06	102.99±3.22
YH-DP	0.20	0.20±0.00	102.22±1.33	0.20	0.18±0.01	91.79±3.29	0.10	0.10±0.00	104.77±1.03
	0.50	0.50±0.02	101.00±3.89	0.50	0.49±0.02	97.12±3.04	0.20	0.20±0.01	101.60±5.12
	1.00	0.96±0.02	96.26±1.71	1.00	1.03±0.02	102.75±1.53	0.50	0.49±0.03	98.46±5.15
YH-Cap	1.0	0.98±0.01	97.89±0.82	0.2	0.19±0.01	95.96±4.89	0.20	0.21±0.01	105.09±4.79
	2.0	1.88±0.08	93.87±4.19	0.5	0.46±0.01	92.88±0.93	0.50	0.52±0.02	103.34±4.24
	5.0	4.70±0.13	93.97±2.64	1.0	1.04±0.04	103.69±3.51	1.00	1.02±0.04	102.16±3.71
SHL-S-Cap	0.2	0.19±0.01	96.69±5.10	0.1	0.09±0.00	89.22±2.07	0.1	0.09±0.01	93.09±4.80
	0.5	0.48±0.01	95.11±2.07	0.2	0.19±0.01	93.39±2.45	0.2	0.18±0.00	90.84±0.64
	1.0	1.04±0.01	104.35±1.37	1.0	0.97±0.01	97.00±0.70	1.0	0.89±0.01	89.89±0.80

2.3.4 Application

Due to the co-existing multiple bioactive components in the traditional Chinese medicinal products, it is far from enough to just monitor one component for the quality control of its raw material and proprietary traditional Chinese medicine products. Therefore, current study developed a simple and accurate assay method for simultaneous determination of six major bioactive flavones in RS. Due to the easy access of HPLC in TCM industry, the developed provided a relatively simple and easy to conduct quality control method for RS. In addition, the constituents of mobile phase as well as sample preparation were easy to obtain and handle.

The validated HPLC/UV method was applied to the simultaneous determination of baicalein, baicalin, wogonin, wogonoside, oroxylin A and oroxylin A-7-O-glucuronide in the reference herb of *Radix Scutellariae* as well as six commercial products containing RS, i.e. HQ-Tab, C-HQ-Tab, YH-Cap, YH-DP, SHL-Cap, SHL-S-Cap. The results are shown in Table 3.

The content of BG was reported to be the most abundant amount in the pharmacopeia and the literatures (The Pharmacopoeia Commission of PRC, 2005, Lin et al., 1999, Zhang et al., 1998, Wu et al., 2005). Its content under the extraction and determination method in the current study complied with the literature report and requirement of Chinese Pharmacopoeia, which should not be less than 9% (w/w). Furthermore, the content of each studied flavones showed marked variations among different dosage forms. The amount of glycosides (BG, WG, OAG) ranked the highest in the reference herb, and the YH-Cap contained the highest amount of aglycones (B, W, OA). W and WG could not be detected in the dripping pill. In

addition, the contents of the aglycones are the least among in all the products tested. This might result from the raw material that have been used or the procedure of extraction and pharmaceutical preparation of different dosage forms. It has been observed that the content of each flavone in the raw material of RS from different areas showed a great extent of variation (Zhou et al., 2006, Yang et al., 2002, Zhang et al., 2005) and the content of BG in plants from some areas were even below 9%. In the cases of YH-DP and SHL-S-Cap, the variances in solubility of different flavones in the formulation bases might cause the content variances in the final products. Particularly, HQ-Tab and C-HQ-Tab were extracted without removing the sugar coating and the content of the six flavones were calculated with the weight of the sugar coating, which might contribute to the relatively low amount of the flavones detected.

Table 2.3   Content of six bioactive flavones in reference herb and commercial PTCM products of RS

Products	Content (n=3, mean±S.D., mg/100mg)					
	BG	WG	OAG	B	W	OA
SHL-Cap	16.32±0.07	0.23±0.01	1.19±0.04	0.39±0.01	0.10±0.01	0.03±0.00
SHL-S-Cap	6.19±0.04	0.03±0.00	0.35±0.01	0.22±0.00	0.04±0.00	0.02±0.00
YH-Cap	7.72±0.01	1.78±0.01	1.27±0.01	1.22±0.02	0.39±0.00	0.09±0.00
YH-DP	10.52±0.12	N.D.	0.22±0.01	0.15±0.00	N.D.	0.01±0.00
HQ-Tab	4.59±0.08	0.81±0.01	0.84±0.01	0.64±0.01	0.39±0.01	0.10±0.01
C-HQ-tab	2.25±0.01	0.67±0.02	0.38±0.01	0.53±0.02	0.19±0.02	0.04±0.00
RH	18.54±0.71	3.54±0.18	2.84±0.14	0.53±0.01	0.21±0.01	0.06±0.00

N.D.: not detectable

2.4   Conclusion

In the present study, a simple and accurate HPLC/UV method has been established and validated to simultaneously determine six main bioactive flavones (baicalein, baicalin, wogonin, wogonoside, oroxylin A and oroxylin A-7-O-glucuronide) in the reference herb and commercial PTCM of RS. It produced good linearity, intra-day and inter-day precision and accuracy as well as high extraction efficiency. The assay method is helpful to improve the quality control of authentic material of RS and its proprietary traditional Chinese medicines.

Chapter Three

Identification and quantification of baicalein, wogonin, oroxylin A and their major glucuronide conjugated metabolites in rat plasma after oral administration of *Radix Scutellariea* product

3.1 Introduction

Radix Scutellariea (RS) has been extensively applied in various commercial proprietary traditional Chinese medicine products such as Huang Qin tablet, Shuang-Huang-Lian capsule, Shuang-Huang-Lian Soft Capsule, Shuang-Huang-Lian Injection, Yin Huang Capsule, Yin Huang Dripping Pill etc.. In addition, RS functions as a major ingredient in various herbal decoctions including Xiexin decoction, Shuang-Huang-Lian and Huangqin-Tang.

With the fast development and extensive application of proprietary traditional Chinese medicine (PTCM) products, there comes an urgent requirement for their modernization, in which the investigation of their pharmacokinetic profiles is essential. There have been a few reports on the pharmacokinetic studies of the pure compounds of B, BG and W after different administration routes to rats. It was found that B could be readily absorbed with a fast and extensive first-pass metabolism, while BG was firstly hydrolyzed to B by LPH in GI tract followed by absorption (Lai et al., 2003, Akao et al., 2000, Xing et al., 2005, Lu et al., 2007, Kim et al., 2007, Li et al., 2005, Zhang et al., 2004). In addition to the rats, there are only two reports on the pharmacokinetics of B and BG in humans (Lai

et al., 2003, Che et al., 2001). For the study of W, it was found that W-7β-D-glucuronide was its major metabolites after oral administration to Wistar rat and the plasma concentration of W was quite low (Chen et al., 2002). The subchronic toxicity and plasma pharmacokinetic studies of W were also carried out in Beagle dogs (Peng et al., 2009). There has been no report about the pharmacokinetic study of pure OA yet.

The pharmacokinetic characteristics of the bioactive components in the herb extract and decoction or of RS, such as Huang-Lian-Jie-Du-Tang and Xiexin decoction were also investigated in rats (Lu et al., 2007, Kim et al., 2007, Zhang et al., 2006, Yan et al., 2007, Kim et al., 2006). Moreover, since it is usually more than one herb in the decoction, the effects of other co-existing ingredients on the pharmacokinetics of the major components of RS were also investigated in Xiexin decoction, Shuang-Huang-Lian and Huangqin-Tang (Li et al., 2005, Di et al., 2006, Zuo et al., 2003). Because of the complexity of ingredients for the herbal medicines, it is extremely important to simultaneously monitor the bioactive components as much as possible using advanced analytical tools. So far, most of the assay methods in plasma concentrated on the determinations of B, W, BG and WG after the administration of the products containing RS. Till now, there were just two articles that have been found to report the *in vivo* pharmacokinetics profiles of OA, but none of them has quantified the plasma concentration of OAG (Kim et al., 2007, Zuo et al., 2003). Sharing the similar chemical structure as B and W, it is expected that OA might also undergo extensive Phase II metabolism. In addition, the content of OA also exist in relatively high amount in the reference herb and proprietary traditional Chinese

medicine products of RS (Li et al., 2009). As a result, it is necessary to develop an assay method to simultaneously determine all the six bioactive flavones in plasma.

In the present study, a specific HPLC method has been developed for the simultaneous determination of three bioactive flavones as well as their major metabolites of glucuronic acid conjugates. Subsequently, this method has been successfully applied to determine the plasma concentration of the six flavones after oral administration of Shuang-Huang-Lian Capsule (SHL-Cap, a commercial available capsule product of RS) to male Sprague-Dawley rats.

3.2   Materials and methods

3.2.1   Materials and reagents

Baicalein (B) and baicalin (BG) with purity over 98% were purchased from Sigma-Aldrich Chem. Co. (Milwaukee, WI, USA). Wogonin (W) and wogonoside (WG) with purity over 98% were purchased from AvaChem Scientific LLC (San Antonio, TX, USA). Oroxylin A (OA, purity over 98%) and Oroxylin A-7-O-glucuronide (OAG, purity over 95%) were supplied by Shanghai u-sea biotech co., Ltd (Shanghai China). The internal standard (IS), 3, 7-dihydroxyflavone with purity of 97%, was purchased from Indofine Chemical Company (Hillsborough, NJ, USA). Waters Oasis® hydrophilic-lipophilic-balanced (HLB, 1cc) copolymer extraction cartridges were purchased from Waters. Acetonitrile (Labscan Asia, Thailand) and methanol (TEDIA company, Inc., USA) were HPLC grade and used without further purification. All other reagents were of at least

analytical grade. Distilled and deionized water was prepared from Millipore water purification system (Millipore, Milford, USA).

3.2.2 Instrumentation and chromatographic conditions

3.2.2.1 HPLC/UV assay for the quantification of bioactive flavones in RS

The HPLC system consists of Waters 600 controller (pump), Waters 717 auto sampler and Waters 996 Photodiode Array UV detector. The separation of all the analytes was performed by using a Thermo BDS Hypersil column (250 mm× 4.6 mm; 5 μm particle size) connected to a guard column (Delta-Pak C18 Guard-Pak, Waters). Data were collected by Waters Millennium software (version 3).

The mobile phase consisting of eluent A (20 mM sodium dihydrogen phosphate buffer, pH 4.6) and B (acetonitrile) was run at 1 ml/min. The linear gradient elution program was set as follows: eluent A decrease from 90 to 70% in the first 10 min, decrease from 70 to 40% in the next 2 min, maintained at 40 % for 4 min, then eluent A increased from 40 to 90% from 16 to 20 min and equilibrated for 5 min before the next injection. The detection wavelength was set at 320 nm and the injection volume was 100 μl.

3.2.2.2 LC-MS/MS assay for the metabolites identification of bioactive flavones in RS

The LC-MS/MS system consisted of ABI 2000 Q-Trap triple quadrupole mass spectrometer equipped with an electrospray ionization source (ESI), TWO Perkin-Elmer PE-200 series micro-pumps and auto-sampler (Perkin-Elmer, Norwalk, CT, USA). All

the analytes were separated using an Alltima C_{18} column (150 mm×4.6 mm, i.d., 5 μm particle size, Alltech) protected by a collared frit (4/4.6 mm i.d., 0.5 μm pore size, Thermo Scientific).

The elution gradient for LC analysis consisted of two solvent compositions: acetonitrile (A) and 0.1% formic acid (B). The gradient began with 35% eluent A for 1min, changed linearly to 60% A in 6 min and remained for further 3min before changing back to10% A in 0.5 min and equilibrating for 2.5 min prior to next injection. Throughout the LC process the flow rate was set at 1ml/min. The temperatures of auto-sampler and the analytical column were set at 4 °C and ambient, respectively. The sample injection volume was 20 μl. Prior to the ESI source, 60% of the LC eluent was split off and only 40% of the effluent was introduced.

The mass spectrometer was set at positive ionization mode. Typical instrumental conditions were: ion spray voltage at 5000 V; nitrogen as nebulizer gas, auxiliary gas, curtain gas at 30, 70, 30 and collision gas at 3 psi, respectively; auxiliary gas temperature at 350 °C and interface heater temper at 100 °C. Other instrumental parameters were analyte specific and were optimized prior to analysis. Data acquisition was conducted at multiple reaction monitoring (MRM), with m/z 271→m/z 122.9 for B, m/z 285→m/z 270 for W and OA, m/z 447→m/z 270.9 for BG, m/z 461→m/z 285 for WG and OAG.

3.2.3 Preparation of standard solutions

The stock solution of B, BG, W, WG, OA and OAG (1 mg/ml) were prepared by dissolving appropriate amount of each authentic compound in DMSO separately. The working solutions of calibration curve were prepared by mixing and diluting the stock solutions of each compound with methanol and phosphate buffer (25 mM, pH 2.5) comprising 1% ascorbic acid (50: 50, v/v) to yield concentrations of 0.2, 0.4, 1.0, 2.0, 4.0, 10.0, 20.0, 40.0 μg/ml, respectively. Standard solution of IS was prepared by dissolving appropriate amount of 3, 7-dihydroxyflavone in methanol at a final concentration of 10 μg/ml.

The samples of calibration curve in plasma were prepared by spiking 50 μl of the above working solutions into 100 μl of blank plasma to yield the concentration at 0.1, 0.2, 0.4, 1.0, 2.0, 4.0, 10.0, 20.0 μg/ml for all the six flavones. Low, medium and high concentrations of quality control (QC) samples were chosen to be 0.8, 4.0 and 8.0 μg/ml in plasma.

3.2.4 Sample preparation

The procedure of plasma sample preparation was similar to our previous study (Zhang et al., 2004). Briefly, the Oasis® HLB cartridges were preconditioned with 1 ml of methanol, followed by 1 ml of 25 mM sodium dihydrogen phosphate buffer (pH 2.5). In 100 μl of plasma sample, 50 μl of 50% methanol in phosphate buffer (pH 2.5) comprising 1% ascorbic acid and 20 μl of internal standard (3, 7-dihydroxyflavone, 10 μg/ml) were added. The mixture was diluted with 1 ml of 35% methanol in 25 mM sodium

dihydrogen phosphate buffer (pH2.5) containing 1% ascorbic acid. After vortexing for 15 sec and centrifuged at 16,000×g for 10 min, the surpernatant was loaded onto the preconditioned HLB cartridge. The cartridge was flushed with 1 ml of 25 mM sodium dihydrogen phosphate buffer (pH2.5) followed by 1 ml of 35% methanol in 25 mM sodium dihydrogen phosphate buffer (pH2.5) containing 1% ascorbic acid. All the analytes were eluted by 1 ml methanol from the cartridge. The eluent was evaporated to dryness in a Centrivap concentrator, and the residue was reconstituted by 150 μl of 50% methanol in phosphate buffer (pH 2.5) comprising 1% ascorbic acid. After centrifuged at 16,000×g for 10 min, an aliquot of 100 μl supernatant was injected into HPLC system for analysis.

3.2.5 Validation of the developed assay method

3.2.5.1 Specificity

The specificity of the method was evaluated by comparing the chromatogram of blank plasma samples from 6 rats with that of blank plasma spiked with standard solution and chromatogram of rat plasma samples after oral administration of SHL-cap suspension.

3.2.5.2 Sensitivity

The limit of detection (LOD) was defined as the lowest concentration of the drug resulting in a signal-to-noise ratio of 3:1. The limit of quantification (LOQ) was defined as the lowest concentration of the drug resulting in a signal-to-noise ratio of 10:1 with precision below 20% and accuracy below ±20% (FDA, 2001).

3.2.5.3 Calibration curve

The calibration curves were plotted using a $1/x^2$ weighted linear regression of the peak-area ratio of each analyte to internal standard versus the plasma concentrations of each analyte.

3.2.5.4 Precision and accuracy

The intra-day precision was determined by analyzing five replicates of QC samples within one day. The inter-day precision was determined by analyzing the QC samples on five separate days. The intra-day and inter-day precision was defined as the relative standard deviation (R.S.D.) and accuracy was defined as relative error (R.E.).

3.2.5.5 Recovery

Recovery was calculated by comparing the peak areas of the extracted QC samples to that of the un-extracted standard solutions containing the equivalent amount of analytes.

3.2.5.6 Stability

Freeze-thaw stability was determined by exposing QC samples to three freeze-thaw cycles before sample preparation. Stability at room temperature and long-term stability were evaluated by keeping QC samples at room temperature for 2 h and at -80°C for 10 days before sample preparation. The stability of samples in auto-sampler was evaluated by analyzing extracted QC samples after being placed in the auto-sampler at room temperature for 24 h.

3.2.6   Assay application

Male Sprague-Dawley rats (body weight, 230-250 g) were supplied by the laboratory Animal Services Center at the Chinese University of Hong Kong. The experiment was conducted under the approval by Animal Ethics Committee of the Chinese University of Hong Kong. The rats were anesthetized with an intramuscular injection of a cocktail containing 60 mg/kg ketamine and 6 mg/kg xylazine. Right jugular vein was cannulated with a polyethylene tubing (0.5 mm ID, 1 mm, Portex Ltd., Hythe, Kent, England) for blood sampling.

The content of SHL-Cap was taken out from the capsule and suspended in water to prepare a suspension of 0.4 g/ml. The suspension of SHL-Cap was prepared by mixing thoroughly and 2 ml of the prepared suspension was delivered by a 5 ml syringe to rats via gavage at dose of 3.2 g/kg. Blood samples were taken at 10, 30, 60, 120, 240, 360, 480, 720 and 1440 min, respectively. Plasma samples were collected after centrifugation at 16, 000×g for 3 min and stored at -80 °C until analysis.

In order to confirm the new metabolite of W, SD rats were orally administrated with pure compound of W, which was prepared in the mixture of PEG 400 and 20% Solutol ® HS15 (3:7, v/v). Plasma samples were collected via jugular vein catheter at 10 min after administration.

3.3   Results and discussions

3.3.1 Method validation

The representative chromatograms of blank plasma, calibration curve and plasma sample obtained after oral administration of SHL-cap were shown in Fig. 3.1. Under the established chromatographic condition, there was no endogenous interference in the plasma and all the six flavones as well as the internal standard could be well separated from each other.

(I)

(II)

(III)
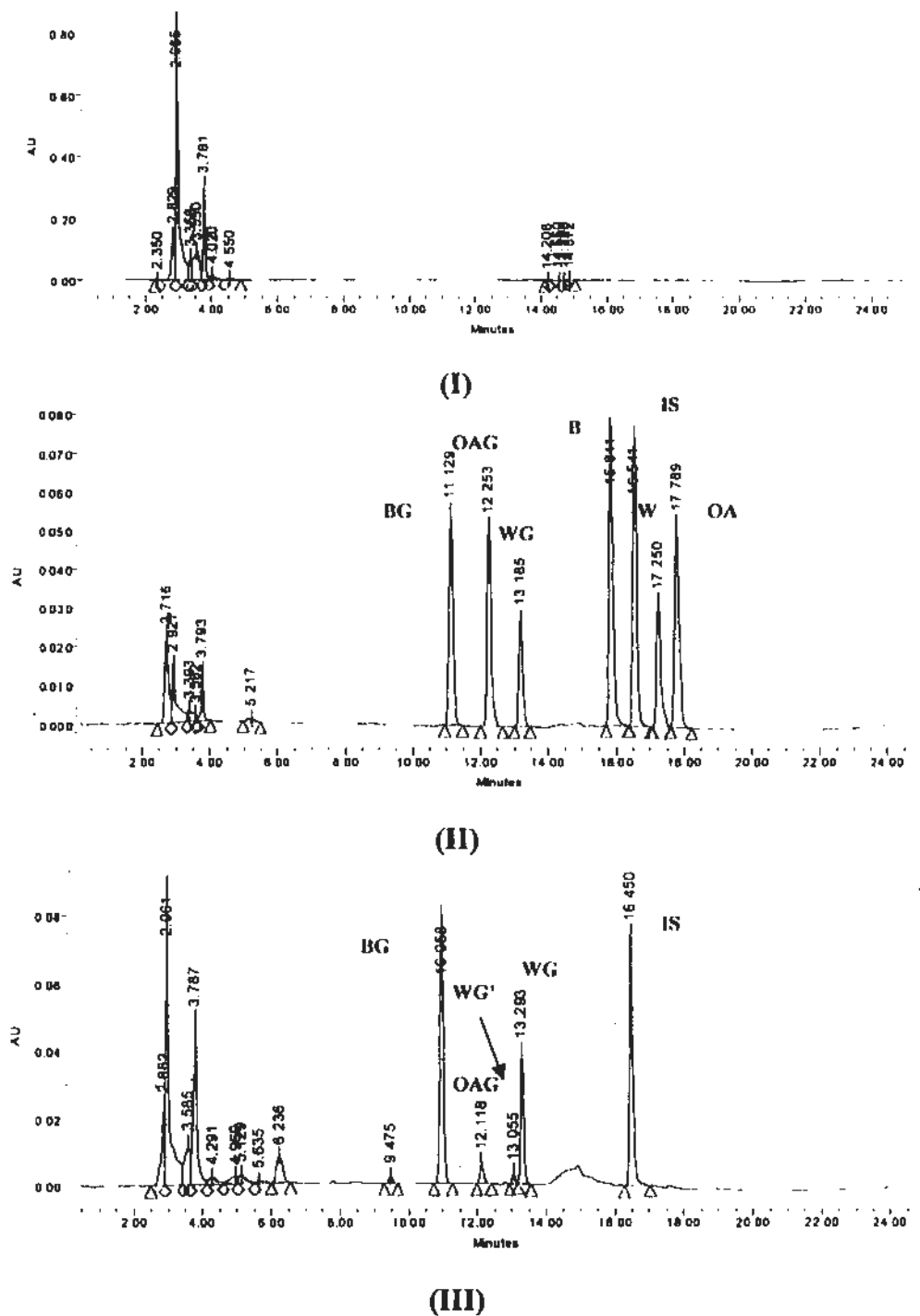
Fig. 3.1   **Representative HPLC/UV chromatograms of rat blank plasma (I); blank plasma spiked with BG, WG, OAG, B, W and OA at the concentration of 2.0 µg/ml (II); rat plasma sample obtained at 480 min after oral administration of SHL-Cap (3.2 g/kg) (III)**

In the range of 0.1-20 µg/ml, the calibration curve produced good linearity ($r^2 \geq 0.999$) using a $1/x^2$ weighted linear regression. The LOD was 0.05 µg/ml and the LOQ was 0.1 µg/ml for all the six analytes. The intra-day and inter-day precision and accuracy of the assay method are listed in Table 3.1. The R.S.D. of both intra-day and inter-day precision at low, medium and high concentrations for all the analytes were below 10.01%. Besides, the intra-day and inter-day accuracy calculated by R.E. were within the range of -10.83% to 15.13%.

The recoveries of six analytes at low, medium and high concentrations as well as internal standard were 72.04% to 82.98% for BG, 70.17% to 84.65% for WG, 75.28% to 87.28% for OAG, 79.41% to 94.79% for B, 81.60% to 97.71% for W, 76.15% to 91.48% for OA. The results were also summarized in Table 3.1. The average recovery for internal standard was 75.28±9.33%.

The results of stability tests under various conditions are listed in Table 3.2. Stability results indicated that all the six flavones were stable for at least three freeze-thaw cycles and they were stable at -80 °C for 10 days at least. Besides, all the six flavones were stable in the prepared samples for 24h at room temperature and they were stable in plasma for at least 2h at room temperature.

Table 3.1 Regression equation, intra-day and inter-day precision and accuracy as well as recoveries of six flavones in rat plasma QC samples

Flavones	Linear range (µg/ml)	Regression equation	R²	Nominal conc. (µg/ml)	Recovery (%, n=3)	Intra-day (n=5)			Inter-day (n=5)		
						Determined conc. (µg/ml)	Precision (%R.S.D.)	Accuracy (%R.E.)	Determined conc. (µg/ml)	Precision (%R.S.D.)	Accuracy (%R.E.)
BG	0.1-20	y=0.1249X-0.0429	0.9995	0.8	72.04±9.80	0.74±0.05	6.86	7.77	0.79±0.06	7.71	1.11
				4.0	73.30±19.19	3.86±0.30	7.87	3.54	4.15±0.16	3.90	-3.63
				8.0	82.98±13.98	8.18±0.19	2.27	-2.23	7.92±0.54	6.83	1.02
WG	0.1-20	y=0.0819X-0.0088	0.9998	0.8	70.17±9.24	0.69±0.04	6.00	13.93	0.75±0.04	4.79	6.00
				4.0	72.43±16.94	3.87±0.29	7.61	3.34	4.18±0.16	3.74	-4.48
				8.0	84.65±11.13	8.08±0.21	2.58	-0.94	8.08±0.58	7.12	-1.00
OAG	0.1-20	y=0.1523X-0.0268	0.9989	0.8	78.01±11.00	0.68±0.06	8.48	15.13	0.78±0.03	4.38	2.50
				4.0	75.28±17.25	3.81±0.29	7.53	4.64	4.23±0.19	4.59	-5.86
				8.0	87.28±11.78	7.98±0.21	2.68	0.26	8.16±0.59	7.25	-1.94
B	0.1-20	y=0.2233X-0.0762	0.9987	0.8	80.18±11.38	0.78±0.05	5.90	2.41	0.89±0.09	10.01	-10.83
				4.0	79.41±18.42	3.88±0.13	3.42	2.99	4.01±0.24	6.01	-0.21
				8.0	94.79±17.41	7.72±0.28	3.62	3.50	7.98±0.72	9.03	0.24
W	0.1-20	y=0.1258X-0.0100	0.9996	0.8	85.40±12.69	0.75±0.03	3.62	6.07	0.75±0.04	5.21	6.42
				4.0	81.60±9.39	4.04±0.13	3.20	-0.99	4.05±0.20	4.89	-1.30
				8.0	97.71±17.70	7.81±0.33	4.27	2.43	8.04±0.68	8.50	-0.55
OA	0.1-20	y=0.2581X-0.0137	0.9999	0.8	78.46±13.05	0.80±0.03	4.28	0.21	0.79±0.03	4.04	1.51
				4.0	76.15±10.64	3.81±0.12	3.15	4.82	4.02±0.18	4.57	-0.39
				8.0	91.48±16.75	7.58±0.24	3.21	5.22	7.93±0.66	8.28	0.93

Table 3.2   Stability experiments of six flavones under different conditions

Flavones	Nominal conc. (µg/ml)	Determined concentration (µg/ml)			
		Three freeze-thaw cycle	Room temperature for 2 h	-80 °C for 10 days	Auto-sampler for 24 h
BG	0.8	0.75±0.02	0.67±0.05	0.82±0.02	0.77±0.02
	4.0	3.61±0.17	4.17±0.29	4.03±0.12	4.01±0.06
	8.0	6.88±0.62	8.21±0.21	7.21±0.08	8.00±0.19
WG	0.8	0.73±0.03	0.68±0.04	0.77±0.01	0.75±0.02
	4.0	3.69±0.19	4.15±0.30	4.26±0.08	4.00±0.05
	8.0	7.22±0.80	8.20±0.28	8.12±0.19	7.65±0.21
OAG	0.8	0.74±0.02	0.70±0.04	0.81±0.01	0.76±0.03
	4.0	3.83±0.15	4.21±0.29	4.34±0.08	3.99±0.06
	8.0	7.45±0.78	8.25±0.28	8.13±0.16	7.92±0.21
B	0.8	0.89±0.04	0.91±0.05	0.94±0.01	0.92±0.04
	4.0	3.68±0.07	3.95±0.14	3.94±0.05	3.65±0.09
	8.0	7.42±0.16	8.40±0.64	8.05±0.03	7.73±0.07
W	0.8	0.68±0.00	0.78±0.03	0.77±0.01	0.78±0.02
	4.0	3.70±0.27	4.01±0.14	4.16±0.04	3.94±0.04
	8.0	7.72±0.53	8.12±0.81	7.97±0.18	7.07±0.69
OA	0.8	0.71±0.01	0.76±0.04	0.78±0.01	0.77±0.02
	4.0	3.76±0.23	4.03±0.10	4.05±0.08	3.84±0.07
	8.0	7.46±0.35	8.12±0.71	7.85±0.15	7.84±0.21

3.3.2 Application to *in vivo* pharmacokinetic study

Although studies on the pharmacokinetic profiles of bioactive flavones in traditional RS decoctions have been reported, none of the studies provided the pharmacokinetic information of bioactive flavones in commercially available PTCM products of RS. The decoctions are the water extract of a single herb or various herbs, while the PTCM products might introduce the impact of other excipients. Due to the extensive application of commercial PTCM RS products, the current assay is proposed aiming to test the pharmacokinetics of its bioactive flavones in these commercial products. Contents of each studied bioactive flavones are essential for the proposed pharmacokinetics studies. Our previously developed assay has simultaneously quantified the six major bioactive components in the studied SHL-Cap and indicated the contents of six flavones to be 522.24, 7.36, 38.08, 12.48, 3.20 and 0.96 mg/kg for BG, WG, OAG, B, W and OA (Li et al., 2009). The same product was used in the current *in vivo* pharmacokinetic study.

In all the plasma samples, just the glucuronic acid conjugates of B, W and OA rather than their aglycones could be detected. BG and WG were detectable for all the time points after the oral administration of SHL-Cap, whereas OAG could only be detected in plasma for a few time points around the t_{max} of 360 min, possibly due to the low content of OAG plus OA in SHL-Cap. The plot of plasma drug concentration versus time for BG, WG was shown in Fig. 3.3.
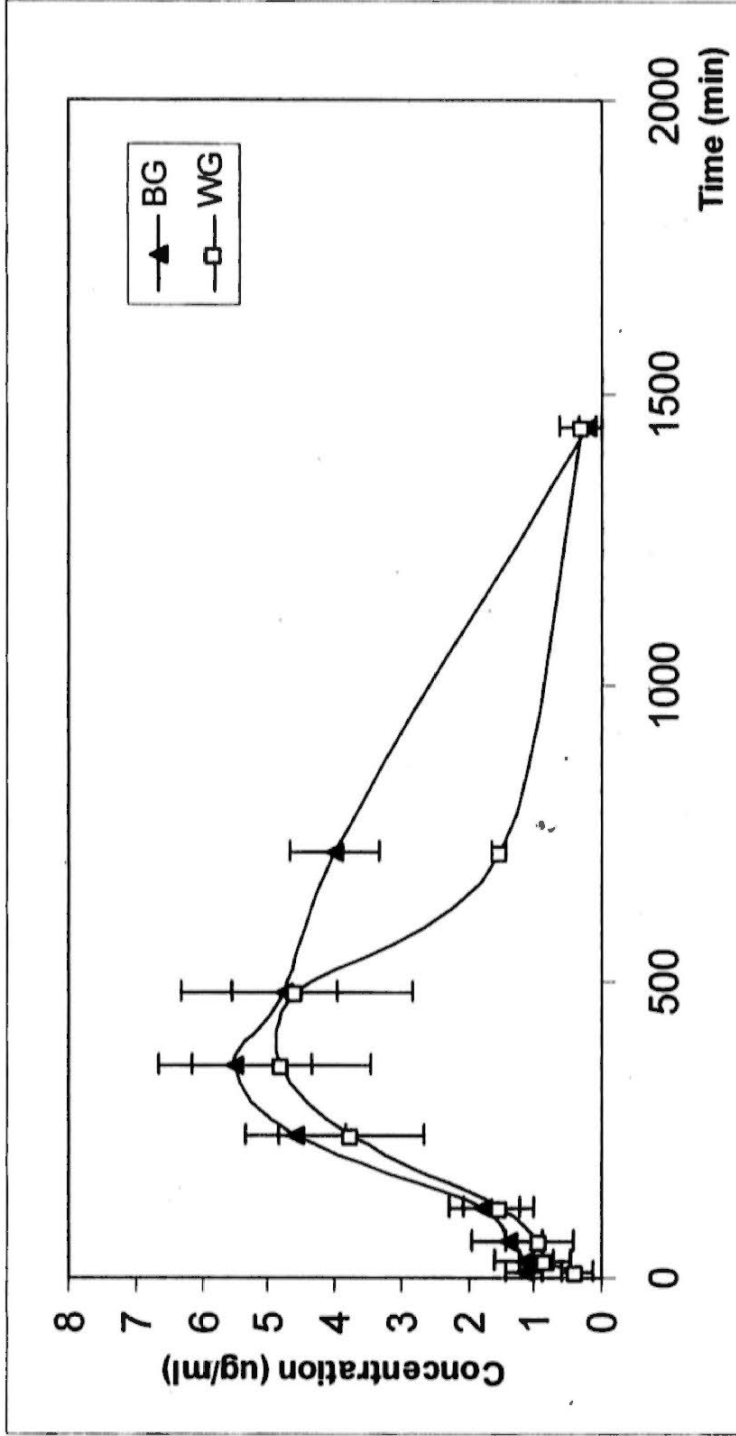
Fig. 3.2   Plasma concentrations versus time profiles of BG and WG after oral
administration of SHL-Cap at 3.2 g/kg to rat (n=6)

The reason for undetectable aglycones of B, W, and OA could be explained by their potential extensive first pass metabolisms. Our previous studies of B by *in situ* and *in vitro* models confirmed that during its intestinal absorption, B underwent a fast and extensive Phase II metabolism to form glucuronic acid and/or sulfate conjugates, in which UGT (Urindine 5'-diphospho-glucuronosyltransferase, UDP-glucuronosyltransferase) and SULT (Sulfotransferase) might be involved (Zhang et al., 2007, Zhang et al., 2005). Besides, the study of B in rat showed that B could not be detectable after 20 min after i.v. administration (Zhang et al., 2004). Although the relatively high P_{app} value observed on Caco-2 monolayer model indicated a good absorption for B, the first-pass metabolism might be the main reason for its low bioavailability after oral administration. Due to the similarity of chemical structure among B, W and OA, it is expectable that W and OA will undergo extensive Phase II metabolism.

Because of the first-pass metabolism at intestine and liver as well as the relatively low content of aglycones in the PTCM products of RS, their corresponding glucuronides are the predominant form in systematic circulation. The monitoring of glucuronides seems to be more important than that of aglycones, especially after oral administration route. Nevertheless, a number of assay method quantified the concentration of glucuronides using an indirect way which calculated the amount of aglycones before and after hydrolysis. It is not accurate enough and quite sample consuming. Consequently, the development of the assay method to analyze aglycones and glucuronides simultaneously seems to be more necessary.

From the HPLC chromatograms of the plasma sample after oral administration of SHL-Cap in rat, there was a new peak appearing just before the peak of WG. Its UV spectrum resembled that of WG. Subsequently, LC/MS/MS was employed to further identify this new compound. Under the mode of positive MRM, there were three peaks under the *m/z* from 461 to 285 indicating the loss of glucuronic acid group. Similarly, there were two peaks found in the plasma sample after oral administration of pure W to rat. The retention time of one peak was identical to that of standard solution of WG. However, there was only one peak appearing under the *m/z* from 461 to 285 after oral administration of pure OA to rat. Additionally, there was just one peak of OAG in the HPLC chromatogram after oral administration of pure OA to rat. The MRM chromatograms are shown in Fig. 2.3. All the evidences above indicated the existence of the isoform of WG. Considering only one more hydroxyl group in W available for forming glucuronic acid conjugates except the one at 7-C, the isoform of BG might be the glucuronic acid conjugate of W at 5-OH. In the study by Chen et al. (Chen et al., 2002), there was only one glucuronic acid conjugate at 7-OH found in the plasma samples after oral administration W to rat at 5 mg/kg. Such discrepancy might be caused by different rat species between Wistar rat and SD rat. Chen et al. used Wistar rat and we employed male Sprague-Dawley rats in the experiment. However, as it mentioned in the article, the existence of wogonin-5β-D-glucuronide in rat plasma sample could not be excluded at that stage. Since the formation of wogonin-7β-D-glucuronide is predominant in rat plasma, their method may not be sensitive enough to identify the conjugate at 5-OH.
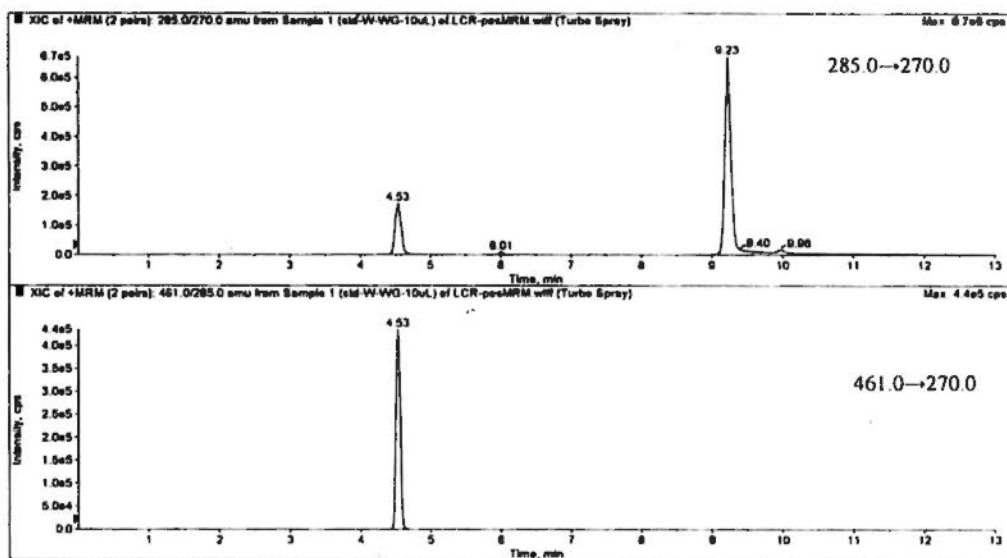
(I)
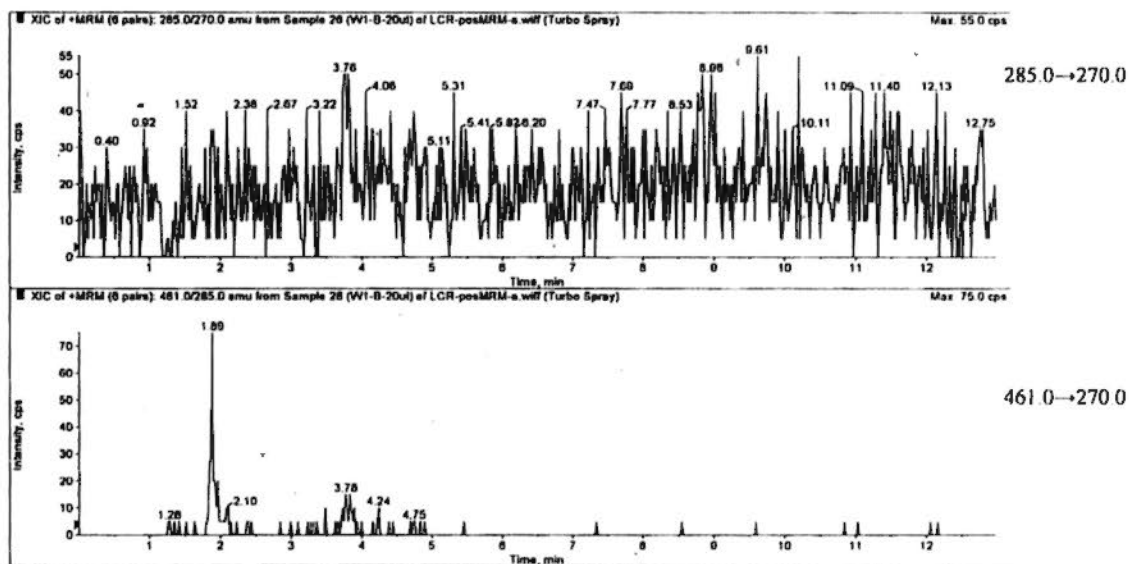
(II)

Fig. 3.3 Positive ion mode MRM chromatograms of standard solution of W and WG mixture at 1 µg/ml (I); rat blank plasma (II); rat plasma sample after oral administration of SHL-Cap at 3.2 g/kg (III); pure W at 5 mg/kg (IV); pure OA at 5 mg/kg (V)
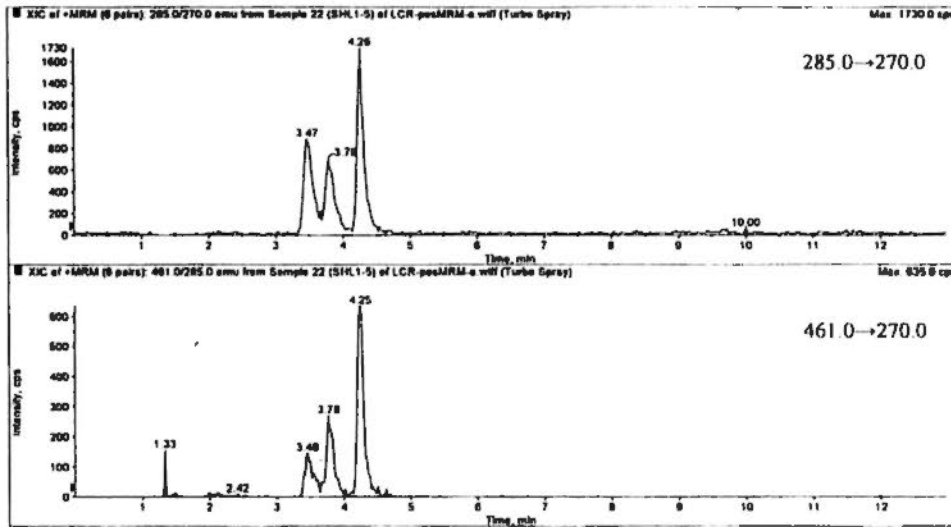
(III)
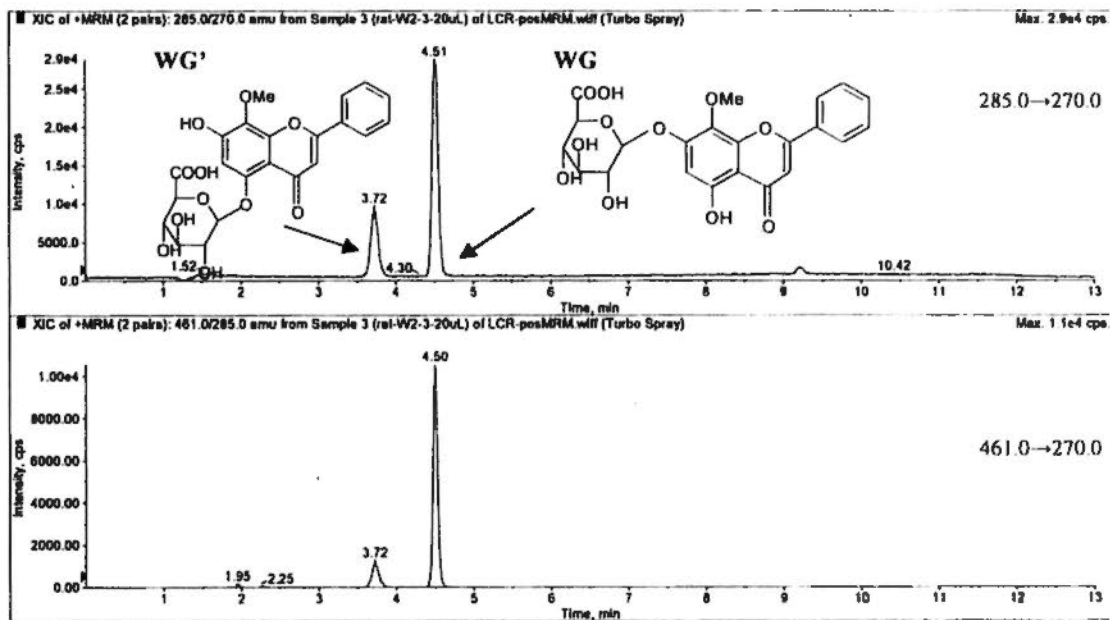
(IV)

Fig. 3.3 **Positive ion mode MRM chromatograms of standard solution of W and WG mixture at 1 µg/ml (I); rat blank plasma (II); rat plasma sample after oral administration of SHL-Cap at 3.2 g/kg (III); pure W at 5 mg/kg (IV); pure OA at 5 mg/kg (V) (continued)**

(V)
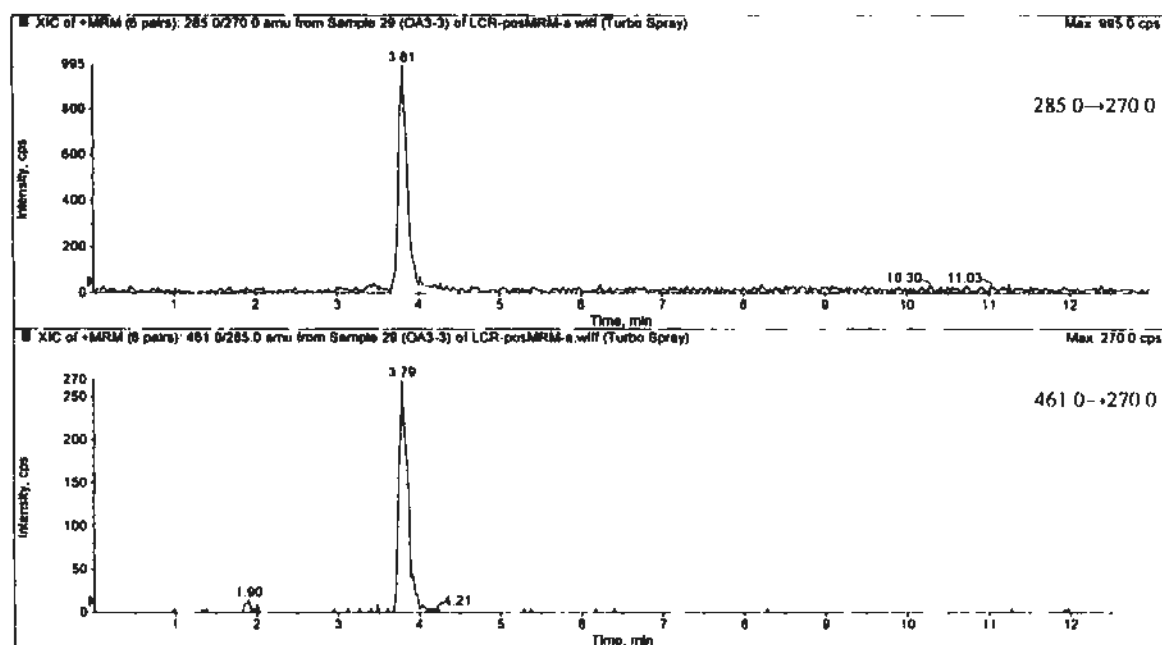
Fig. 3.3   **Positive ion mode MRM chromatograms of standard solution of W and WG mixture at 1 µg/ml (I); rat blank plasma (II); rat plasma sample after oral administration of SHL-Cap at 3.2 g/kg (III); pure W at 5 mg/kg (IV); pure OA at 5 mg/kg (V) (continued)**

It was assumed that OA should have the same metabolic pathways as W because of their structural similarity. However, based on the results from pharmacokinetic study *in vivo*, W could be metabolized to two isoforms of WG, whereas OA could just form the glucuronic acid conjugate at 7-OH. Both compounds could form the similar H bond due to the proximity of the C-4 carbonyl group with C-5 hydroxyl group, respectively. However, the strength of H-bond of OA is different from that of W. The ortho methoxyl group in OA had stronger inductive effect on the hydroxyl group at C-5 than the para

methoxyl group in W. As a result, the difference in structure made the electron density at C-5 in OA lower compared with that in W, which leads to a more significant H bond effect in OA and prevents a second esterification occurring at C-5.

3.4   Conclusion

A simple and specific HPLC/UV method has been developed and validated for the simultaneous determination of B, W, OA, BG, WG and OAG in rat plasma following a solid phase extraction procedure. The assay method demonstrated good sensitivity, accuracy, precision, linearity, stability and recovery. Subsequently, this method was successfully applied to determine the concentration of the flavones in plasma after oral administration of SHL-Cap to male Sprague-Dawley rat. In addition to WG, a new metabolite of W has been found and confirmed using LC/MS/MS for the first time.

Chapter Four

Mechanistic studies on the intestinal absorption and disposition of wogonin and oroxylin A

4.1 Introduction

Our previous study on B (Zhang et al., 2007a) found that although it exhibited favorable permeability, the extensive first-pass metabolism during its intestinal absorption limited its bioavailability. Glucuronidation of B was the major route for its metabolism with various intestinal and hepatic UGT isozymes involved. UGT 1A9 mainly catalyzed the formation of BG in human liver. The intracellularly formed glucuronide could be effluxed to the apical side (lumen side) and basolateral side (mesenteric blood side) by membrane transporters, in which MRPs were mainly involved. As shown in Fig. 1.2, W and OA, the other two major bioactive components in *Radix Scutellariae* (RS), share the similar chemical structure as B. It was hypothesized that W and OA would also undergo the similar absorption and disposition pathways as B. Although there are some reports about the pharmacokinetic profile of W and OA after oral administration of the extract or proprietary traditional Chinese medicine products of RS, the mechanisms of their absorption and disposition at cellular or organ level have not been investigated. Since intestine is the first barrier that drug meets after oral administration, it is of great importance to elucidate their potential intestinal absorption and disposition mechanisms. As a result, two classical absorption models of Caco-2 cell monolayer model and rat *in*

situ single-pass intestinal perfusion model were employed for the purpose of intestinal absorption and disposition mechanism study.

For the sake of high throughput screening of new compound entities, a number of *in vitro* and *in situ* models have been developed to study the pharmacokinetic characteristics, especially drug absorption in the early stage of drug development and enhance the probability of success in clinical trials. They are usually simple systems and the experiments are easy to operate. In addition, they are time and cost saving. Often, some mechanistic information could be derived (Venkataramanan et al., 2006). Till now, several *in vitro* models have been successfully established and utilized to investigate drug permeability such as Parallel Artificial Membrane Permeability Assay (PAMPA) system (Kansy et al., 1998, Hämäläinen et al., 2004), Ussing chamber (Boisset et al., 2000), and intestinal cell models obtained from human colon cancer like Caco-2 cells, HT-29 cells and T84 (Barthe et al., 1999).

Among these cell models, Caco-2 cell monolayer model is one of the most successfully and extensively employed models. Caco-2 cells originate from human colon adenocarcinoma cells (Artursson et al., 1997). It differentiates in culture and shows morphological and functional similarities to human small intestine epithelium such as the microvilli, apical brush border and tight junction (Peterson et al., 1992). Moreover, Caco-2 cells also express membrane transporters such as Pgp, MRPs, BCRP and organic anion transporters et al. (Hunter et al., 1993, Hirohashi et al., 2000, Kobayashi et al., 2003, Darnell et al., 2010). There are also metabolic enzymes expressed in the system including

cytochrome P450, UDP-glucuronosyltransferase, sulfotransferase, glutathione S-transferase, N-acetyltransferase and acyltransferase (Sun et al., 2002, Paine et al., 2000, Siissalo et al., 2008 and 2010). Caco-2 cell monolayer model is often used to predict intestinal drug absorption by different transport routes (Artursson et al., 2001) for the good correlation with the *in vivo* permeability (Grès et al., 1998). In addition to its application in drug screening, it has been extensively used in rapid evaluation of prodrugs for enhanced oral absorption, drug transport from delivery systems, cellular uptake studies, selection of absorption-promoting excipients, assessment of presystemic metabolism of drugs in the intestinal epithelium, drug-drug and drug-excipient interaction related to membrane transporters as well as cytotoxicological studies (Shah et al., 2006).

However, there are still some limitations of Caco-2 cell monolayer model such as the long culturing time, low expression of cytochrome P450 3A4, lack of mucus layer, higher TEER than small intestine, variable expression of membrane transporters (Shah et al., 2006). Although *in vivo* studies provide useful information of overall drug exposure, the results are always complicated with the comprehensive effects of several factors such as the simultaneous function of several organs. In order to better mimic the real situation that a drug undergoes in a specific organ, the *in situ* models are more relevant. In the present study, rat *in situ* single-pass intestinal perfusion model was further employed to study the characteristics of W and OA during their intestinal absorption and disposition. It possesses several advantages over the *in vivo* and *in vitro* models such as the easy control of experiment parameters, exclusion of impact of other organs and the maintain of intact intestinal blood supply (Cook et al., 2003). Rat *in situ* single-pass intestinal

perfusion model has been successfully applied in the study of drug intestinal absorption and metabolism (Hu et al., 2003, Liu et al., 2002, Wang et al., 1997, Okudaira et al., 2000, Fagerholm et al., 1996, Liu et al., 2009). Therefore, Caco-2 cell monolayer model and rat *in situ* single-pass intestinal perfusion model were employed to carry out the mechanistic study of the absorption and disposition of W and OA at small intestine.

4.2   Materials

Baicalein (B) and baicalin (BG) with purity over 98% were purchased from Sigma-Aldrich Chem. Co. (Milwaukee, WI, USA). Wogonin (W) and wogonoside (WG) with purity over 98% were purchased from AvaChem Scientific LLC (San Antonio, TX, USA). Oroxylin A (OA, purity over 98%) and Oroxylin A-7-*O*-glucuronide (OAG, purity over 95%) were supplied by Shanghai u-sea biotech co., Ltd (Shanghai China). 3, 7-dihydroxyflavone (IS) as internal standard with purity of 97% was purchased from Indofine Chemical Company (Hillsborough, NJ, USA). Estrone 3- sulfate (ES), estradiol glucuronide (EG), verapamil (Vera) and mitoxantrone dihydrochloride (MTX) were purchased from Sigma-Aldrich Chem. Co. (Milwaukee, WI, USA). Phenol red, calcium chloride and sodium dihydrogen phosphate were purchased from BDH chemical Ltd (Poole, England). Potassium chloride, PEG 400 and ascorbic acid were supplied by Wing Hing Chemical Co. (Hong Kong). Potassium dihydrogen phosphate was purchased from Merck (Darmstadt, Germany). Acetonitrile (Labscan Asia, Thailand) and methanol (TEDIA company, Inc., UAS) were HPLC grade and used without further purification. All other reagents were of at least analytical grade. Distilled and deionized water used throughout the experiment.

For cell culture, Dulbecco's modified Eagle's medium, fetal bovine serum, 0.25% trypsin-EDTA, penicillin-streptomycin and non-essential amino acids were purchased from Gibco BRL (Carlsbad, CA, USA) and Life Technologies (Grand Island, NY, USA). Phosphate buffered saline tablets were purchased from Sigma Chemical Co. (St. Louis, MO, USA).

4.3   Methods

4.3.1   Caco-2 and MDCK cell monolayer models

4.3.1.1 Cell culture

Caco-2 cells were purchased from American Type Culture Collection (ATCC). MDCK cell lines used in the experiment were a kind gift from Prof. P. Borst (The Netherlands Cancer Institute). Four types of MDCK cell lines were employed including the wild type of MDCK (MDCK/WT), MDCK cell line transfected with human MDR1 gene (MDCK/MDR1) as well as MDCK cell line transfected with human MRP2 and MRP3 genes (MDCK/MRP2 and MDCK/MRP3).

For cell culture, Caco-2 and MDCK cells were cultured in Dulbecco's modified Eagle's medium at 37 °C, supplemented with 10% fetal bovine serum, 1% non-essential amino acids, in an atmosphere of 5% CO_2 and 90% relative humidity. Caco-2 cells were subcultured at 70-80% confluence by trypsinization with 0.25% trypsin-EDTA and plated onto 6-well plates Transwell® inserts (24 mm I.D., 0.4 mM pore size, 4.71 cm^2,

polycarbonate filter, Corning Costar Co., NY) coated with a collagen layer at a density of 3×10^5 cells/ well and cultured for 21 days prior to transport studies. For MDCK cells, the seeding density was 2×10^6 cell/well and cells were cultured for 3 days before transport study. TEER (transepithelial electrical resistance) was used to monitor the integrity of the Caco-2 and MDCK cell monolayer. Caco-2 monolayers with TEER above 600 ohms cm^2 and MDCK monolayers with TEER above 150 ohms cm^2 were employed in the transport study. Caco-2 cells grown in Transwell® at passage 38-41 were used for the experiment.

4.3.1.2 Preparation of transport buffer

The transport study was carried out in phosphate buffer saline supplemented with 0.45 mM calcium chloride and 0.4 mM potassium chloride with pH value adjusted to 6.0 (PBS^+).

4.3.1.3 Stabilities of W, OA, WG and OAG in transport buffer

Solutions of W, OA, WG and OAG at concentration of 1 µg/ml in transport buffer (PBS^+, pH 6.0) were incubated in 37 °C water bath for 3 h. Samples were taken at 0, 30, 60, 90, 120, 150, 180 min to determine the percentage of compound remaining.

4.3.1.4 Cytotoxicities of W, OA, WG and OAG to Caco-2 and MDCK cells

MTT assay was employed to test the cytotoxicity of the four compounds to Caco-2 cells and MDCK cells. Briefly, cells were seeded onto the 96-well plate in DMEM culture medium at the density of 5×10^4 cells/well for Caco-2 cells and 1.5×10^4 cells/well for MDCK cells. Then the plate was incubated at 37 °C for 24 h. Subsequently, the culture

medium was replaced by 150 μl of PBS$^+$ (pH 6.0) containing different flavones at a series of concentrations. For Caco-2 cells, 0.35, 0.88, 1.76, 2.82, 3.52, 5.28, 8.80, 17.61 μM of W or OA and 2.17, 10.87, 21.74, 43.48, 86.96, 130.43, 173.91, 217.39 μM of WG or OAG were employed. For MDCK cells, 0.37, 1.85, 3.70, 18.52, 37.04 μM of BG as well as 0.35, 1.76, 3.52, 17.61, 35.21 μM of WG and OAG were employed. The blank PBS$^+$ (pH 6.0) was employed as a negative control. The plate with studied compounds was incubated for 4 h at 37 °C. Then 20 μl of MTT [3-(4, 5-dimethylthiazole-2-yl)-2, 5-diphenyl tetrazolium bromide, 5 mg/ml] solution in PBS$^+$ was added to each well and the 96-well plate was incubated at 37 °C for another 2 h. The solution in each well was removed and 200 μl of DMSO was used to dissolve the cell remains. Finally, the absorbance of the solution in each well was measured at 595 nm by a Kinetic microplate reader (Molecular Devices).

4.3.1.5 Bidirectional transport studies of W and OA on Caco-2 cell monolayer model

Caco-2 cell monolayer grown for 21 days were rinsed twice and equilibrated with transport buffer at 37°C for 15 min before experiment. The transport study was conducted in a bidirectional way. W, WG, OA, OAG at different concentrations in PBS$^+$ were loaded into the apical side (AP, 1.5 ml of transport buffer) or basolateral side (BL, 2.6 ml transport buffer), namely the donor chamber. Aliquots of 0.5 ml samples were taken from the other side, namely the receiver chamber, at different time intervals (30, 60, 90, 120 min). Same volume of blank PBS$^+$ was added to the receiver chamber after each sampling. All the samples were stabilized with 0.2 ml mixture of methanol: 20% ascorbic acid solution (1:1, v/v) and stored at -80 °C until analysis.

To determine the cell uptake of W and OA, the Caco-2 monolayer was cut off from the filter of Transwell® after the transport experiment and rinsed twice by ice-cold saline. After spiking with 20 µl internal standard (100 µg/ml), the monolayer was lysed with 3 ml methanol followed by 30 min sonication. Afterwards, the liquid mixture was centrifuged at 10,000 rpm for 10 min and the supernatant was evaporated under the flow of nitrogen in room temperature. The residue was reconstituted with 100 µl of 35 % methanol in 25 mM sodium dihydrogen phosphate buffer (pH 2.5) containing 1% ascorbic acid. An aliquot of 50 µl was injected into HPLC for analysis.

For the purpose of investigating the potential membrane transporters which might be involved during the transport of W, OA, WG and OAG, various transporter inhibitors or substrates at appropriate concentrations were preloaded onto both the apical and basolateral sides for 30 min. The transport inhibition studies were conducted in the presence of selected inhibitors following the general bidirectional transport procedure described above.

In order to verify the role of the paracellular pathway in the absorption of WG and OAG, the Caco-2 cell monolayer was pre-incubated with PBS^+ containing 2.5 mM EGTA for 45 min followed by the apical to basolateral transport of WG and OAG in the presence of 2.5 mM EGTA.

4.3.1.6 Basolateral to apical transport study of WG and OAG on transfected MDCK cell model

To identify potential membrane transporters, the basolateral to apical transport study was carried out in phosphate buffer saline supplemented with 0.45 mM calcium chloride and 0.4 mM potassium chloride with pH value adjusted to 6.0 (PBS$^+$). Cell monolayer of MDCK/WT, MDCK/MDR1, MDCK/MRP2 and MDCK/MRP3 grown for 3~4 days were rinsed twice and equilibrated with transport buffer at 37°C for 15 min before experiment. WG and OAG at the concentrations of 2.17 μM in PBS$^+$ were loaded into the basolateral side (BL, 2.6 ml transport buffer), namely the donor chamber. Aliquots of 0.5 ml samples were taken from the other side, namely the receiver chamber, at different time intervals (30, 60, 90, 120 min). Same volume of blank PBS$^+$ was added to the receiver chamber after each sampling. All the samples were stabilized with 0.2 ml mixture of methanol: 20% ascorbic acid solution (1:1, $v:v$) and stored at -80 °C until analysis.

4.3.2 Rat *in situ* single-pass intestinal perfusion model

4.3.2.1 Preparation of perfusate buffer

The perfusion buffer was isotonic (288 mOsm/l) and composed of 2.7 mM KCl, 1.3 mM KH$_2$PO$_4$, 8.1 mM Na$_2$HPO$_4$, 0.9 mM CaCl$_2$, 0.4 mM MgCl$_2$, and 7% PEG 400 ($v:v$) with pH 5.0 at 37 °C. In addition, 10 μg/ml of phenol red was added to the perfusate as a non-absorbable marker. The flow rate of perfusate applied to the intestinal lumen of the rat was set at 0.3 ml/min.

4.3.2.2 Stabilities of W and OA in the perfusate buffer

Both W and OA were dissolved in perfusion buffer at a concentration of 1 μg/ml, respectively. The prepared solution was incubated in shaking water bath at 37 °C for 2 h. Samples were taken every 30 min and the concentrations of W and OA were determined by HPLC/UV to calculate the percentage of W or OA remained.

4.3.2.3 Animals and surgical procedures

Male Sprague-Dawley rats, weighing 230 to 250 g, were fasted overnight with free access to water. The rats were anesthetized with an intramuscular injection of a mixture containing 60 mg/kg ketamine and 6 mg/kg xylazine. During the surgical process, the body temperature was maintained at 37 °C by heating lamp. Fresh heparinized blood was collected from donor rats by cardiac puncture. Right jugular vein for infusion of donor blood was cannulated with a polyethylene tubing (0.5 mm ID, 1 mm OD, Portex Ltd., Hythe, Kent, England). The infusion rate of donor blood via right jugular vein was controlled by a syringe pump at 0.3 ml/min (Cole parmer 74900 series, New hope, PA, USA). A midline incision was made and the small intestine was then exposed. A 7 to 11 cm long segment of jejunum was cannulated with silicon tubing (2.4 mm ID, 4.0 mm OD) connected to a peristaltic pump (Minipuls® 3, Gilson, France). The cannulated segment was then flushed with warm saline to remove intestinal content. The mesenteric vein blood was collected from the specific segment of intestine through a polyethylene tubing (0.5 mm ID, 1 mm OD, Portex Ltd., Hythe, Kent, England). Both the mesenteric blood and perfusate were collected into the pre-weighted microtubes every 5 min and lasted for 40 min.

4.3.2.4 In situ intestinal perfusion of W and OA

Our previous study of B and the other investigation on other flavonoids indicated that the glycosides of flavonoids could not be absorbed at intestine. They were hydrolyzed to their corresponding aglycone forms prior to absorption. As a result, the intestinal absorption and disposition mechanism was studied only for W and OA, rather than WG and OAG, on rat *in situ* perfusion model. The perfusate buffer loaded with 50 μM of W or OA was perfusated through the cannulated intestine segment. Perfusate and blood samples were collected from the outlet of the intestine and the mesenteric vein respectively. All samples were kept on ice until the end of the experiment. The blood samples were centrifugation at 16,000 g for 3 min and the plasma were transferred to another tube. All the perfusate and plasma samples were kept at -80 ° C until analysis.

4.3.2.5 Sample preparation

For the collected samples from perfusate, 500 μl of each perfusate sample was mixed with 200 μl of methanol and 100 μl of 20 % ascorbic acid. Then, 100 μl of above perfusate mixture was added with 20 μl internal standard (3, 7-dihydroxyflavone, 100 μg/ml) and 50 μl of the resultant solution was injected into HPLC system for analysis.

For the plasma samples collected from mesenteric blood, the plasma sample preparation followed the procedure described in section 3.2.4 of Chapter Three. Briefly, the Oasis® HLB cartridges were preconditioned with 1 ml of methanol, followed by 1 ml of 25 mM sodium dihydrogen phosphate buffer (pH 2.5). In 100 μl of plasma sample, 50 μl of 50% methanol in phosphate buffer (pH 2.5) comprising 1% ascorbic acid and 20 μl of internal

standard (3, 7-dihydroxyflavone, 10 μg/ml) were added. The mixture was diluted with 1 ml of 35% methanol in 25 mM sodium dihydrogen phosphate buffer (pH 2.5) containing 1% ascorbic acid. After vortexing for 15 sec and centrifuged at 16,000 ×g for 10 min, the supernatant was loaded onto the preconditioned HLB cartridge. The cartridge was flushed with 1 ml of 25 mM sodium dihydrogen phosphate buffer (pH 2.5) followed by 1 ml of 35% methanol in 25 mM sodium dihydrogen phosphate buffer (pH 2.5) containing 1% ascorbic acid. All the analytes were eluted by 1 ml methanol from the cartridge. The eluent was evaporated to dryness in a Centrivap concentrator, and the residue was reconstituted by 150 μl of 50% methanol in phosphate buffer (pH 2.5) comprising 1% ascorbic acid. After centrifugation at 16,000×g for 10 min, an aliquot of 100 μl supernatant was injected into HPLC system for analysis.

4.3.3   Chromatographic and instrumental conditions

To quantify the concentration of W and OA as well as their corresponding glucuronides after the study by Caco-2 cell monolayer model and rat *in situ* single-pass intestinal perfusion model, a HPLC/UV method has been established in Chapter Three. Furthermore, a LC-MS/MS method was employed to identify the corresponding metabolites of W and OA during the studies.

4.3.3.1 HPLC/UV analysis for the quantification of W, OA, WG and OAG

The instrumental and chromatographic conditions were described in the section 3.2.2.1 in Chapter Three.

The detection wavelength was set at 270 nm for the analysis of cell model samples and perfusate samples. Due to the interference from plasma sample, the detection wavelength was set at 320 nm for the analysis of plasma samples.

Due to the commercial unavailability of the standard compounds of WS and OAS, the concentrations of WS and OAS after the transport study in Caco-2 cell monolayer model was quantified indirectly based on the assumptions that WS/OAS has the same UV absorbance group as W/OA and one molar of W/OA produce one molar of WS/OAS. As a result, the calibration curve was firstly plotted with the molar concentrations of W/OA versus the peak area ratios of W/OA to IS. The molar concentration of WS/OAS was calculated based on their observed peak are ratios from the above calibration curve of W/OA.

4.3.3.2 LC-MS/MS analysis for identification of metabolites of W and OA

The LC-MS/MS system consisted of and ABI 2000 Q-Trap triple quadrupole mass spectrometer equipped with an electrospray ionization source (ESI), TWO Perkin-Elmer PE-200 series micro-pumps and auto-sampler (Perkin-Elmer, Norwalk, CT, USA). A thermo BDS Hypersil column (250 mm× 4.6 mm; 5 μm particle size) was eluted with a gradient program at a flow rate of 1 ml/min.

The elution gradient for LC analysis consisted of two solvent compositions: acetonitrile (A) and 0.04% formic acid (B). The gradient began with 20% eluent A. Then it was changed linearly to 40% A in 5 min and remained for further 11 min before changing

back to 20% A in 2 min. Prior to the ESI source, 80% of the LC eluent was split off and only 20% of the effluent was introduced.

The mass spectrometer was set at negative ionization mode. Other mass spectrometer parameters were: orifice voltage, -71V; ring voltage, -80V; nebulization gas, 45psi; auxiliary gas, 80 psi; nebulizer temperature, 400 °C. Other instrument parameters were: collision energy, 27 eV; cell entrance potential, 22 eV; cell exit potential, 16 eV.

4.3.3.3 Analysis of phenol red

Phenol red was used to monitor the integrity of intestinal epithelium and to adjust the concentration of analytes in perfusate. The concentrations of the analytes in the perfusate were corrected for the water flux as $Conc_{corrected}=Conc_{measured} \times$ (Phenol red)$_{in}$/(Phenol red)$_{out}$ before other calculations were performed. For the analysis of phenol red, 10 μl of sodium hydroxide (1M) was added into 200 μl of the perfusate samples after the study by rat *in situ* single-pass intestinal perfusion model to adjust the pH value. Then the concentrations of phenol red were determined using a 96-well plate reader at 595 nm (Bio-rad, Hercules, CA, USA).

4.3.4 Data analyses

4.3.4.1 Caco-2 cell monolayer model and MDCK cell lines

The permeability coefficients (P_{app}) of W, OA, WG and OAG on Caco-2 and MDCK cell model were calculated as described previously using the following equations (Artursson, and Karlsson, 1991).

$$P_{app} = [(dC/dt \times V)]/ (A \times C)$$

dC/dt: change of the drug concentration in the receiver chambers over time

V: volume of the solution in the receiver chambers (In the current setting, it was 2.6 cm^3 for apical to basolateral transport; 1.5 cm^3 for basolateral to apical transport)

A: membrane surface area (4.71 cm^2 for 6 well cell culture plate)

C: loading concentration in the donor chambers

Besides, the percentage of metabolism of W and OA during their intestinal absorption on Caco-2 cell monolayer model was calculated according to the following equation, in which "AP" represented cumulative amount in apical side, "BL" represented cumulative amount in basolateral side and "uptake" represented cell uptake.

$$\% \text{ of metabolism} = \frac{\Sigma metabolite_{(AP+BL+uptake)}}{\Sigma parent\ drug_{(AP+BL+uptake)} + \Sigma metabolites_{(AP+BL+uptake)}}$$

All the values were presented as mean ± SD. Statistically significant difference between two groups or more than two groups was evaluated by Student's t-test and one-way ANOVA respectively. A $p < 0.05$ was considered significant for all tests.

4.3.4.2 Rat in situ single-pass intestinal perfusion model

Permeability coefficients of parent drugs were calculated based on the appearance of the compounds in the mesenteric blood (P_{blood}) and the disappearance of the compound in the perfusate (P_{lumen}) according to the following equations.

$$P_{blood} = \frac{dX/dt}{AC_0}$$ (Amidon et al., 1980, Johnson et al., 2003)

Where dX/dt is the rate of drug appearance in mesenteric blood, A is the area of the perfusated intestine segment and C_0 is the initial drug concentration in the perfusate buffer.

$$P_{lumen} = -\frac{Q}{A} \ln \frac{C_{out}}{C_{in}}$$ (Cummins et al., 2003)

Where A is the area of the perfused intestine segment, Q is the perfusion flow rate, C_{in} is the drug concentration in the inlet of the perfusate entering the intestinal segment, C_{out} is the drug concentration in the exiting perfusate at the steady state.

Cummins's extraction ratio (ER) was employed to evaluate the extent of intestinal metabolism of W and OA (Cummins et al., 2003). Cummins's ER was the ratio of the total amount of metabolites found during the perfusion process divided by a sum of the total amount of metabolites formed and the parent compound present in the mesenteric blood.

$$ER = \frac{\Sigma metabolite_{(perfusate+blood)}}{\Sigma parent\ drug_{(blood)} + \Sigma metabolites_{(perfusate+blood)}}$$

4.4   Results

4.4.1   Caco-2 cell and MDCK cell monolayer models

4.4.1.1 Stabilities of W, OA, WG and OAG in transport buffer

The results of stability test were shown in Fig. 4.1. After incubation, the percentages of compound remaining of W, OA, WG and OAG were around 100%, indicating that the four compounds would be stable at 37 °C in the transport buffer for at least 3 h.
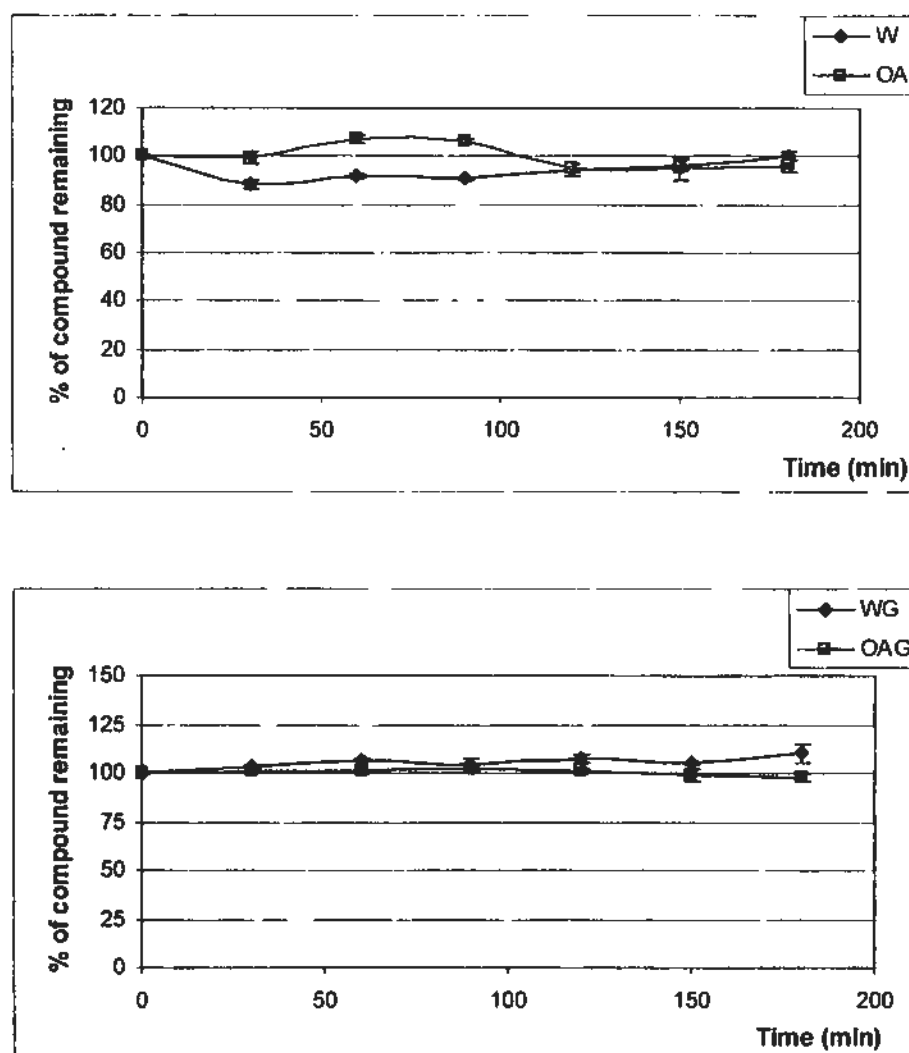
Fig. 4.1   **Stabilities of W, OA, WG and OAG in transport buffer (PBS⁺, pH 6.0) under 37 °C for 3 h (n=3)**

4.4.1.2 Cytotoxicities of W, OA, WG and OAG to Caco-2 cell and MDCK cells

As shown in Fig. 4.2 and Fig. 4.3, the relative absorbance of the studied flavones to the negative control showed no decrease. The results indicated that the four flavones had no cytotoxicity to Caco-2 cells and MDCK cells at the tested concentrations range.
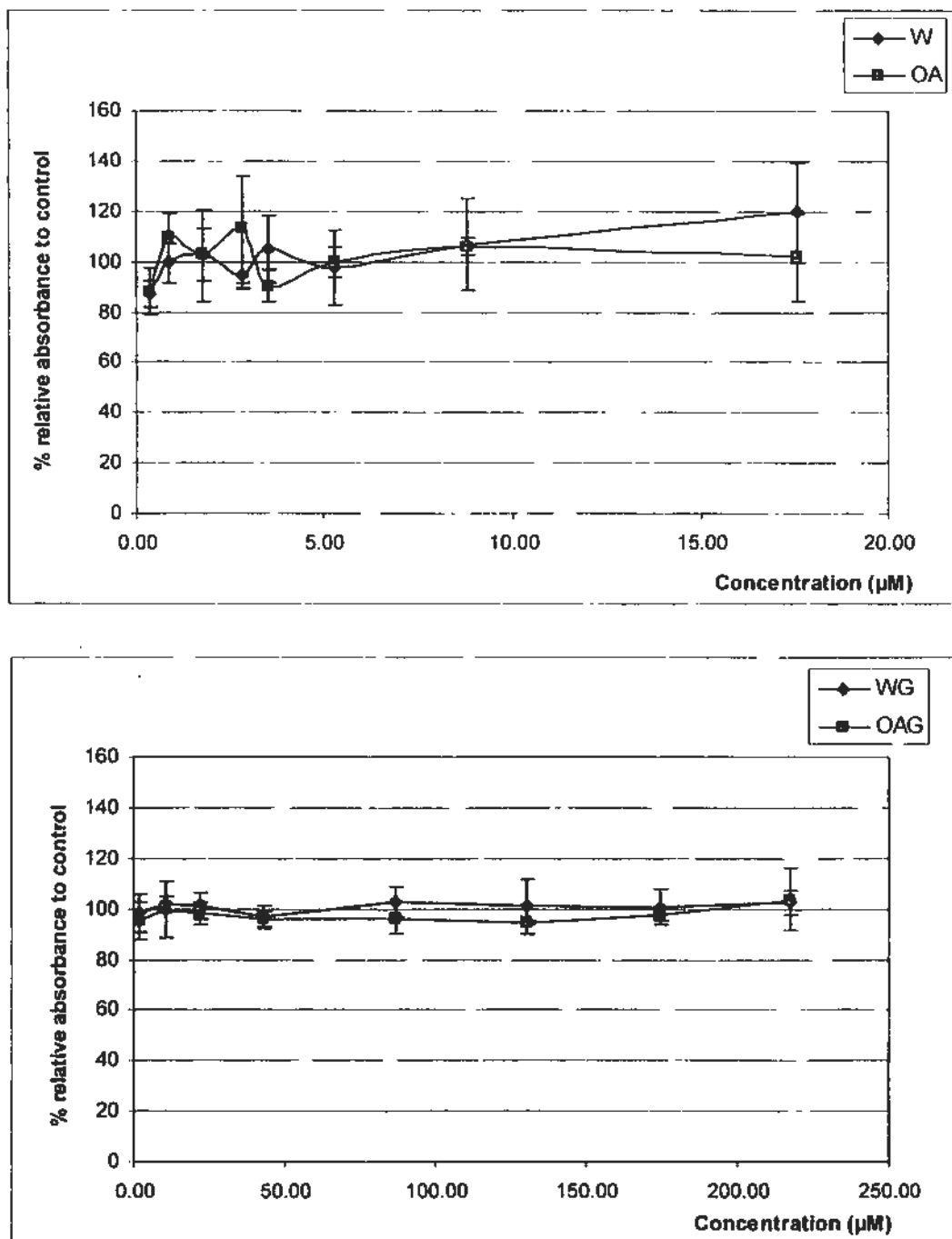
Fig. 4.2   **Cytotoxicities of W, OA, WG and OAG to Caco-2 cells by MTT assay**
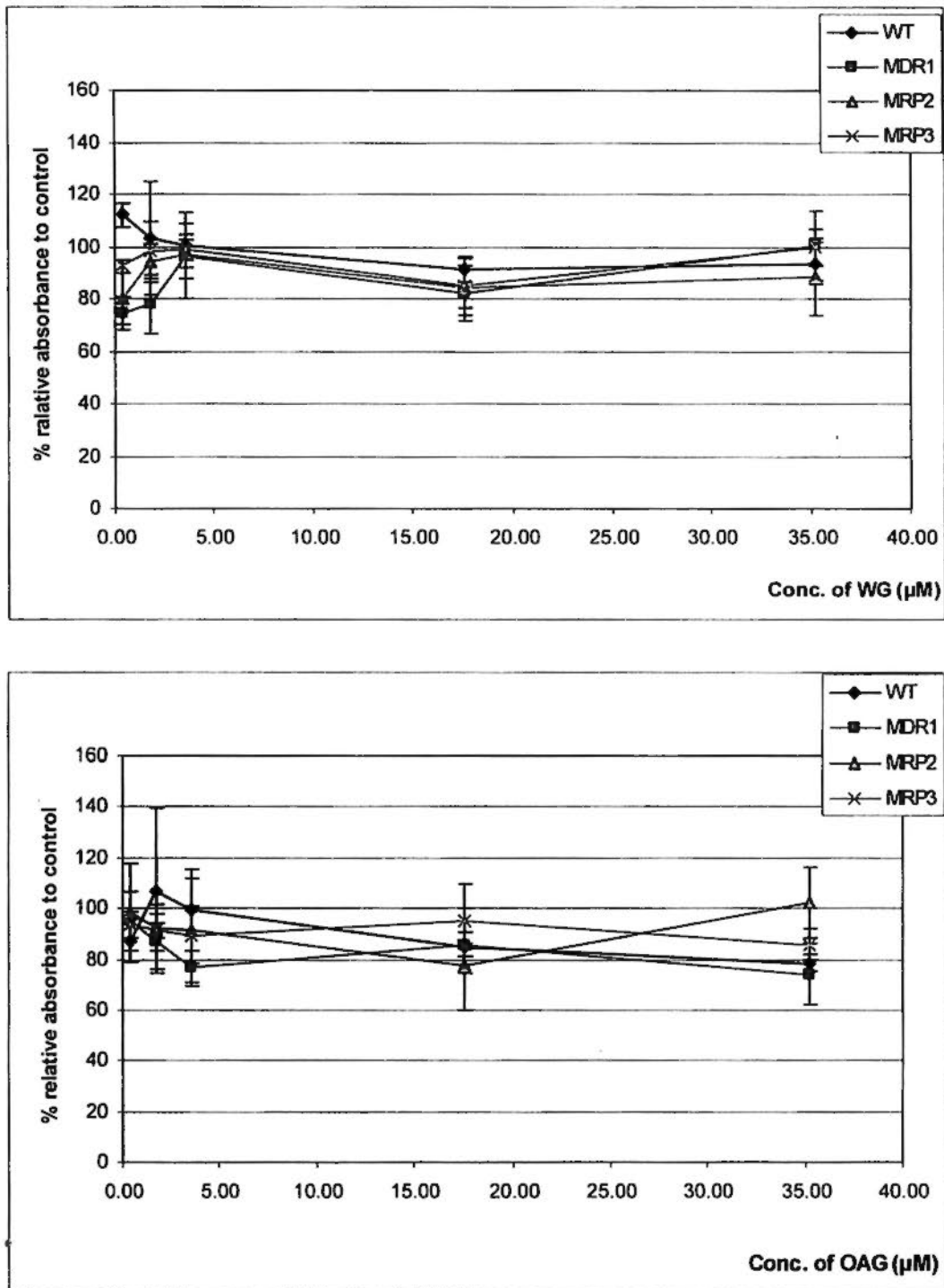
Fig. 4.3   Cytotoxicities of WG and OAG to MDCK cells by MTT assay
WT: wild type of MDCK cell
MDR1: MDCK cell transfected with human MDR1 gene
MRP2: MDCK cell transfected with human MRP2 gene
MRP3: MDCK cell transfected with human MRP3 gene

4.4.1.3 Identification of metabolites of W and OA in Caco-2 cell model

During the bidirectional transport studies of W and OA, there were two metabolites identified for both flavones at both sides of the Caco-2 cell monolayer model (Fig. 4.4a and Fig. 4.4b).

The UV spectra of both metabolites resembled those of W and OA, respectively. In the HPLC/UV chromatograms of the transport study samples of W and OA, there were two more peaks appearing in addition to the peaks of the parent compounds. The retention times of their first elutes were identical to those of WG and OAG, respectively. Moreover, the LC-MS/MS analysis at negative ion mode demonstrated that the molecular ion of the first elutes were at the m/z of 459 and the major fragment of this molecular ion were at m/z of 283 indicating the loss of glucuronic acid moiety (176 amu). For the second elutes, their molecular ion appeared at m/z of 363 and their major fragment ion were at m/z of 283, indicating the loss of sulfate acid moiety (80 amu) (Fig. 4.5a and Fig. 4.5b). Consequently, W and OA were suggested to be metabolized as the conjugates of glucuronic acid and sulfate during their bidirectional transport in Caco-2 cell monolayer model.
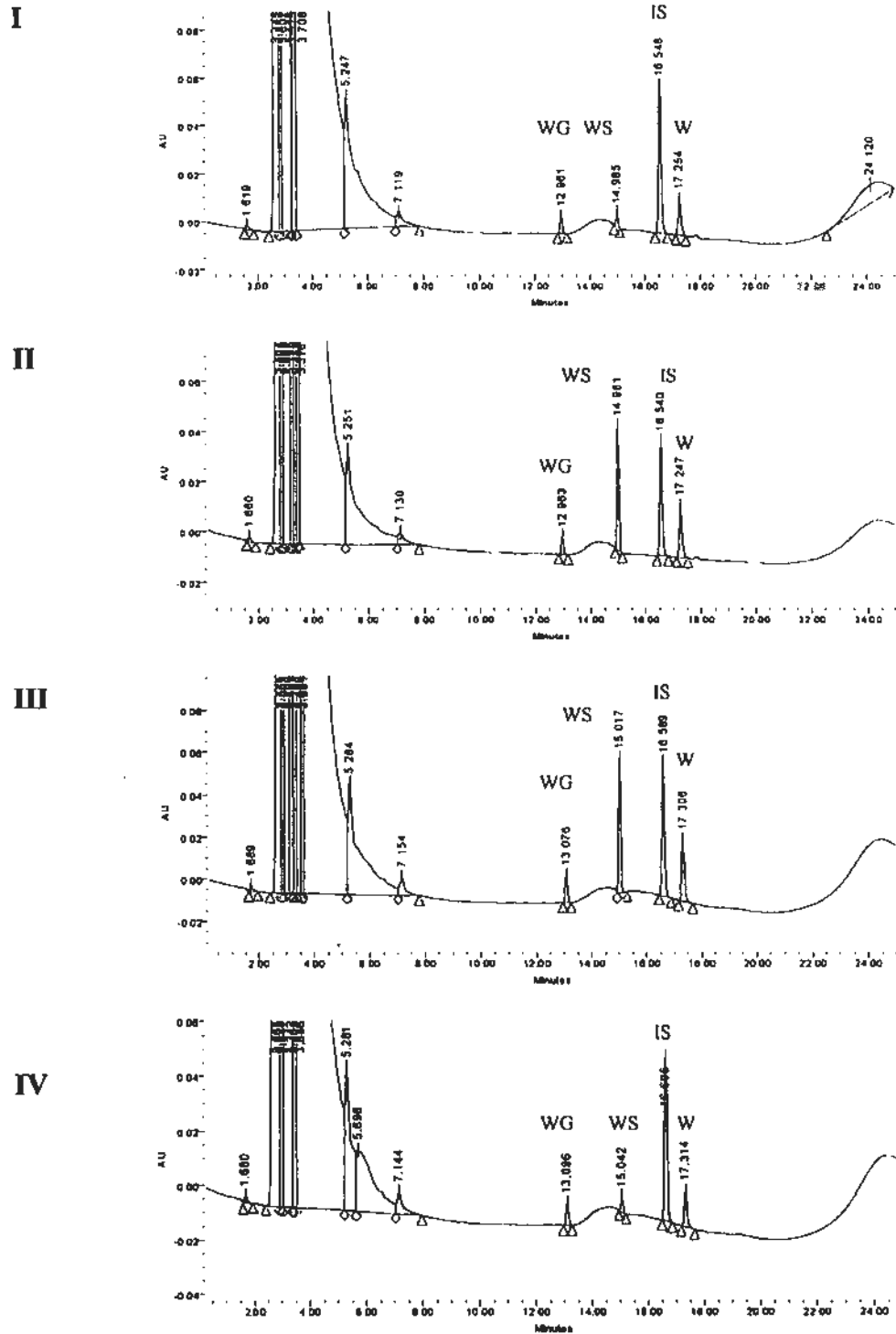
Fig. 4.4a   **Representative HPLC/UV chromatograms of basolateral sample (I), apical sample (II) in apical to basolateral transport of W as well as apical sample (III) and basolateral sample (IV) in basolateral to apical transport study of W**
W: wogonin; WG: wogonoside; WS: sulfate of W
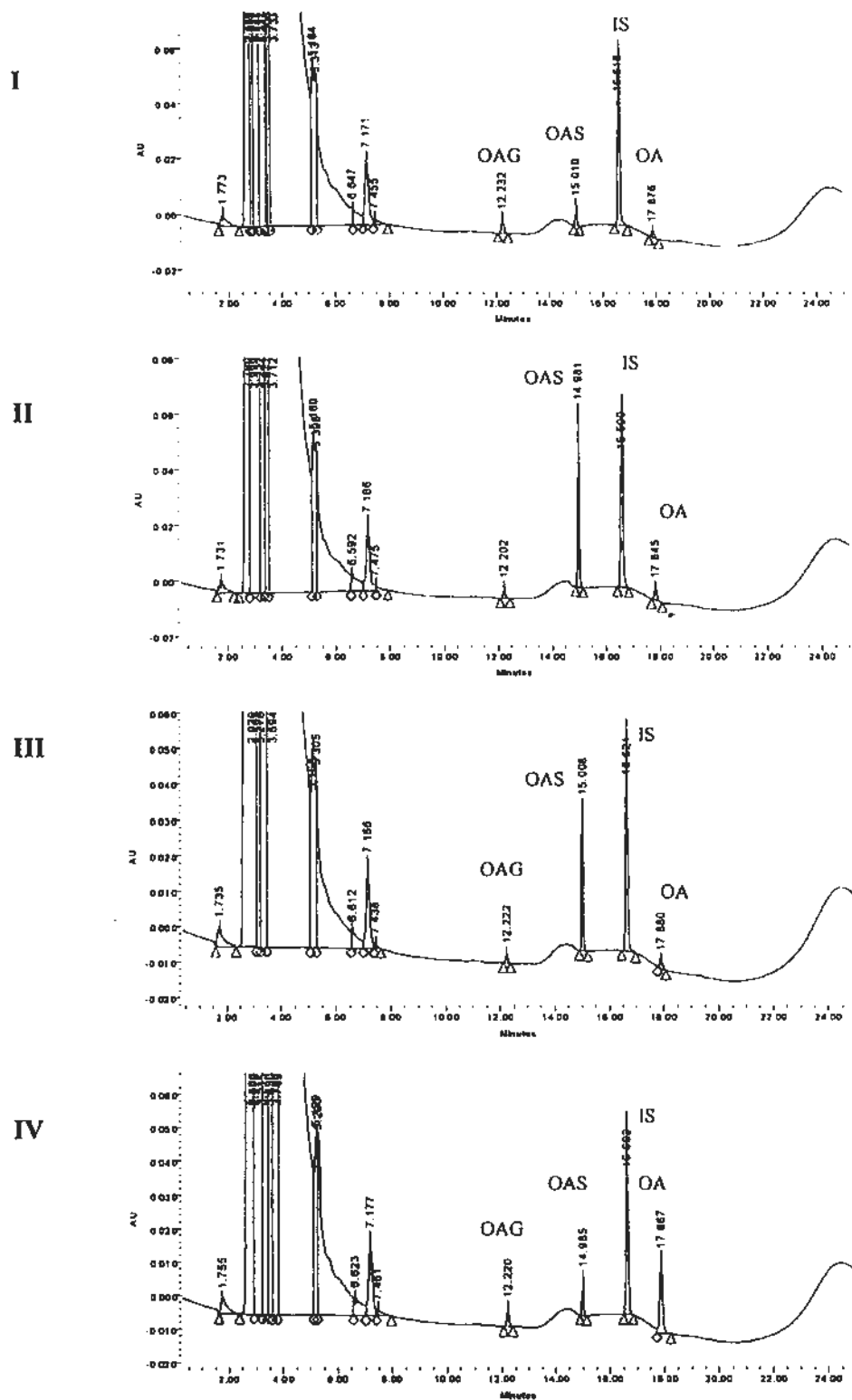
Fig. 4.4b Representative HPLC/UV chromatograms of basolateral sample (I), apical sample (II) in apical to basolateral transport of OA as well as apical sample (III) and basolateral sample (IV) in basolateral to apical transport study of OA

OA: oroxylin A; OAG: oroxylin A-7-O-glucuronide; OAS: sulfate of OA
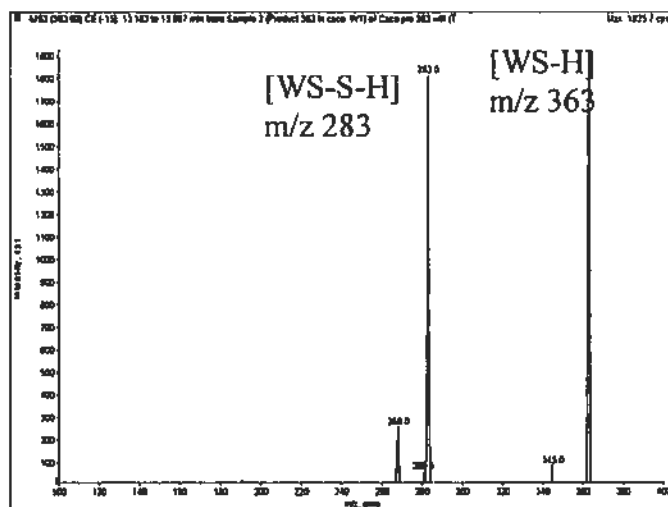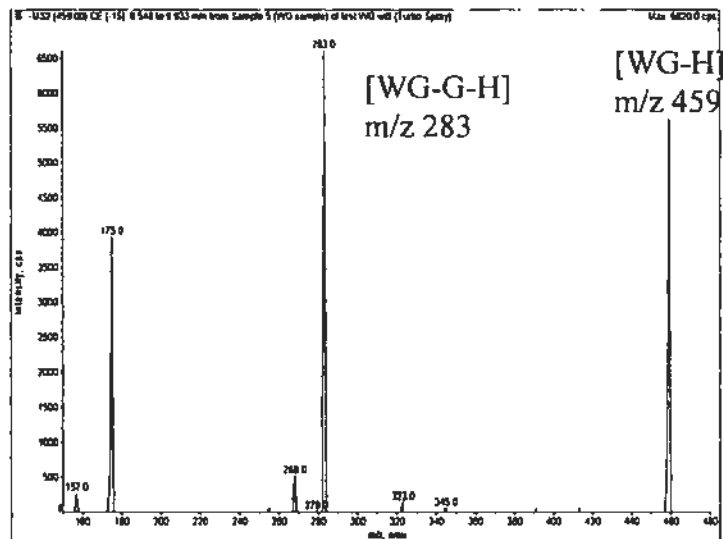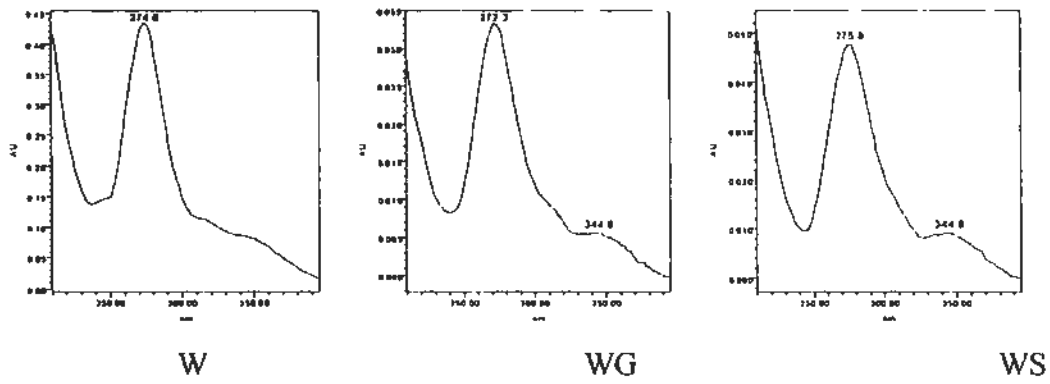
Fig. 4.5a   UV and mass spectra of two metabolites of W found in Caco-2 cell
monolayer model
W: wogonin; WG: wogonoside; WS: sulfate of W

OA   OAG   OAS

[OAG-G-H]

[OAG-H]
m/z 459

[OAS-S-H]
m/z 283

[OAS-H]
m/z 363
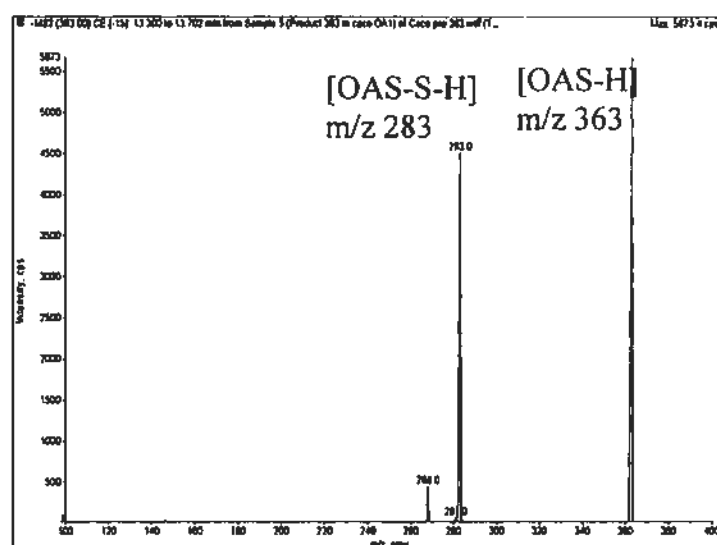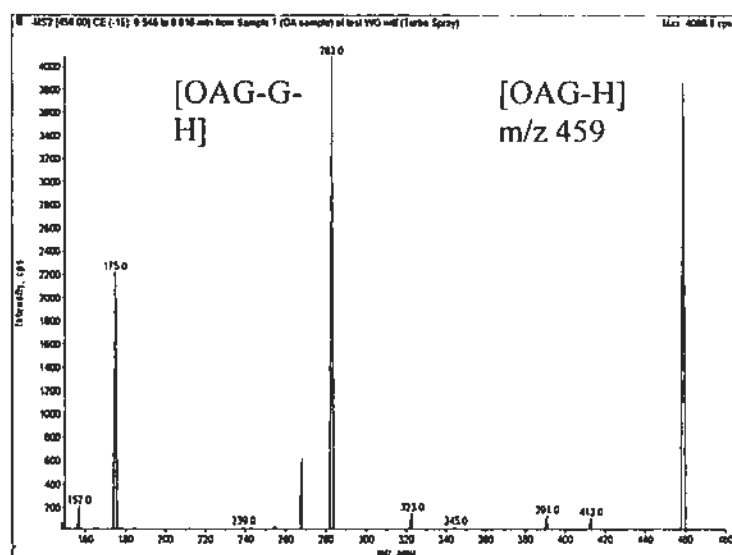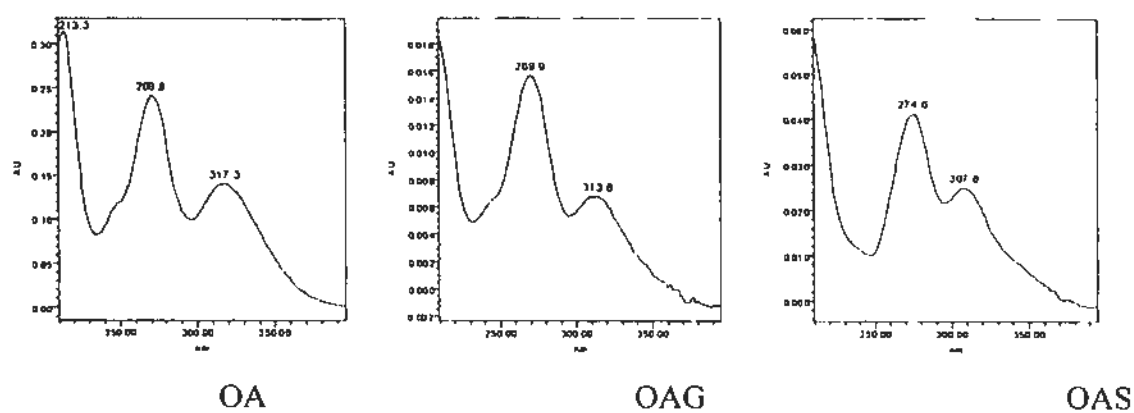
Fig. 4.5b   **UV and mass spectra of two metabolites of OA found in Caco-2 cell monolayer model**

OA: oroxylin A; OAG: oroxylin A-7-*O*-glucuronide; OAS: sulfate of OA

4.4.1.4 Transport and metabolism of W and OA on Caco-2 cell model

Due to the similarity in chemical structure, the transport and metabolism of W and OA showed similar profiles in Caco-2 cell monolayer model. The amount of W or OA at receiver side increased linearly over the 2 h transport study. The apparent permeability from absorptive transport of W and OA were $12.64\pm0.55\times10^{-6}$ cm/sec at 18.94 μM and $5.73\pm0.19\times10^{-6}$ cm/sec at 17.36 μM, respectively, which demonstrated an efficient permeability of both W and OA (Artursson and Karlsson, 1991; Yee, 1997). Besides, the P_{app} values of W and OA at low and high concentrations demonstrated no dose dependence, indicating that there might not be any active transport involved.

During their bidirectional transport, extensive Phase II metabolism has been observed for both W and OA. The formation of their glucuronic acid and sulfate conjugates of W and OA were also monitored. It was found that the amount of these metabolites increased linearly versus time at both apical side and basolateral side in the bidirectional transport study. The percentage of metabolism (Section 4.3.4.1) showed a tendency of decrease with the increase of loading concentration, indicating a saturation profile of metabolism (Table 4.1a and Table 4.1b). Over the 2 h transport study, the amount of W and OA as well as their metabolites increased linearly versus time (Fig. 4.6 a-d). At the same loading concentration, the extent of sulfation was greater than the extent of glucuronidation for both W and OA. Comparison of the total amount of glucuronides and sulfates at different loading concentrations showed a different saturation behavior for glucuronidation and sulfation. Sulfation was saturated at 3.79 μM for W and at 3.47 μM for OA, whereas glucuronidation showed a linear increase over the studied loading concentration range

(Fig. 4.7a and Fig. 4.7b). Without considering the amount trapped intracellularly, the amount of WG or OAG transported to apical and basolateral side had significant difference ($p<0.05$). It was observed that the formed WG or OAG was preferentially extruded to the basolateral side whereas the formed WS or OAS was easier to reach the apical side regardless of the side of loading (Fig. 4.8 a-d).

Table 4.1a   **Bidirectional transport permeability and metabolism of W in Caco-2 cell monolayer model**

Loading Concentration of W (µM)	A to B		B to A	
	P_{app} ($\times 10^{-6}$ cm/s)	% of metabolism	P_{app} ($\times 10^{-6}$ cm/s)	% of metabolism
3.79	N.D.	95.92±2.16	N.D.	53.02±0.34
7.58	10.50±2.91	53.09±5.13	7.29±1.25	43.80±1.31
18.94	12.64±0.55	32.11±0.98	8.96±1.36	28.45±1.35

A to B: apical to basolateral transport
B to A: basolateral to apical transport

Table 4.1b   **Bidirectional transport permeability and metabolism of OA in Caco-2 cell monolayer model**

Loading Concentration of OA (µM)	A to B		B to A	
	P_{app} ($\times 10^{-6}$ cm/s)	% of metabolism	P_{app} ($\times 10^{-6}$ cm/s)	% of metabolism
3.47	N.D.	99.79±0.02	N.D.	79.02±1.09
6.94	2.91±0.44	90.31±0.20	4.43±0.90	67.68±1.14
17.36	5.73±0.19	55.62±1.91	5.62±0.55	36.77±1.55

A to B: apical to basolateral transport
B to A: basolateral to apical transport
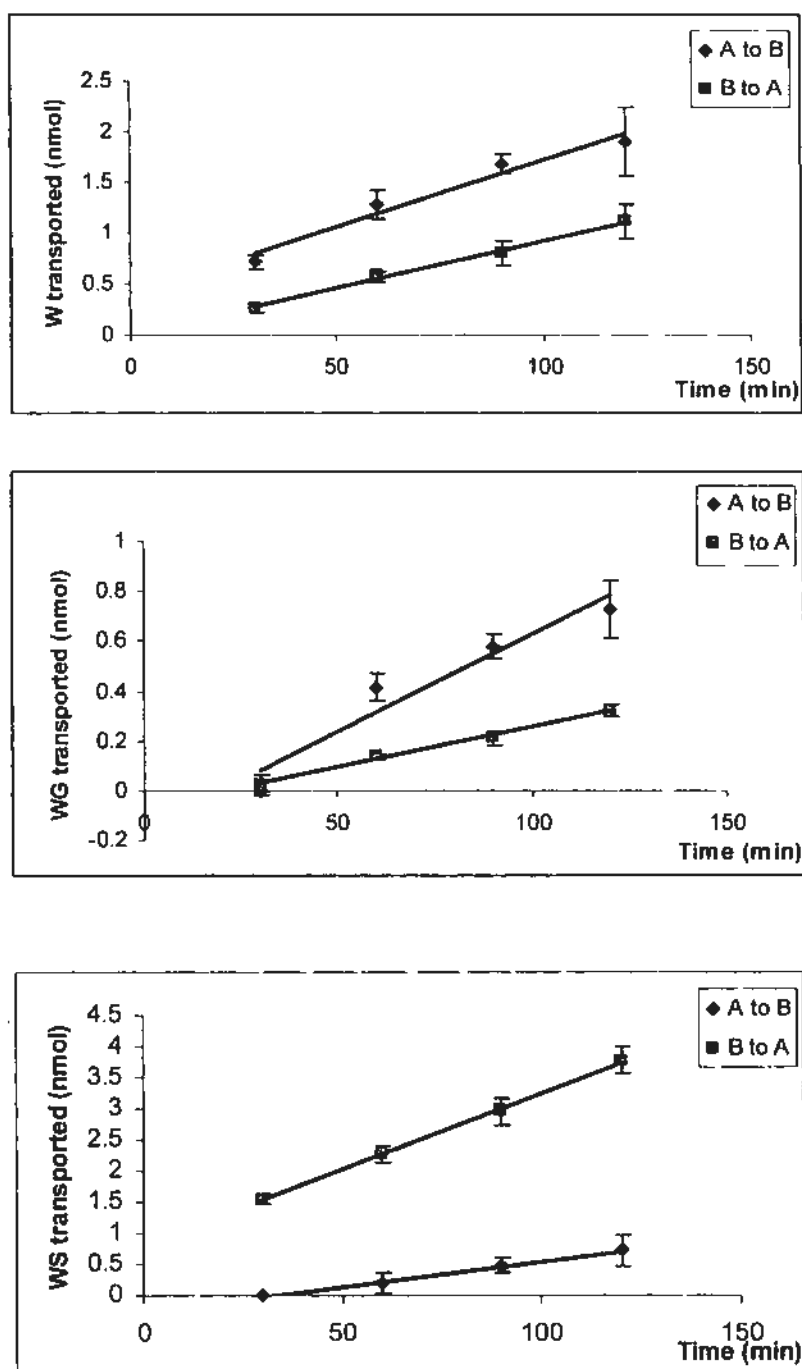
Fig. 4.6a   Cumulative amount of W, WG and WS at the receiver side as a function of time in the bidirectional transport of W (7.58 μM) in Caco-2 cell monolayer model

W: wogonin, WG: wogonoside, WS: sulfate of wogonin

A to B: apical to basolateral transport, B to A: basolateral to apical transport
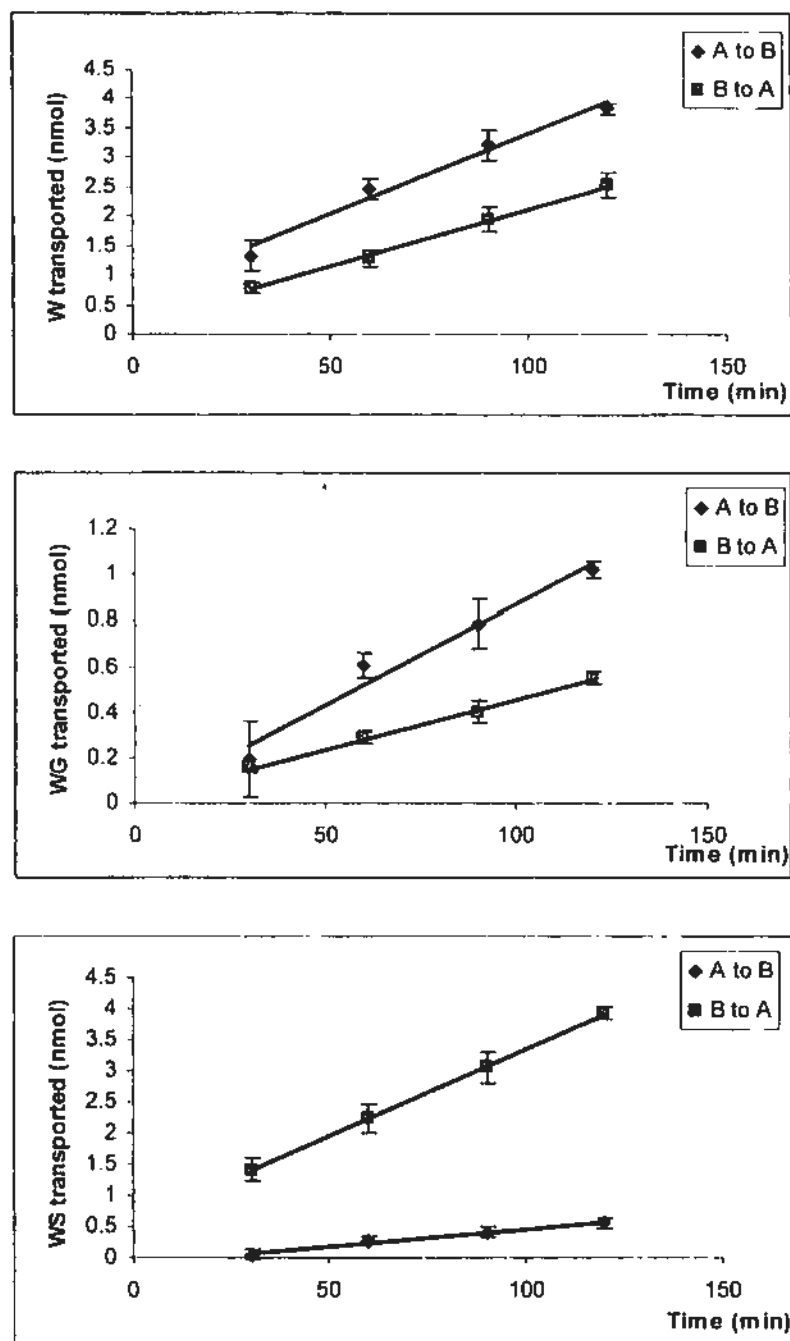
Fig. 4.6b   Cumulative amount of W, WG and WS at the receiver side as a function of
time in the bidirectional transport of W (18.94 μM) in Caco-2 cell monolayer
model
W: wogonin, WG: wogonoside, WS: sulfate of wogonin
A to B: apical to basolateral transport, B to A: basolateral to apical transport
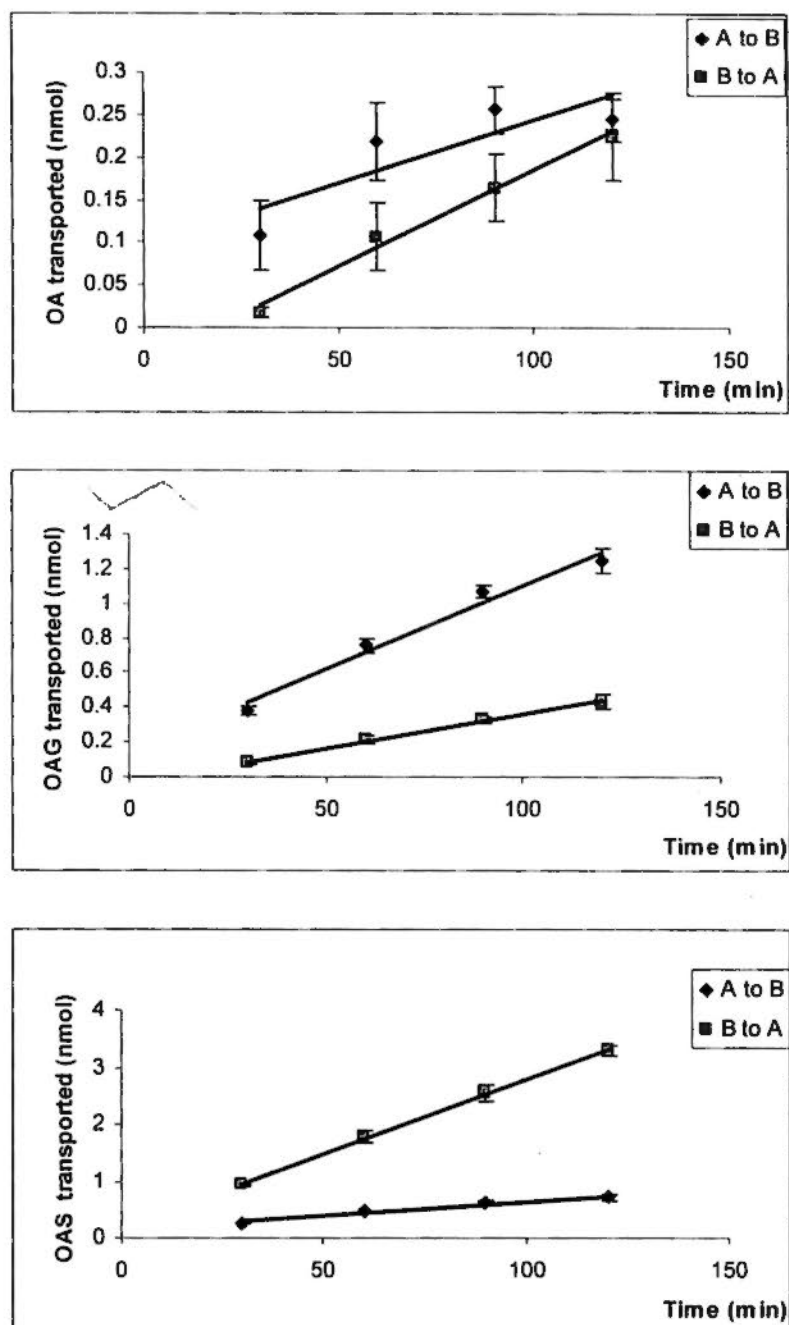
Fig. 4.6c   Cumulative amount of OA, OAG and OAS at the receiver side as a function of time in the bidirectional transport of OA (6.94 µM) in Caco-2 cell monolayer model
OA: oroxylin A, OAG: oroxylin A-7-glucuronide, OAS: sulfate of oroxylin A
A to B: apical to basolateral transport, B to A: basolateral to apical transport
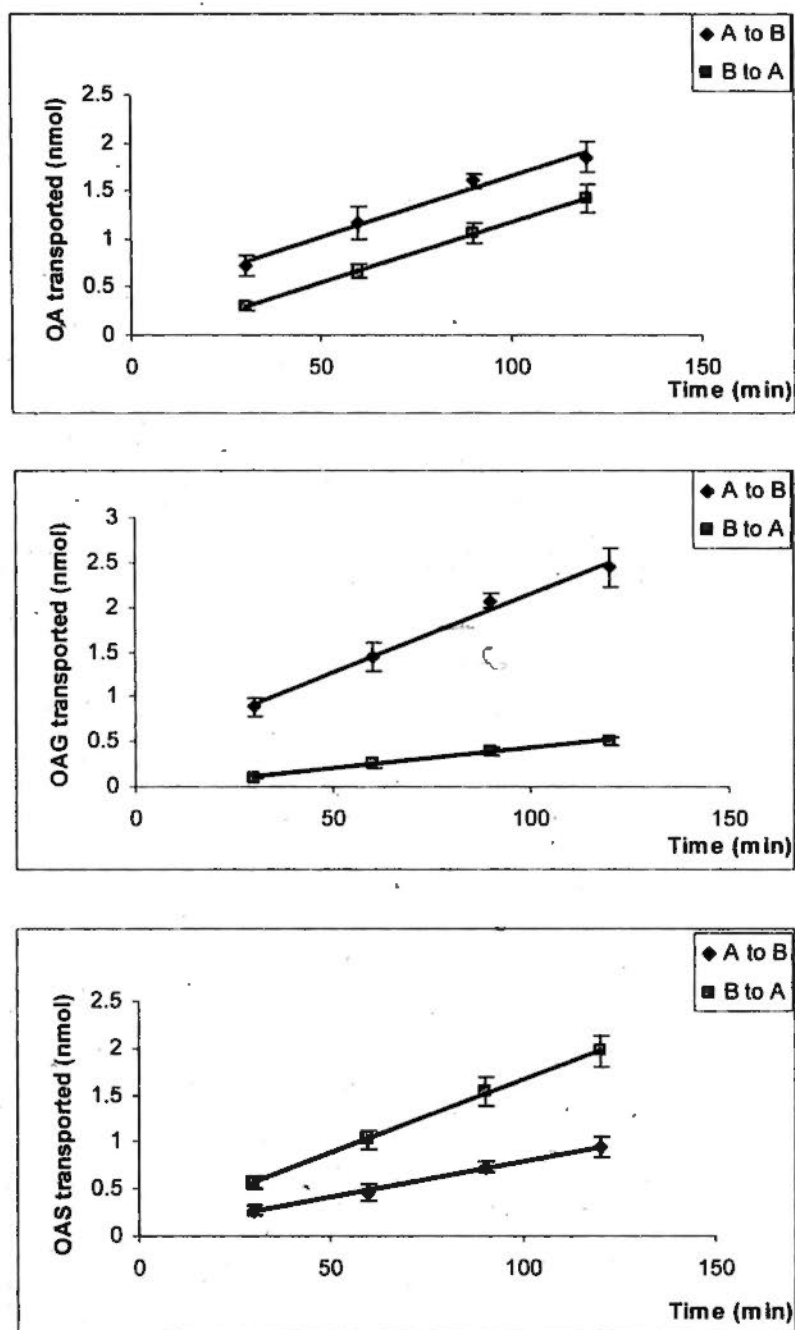
Fig. 4.6d   Cumulative amount of OA, OAG and OAS at the receiver side as a function of
time in the bidirectional transport of OA (17.36 µM) in Caco-2 cell monolayer
model
OA: oroxylin A, OAG: oroxylin A-7-glucuronide, OAS: sulfate of oroxylin A
A to B: apical to basolateral transport, B to A: basolateral to apical transport
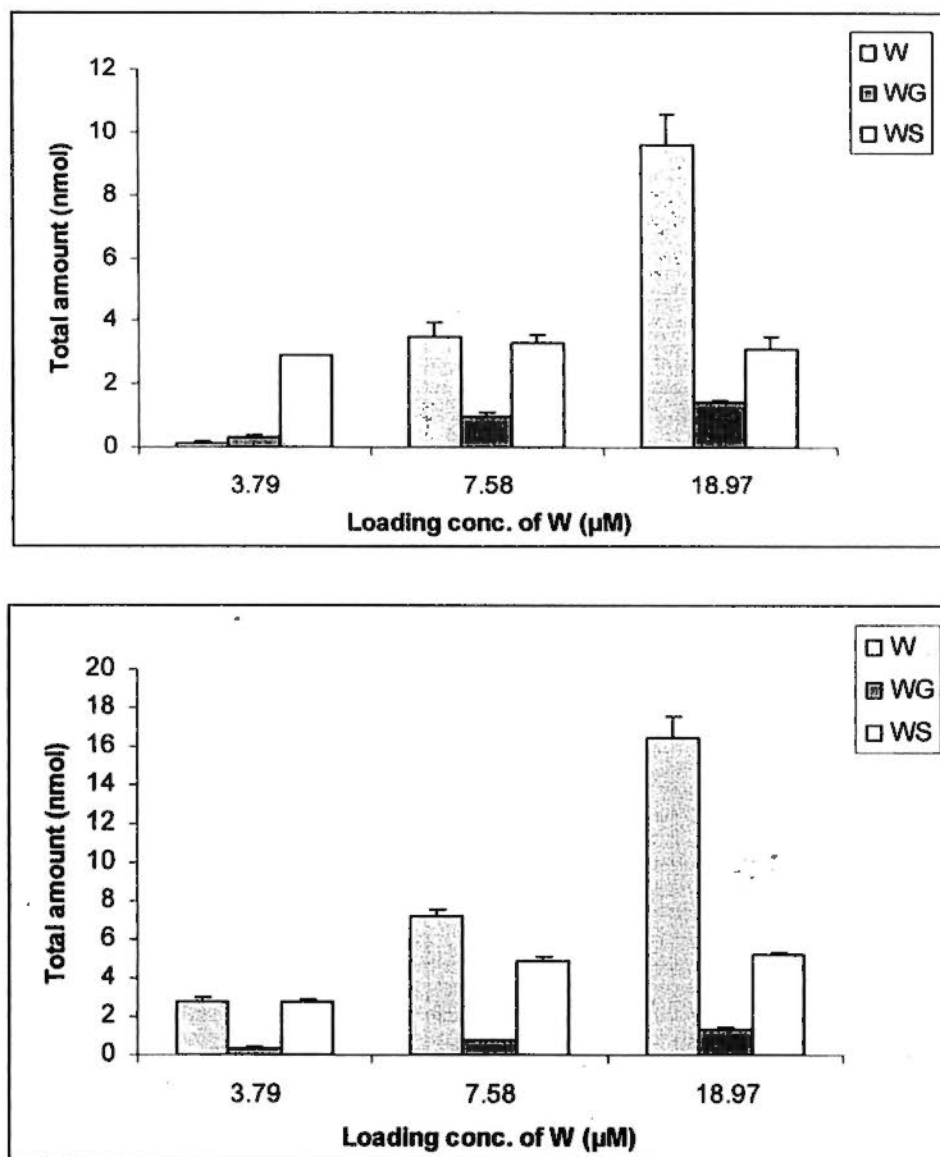
Fig. 4.7a   Total amount (basolateral side + apical side +intracellular amount) of W and its metabolites formed during apical to basolateral transport (upper) and basolateral to apical transport of W (lower) on Caco-2 cell monolayer model
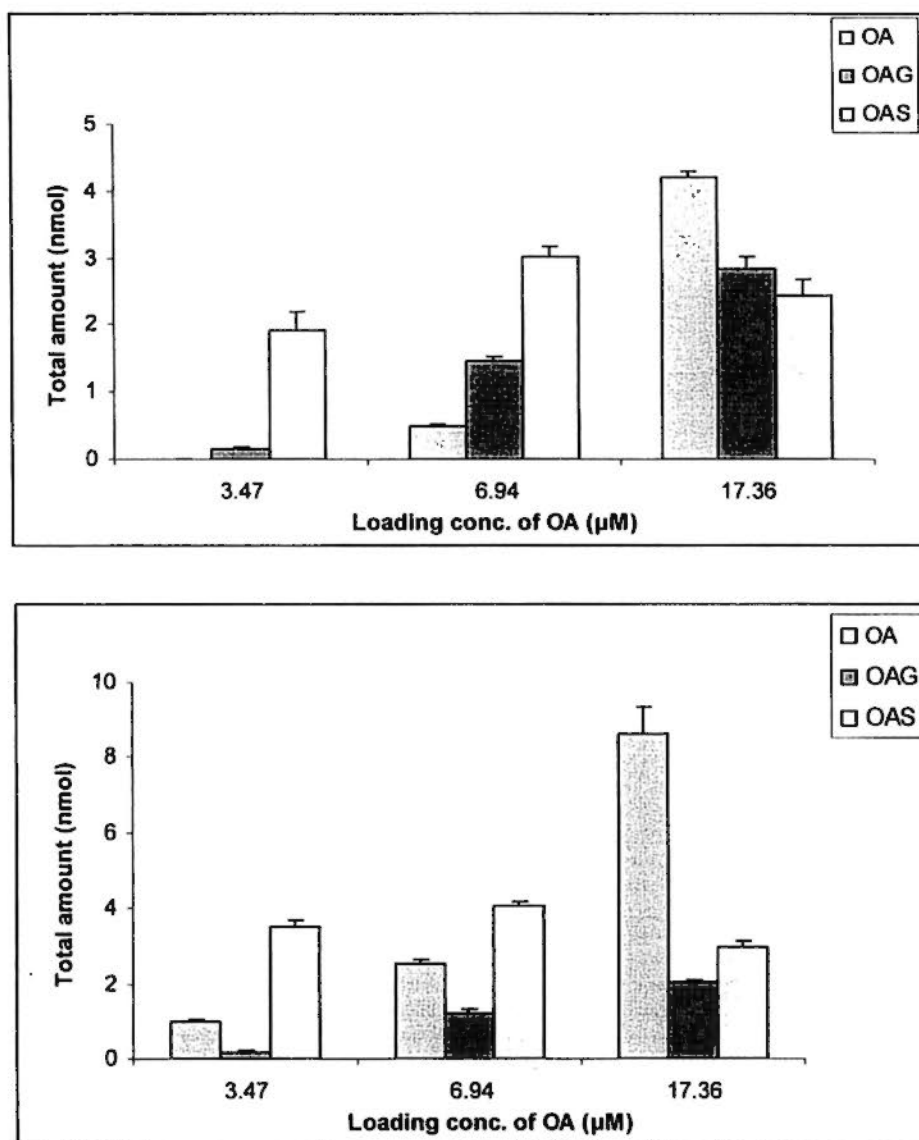
Fig. 4.7b **Total amount (basolateral side + apical side +intracellular amount) of OA and its metabolites formed during apical to basolateral transport (upper) and basolateral to apical transport of OA (lower) on Caco-2 cell monolayer model**
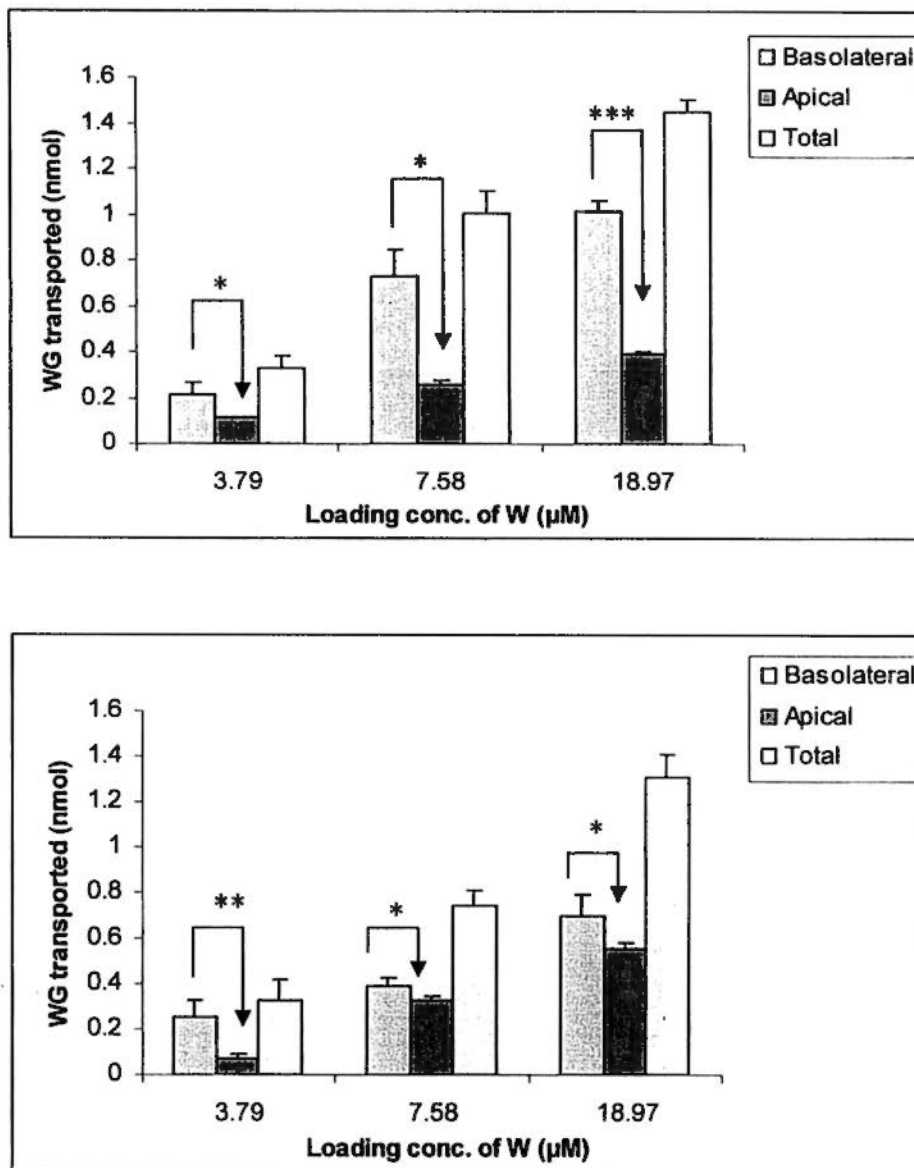
Fig. 4.8a **Efflux transport of WG during bidirectional transport of W at various concentrations: apical to basolateral transport (upper) and basolateral to apical transport (lower) in Caco-2 cell monolayer model *: $p<0.05$, **: $p<0.01$, ***: $p<0.001$**
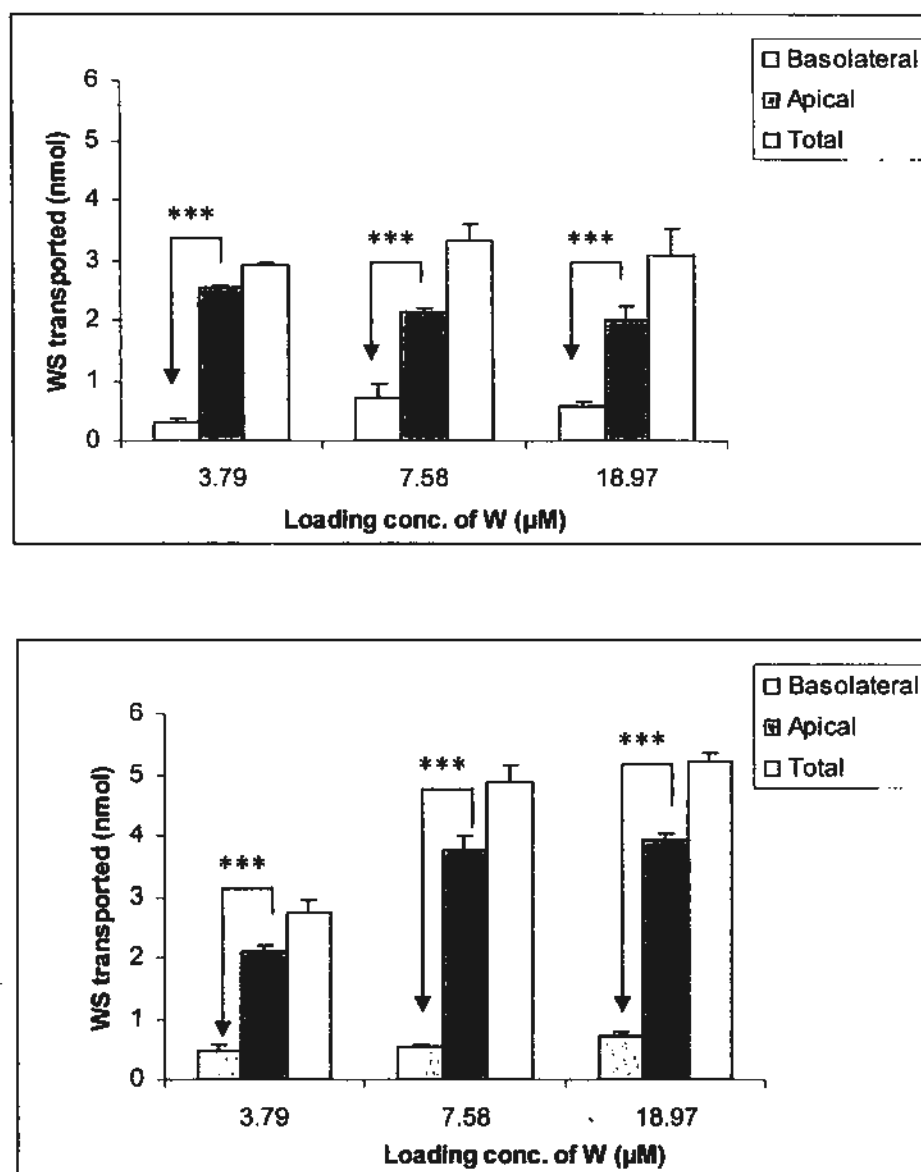
Fig. 4.8b   **Efflux transport of WS during bidirectional transport of W at various concentrations: apical to basolateral transport (upper) and basolateral to apical transport (lower) in Caco-2 cell monolayer model**
***: $p<0.001$
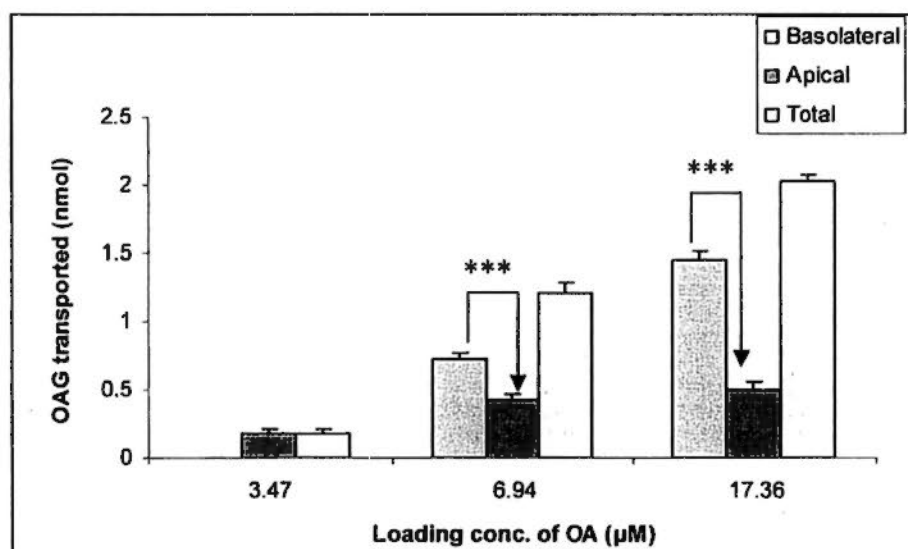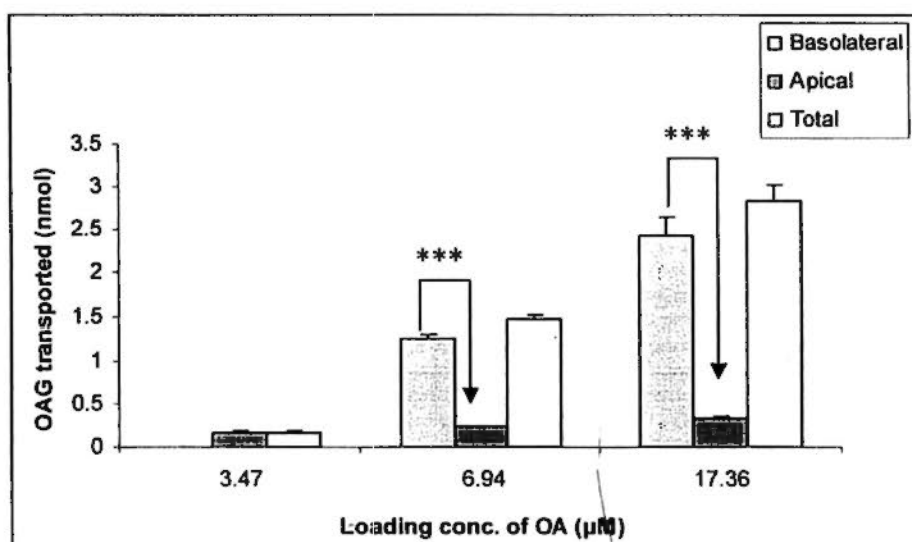
Fig. 4.8c   Efflux transport of OAG during bidirectional transport of OA at various concentrations: apical to basolateral transport (upper) and basolateral to apical transport (lower) in Caco-2 cell monolayer model
***: p<0.001
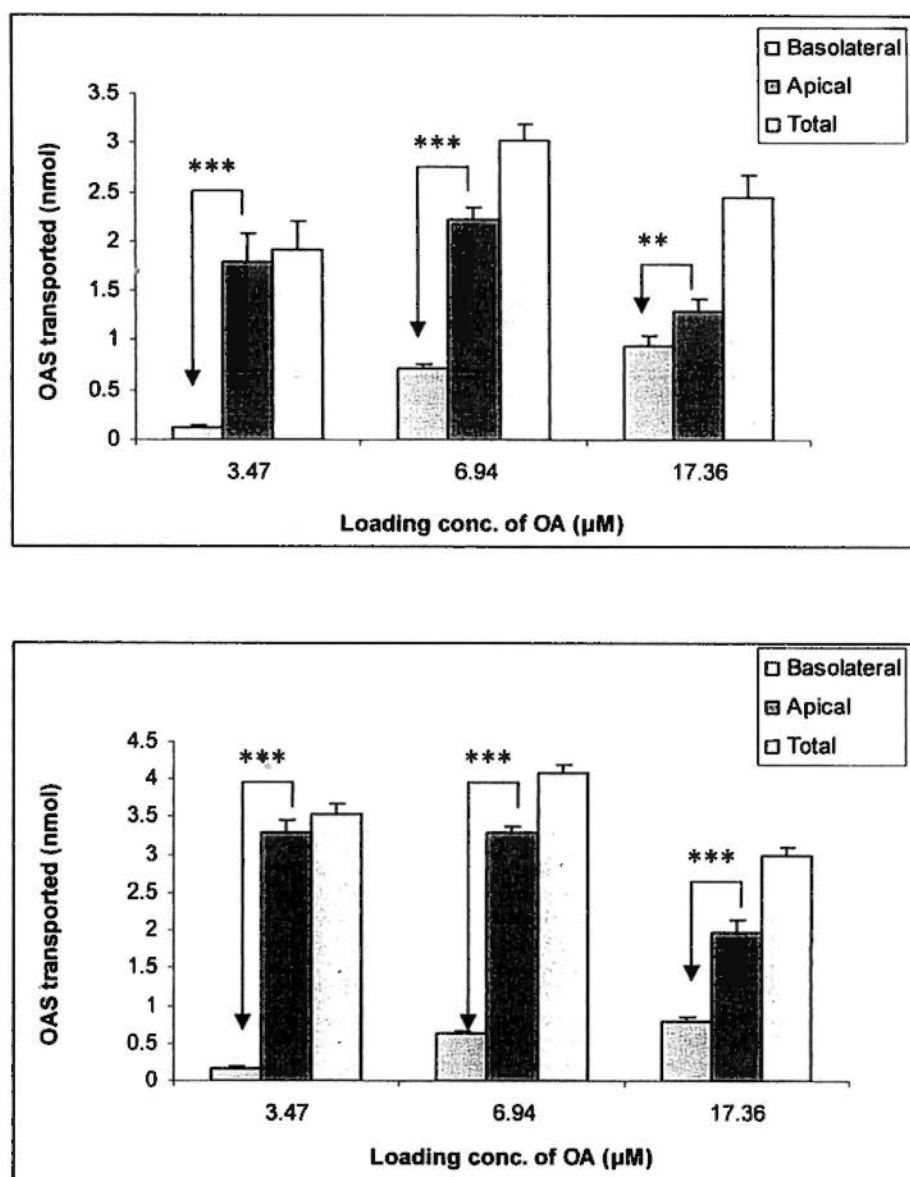
Fig. 4.8d   **Efflux transport of OAS during bidirectional transport of OA at various concentrations: apical to basolateral transport (upper) and basolateral to apical transport (lower) in Caco-2 cell monolayer model**
**: $p<0.01$, ***: $p<0.001$

4.4.1.5 Dose-dependent transport of WG and OAG

The transport profile of WG and OAG showed difference between the apical to basolateral transport and basolateral to apical transport. Both glycosides could not be detected at the receiver side in the apical to basolateral transport study at the concentration of 43.48 μM or below. On the contrary, their P_{app} value in the basolateral to apical transport study decreased with the increase of loading concentration. The transport kinetics complied with a saturable profile with WG saturated at 33.98 μM and OAG saturated at 43.48 μM (Fig. 4.9).
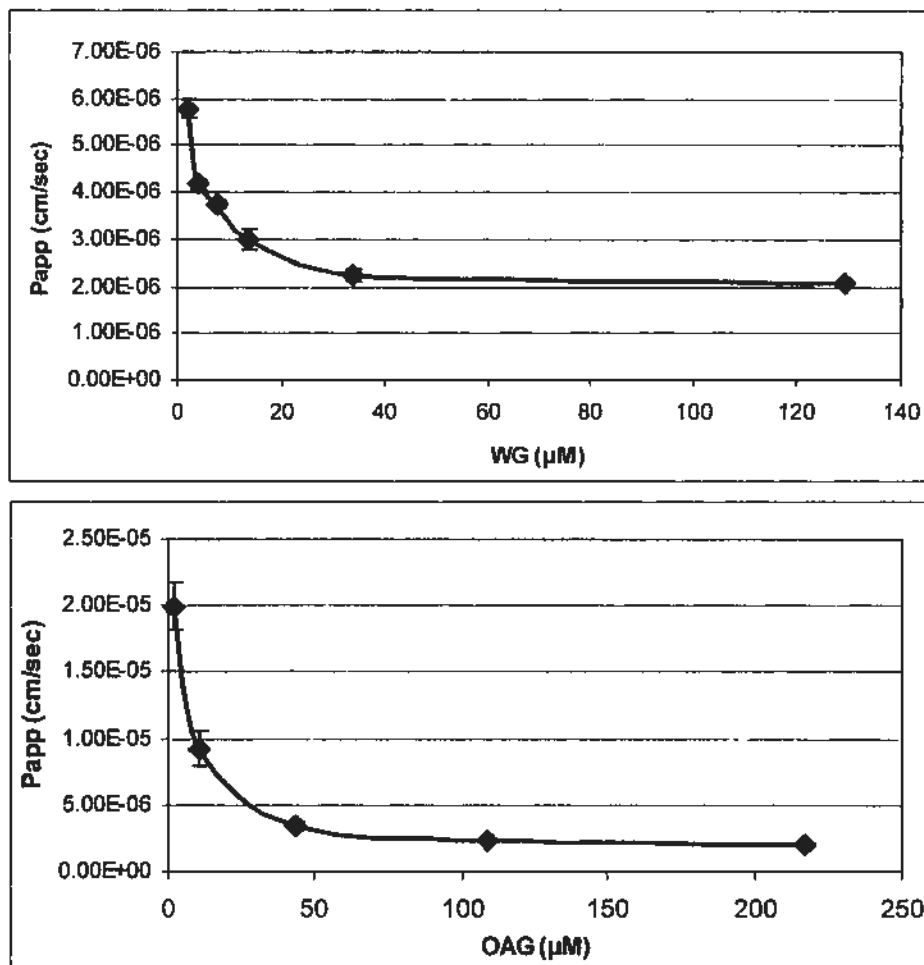
Fig. 4.9 P_{app} values of WG (upper) and OAG (lower) in their basolateral to apical transport at various loading concentrations in Caco-2 cell monolayer model

4.4.1.6 Transport inhibition study during the absorptive transport of W and OA in Caco-2 cell model

Our previous transport studies of WG and OAG in section 4.4.1.4 have proved that they could not pass through the membrane in the apical to basolateral direction. However, both glucuronic acid and sulfate conjugates could be detected in both apical and basolateral samples after the bidirectional transport study of their parent flavones. This suggested that they might be the substrate of the efflux membrane transporters. This part of experiment was conducted to identify the potential transporters that might be involved in the efflux of their metabolites during the absorptive transport of W and OA at the loading concentration of 17.60 μM. The results showed that the basolateral transport of WG was significantly inhibited by verapamil (Vera), estrone 3-sulfate (ES), estradiol glucuronide (EG), mitoxantrone (MTX) and MK571 (MK); ES, EG, MTX and MK were found capable of inhibiting the apical transport of WG, indicating the involvement of P-gp, MRPs and BCRP in the apical and basolateral transport of BG. Among the tested inhibitors, ES and MK showed significant inhibition effect on the basolateral transport of WS; the apical transport of WS was strongly inhibited by Vera, MTX and MK, suggesting the role of P-gp, MRPs and BCRP in the apical and basolateral transport of WS.

Due to the detection interference from the possible impurities in EG standard compound , the inhibition effect of EG was not conducted on OA. It was found that the basolateral transport of OAG was inhibited only by MK, while the apical transport of OAG could be significantly inhibited by Vera, MTX, ES and MK, indicating the involvement of P-gp,

MRPs and BCRP in the apical and basolateral transport of OAG. The basolateral and apical transport of OAS were only inhibited by MK, while the basolateral transport of OAS could be significantly inhibited by ES and MK, indicating the involvement of MRPs in the apical and the basolateral transport of OAS. Based on the inhibition extent of the tested inhibitor/substrate as shown in Fig. 4.10a and Fig. 4.10b, it was concluded that MRPs might be the most potent membrane transporter involved in the efflux of WG, OAG, WS and OAS.
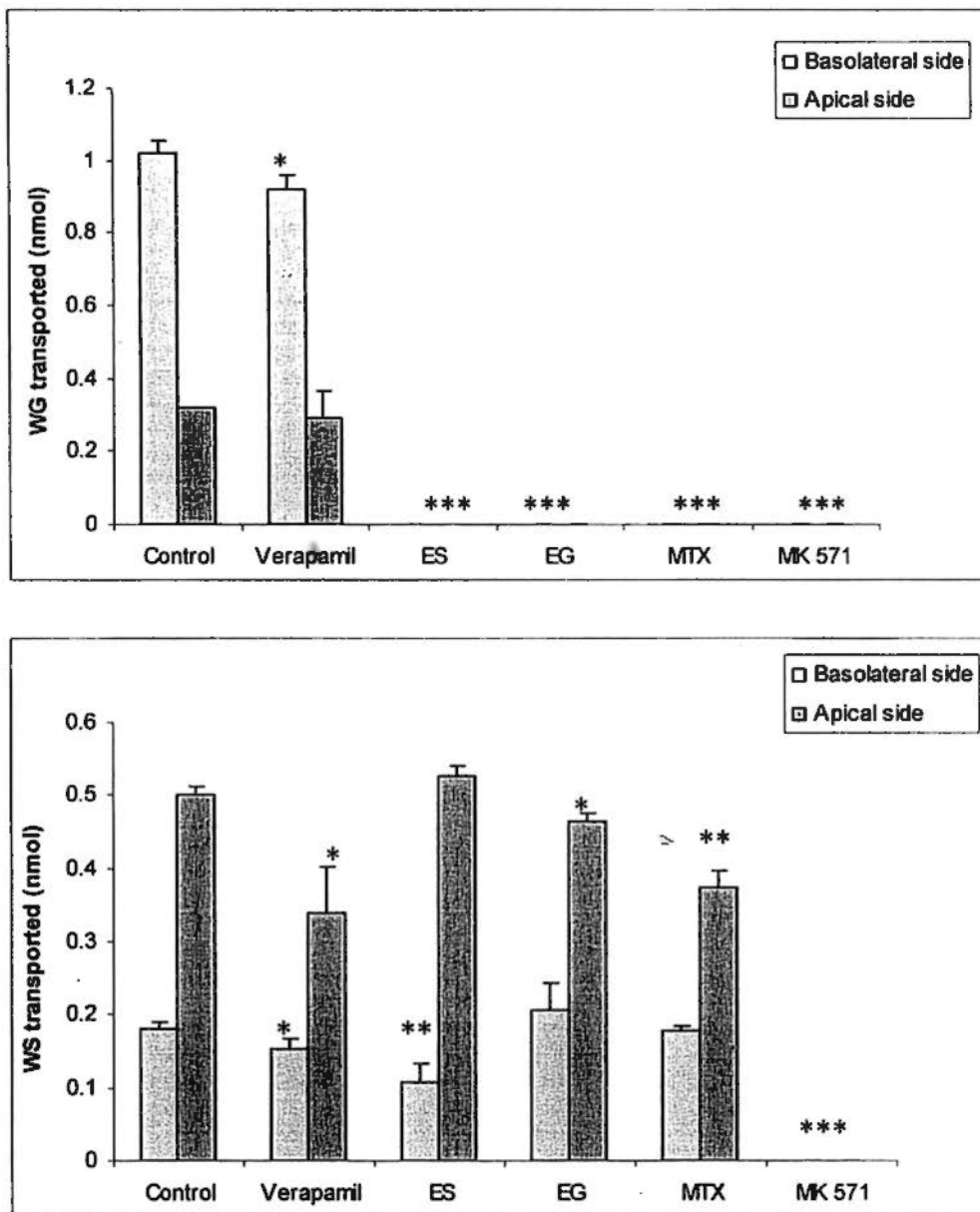
Fig. 4.10a **Effects of transporter inhibitors on the efflux of WG (upper) and WS (lower) formed during absorptive transport of W in Caco-2 cell monolayer model**
W: wogonin, WG: wogonoside, WS: sulfate of wogonin
***: $p<0.001$, **: $p<0.01$, *: $p<0.05$ compared with control
ES: estrone 3-sulfate, EG: estradiol glucuronide, MTX: mitoxantrone dihydrochloride
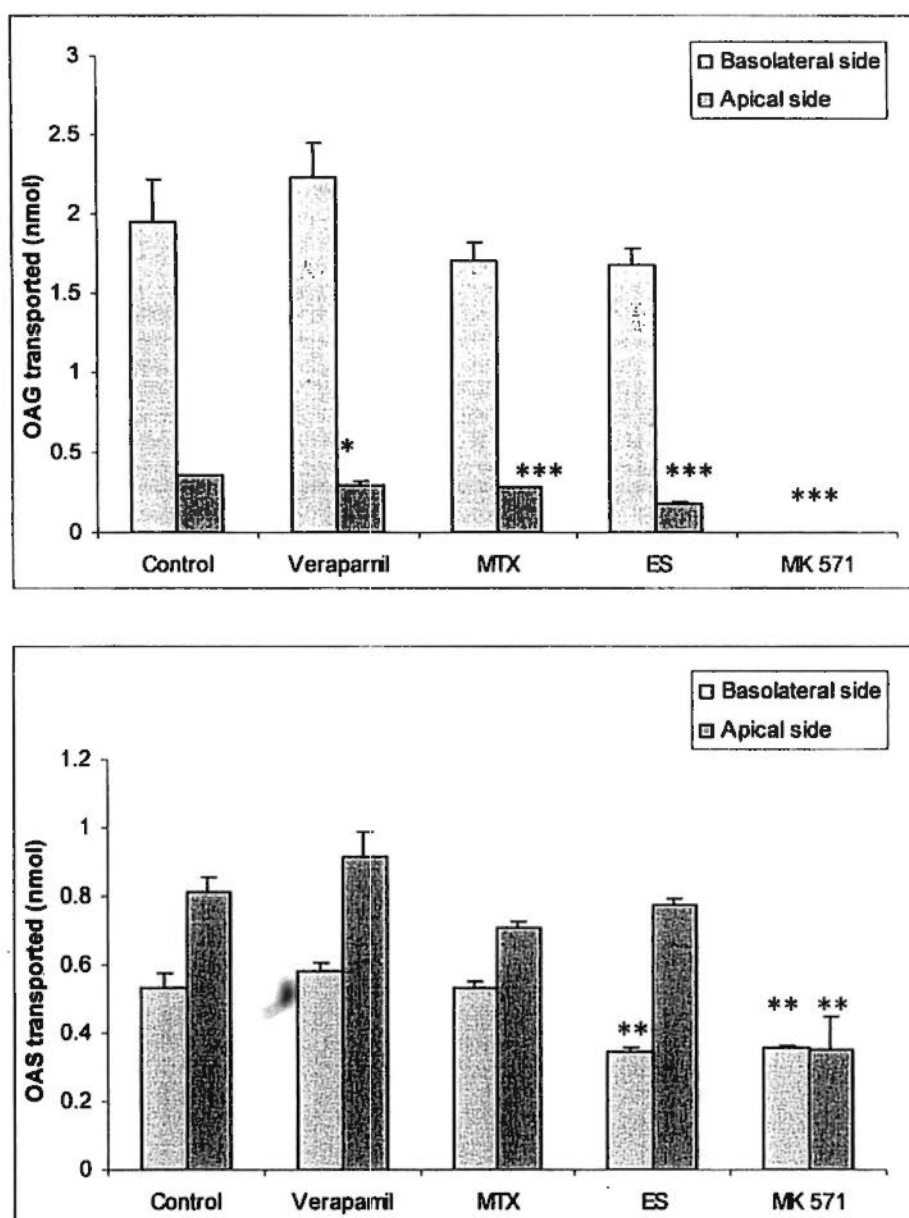
Fig. 4.10b **Effects of transporter inhibitors on the efflux of OAG (upper) and OAS (lower) formed during absorptive transport of OA in Caco-2 cell monolayer model**
OA: oroxylin A, OAG: oroxylin A-7-O-glucuronide, OAS: sulfate of oroxylin A
***: $p<0.001$, **: $p<0.01$, *: $p<0.05$ compared with control
ES: estrone 3-sulfate, EG: estradiol glucuronide, MTX: mitoxantrone dihydrochloride

4.4.1.7 Inhibition of basolateral to apical transport of WG and OAG in Caco-2 cell monolayer model

The basolateral to apical transport of WG and OAG were also carried out in the presence of the above mentioned membrane transporters inhibitor/substrate in section 4.4.1.6. The results were consistent with those observed in the inhibition study during the absorptive transport of W and OA in section 4.4.1.6. ES (50 μM) and MK571 (25 μM) could significantly inhibit the basolateral to apical transport of WG and OAG (Tab 4.2) at the concentration of 2.17 μM, indicating the role of MRPs in the apical efflux of WG and OAG. Furthermore, EG (50 μM) reduced the secretive transport of WG indicating the involvement of MRPs in the apical efflux of WG. Vera (50 μM) showed no effect on reducing the basolateral to apical transport of both WG and OAG indicating possible no involvement of P-gp in the apical efflux of WG and OAG.

Table 4.2 P_{app} values of WG and OAG during excretive transport of WG and OAG at 2.17 µM in presence and absence of various membrane transporter inhibitor/substrate in Caco-2 cell monolayer model

Flavones	Control	Verapamil	ES	EG	MTX	MK571
		P-gp inhibitor	Substrate of MRPs		Substrate of BCRP	Inhibitor of MRPs
WG ($\times 10^{-6}$ cm/sec)	5.78±0.15	5.76±0.64	N.D.***	4.65±0.34*	5.61±0.16	N.D.***
OAG ($\times 10^{-5}$ cm/sec)	1.99±0.18	2.00±0.08	0.66±0.01***	N.A.	2.38±0.09**	N.D.***

N.A.: the experiment was not conducted
N.D.: compound was not detectable at apical side
*: $p<0.05$, **: $p<0.01$, ***: $p<0.001$ compared with control

4.4.1.8 Further identification of potential membrane transporters for BG, WG and OAG using transfected MDCK cell lines

The transport study of WG and OAG in basolateral to apical direction was carried out on various MDCK cell lines including the wild type and transfected with human MDR1, MRP2 and MRP3 gene. For the transport of BG on MDCK cell lines has not been conducted before, the basolateral to apical transport of BG on MDCK cell lines was also carried out. The cumulative amount of flavones at apical side and the excretive P_{app} values were calculated and shown in Fig. 4.11. Comparing with their results on MDCK/WT, the cumulative amount at apical side of BG, WG and OAG and their P_{app} value were significantly increased in MDCK/MRP2 cell model. However, the cumulative amount at apical side of three glucuronides and their P_{app} in MDCK/MDR1 and MDCK/MRP3 showed no significant different from that in MDCK/WT, indicating no significant involvement of MDR1 and MRP3 in the efflux transport of BG, WG and OAG. The above results suggested that MRP2 might be the most potent membrane transporter responsible for the efflux of BG, WG and OAG.
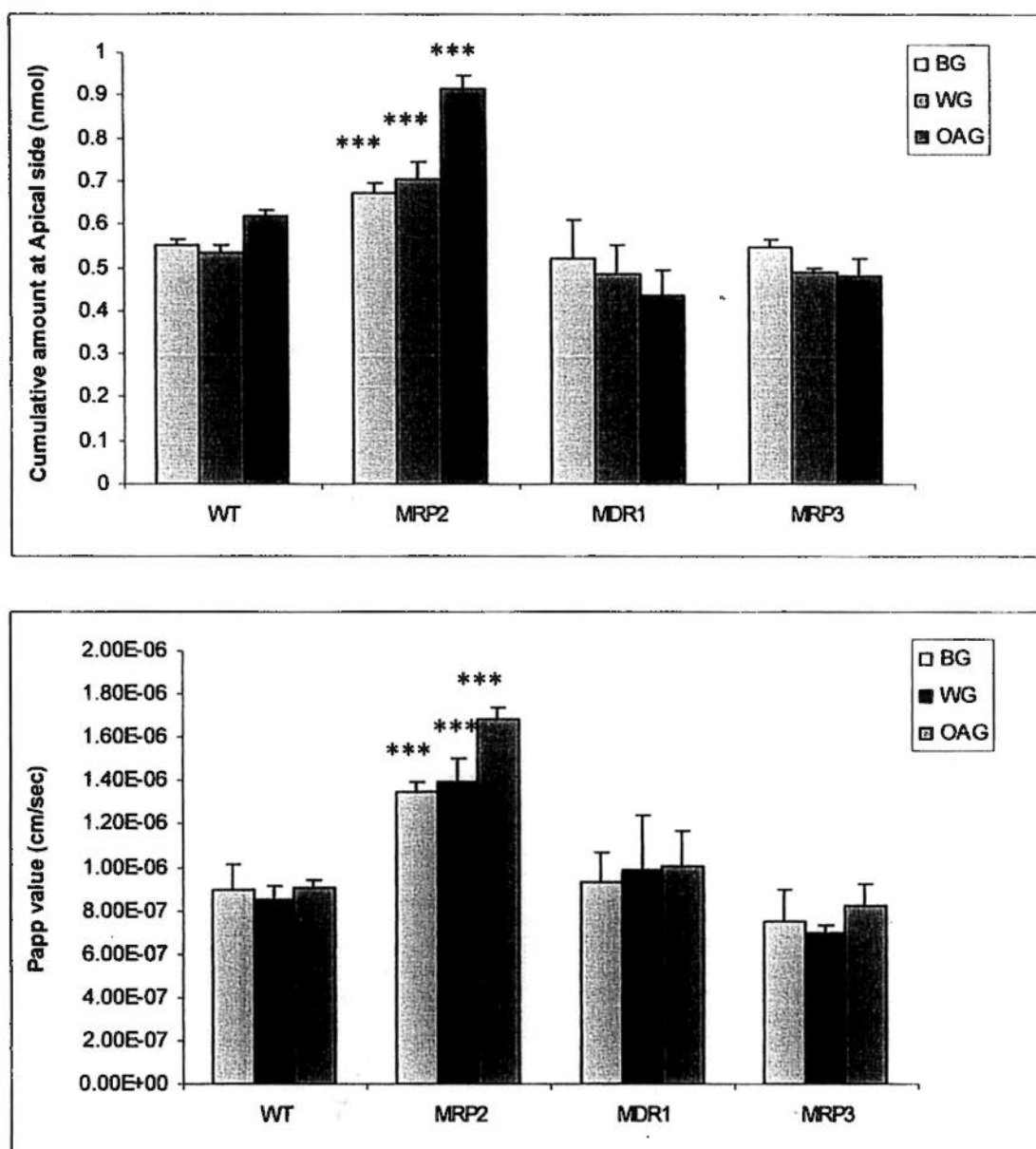
Fig. 4.11   **Cumulative amount at apical side (upper) and apparent permeability Coefficient (lower) of BG, WG and OAG after their basolateral to apical transports in MDCK cell model**
***: $p < 0.001$

4.4.1.9 Role of the paracellular pathway in the absorption transport of WG and OAG

After the pre-incubation with EGTA to open the intracellular tight junction, the P_{app} of WG and OAG were significantly increased to $1.08 \pm 0.07 \times 10^{-5}$ and $1.17 \pm 0.003 \times 10^{-5}$

cm/sec from zero as shown in section 4.4.1.5 with the same loading concentration of 43.48 μM.

4.4.2   Rat *in situ* single-pass intestinal perfusion model

4.4.2.1 Stabilities of W and OA in perfusate buffer

The result of stability tests of W and OA was shown in Fig. 4.12. From the results, W and OA were stable in perfusate buffer at 37 °C for at least 2 h.
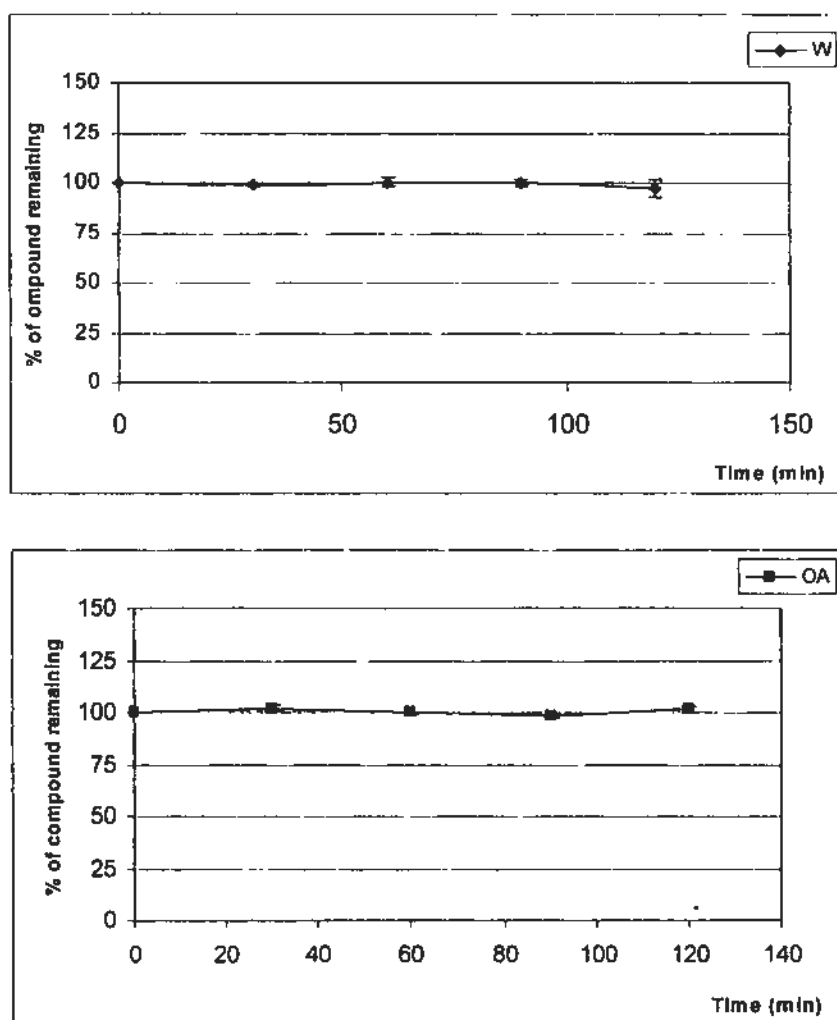
Fig. 4.12   **Stability of W (upper) and OA (lower) in the perfusate buffer at 37 °C for 120 min in the rat *in situ* single-pass intestinal perfusion model**

4.4.2.2 Intestinal absorption and disposition of W and OA in rat in situ single-pass intestinal perfusion model

During the intestinal absorption of W and OA, extensive Phase II metabolism was observed once again. There were glucuronides appearing in both the perfusate samples and mesenteric blood samples of both W and OA. The representative HPLC/UV chromatograms of perfusate samples and the plasma samples are shown in Fig. 4.13 and Fig. 4.14, respectively.
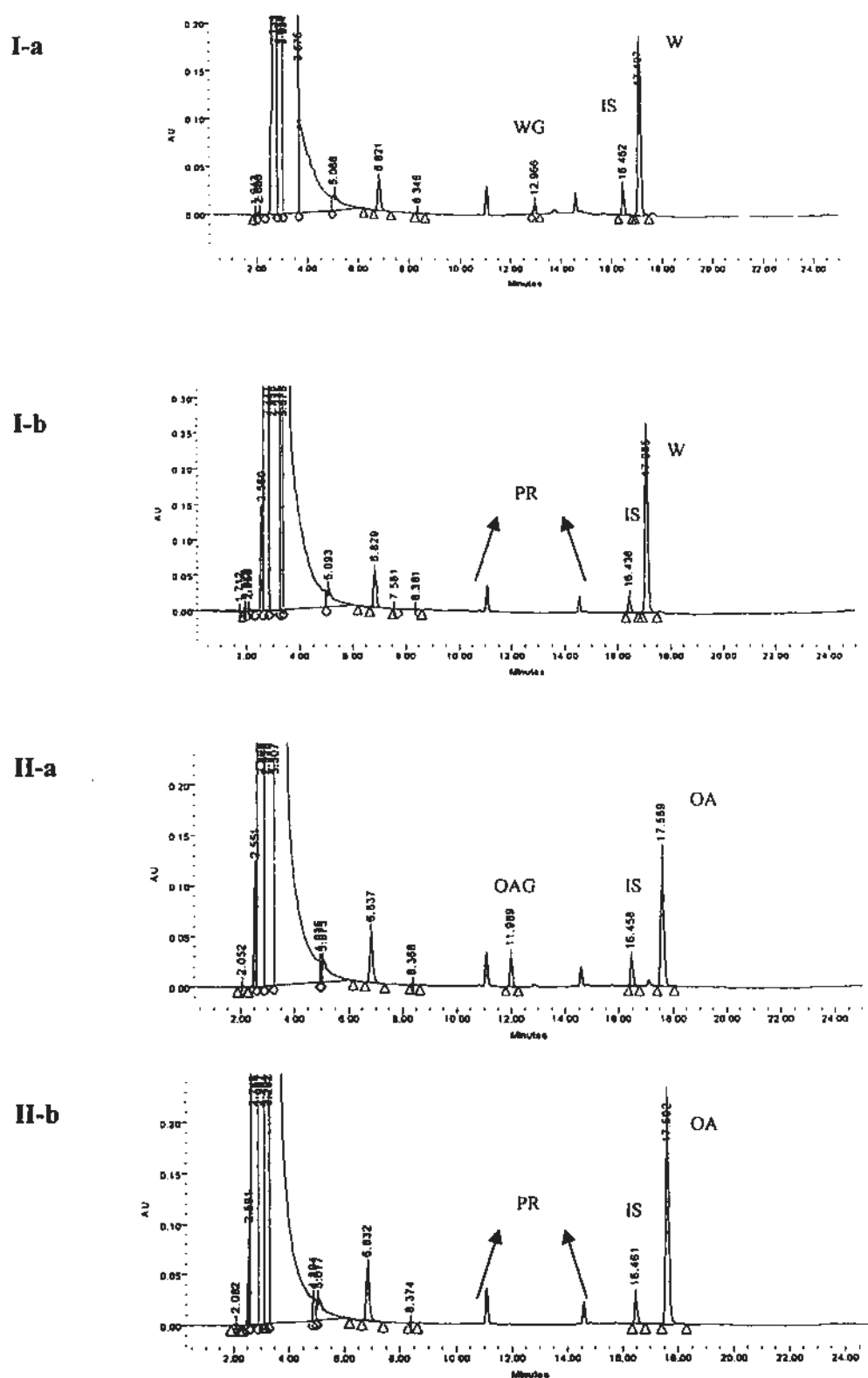
Fig. 4.13   **Representative HPLC/UV chromatograms of perfusate samples obtained after (a) and before (b) perfusing 50 μM of W (I) and OA (II) into rat small intestine PR: phenol red, W: wogonin, WG: wogonoside, OA: oroxylin A, OAG: oroxylin A-7-O-glucuronide, IS: internal standard**
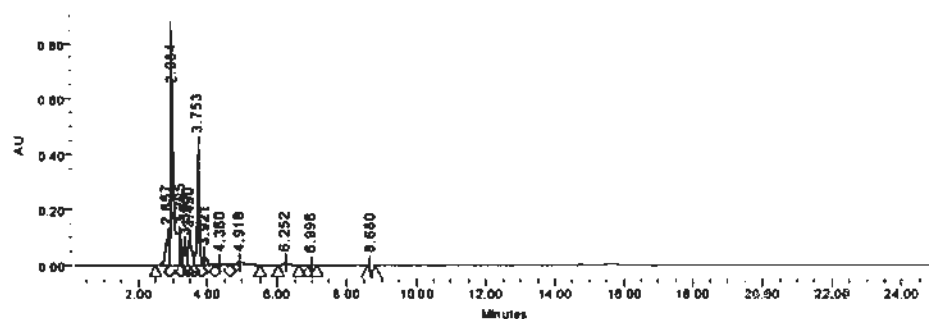
(I)
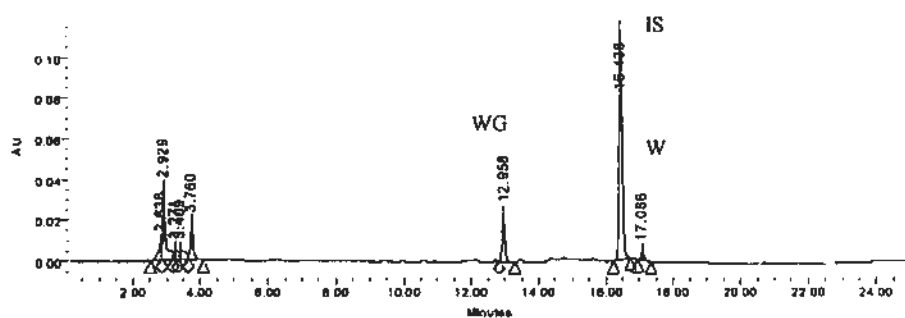
(II)
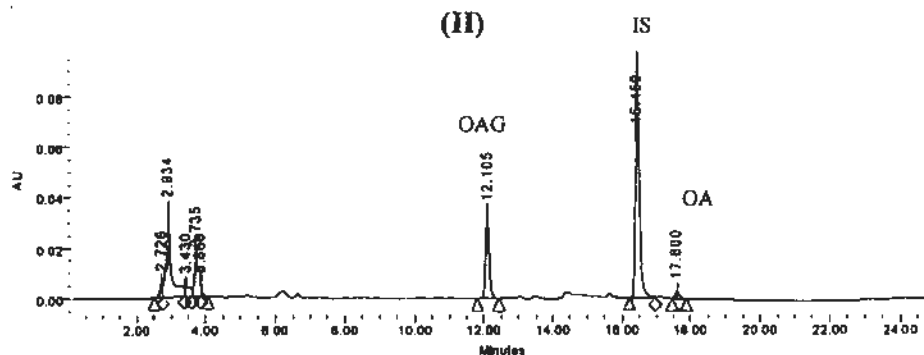
(III)

Fig. 4.14   **Representative HPLC/UV chromatograms of blank plasma (I) and plasma samples obtained after rat *in situ* single-pass intestinal perfusion of W (II) and OA(III)**

Both W and OA showed favorable permeability across the epithelium of small intestine. The permeability coefficient (P_{lumen}) of W and OA determined based on the disappearance of parent drug in the intestine lumen were calculated to be $2.27 \pm 1.26 \times 10^{-4}$ cm/sec and $3.50 \pm 1.46 \times 10^{-4}$ cm/sec, respectively (Table 4.3). Their permeability coefficients were comparable to the value of antipyrine which is often used as a reference probe of passive absorption ($P_{lumen} = 1.6 \pm 0.4 \times 10^{-4}$ cm/sec, Fagerholm et al., 1996).

Table 4.3   **Permeability coefficients of W and OA calculated as P_{lumen} and P_{blood} in rat *in situ* single-pass intestinal perfusion model (n=6)**

Compound	P_{lumen} ($\times 10^{-4}$ cm/sec)	P_{blood} ($\times 10^{-6}$ cm/sec)
W	2.27 ± 1.26	4.48 ± 1.86
OA	3.50 ± 1.46	3.00 ± 1.51

In the mesenteric blood samples, the amount of glucuronic acid conjugates of W and OA were much higher than their corresponding parent drugs. The permeability coefficient (P_{blood}) based on the appearance of parent drug in mesenteric blood were calculated to be $(4.48 \pm 1.86) \times 10^{-6}$ cm/sec and $(3.00 \pm 1.51) \times 10^{-6}$ cm/sec for W and OA, respectively (Table 4.3).

The cumulative amount of parent drug and formed glucuronides in mesenteric blood as well as the metabolites in perfusate were summarized in Table 4.4. It was noticed that the amount of formed glucuronides was much higher than that of parent drugs for both W and OA. Besides, the Cummins's extraction ratios were calculated to be 0.91 ± 0.03 and 0.95 ± 0.02 for W and OA, respectively. Both results indicated that W and OA underwent extensive Phase II metabolism during their absorption across intestinal epithelium. The

cumulative amount of glucuronides effluxed to mesenteric blood and perfusate was calculated and compared in Fig. 4.15. It was noticed that the amount of WG was higher in mesenteric blood than that in perfusate, whereas the amount of OAG in blood and perfusate was comparable.

Table 4.4 **Metabolism of W and OA during their *in situ* single-pass intestinal perfusion in rat (n=6)**

Flavones	Cumulative amount (nmol)			
	Glucuronide in blood	Glucuronide in perfusate	Parent flavone in blood	ER
W	47.87±14.33	25.07±10.21	6.80±2.33	0.91±0.03
OA	41.11±7.39	40.61±7.79	4.29±1.99	0.95±0.02

ER: extraction ratio
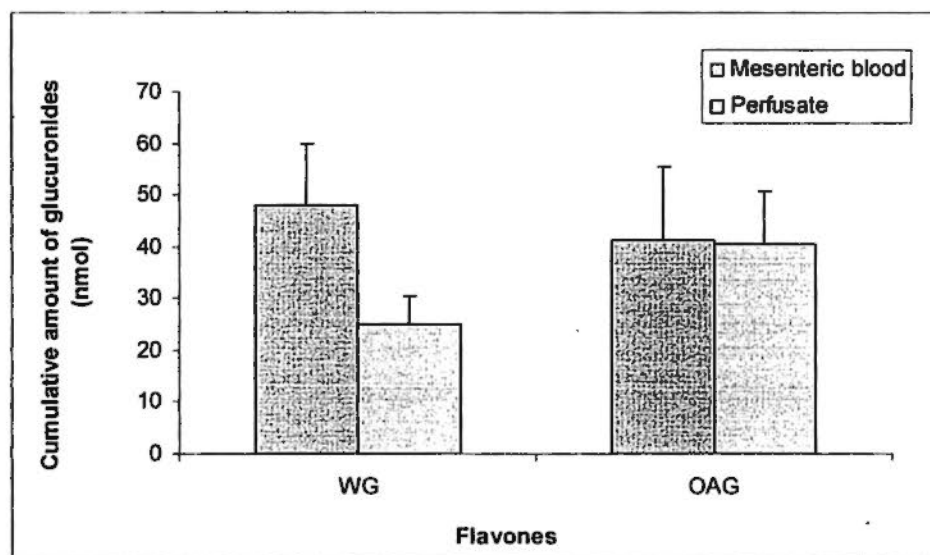
Fig. 4.15 **Cumulative amount of corresponding glucuronides for W and OA in mesenteric blood and perfusate after perfusing W and OA into rat small intestine (n=6)**

4.5 Discussion

4.5.1 Findings from cell monolayer models

During the absorptive and excretive transports of W and OA, good apparent permeability has been observed for both flavones, which means that W and OA could be readily absorbed in the small intestine. Our previous transport study on B also exhibited a favorable permeability of B, but the P_{app} value of B was relatively lower than that of W and OA, suggesting a lower permeability of B than that of W and OA. However, an extensive first-pass metabolism occurred simultaneously with the good permeation of three flavones. At low loading concentrations, extent of metabolism was even over 90% for W and OA. To compare the absorption and metabolism of W and OA, it was found that at similar loading concentrations, the P_{app} value of W was higher than that of OA, whereas the metabolism rate of OA was greater than that of W. So it was suggested that the higher metabolism of OA might result in its lower permeation in cell monolayers.

As the Phase II metabolites of W and OA, their glucuronic acid and sulfate conjugates have increased molecular weight and polarity. Due to the poor lipophilicity, it was hard for Phase II metabolites to pass across the intestinal epithelium via passive diffusion. Afterwards, this presumption has been proved by the fact that there was no absorption of WG and OAG during their apical to basolateral transport study. Nevertheless, the absorptive P_{app} of WG and OAG were significantly enhanced in the presence of calcium chelator of EGTA by opening the tight junction. With all the information taken together, it was suggested that WG and OAG were absorbed via paracellular pathway. Similar

results were obtained for BG, during its apical to basolateral transport study with/without EGTA.

In the basolateral samples and the apical samples after bidirectional transport study of W and OA, both glucuronides and sulfate conjugates have been identified, respectively. Since the metabolism of W and OA occurred intracellularly and the formed conjugated metabolites inside the intestinal epithelium were too polar to across the intestinal epithelium, the appearance of glucuronic acid and sulfate conjugates at both sides might be due to the function of membrane transporters. There have been a number of literatures reporting the interaction between flavonoids and membrane transporters. Among these membrane transporters, ATP binding cassette (ABC) transport proteins have attracted special attention. P-glycoprotein (Pgp), multidrug resistance associated proteins (MRPs) and breast cancer resistance protein (BCRP) have been particularly investigated because of their important role in the development of multidrug resistance and drug-drug or drug-herb interactions. In addition to tumor tissues, these membrane transporters also are highly expressed level in normal tissues. Pgp has been detected at the apical membranes of epithelial cells in the excretory organs, such as intestine, liver and kidney and the luminal side of endothelial cells in the blood brain barrier (Morris, et al., 2006). Additionally, MRP2 and BCRP are located at the apical membrane, whereas MRP1, MRP3 and MRP5 are localized at the basolateral membrane (Brand, et al., 2006). Based on the cumulative amount of metabolites at the apical side and basolateral side, it was found that glucuronides of W and OA preferentially went to the basolateral side, whereas the amount of their sulfate conjugates were much higher at the apical side, regardless of

the side of loading. As a result, it was suggested that the glucuronides might have higher affinity to the basolateral transporters and the apical transporters might mediate the efflux of sulfates. Furthermore, the absorptive transport studies of W and OA were conducted in the presence of transporter inhibitors or substrates including Vera (Bansal, et al., 2009, Wang et al., 2006), MK (Bousquet et al., 2008, Videmann, 2007), EG and ES (Leslie et al., 2005, Tiwari et al., 2009, Campbell et al., 2004, Hagenbuch, 2007), MTX (Mahringer, et al., 2009, Rosenberg et al., 2010). The findings strongly suggested that MRPs and BCRP might be involved in the efflux of metabolites of W and OA.

In addition to the ABC transporters, there are other transporters at the intestinal membrane such as organic anion transporting polypeptides (OATPs). The subfamily of OATP2B1 is located at the endothelial cells of blood brain barrier, intestine, hepatocytes et al and is responsible of transporting its substrate into the cells. Since there was no absorptive transport of WG and OAG but these two glucuronides could pass through Caco-2 cell monolayer from basolatera to apical side, we speculated that OATPs might be involved in the secretory transport of WG and OAG. Consequently, this assumption was confirmed by the inhibition study in the basolateral to apical transport of WG and OAG, in which the P_{app} of WG and OAG were significantly decreased as a function of ES and MK571. Conclusively, on the basis of the inhibition studies, it was suggested that OATPs might be involved in the influx of WG and OAG, while their efflux might be mediated by MRPs and BCRP. Bases on the results, MRPs inhibitor seemed to show a stronger effect than other inhibitors. Nevertheless, this might be due to that WG and OAG had higher affinity to MRPs or MRPs had higher expression level than BCRP and

OATP in Caco-2 cells that we employed in the experiment. Our previous studies on B found that the intracellularly formed BG might be the substrate of MRPs and OATPs (Zhang et al., 2007a).

Furthermore, using membrane transporter inhibitors or substrate to investigate the drug-transporter interaction may not be reliable enough, especially in a complicated system like Caco-2 cell monolayer model. In fact, there is no so-called specific transporter inhibitor. Some studies pointed out that some efflux transporter inhibitors also inhibit influx transporters such as cyclosporine A (Hirano et al., 2006). It is necessary to combine the information originated from the transport study using membrane transporter inhibitors with the results from genetically modified cell lines (Wang et al., 2008). As a result, MDCK cell lines transfected with human transporter genes were utilized to provide further information for the identification of potential membrane transporters. MDCK, Madin-Darby canine kidney, epithelial cell line is derived from the kidney of a normal male cocker apaniel. It shows good correlation with Caco-2 cell line in the evaluation of drug permeability and it has been used extensively to predict absorption of drugs or new compound entities across membrane epithelium (Ranaldi, et al., 1992 and 1996, Irvine et al., 1999, Taub et al., 2002). Morphologically and physiologically, it exhibits apical microvilli, junctional complexes, lateral membrane enfolding as well as tight junction (Herzlinger et al., 1982). MDCK cell line posses some superiorities over Caco-2 cell lines such as the short maturation time and the high expression of single membrane transporter proteins. As a result, transfected MDCK cell line with membrane transporters such as MDR1, MRPs, BCRP, CMOAT etc. are extensively employed to

identify the potential substrate or inhibitor of membrane transporters (Luo, et al., 2002, Barthomeuf et al., 2005, Giri et al., 2009, Souza et al., 2009, Wortelboer et al., 2008). In the present study, after the basolateral to apical transport study of BG, WG and OAG, their permeabilities were significantly increased in MDCK/MRP2 cell model but had no significant changes in MDCK/MDR1 and MDCK/MRP3 cell models, indicating the important role of MRP2 in the efflux of BG, WG and OAG rather than MDR1 and MRP3. Nevertheless, our previous bidirectional transport studies of B (Zhang et al., 2007a), W and OA(section 4.4.1.6) found that the intracellularly formed BG, WG and OAG showed preferential biding to the basolateral transporters such as MRP1, MPR3 and MRP5 than the apical transporters such as Pgp, MRP2 and BCRP. It seemed that the results from transport studies in Caco-2 cell model may not be consistent with the results from MDCK cell model. However, we could not rule out the possibility that the roles of MRP1 and MRP5 were much more significant than MRP3, which has not been conducted in the current study in MDCK cell model. In addition, there was also possibility that the different expression level of MRP3 in the Caco-2 cells and MDCK cells caused such discrepancy in results. In order to identify the affinities of the studied compound to specific MRPs, experiments such as the ATPase assay using membranes from Sf9 cells overexpressing the specific transporter could provide further information.

4.5.2 Findings from rat *in situ* single-pass intestinal perfusion models

Based on the results of transport studies of W and OA in Caco-2 cell model, W and OA underwent extensive metabolism during their intestinal absorption. In the current rat intestinal perfusion study, we expected that the metabolism of W and OA would also be

extensive. Since our purpose was to investigate the absorption of W and OA, we would like to monitor both the parent flavones of W and OA as well as their metabolites in the mesenteric blood of the rat *in situ* intestinal perfusion model. Thus, a relatively high loading concentration was necessary to ensure the detection of both W/OA and their metabolites. However, the poor aqueous solubilities of W and OA (about 0.3 µg/ml based on our preliminary study) would limit the use of high concentrations of W/OA. The concentration of 50 µM was eventually chosen to ensure the aqueous solubilities of W and OA in perfusate buffer as well as the detection of both the parent compound and metabolites of W and OA.

Effective permeabilities were observed for W and OA on rat *in situ* single-pass perfusion model. The permeability coefficients (P_{lumen}) of W and OA were comparable to the well-absorbed marker, antipyrine. Besides, the P_{lumen} of W and OA were higher than that of B which was obtained in our previous study. However, the P_{lumen} was calculated based on the disappearance of parent drug from the perfusate buffer. The disappearance of parent drugs from the perfusate might be caused by the absorption or metabolism. Then the permeability coefficient (P_{blood}) was calculated based on the appearance of parent into the mesenteric blood, which should reflect the real absorption of the drug *in vivo*. The calculated P_{blood} values for W and OA were much lower than their corresponding P_{lumen}, indicating that good permeability might not guarantee a high exposure of parent flavones in the mesenteric blood.

In the *in situ* rat perfusion model, the parent flavones of W and OA were metabolized in the intestinal epithelium and the formed Phase II metabolites were then effluxed into the mesenteric blood or back to the perfusate by some membrane transporters. The cumulative amount of glucuronides at both sides were calculated and compared for both W and OA. Similar results were observed in our previous study on B using the same model. It was found that the amount of glucuronides in mesenteric blood was much higher than that in perfusate. Such difference in the amount from two sides was more significant for BG, WG than OAG. This finding demonstrated that the intracellularly formed glucuronides were preferentially effluxed to the mesenteric blood, which complied with the results from Caco-2 cell monolayer model.

4.5.3 Comparison between the findings from Caco-2 cell monolayer model and rat *in situ* single-pass intestinal perfusion model

The intestinal absorption and disposition of W and OA were investigated using both Caco-2 cell monolayer model and rat *in situ* single-pass intestinal perfusion model. The proposed mechanistic explanation of intestinal absorption and disposition of W and OA was summarized in Fig. 4.16. W and OA exhibited favorable permeability on both models. Nevertheless, the P_{app} values from *in situ* model were much higher than those obtained from cell model, which was similar to our findings on B. This could be explained by the higher TEER of Caco-2 cell model and larger surface area of the intestine epithelium (Shah et al., 2006). Extensive metabolism of W and OA were observed on both models. The percentage of metabolism was higher than 90% in Caco-2 cell model and the extraction ratio was above 0.9 in rat *in situ* perfusion model for both

W and OA. Nevertheless, there were two pathways of metabolism on Caco-2 cell model which were glucuronidation and sulfation. Only corresponding glucuronides of W and OA were found on rat *in situ* single-pass intestinal perfusion model. This finding indicated that there might be species difference for the metabolism of both W and OA.

4.6 Conclusion

Caco-2 cell monolayer model and rat *in situ* single-pass intestinal perfusion model were employed to investigate the intestinal absorption and disposition of W and OA. Based on the results from the two models, W and OA were readily absorbed with moderate permeability. However, similar to B, extensive Phase II metabolism was observed during their intestinal absorption and MRPs might be involved in the efflux of their intracellularly formed glucuronides and sulfates. Besides, there were species difference in the metabolisms of W and OA.
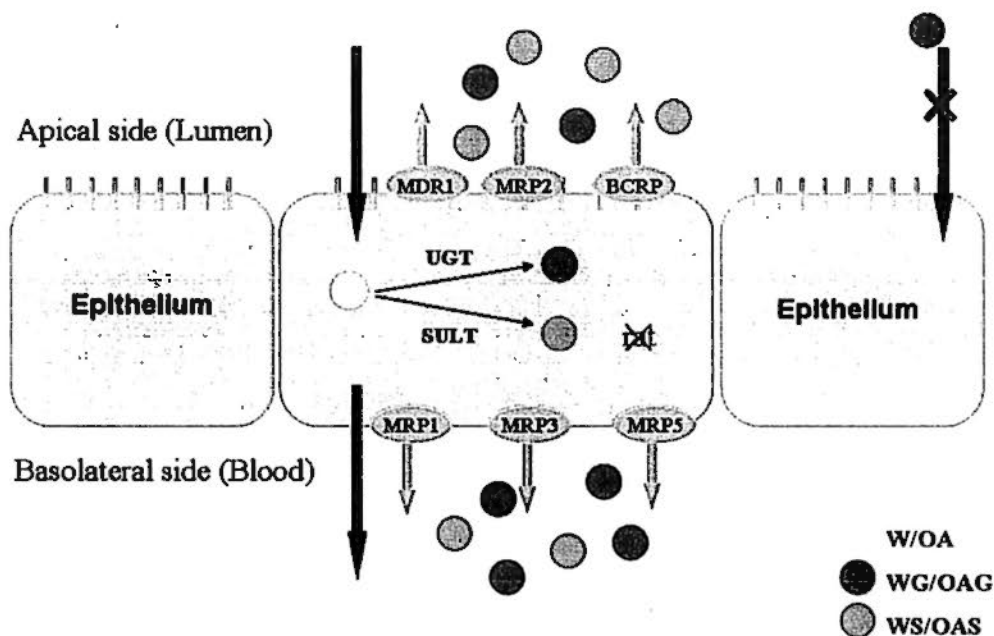
Fig. 4.16   Proposed mechanisms for the intestinal absorptions and dispositions of W and OA

Chapter Five

Intestinal and hepatic metabolism of W and OA

5.1   Introduction

Based on previous findings from Caco-2 cell monolayer model and rat *in situ* single-pass intestinal perfusion model, similar to B, W and OA underwent extensive Phase II metabolism with glucuronic acid and sulfate conjugates identified as major metabolites for both of them. Although intestine is the first barrier that drugs meet after oral administration, liver is still the predominant site for drug metabolism after absorption. Thus, both the intestinal and hepatic metabolisms are essential to predict the *in vivo* drug disposition.

The investigation of liver drug metabolism plays an important role in pre-clinical drug development, in which many *in vitro* and *in situ* approaches have been developed, such as the organ based liver perfusion model (Miller et al., 1973, Zaman et al., 1996), precision-cut liver slice (Guo et al., 2007), primary culture of hepatocytes (Maurel, 1996, Gläβer et al., 2002). Sub-cellular fractions including microsome, S9 fractions and cytosol are extensively used to study drug metabolism. Since it is a high-throughput method and the reaction conditions are easy to handle, *in vitro* incubation of sub-cellular fractions with studied compound is often used in preclinical studies in the pharmaceutical industry to investigate the Phase I and Phase II metabolism.

Our previous *in vitro* enzymatic studies on B found that it demonstrated extensive first-pass glucuronidation in both liver and intestine and UGT 1A9 mainly catalyzed the formation of BG in human liver (Zhang et al., 2007b). In comparison, hepatic sulfation of B was less extensive. Nevertheless, the intestinal and hepatic metabolism of W and OA has not been systematically investigated, although the pharmacokinetic studies about W and OA found that both flavones also underwent extensive glucuronidation after oral administration of the RS extract to rat (Kim et al., 2006, Zuo et al., 2003, Li et al., 2005).

Based on the results from Caco-2 cell monolayer model, it has been found that extensive Phase II metabolism occurred during the intestinal absorption of both W and OA. There were two metabolites that have been confirmed for W and OA, respectively. As a result, glucuronidation and sulfation were suggested to be two major metabolic pathways for both W and OA in human intestine. However, the data generated from rat *in situ* single-pass perfusion indicated that both W and OA could only be transformed into their corresponding glucuronides rather than sulfates in rat small intestine. Such difference in the types of metabolites suggested that species difference might occur between human and rat in the metabolic pathways for W and OA. Caco-2 cell originated from human epithelial colorectal adenocarcinoma cells. Although its morphology and function resemble human small intestine such as the expression of tight junction, microvilli, enzymes and membrane transporters, the study on this model alone cannot predict the *in vivo* metabolism of the flavones. Considering the species difference between human and rat and the limitations of Caco-2 cell monolayer model, the *in vitro* enzymatic kinetic studies using various organ sub-cellular fractions from human and rat should be

employed aiming to provide a thorough investigation on the metabolism of W and OA as well as the competition among B, W and OA in different species and organs.

In the current study, intestinal and liver microsomes, S9 fractions as well as cytosol originating from rat or human were employed to study the glucuronidation and sulfation of W and OA in liver and intestine. In addition, recombinant human UDP-glucuronosyltransferase isoforms were used to further characterize the glucuronidation of W and OA. Moreover, species difference and organ preference for the metabolism of the studied flavones were investigated.

5.2 Material and reagents

Baicalein (B) and baicalin (BG) with purity over 98% were purchased from Sigma-Aldrich Chem. Co. (Milwaukee, WI, USA). Wogonin (W) and wogonoside (WG) with purity over 98% were purchased from AvaChem Scientific LLC (San Antonio, TX, USA). Oroxylin A (OA, purity over 98%) and Oroxylin A-7-*O*-glucuronide (OAG, purity over 95%) were supplied by Shanghai u-sea biotech co., Ltd (Shanghai China). 3, 7-dihydroxyflavone with purity of 97% was purchased from Indofine Chemical Company (Hillsborough, NJ, USA).

Uridine 5'-diphosphoglucuronic acid (UDPGA), adenosine 3'-phosphate 5'-phosphosulfate (PAPS) and alamethicin were obtained from Sigma-Aldrich Chem. Co. (Milwaukee, WI, USA). Pooled human liver and intestine microsomes, pooled human liver S9, pooled human liver cytosol; pooled male rat liver microsomes, pooled male rat

liver cytosol, pooled male rat liver and intestinal S9 (Sprague-Dawley); recombinant human UGT1A1, UGT1A3, UGT1A7, UGT1A8, UGT1A9, UGT1A10, UGT2B4, UGT2B15 were purchased from BD Biosciences (Woburn, MA, USA).

Acetonitrile (Labscan Asia, Thailand) and methanol (TEDIA company, Inc., USA) were HPLC grade and used without further purification. All other reagents were of at least analytical grade. Distilled and deionized water was prepared from Millipore water purification system (Millipore, Milford, USA).

5.3   Methods

5.3.1   HPLC/UV method for quantification of conjugated metabolites of W and OA

The HPLC system consists of Waters 600 controller (pump), Waters 717 auto sampler and Waters 996 Photodiode Array UV detector. The separation of all the analytes was performed by using a Thermo BDS Hypersil column (250 mm× 4.6 mm; 5 μm particle size) connected to a guard column (Delta-Pak C18 Guard-Pak, Waters). Data were collected by Waters Millennium software (version 3).

The mobile phase consisting of eluent A (20 mM sodium dihydrogen phosphate buffer, pH 4.6) and eluent B (acetonitrile) was run at 1 ml/min. The linear gradient elution program was set as follows: eluent A decreased from 90 to 70% in the first 10 min, decreased from 70 to 40% in the next 2 min, maintained at 40 % for 4 min, then eluent A

increased from 40 to 90% from 16 to 20 min and equilibrated for 5 min before the next injection. The detection wavelength was set at 270 nm.

Due to the commercial unavailability of the standard compounds of WS and OAS, the concentrations of WS and OAS after the transport study in Caco-2 cell monolayer model was quantified indirectly based on the assumptions that WS/OAS has the same UV absorbance group as W/OA and one molar of W/OA produce one molar of WS/OAS. As a result, the calibration curve was firstly plotted with the molar concentrations of W/OA versus the peak area ratios of W/OA to IS. The molar concentration of WS/OAS was calculated based on their observed peak are ratios from the above calibration curve of W/OA.

5.3.2   HPLC/UV assay method validation

In order to measure metabolites formation, a HPLC/UV method to quantify BG, WG and OAG has been established. Since all the collected samples were centrifuged without further treatment, the HPLC/UV method for BG, WG and OAG was further validated using rat liver microsome with the final protein concentration at 0.2 mg/ml. The linearity, intra-day and inter-day precision and accuracy were employed for method validation. The intra-day precision was determined within one day by analyzing three replicates of quality control samples at concentrations of 0.5, 1.0, 10.0 μg/ml. The inter-day precision was determined on three separate days for the quality control samples. The intra-day and inter-day precision were defined as the relative standard deviation (R.S.D.) and the accuracy was determined by calculating the relative error (R.E.). The limit of detection (LOD) was defined as the lowest concentration of the drug resulting in a signal-to-noise

ratio of 3:1. The limit of quantification (LOQ) was defined as the lowest concentration of the drug resulting in a signal-to-noise ratio of 10:1 with precision below 20% and accuracy below ±20%. Extraction recovery was calculated by comparing the peak areas of the quality control samples to that of the standard solutions containing the equivalent amount of analytes.

5.3.3 Glucuronidation activity assay

The glucuronidation reaction followed our previously described procedure (Zhang et al., 2006). Briefly, a series of concentration of W or OA (0.35-35 μM) were pre-incubated with different sub-cellular fractions or UGT isozymes in 50 mM Tris-HCl buffer (pH 7.4) containing 8 mM of $MgCl_2$ and 25 μg/ml of alamethicin for 5 min at 37 °C. The reaction was initiated by the addition of 2 mM UDPGA. The optimized concentrations of sub-cellular fractions and the UGT isozymes as well as the incubation time were listed in Table 5.1. The protein concentrations and incubation times were optimized to ensure linearity for metabolite formation. All the experiments were performed in triplicate.

Table 5.1   **Summary of optimized protein concentration and reaction time for the enzymatic kinetic study of glucuronidation using various sub-cellular fractions and UGT isozymes**

Sub-cellular fraction/ isozymes	Protein concentration (mg/ml)	Reaction time (min)
HLM	0.2	10
HIM	0.1	10
RLM	0.2	10
HLS9	0.8	10
RL S9	0.8	10
RIS9	0.8	10
UGT 1A1	0.2	10
UGT 1A3	0.2	10
UGT 1A7	0.5	10
UGT 1A8	0.2	5
UGT 1A9	0.2	10
UGT 1A10	0.2	10
UGT 2B4	0.2/0.8	10/30
UGT 2B15	0.2	10

HLM: human liver microsome; RLM: rat liver microsome; HIM: human intestine microsome; RLS9: rat liver S9 fraction; HLS9: human liver S9 fraction; RIS9: rat intestine S9 fraction

5.3.4 Sulfation activity assay

Similar to the condition of glucuronidation, different concentrations of W or OA (0.35-35 μM) was pre-incubated with pooled human, rat liver cytosol and rat intestinal S9 fraction at a final protein concentration of 0.8 mg/ml at 37 °C min in 50 mM Tris-HCl buffer (pH 7.4) containing 5 mM MgCl₂, 8 mM dithiothreitol and 0.0625 % bovine serum albumin. The reaction was initiated by addition of 200 μM of PAPS and lasted for 10 min.

5.3.5 Sample preparation

All the enzymatic reactions were terminated by the addition of 40 μl of ice cold acetonitrile / acetic acid (9:1, *v/v*) containing 40 μg/ml internal standard (3, 7-dihydroxyflavone). The mixture was centrifuged at 16, 000 g for 10 min and the supernatant was directly injected into HPLC/UV system for analysis.

5.3.6 Data analysis

Reaction rate of glucuronidation and sulfation in various sub-cellular fractions and UGT isozymes was expressed as amount of metabolites formed per min per mg protein (nmol/min/mg). All the reported values were presented as mean ± SE. The enzyme kinetic parameters of glucuronidation were obtained by fitting data to the Michaelis-Menten equation or substrate inhibition profile using the software of Prism (GraphPad Software, Inc.). Eadie-Hofstee plot was also employed to determine whether the obtained enzymatic kinetic profile is fitted to Michaelis-Menten or substrate inhibition profile as shown in the following equations:

Michaelis-Menten equation: $V = V_{max} \times C / (K_m + C)$;

Substrate inhibition profile: $V = V_{max} / (1 + K_m/C + C/K_i)$

Where V_{max} is the maximal velocity; K_m is the substrate concentration at half maximal velocity; K_i is the inhibition constant, V is the metabolic formation rate, C is the substrate concentration.

5.4   Results and discussions

5.4.1   HPLC/UV method assay validation

The representative HPLC/UV chromatograms of blank rat liver microsome and blank rat liver microsome spiked with standard solution of BG, WG, and OAG are shown in Fig. 5.1. Under the established chromatographic condition, there was no endogenous interference to the peaks of BG, WG and OAG and a good separation from each other has been demonstrated for all the tested analytes. Representative chromatograms of samples from different sub-cellular fractions and UGT isozymes for W and OA are shown in Fig. 5.2a and Fig. 5.2b.
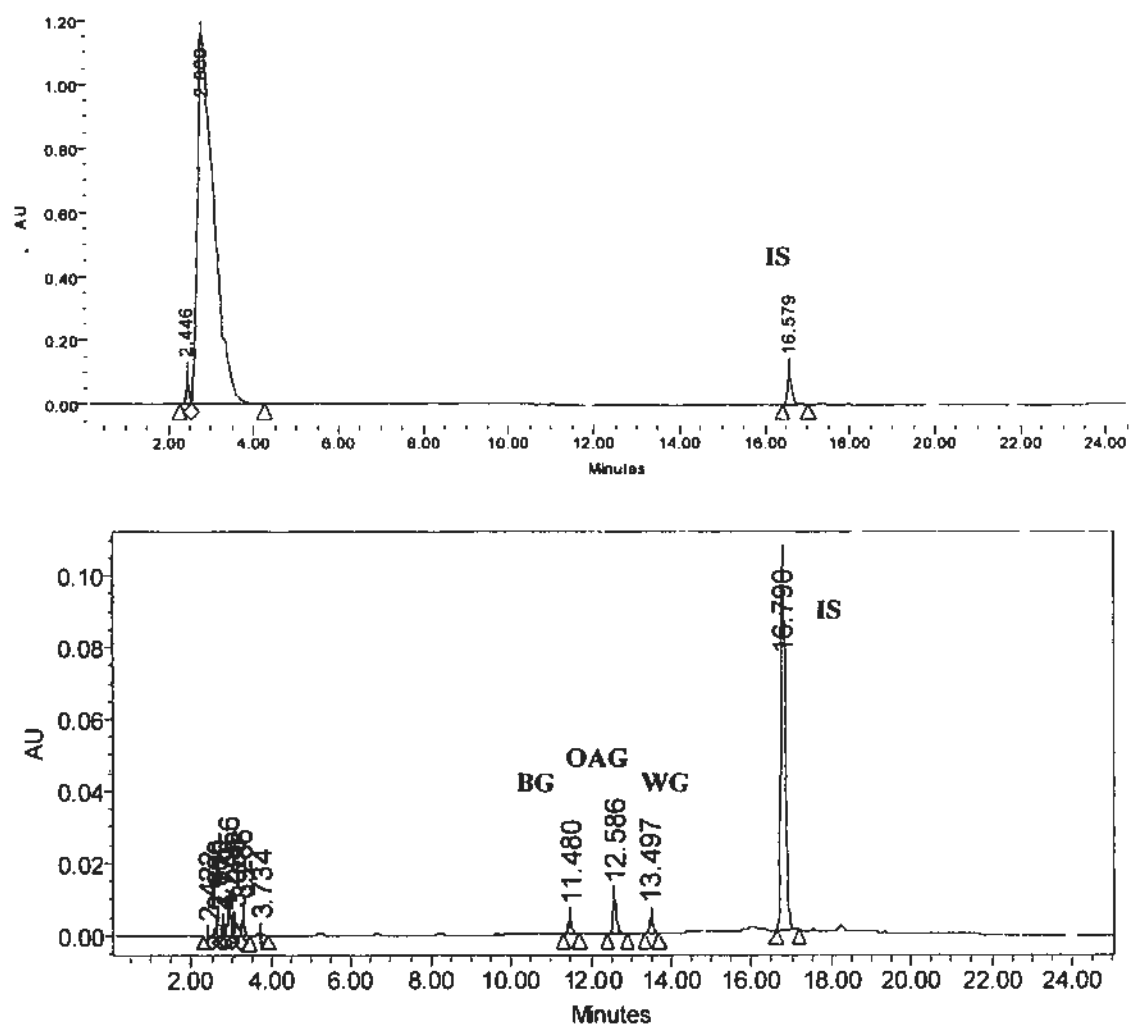
Fig. 5.1   Representative HPLC/UV chromatograms of rat liver microsome (upper); rat liver microsome spiked with standard solution of BG, WG and OAG at 0.2 µg/ml (lower)
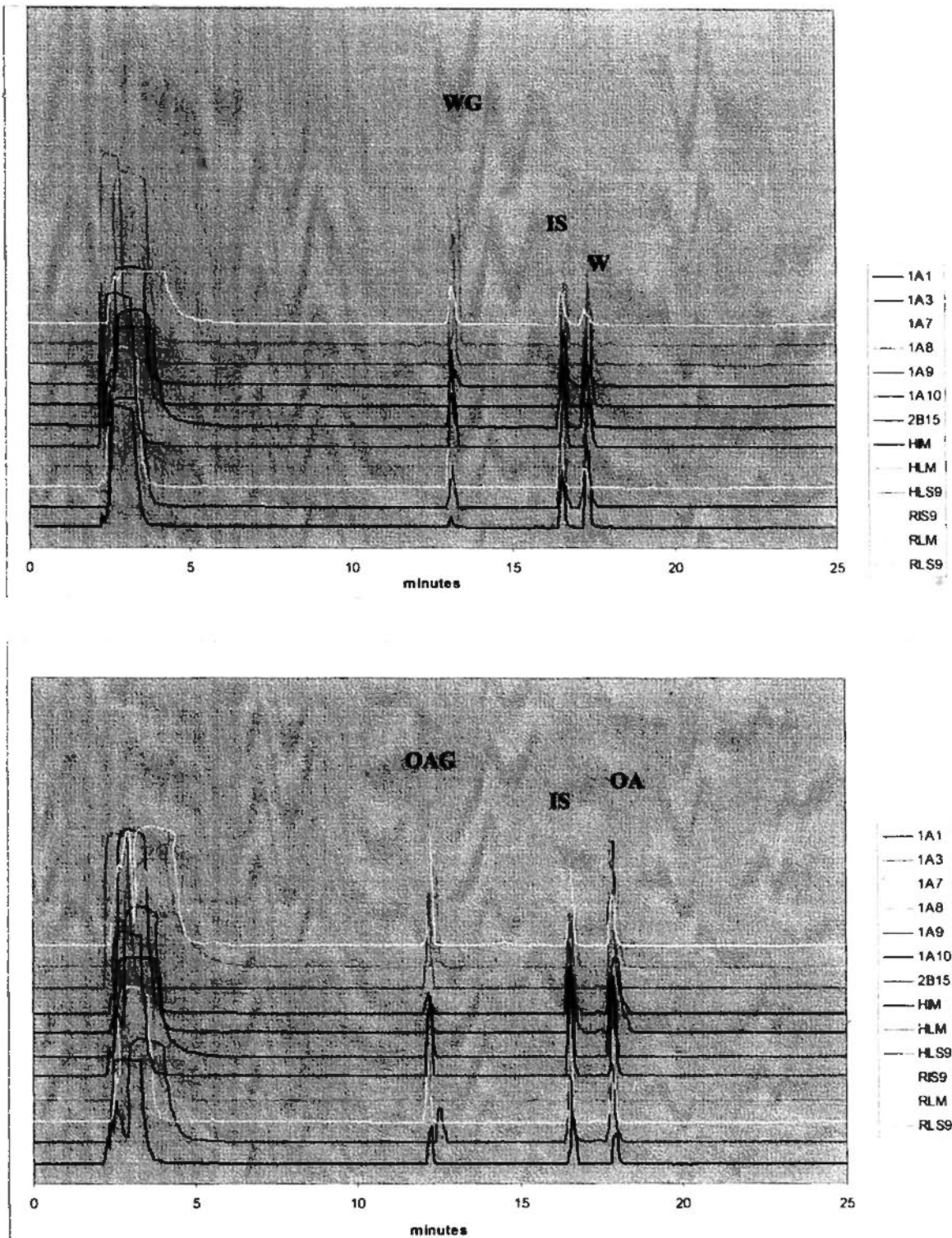
Fig. 5.2a   Representative HPLC/UV chromatograms of samples from *in vitro* glucuronidation kinetic study in various sub-cellular fractions and UGT isozymes of W (upper) and OA (lower)
HLM: human liver microsome; RLM: rat liver microsome
HIM: human intestine microsome; RLS9: rat liver S9 fraction
HLS9: human liver S9 fraction; RIS9: rat intestine S9 fraction
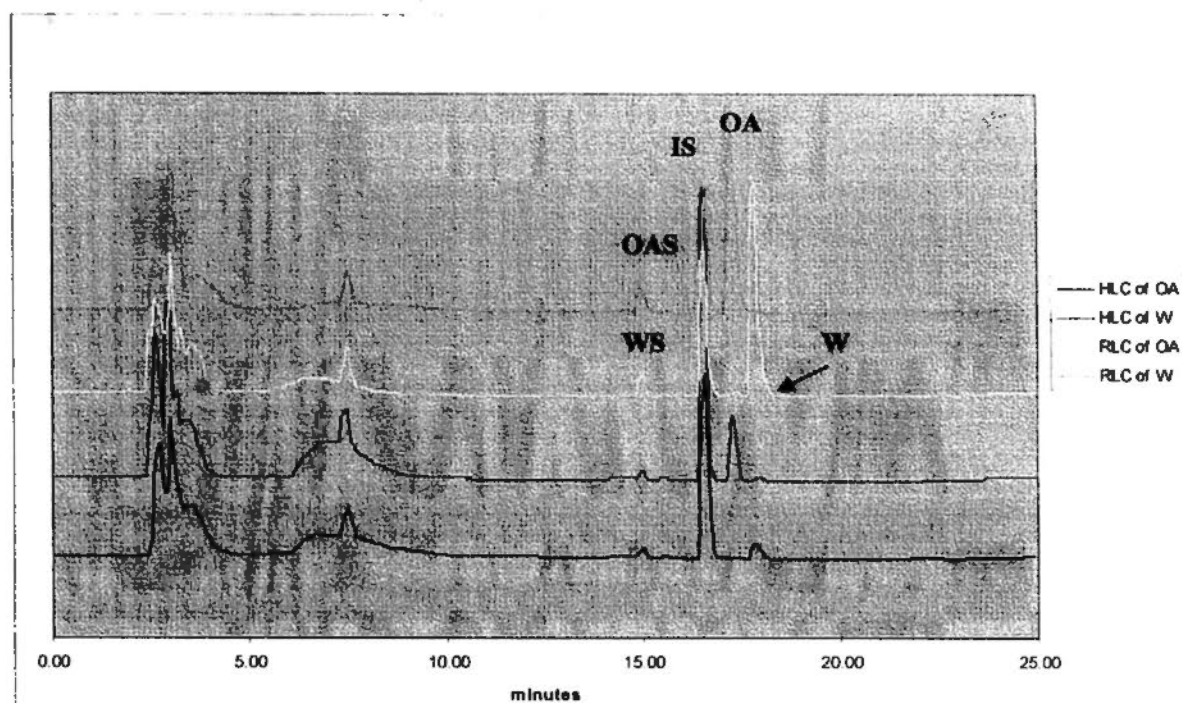
(III)

Fig. 5.2b **Representative HPLC/UV chromatograms of samples from *in vitro* sulfation kinetic study of W and OA in human/rat liver cytosols**
HLC: human liver cytosol; RLC: rat liver cytosol

In the range of 0.1-20 µg/ml, the calibration curve produced good linearity ($r^2 \geq 0.99$). The LOD was 0.05 µg/ml and the LOQ was 0.1 µg/ml for BG, WG and OAG. The intra-day and inter-day precision and accuracy of the assay method were listed in Table 5.2. The R.S.D. of both intra-day and inter-day precision at low, medium and high concentrations were below 13.39% for all the analytes. Besides, the intra-day and inter-day accuracy calculated by R.E. were within the range of -13.35% to 8.73%.

As shown in Table 5.3, the extraction recoveries of BG, WG and OAG at low, medium and high concentrations were above 89.42%.

Table 5.2 Linearity, intra-day and inter-day precision and accuracy of the developed HPLC/UV method for BG, WG and OAG

Flavones	Linear range (µg/ml)	Regression equation	R^2	Nominal conc. (µg/ml)	Intra-day (n=5)			Inter-day (n=3)		
					Determined conc. (µg/ml)	Precision (%R.S.D.)	Accuracy (% R.E.)	Determined conc. (µg/ml)	Precision (%R.S.D.)	Accuracy (% R.E.)
BG	0.1-20	Y=0.1888X-0.0149	0.9989	0.5	0.483±0.027	5.67	-3.44	0.544±0.062	11.40	8.73
				1.0	0.876±0.079	9.07	-12.38	0.987±0.044	4.50	-1.25
				10.0	9.241±0.827	8.95	-7.59	10.008±0.457	4.57	0.08
WG	0.1-20	Y=0.2258X-0.0522	0.9947	0.5	0.478±0.022	4.57	-4.44	0.525±0.022	4.13	5.06
				1.0	0.890±0.070	8.80	-10.96	0.953±0.022	2.23	-4.73
				10.0	8.801±0.635	7.22	-11.99	9.756±0.749	7.67	-2.44
OAG	0.1-20	Y=0.2023X-0.0247	0.9991	0.5	0.433±0.019	4.34	-13.35	0.509±0.068	13.39	1.88
				1.0	0.913±0.056	6.12	-8.74	1.010±0.062	6.13	1.03
				10.0	9.055±0.520	5.74	-9.45	9.681±0.353	3.64	-3.19

Table 5.3 Sample extraction recoveries of BG, WG and OAG by of the developed HPLC/ UV method (n=3)

Flavones	Concentration (µg/ml)		
	0.5	1.0	10.0
BG	94.94±13.66	96.77±5.95	99.59±5.17
WG	94.00±9.80	89.42±8.06	98.91±1.15
OAG	97.58±5.63	99.77±8.76	104.82±5.92

5.4.2 Kinetic profiles of glucuronidation of W and OA in various sub-cellular fractions

The enzymatic kinetic profiles of glucuronidation of W and OA by human liver microsome, rat liver microsome, human intestinal microsome, human liver S9, rat liver S9 and rat intestine S9 were obtained and compared (Fig. 5.3). The formation of WG and OAG at various concentrations followed the Michaelis-Menten equation with favorable goodness of fit (R^2>0.9) and the enzymatic kinetic parameters including K_m, V_{max} and Cl_{int} (V_{max}/K_m) were listed in Table 5.4. Comparing the kinetic parameters between W and OA, it was found that W showed higher V_{max} and OA showed lower K_m and higher intrinsic clearance in the six studied sub-cellular fractions. As to the extent of glucuronidation, W and OA demonstrated similar rank order of biotransformation efficiency in the studied sub-cellular fractions, which was RLM>HLM>HIM> HLS9~RLS9~RIS9.

Six sub-cellular fractions were used to study the glucuronidation of both W and OA. There was only one glucuronic acid conjugate found for OA in all the tested systems. However, in addition to WG (Wogonin-7-O-glucuronide), there was the other peak in trace amount, found in the incubation mixture of rat liver microsome. Since the reaction system only allowed the glucuronidation to take place, it was presumed that this new glucuronidated metabolite of W might be the glucuronic acid conjugate at the other available OH site (5-OH) of W, which needs further confirmation.

W and OA shared a similar rank order of glucuronidation formation in various sub-cellular fractions with the highest formation rate for RLM. The curves of formation rate versus substrate concentration in RLS9 and HLS9 almost overlapped with each other for both W and OA. Based on *in vitro* intrinsic clearance in the sub-cellular fraction from the same species, it was found that the intrinsic clearance for transformation from aglycones (W and OA) to glucuronic acid conjugates (WG and OAG) in human were comparable to those in rat. Such findings indicated that there was no species difference in hepatic glucuronidation for W and OA. To find if there was organ preference existing for the glucuronidation of W and OA, the enzymatic kinetic parameters in the sub-cellular fractions from the same species but different organ were compared. It was found that the formation of glucuronides was faster in intestine in human, whereas liver clearance was higher in rat. Nevertheless, both flavones showed high affinity to intestinal microsome or S9 fraction in both species with lower K_m value, indicating that the intestinal glucuronidation of W and OA could be activated at relatively low concentration.
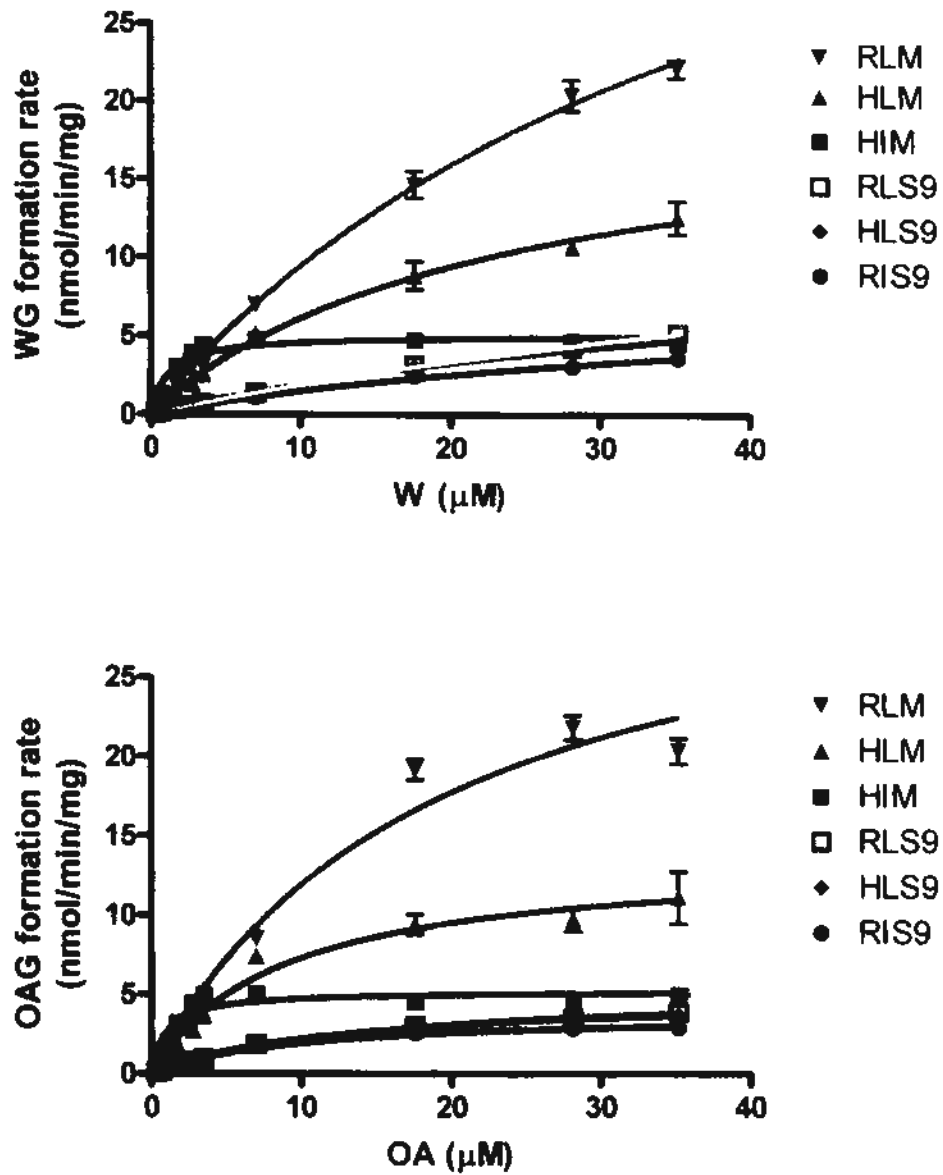
Fig. 5.3   Metabolic formation of WG (upper) and OAG (lower) in various
            sub-cellular fractions (n=3)
            HLM: human liver microsome; RLM: rat liver microsome
            HIM: human intestine microsome; RIS9: rat intestine S9 fraction
            HLS9: human intestine S9 fraction; RLS9: rat liver S9 fraction

Table 5.4   Enzyme kinetic parameters of the glucuronidation for W and OA in various sub-cellular fractions (n=3)

Sub-cellular fractions	W			OA		
	V_{max} (nmol/min/mg)	K_m (μM)	Cl_{int} (μl/min/mg)	V_{max} (nmol/min/mg)	K_m (μM)	Cl_{int} (μl/min/mg)
HLM	20.53±1.80	23.59±4.08	870	13.69±0.94	8.76±1.67	1562
HIM	5.13±0.16	1.23±0.17	4170	5.24±0.24	1.04±0.23	5038
RLM	51.16±5.16	44.31±7.09	1154	34.83±2.97	19.25±3.49	1809
HLS9	37.58±9.99	42.50±18.15	884	18.48±1.68	13.16±2.91	1404
RLS9	60.06±25.83	77.42±45.11	775	20.12±1.98	15.72±3.53	1279
RIS9	8.05±0.56	44.04±4.85	182	3.87±0.14	9.95±0.96	388

HLM: human liver microsome; RLM: rat liver microsome; HIM: human intestine microsome; RLS9: rat liver S9 fraction; HLS9: human liver S9 fraction; RIS9: rat intestine S9 fraction

5.4.3 Enzymatic kinetic profiles of glucuronidation of W and OA in human UGT isozymes

Since the content of specific UGT isozyme in the sub-cellular fraction was unknown, it would be difficult to interpret the enzymatic kinetics data. Therefore, further *in vitro* enzyme kinetic study using human recombinant UGT isozymes were conducted to find out which UGT isozyme was predominantly responsible for the glucuronidation of W and OA. Eight UGT isozyems were selected to investigate the glucuronidation of W and OA in human, in which six of them were from 1A subfamily and two were from 2B subfamily. Majority of the UGT isozymes have high expression in liver. They included UGT 1A1, UGT 1A3, UGT 1A4, UGT 1A6, UGT 1A9, UGT 2B4, UGT 2B7, UGT 2B10, UGT 2B11, UGT 2B15, UGT 2B17 and UGT 2B28 (Kiang et al., 2005). UGT 2B4 and UGT 2B15 have extremely high expression level in liver (Ohno et al., 2009). In the extrahepatic organs, UGT 1A8 and UGT 1A10 are expressed in the gastrointestinal tract (Cheng et al., 1998, Strassburg et al., 1997). UGT 1A7 is only expressed in the esophagus, stomach and lung (Strassburg et al., 1997) and UGT 2B1 is mainly in nasal epithelium (Jeditschky et al., 1999).

Eight human UGTs were selected to investigate the glucuronidation of W and OA in the present study. Not surprisingly, UGT 1A1, UGT 1A3, UGT 1A7, UGT 1A8, UGT 1A9, UGT 1A10 and UGT 2B15 could catalyze the glucuronidation of W and OA with the Cl_{int} ranging from 244 to 1269 nmol/min/mg for W and from 194 to 2274 nmol/min/mg for OA. This result indicated that W and OA could undergo extensive intestinal and hepatic Phase II metabolism in human. The metabolic formation versus substrate

concentrations are shown in Fig. 5.4a and Fig. 5.4b (UGTs 1A1 and 1A3). The kinetic parameters are listed in Table 5.5 and Table 5.6 (UGTs 1A1 and 1A3). Except for UGT 2B4, the other UGT isozymes showed glucuronidation activity toward W and OA. In addition, the enzymatic kinetic profiles of UGTs 1A1 and 1A3 could not be explained by Michaelis-Menten equation, while the profiles of W and OA by other UGT isozymes complied with the typical curves described by Michaelis-Menten equation with favorable goodness of fit ($R^2 > 0.9$). For W, UGT 1A9 displayed the greatest capacity to W with the highest V_{max} and UGT 2B15 had the highest affinity to W with the lowest K_m value. For OA, UGT 1A8, 1A9 and 1A10 displayed similar capacity to it with similar V_{max}. OA showed the highest affinity to UGT 1A9 with the lowest K_m value. Among all the tested UGTs, UGT 1A9 showed the most efficient glucuronidation with the highest Cl_{int} for both W and OA. By comparing intrinsic clearance between W and OA obtained from the same UGT isozyme, it was found that UGT 1A subfamily showed a faster glucuronidation for OA, whereas UGT 2B subfamily exhibited a faster metabolism for W. However, because there was only one isozyme for UGT 2B subfamily tested in the current study, this tendency needs further information to justify. Different from other UGTs, the formation rate curves versus substrate concentration in UGTs 1A1 and 1A3 displayed a substrate inhibition kinetic profile for both W and OA. The formation rate of WG and OAG enhanced with the increase of substrate concentrations at the low concentration range till the maximal formation rate of glucuronides was reached at about 7 μM for both W and OA. Further increase of substrate concentration at high concentration range resulted in the decrease of metabolites formation rate for both W and OA. Although different protein concentrations and reaction times were tested for UGT

2B4, there was no glucuronidation occurred for neither W nor OA under any tested condition.

Although the glucuronidation kinetic profile in all the sub-cellular fractions and majority of UGT isozymes complied with Michaelis-Menten equation, the glucuronidation in UGT 1A1 and UGT 1A3 as well as the sulfation in human and rat liver cytosol, W and OA showed a different kinetic profile. As a result, Eadie-Hofstee plot was generated to determine the kinetic profiles in above mentioned sub-cellular fractions and UGTs. It was found that their Eadie-Hofstee plots showed characteristics of atypical kinetics similar to substrate inhibition (Fig. 5.6). In addition to Eadie-Hofstee plots, the data were also fitted by different models including substrate inhibition, Michaelis-Menten equation and Hill equation using the software of Prism. Based on the Akaike's information criterion values, F-test and correlation coefficient obtained from the fitting, the substrate inhibition model was found to be a suitable model to interpret the kinetic profiles of W and OA in above mentioned sub-cellular fractions and UGTs. Interestingly, B, W and OA had similar kinetic profile in UGT 1A1, but their enzymatic kinetic profile in UGT 1A3 were quite different. In UGT 1A3, the enzyme kinetic profile of B was fitted to a typical Michaelis-Menten equation, whereas the profiles of W and OA complied with a substrate inhibition profile. It was reported that the number of hydroxyl groups showed significant impact on the affinity of flavonoids to UGT 1A3 (Chen et al, 2008). In addition, the methoxy group might also contribute to the affinity of the substrate to UGT 1A3 (Xie et al, 2001). As a result, the existence of methoxy group and the difference in chemical structures might cause the different kinetic profiles between B and W, OA in UGT 1A3.

In a typical Michaelis-Menten kinetic model, there is an initial bi-molecular reaction between the enzyme (E) and substrate (S) to form the Enzyme-Substrate complex (ES) before the formation of the product. In the case of substrate inhibition, there are two binding sites in the enzyme for the substrate. The first molecule of substrate can bind to the enzyme and initiate subsequent reaction to form ES. The second molecule of substrate can further bind to the ES to form an inactive ternary complex (SES). Since the formation of the ES complex must precede the formation of the SES, substrate inhibition usually occurred at high substrate concentrations with lower measured velocity than expected (Copeland, 2000).
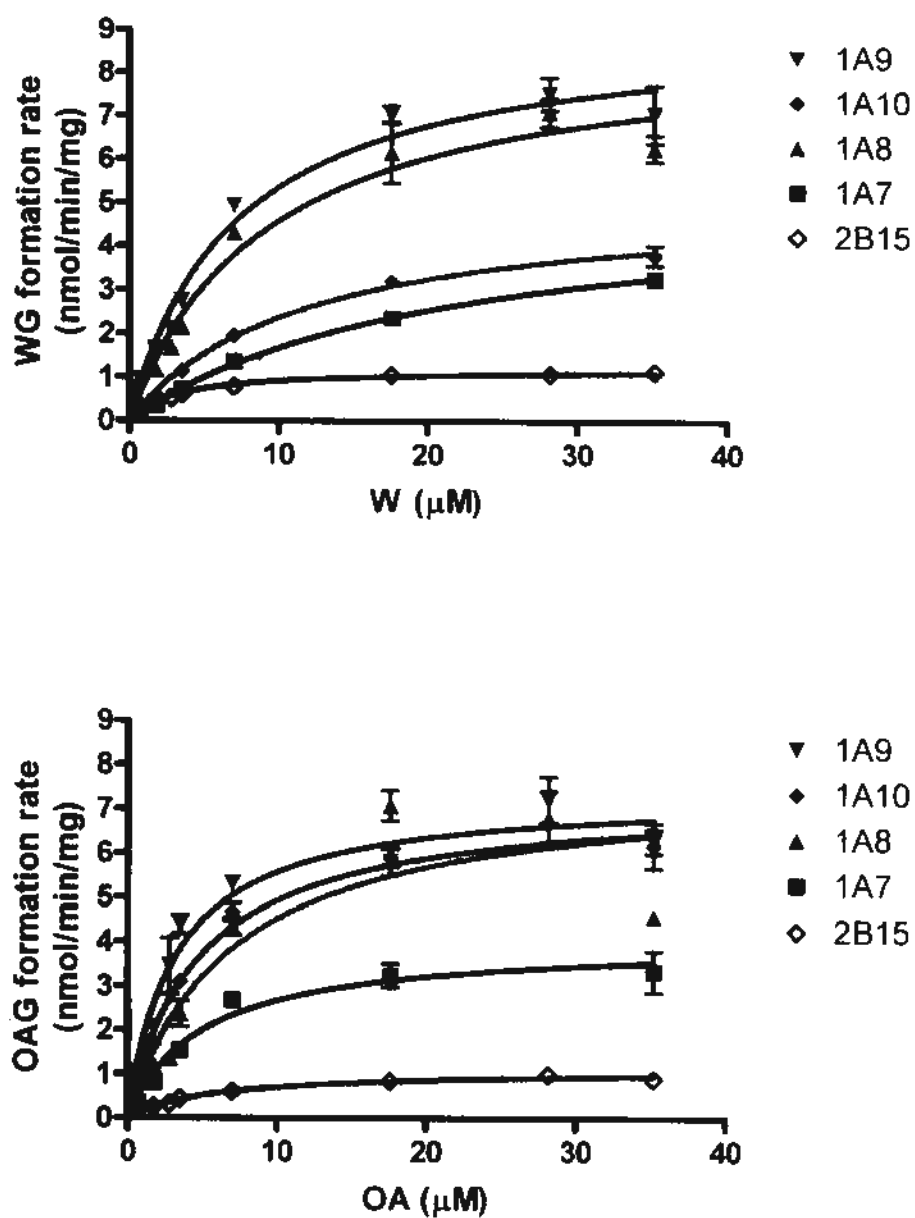
Fig. 5.4a Metabolic formation of WG (upper) and OAG (lower) in various UGT isozymes (n=3)
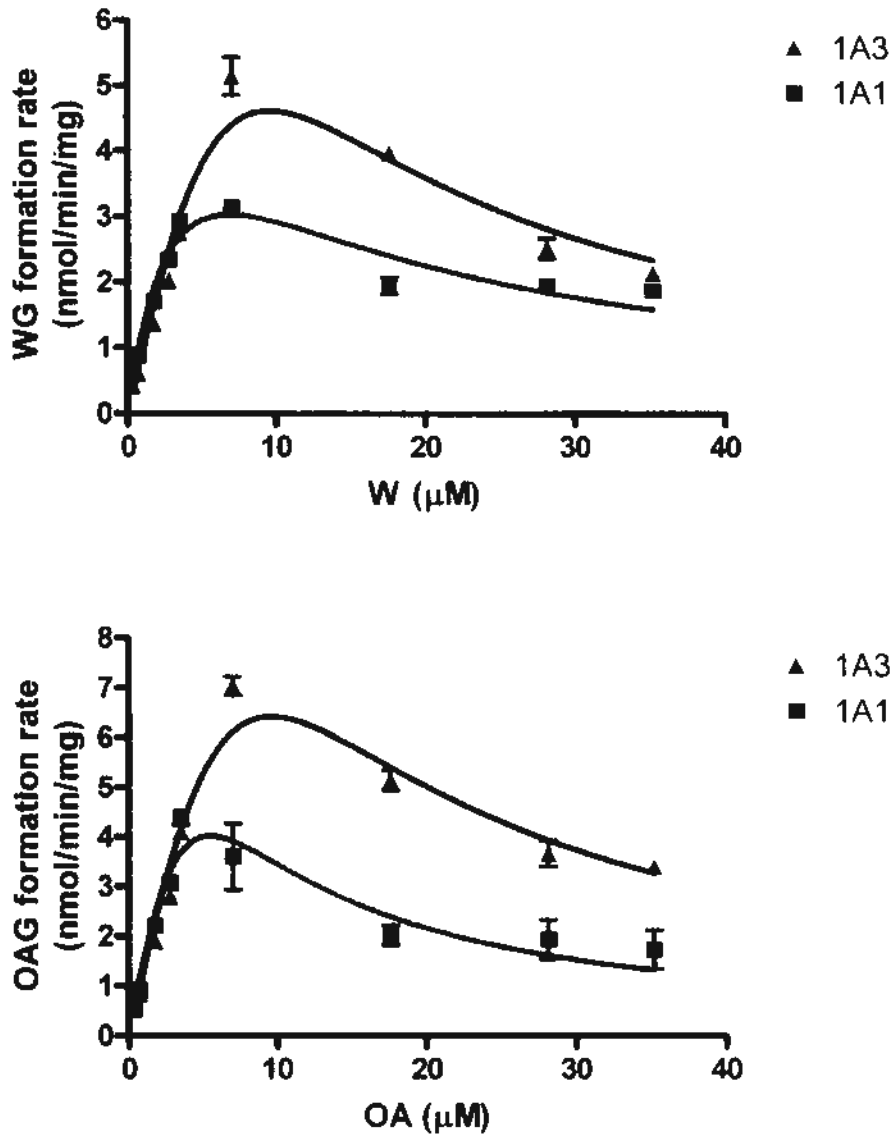
Fig. 5.4b　　Metabolic formation of WG (upper) and OAG (lower) in UGTs
1A1 and 1A3 (n=3)

Table 5.5   Enzyme kinetic parameters of the glucuronidation for W and OA in various UGT isozymes (n=3)

UGT isozyme	W			OA		
	V_{max} (nmol/min/mg)	K_m (μM)	Cl_{int} (μl/min/mg)	V_{max} (nmol/min/mg)	K_m (μM)	Cl_{int} (μl/min/mg)
1A7	5.28±0.32	21.61±2.59	244	4.04±0.31	5.17±1.22	781
1A8	8.86±0.54	9.37±1.54	945	7.65±0.75	6.96±1.99	1099
1A9	9.22±0.42	7.26±0.95	1269	7.37±0.31	3.24±0.48	2274
1A10	5.21±0.29	12.07±1.61	431	7.29±0.33	4.81±0.68	1515
2B4	N.D.	N.D.	N.A.	N.D.	N.D.	N.A.
2B15	1.21±0.03	3.20±0.31	378	1.11±0.03	5.72±0.55	194

N.A.: not available; N.D.: not detectable

5.4.4 Kinetic profiles of sulfation of W and OA in human and rat liver cytosols

W and OA could be transformed into the sulfate conjugates in human and rat liver cytosols in the presence of PAPS. However, the extent of sulfation was much lower than their glucuronidation. The UV spectrum of formed sulfate conjugates resembled those of corresponding aglycones and their structures were further confirmed by LC-MS/MS. The major fragment ions were observed at m/z of 283 from the quasi-molecular ions at m/z of 363, indicating the loss of sulfate group. For W and OA, their kinetic profiles of sulfation complied with substrate inhibition in both human and rat liver cytosol. The curves of metabolite formation rate versus substrate concentration are shown in Fig. 5.5 and the kinetic parameters were listed in Table 5.6.

Due to the commercial unavailability of the standard compounds of WS and OAS, the concentrations of WS and OAS after the transport study in Caco-2 cell monolayer model was quantified indirectly based on the assumptions that WS/OAS has the same UV absorbance group as W/OA and one molar of W/OA produce one molar of WS/OAS. As a result, the calibration curve was firstly plotted with the molar concentrations of W/OA versus the peak area ratios of W/OA to IS. The molar concentration of WS/OAS was calculated based on their observed peak are ratios from the above calibration curve of W/OA. W and OA could be transformed into sulfate conjugates by the sulfotransferase (SULT) in HLC and RLC, whereas there was no reaction in RIS9. This finding is consistent with our previous studies by rat *in situ* single-pass intestinal perfusion model that W and OA underwent only glucuronidation rather than sulfation in rat intestine in Chapter Four. As the human intestinal cytosol and S9 fraction are not commercially

available, the intestinal sulfation of W and OA could not be investigated in enzymatic incubation study at this stage. The enzymatic kinetic study of W and OA in HLC and RLC also showed a substrate inhibition profile with a low intrinsic clearance value. Comparing with the glucuronidation of W and OA in human and rat liver microsomes, their sulfation in corresponding cytosol fractions demonstrated low V_{max} and K_m values, indicating that W and OA had higher affinity but lower capacity to SULTs than UGTs. This was consistent with our previous findings in Caco-2 monolayer model in Chapter Four that sulfation was easier to be saturated. As a result, it was suggested that both glucuronidation and sulfation contributed to the Phase II metabolism of W and OA at low concentration (lower than 10 μM), while glucuronidation was the major metabolic pathway for W and OA at a higher concentration range.
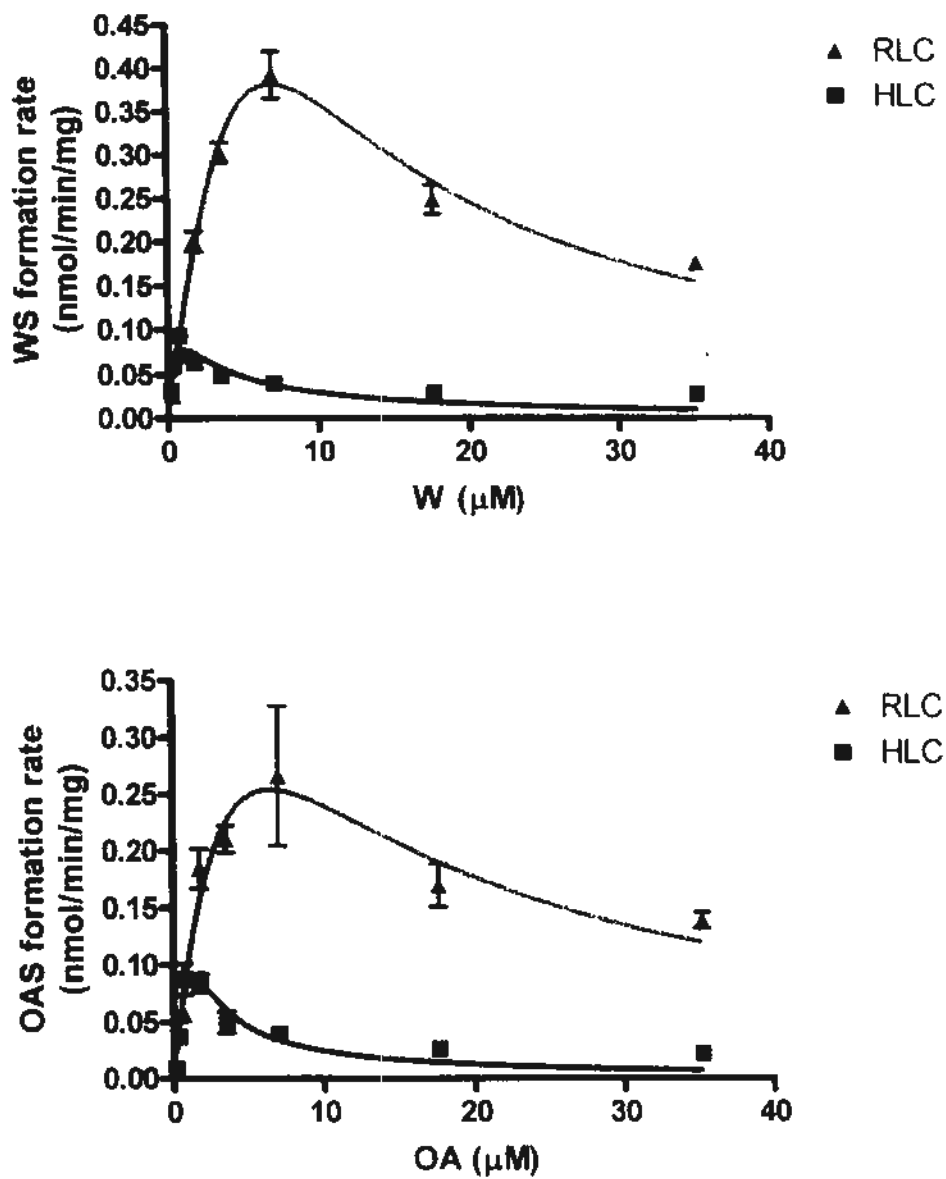
Fig. 5.5   Metabolic formation of WS (upper) and OAS (lower) in human
and rat liver cytosols (n=3)
HLC: human liver cytosol; RLC: rat liver cytosol

Table 5.6 Substrate inhibition enzyme kinetic parameters of W and OA in human and rat liver cytosols and UGTs 1A1 and 1A3 (n=3)

Sub-cellular fraction /Isozyme	W				OA			
	V_{max} (nmol/min/mg)	K_m (μM)	K_i (μM)	Cl_{int}^{*} (μl/min/mg)	V_{max} (nmol/min/mg)	K_m (μM)	K_i (μM)	Cl_{int}^{*} (μl/min/mg)
UGT 1A1	6.78±1.36	4.29±1.35	11.16±3.44	705	19.48±7.69	10.95±5.32	2.77±1.55	1165
UGT 1A3	28.29±4.27	26.51±5.19	3.56±0.76	714	40.58±13.91	27.40±10.73	3.22±2.21	988
HLC	0.14±0.04	0.41±0.23	2.79±1.46	114	0.70±0.49	4.82±3.78	0.38±0.35	147
RLC	2.43±0.55	19.05±5.03	2.56±0.73	122	0.84±0.63	3.35±3.26	2.44±2.49	127

$^{*}Cl_{int}$ was calculated based on the slope of the initial linear portion of the metabolite formation rate versus substrate concentrations plot
HLC: human liver cytosol; RLC: rat liver cytosol

Glucuronidation
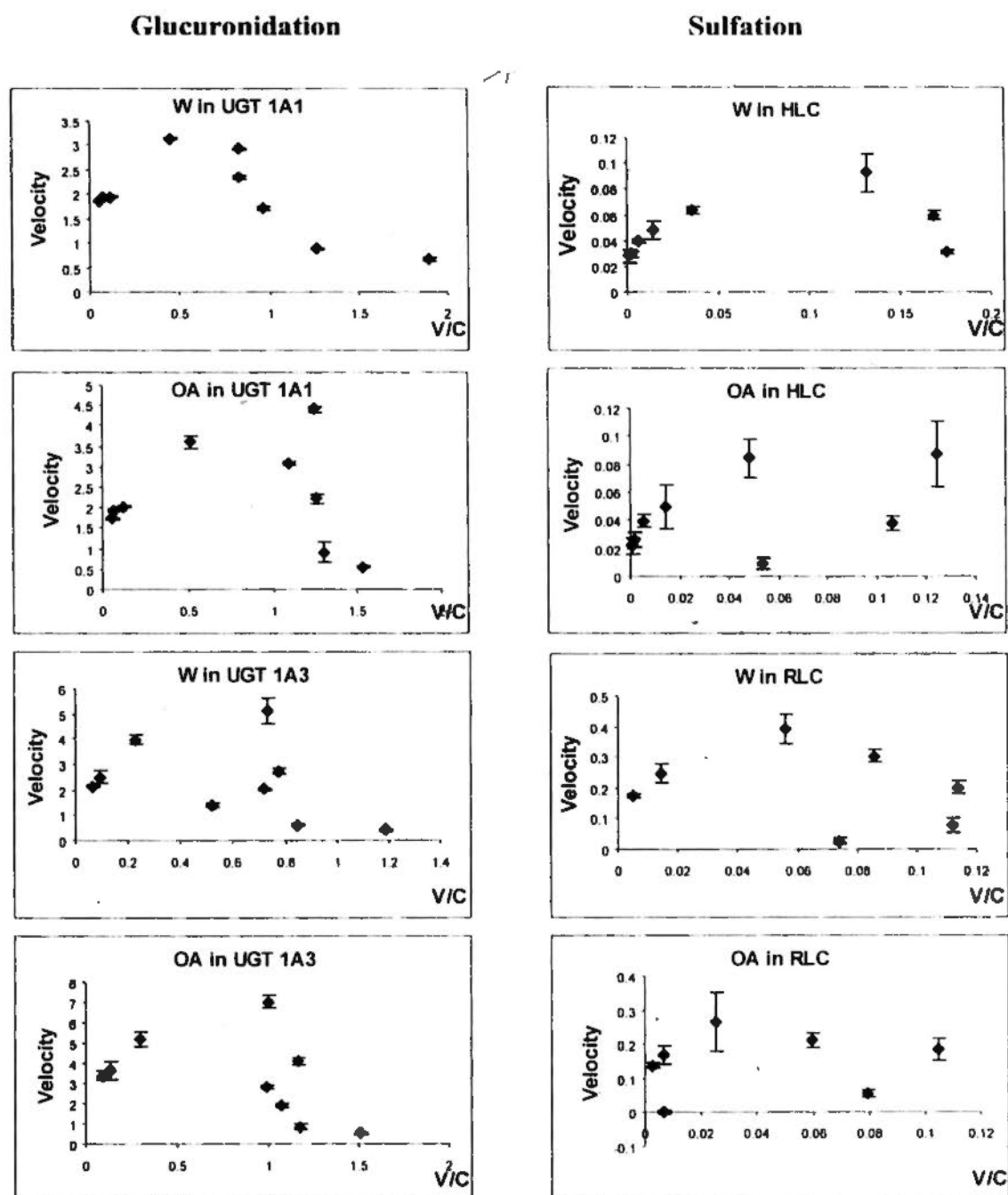
Sulfation

Fig. 5.6   Eadie-Hofstee plots for glucuronidation of W and OA in UGTs
1A1 and 1A3 (left) and sulfation profiles in HLC and RLC (right)
HLC: human liver cytosol; RLC: rat liver cytosol

5.5   Conclusions

The findings in hepatic and intestinal metabolisms of W and OA were summarized in Fig. 5.7. Similar to our previous findings on B, both W and OA would undergo extensive hepatic and intestinal glucuronidation in human and rat. Based on the studies by various recombinant human UGT isozymes, it was found that the hepatic glucuronidation of W and OA was mainly catalyzed by UGT 1A9, whereas UGT 1A8 and UGT 1A10 were responsible for their intestinal glucuronidation. The extent of sulfation for both W and OA was low in human and rat liver cytosol and could not be found in RIS9 fraction. The hepatic glucuronidation and sulfation of W and OA showed no species difference. OA demonstrated the highest glucuronidation rate among B, W and OA.
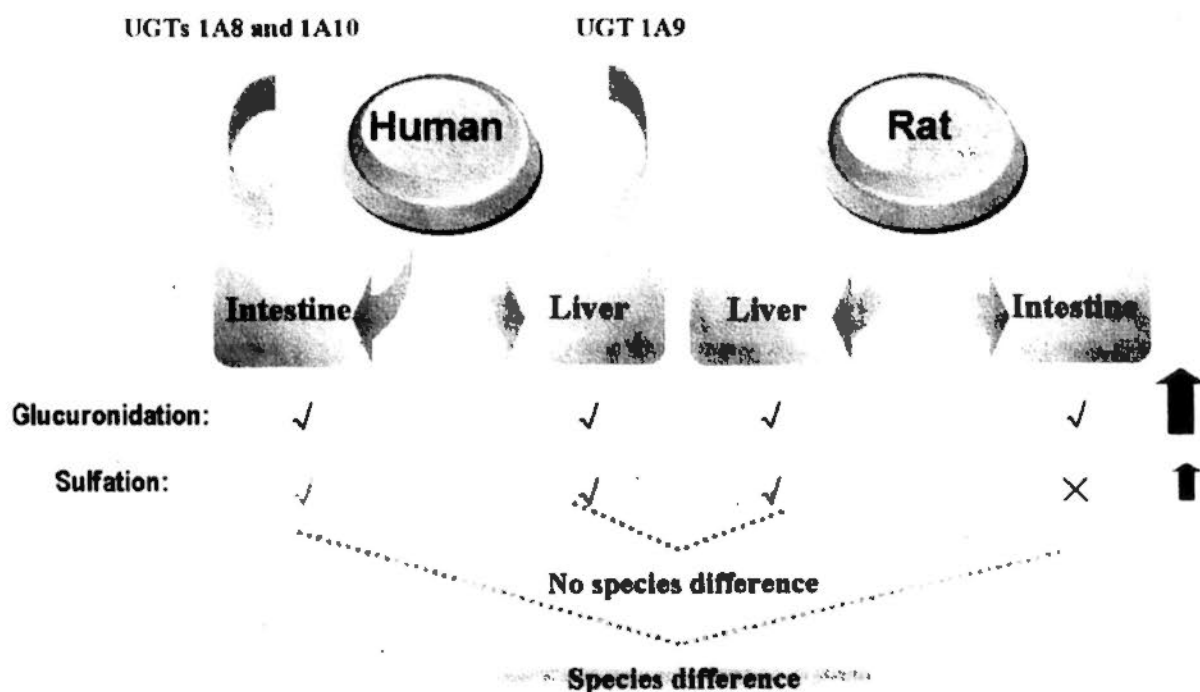
Fig. 5.7   Proposed mechanisms for the hepatic and intestinal metabolisms of W and OA

Chapter Six

Biopharmaceutics and pharmacokinetics interactions among major bioactive components in *Radix Scutellariae*

– *in vitro*, *in situ* and *in vivo* evidences

6.1 Introduction

For most herbal medicines, they are consumed by oral administration in the form of decoction or proprietary traditional Chinese medicine (PTCM) products. Thus, it is of great importance and relevance to investigate their pharmacokinetic characteristics after oral administration to guarantee their safety. Besides, since the components in the herb decoction and PTCM products are complicated, there might be interactions between the ingredients in the same herb or ingredients from different herbs or even between the herbal ingredients with the excipients used in PTCM. As a result, in order to clearly identify the roles of each ingredient in the overall pharmacokinetics of a herbal medicine, the essential step is to investigate the pharmacokinetic characteristics of each single major bioactive components of the studied herbal medicine.

Based on our previous study on B (Zhang et al., 2007a) and our findings on W and OA in Chapter Four and Five, it was demonstrated that these flavones could be readily absorbed, however, would undergo similar absorption and disposition pathways. Previous studies from us and others on flavonoids indicated that the glycosides of flavonoids could not be absorbed at intestine and they were hydrolyzed to their corresponding aglycone forms by

intestinal lactose-phlorizin hydrolase in GI tract for absorption. As a result, the biopharmaceutic and pharmacokinetic interactions were studied only for the aglycones of B, W and OA, rather than their corresponding glucuronides.

Although there are a number of pharmacokinetic studies on B in rat, the *in vivo* pharmacokinetics information about W and OA is rather limited. There is only one report on the plasma concentration versus time profiles for W and WG in Wistar rat after oral administration of pure compound of W (Chen et al., 2002) and one on the pharmacokinetic parameters of W in beagle dogs after intravenous infusion of W (Peng et al., 2009). After oral administration of a purified extract of *Scutellaria baicalensis* Georgi at low, middle and high dose, the parent compound of OA could not be detected in plasma but its glucuronic acid conjugate could be detected in plasma, urine and gastrointestinal tract (Kim et al., 2007). In addition, most pharmacokinetic study about the bioactive components in RS are investigated in the form of traditional Chinese formulations in which other herbs are also included like Shuang-Huang-Lian (Di et al., 2006, Xiexin Decoction (Yan et al., 2007, Li et al., 2005), Huangqin-Tang (Zuo et al., 2002 and 2003), Huang-Lian-Jie-Du-Tang (Deng et al., 2006 and 2008, Lu et al., 2007).

In the present study, the biopharmaceutic and pharmacokinetic interactions among the major bioactive flavones in RS were further investigated by these *in vitro* and *in situ* models mentioned in Chapter Four and Five. Considering the complexity of herbal preparations, the present study also aimed to investigate the pharmacokinetics characteristics of pure compounds of B, W and OA followed by the pharmacokinetic

interactions among these flavones after oral administration of these compounds mixtures at similar dose to pure compounds.

6.2   Material and reagents

Baicalein (B) and baicalin (BG) with purity over 98% were purchased from Sigma-Aldrich Chem. Co. (Milwaukee, WI, USA). Wogonin (W) and wogonoside (WG) with purity over 98% were purchased from AvaChem Scientific LLC (San Antonio, TX, USA). Oroxylin A (OA, purity over 98%) and Oroxylin A-7-*O*-glucuronide (OAG, purity over 95%) were supplied by Shanghai u-sea biotech co., Ltd (Shanghai China). 3, 7-dihydroxyflavone with purity of 97% was purchased from Indofine Chemical Company (Hillsborough, NJ, USA).

Phenol red, calcium chloride and sodium dihydrogen phosphate were purchased from BDH chemical Ltd (Poole, England). Potassium chloride, PEG 400 and ascorbic acid were supplied by Wing Hing Chemical Co. (Hong Kong). Potassium dihydrogen phosphate was purchased from Merck (Darmstadt, Germany).

Uridine 5'-diphosphoglucuronic acid (UDPGA) and alamethicin were obtained from Sigma-Aldrich Chem. Co. (Milwaukee, WI, USA). Pooled human liver microsomes, pooled human intestinal microsomes, pooled male rat liver microsomes, pooled male rat intestinal S9 (Sprague-Dawley), recombinant human UGT1A8 and UGT1A9 were purchased from BD Biosciences (Woburn, MA, USA).

Waters Oasis® hydrophilic-lipophilic-balanced (HLB, 1cc) copolymer extraction cartridges were purchased from Waters. Acetonitrile (Labscan Asia, Thailand) and methanol (TEDIA company, Inc., USA) were HPLC grade and used without further purification. All other reagents were of at least analytical grade. Distilled and deionized water was prepared from Millipore water purification system (Millipore, Milford, USA).

6.3   Methods

6.3.1   Instrumentation and chromatographic conditions

6.3.1.1 HPLC/UV for quantification of six bioactive flavones in RS

The instrumental and chromatographic conditions were described in section 3.2.2.1 of Chapter Three. The UV detection wavelength was set at 320 nm for the assay of plasma sample and set at 270 nm for the assay of sample obtained from transport study on Caco-2 cell monolayer model, *in vitro* enzymatic kinetic study and rat *in situ* single-pass intestinal perfusion model.

Due to the commercial unavailability of the standard compounds of WS and OAS, the concentrations of WS and OAS after the transport study in Caco-2 cell monolayer model was quantified indirectly based on the assumptions that WS/OAS has the same UV absorbance group as W/OA and one molar of W/OA produce one molar of WS/OAS. As a result, the calibration curve was firstly plotted with the molar concentrations of W/OA versus the peak area ratios of W/OA to IS. The molar concentration of WS/OAS was

calculated based on their observed peak are ratios from the above calibration curve of W/OA.

6.3.1.2 *LC-MS/MS for identification of in vivo major metabolites of bioactive flavones from RS*

The LC-MS/MS system, chromatographic condition and mass spectrometer were described in section 3.2.2.2 of Chapter Three.

6.3.2   Caco-2 cell monolayer model

Cell culture procedure was described in section 4.3.1.1 of Chapter Four. Compound mixture of B, W and OA at the ratio of 1:1:1 (B: W: OA, 14.81 μM: 14.08 μM: 14.08 μM) in transport buffer were added into the apical side. The transport study of the compound mixture followed the procedure described in section 4.3.1.5 of Chapter Four.

6.3.3   Rat *in situ* single-pass intestinal perfusion model

Perfusate buffer was prepared as described in section 4.3.2.1 of Chapter Four. Animal surgical procedures were the same as section 4.3.2.3 of Chapter Four. Compound mixture of B, W and OA at the ratio of 1:1:1 (50 μM each) in perfusate buffer was used in the experiment.

6.3.4   *In vitro* enzymatic kinetic study

In order to investigate the metabolism competition among B, W and OA for glucuronidation, the mixture of three flavones at a serial of concentrations with the same

mixing ratio of 1:1:1 were tested for the enzyme reactions in human liver or intestinal microsome; rat liver microsome; rat intestinal S9; UGT 1A8; UGT 1A9. The *in vitro* glucuronidation activity assay and the sample preparation were the same as described in section 5.3.2 and section 5.3.4 of Chapter Five.

6.3.5 Pharmacokinetics characterization and interactions of major bioactive flavones in RS after oral administration

6.3.5.1 Animals and drug administration

Male Sprague-Dawley rats (body weight, 230-250 g) were supplied by the laboratory Animal Services Center at the Chinese University of Hong Kong. The experiment was conducted under the approval by Animal Ethics Committee of the Chinese University of Hong Kong. The rats were anesthetized with an intramuscular injection of a cocktail containing 60 mg/kg ketamine and 6 mg/kg xylazine. Right jugular vein was cannulated with a polyethylene tubing (0.5 mm ID, 1 mm, Portex Ltd., Hythe, Kent, England) for blood sampling. After surgery, the rats were allowed to recover over night under fasting condition with free access to water.

Pure compound of B, W and OA as well as their mixture were prepared in the solvent mixture of PEG 400 and 20% Solutol® HS15 (3:7, *v/v*) at the concentration of 1.25 mg/ml for each flavone both single compound group and compound mixture group (6 rats for each group). Rats were randomly divided into four groups. Three groups were orally administrated with single compound of B, W and OA at 5 mg/kg, respectively and the

forth group was administrated with these compound mixtures (B+W+OA, 5 mg/kg each). Blood samples were taken at 3, 5, 10, 30, 60, 120, 240 and 480 min after dosing. Plasma samples were obtained after centrifugation of the blood samples at 16, 000×g for 3 min and stored at -80 °C until analysis.

6.3.5.2 Sample preparation

All the plasma samples were treated as described in section 3.2.4 of Chapter Three.

6.3.5.3 Data analyses

The plasma concentration versus time profile was analyzed by the software of Win Nonlin (Pharsight Corporation, Mountain View, CA, USA, Version 2.1). Non-compartmental model was chosen to calculate the pharmacokinetic parameters including the area under the plasma concentration-time curve from zero to 480 min ($AUC_{0 \to t}$) and elimination half-life ($t_{1/2\lambda z}$). The peak plasma concentration (C_{max}) and the time reaching C_{max} (T_{max}) were obtained directly from the experimental data.

All data are expressed as the mean ± SD (standard deviation). Student's t-test was employed to compare the biopharmaceutic and pharmacokinetic parameters between the single compound group and compound mixture group. A $p<0.05$ was considered to be statistically significant.

6.4   Results and discussions

6.4.1 Intestinal absorption interactions among B, W and OA in Caco-2 cell monolayer model

To evaluate the capacity of each flavone in the compound mixture, the ratio of 1:1:1 was employed. After co-administration of three aglycones together to the apical side at the ratio of 1: 1: 1 (B: W: OA, 14.81 μM: 14.08 μM: 14.08 μM), the cumulative amount of parent drugs at receiver side and the total amount of glucuronides metabolites (apical side + basolateral side + intracellular amount) were compared with that obtained from the group in which the flavones were loaded alone to the apical side at the same concentration (Fig. 6.1). It was found that the cumulative amount of the all parent drugs transported to receiver side increased, whereas the formation of their metabolites decreased comparing with that from the single compound group. Besides, the apparent permeability was calculated for each compound in both treatment groups. It was found that the P_{app} values of B and W were significantly increased in the compound mixture group. Although the P_{app} value of OA also showed a trend of increase, its difference between the single compound group and compound mixture group was not statistically significant (Table 6.1).

Besides, in order to mimic the compound mixture ratio in RS, the molar ratio of each flavone in RS was estimated based on our previous study on the quantification of major bioactive flavones in the reference herb of RS in Chapter Two. It was calculated based on the molar content ratio of (B+BG): (W+WG): (OA+OAG) and an appropriate ratio of 5:1:1 was obtained. Compound mixture of B, W and OA at 5:1:1 was thus tried in Caco-2 cell model. It was found that the cumulative amount of W and OA at basolateral side was

enhanced in compound mixture group, whereas the cumulative amount of B in basolateral side remained the same. The P_{app} value of W increased from $3.36 \pm 0.45 \times 10^{-6}$ cm/sec in single compound group to $15.11 \pm 1.50 \times 10^{-6}$ cm/sec in compound mixture group and the P_{app} value of OA increased from $2.32 \pm 0.31 \times 10^{-6}$ cm/sec in single compound group to $9.99 \pm 0.54 \times 10^{-6}$ cm/sec in compound mixture group. Such findings in type of compound with enhanced P_{app} differed from what has been observed from compound mixture at the ratio of 1:1:1 shown in Table 6.1. Due to the large amount of B in compound mixture at ratio of 5:1:1, the influence of W and OA on the intestinal absorption and metabolism of B might not be significant as that shown in compound mixture of 1:1:1. The further trial of compound mixture at 5:1:1 was not pursued due to limited solubility of such preparation at the large doses needed for *in situ* and *in vivo* models.
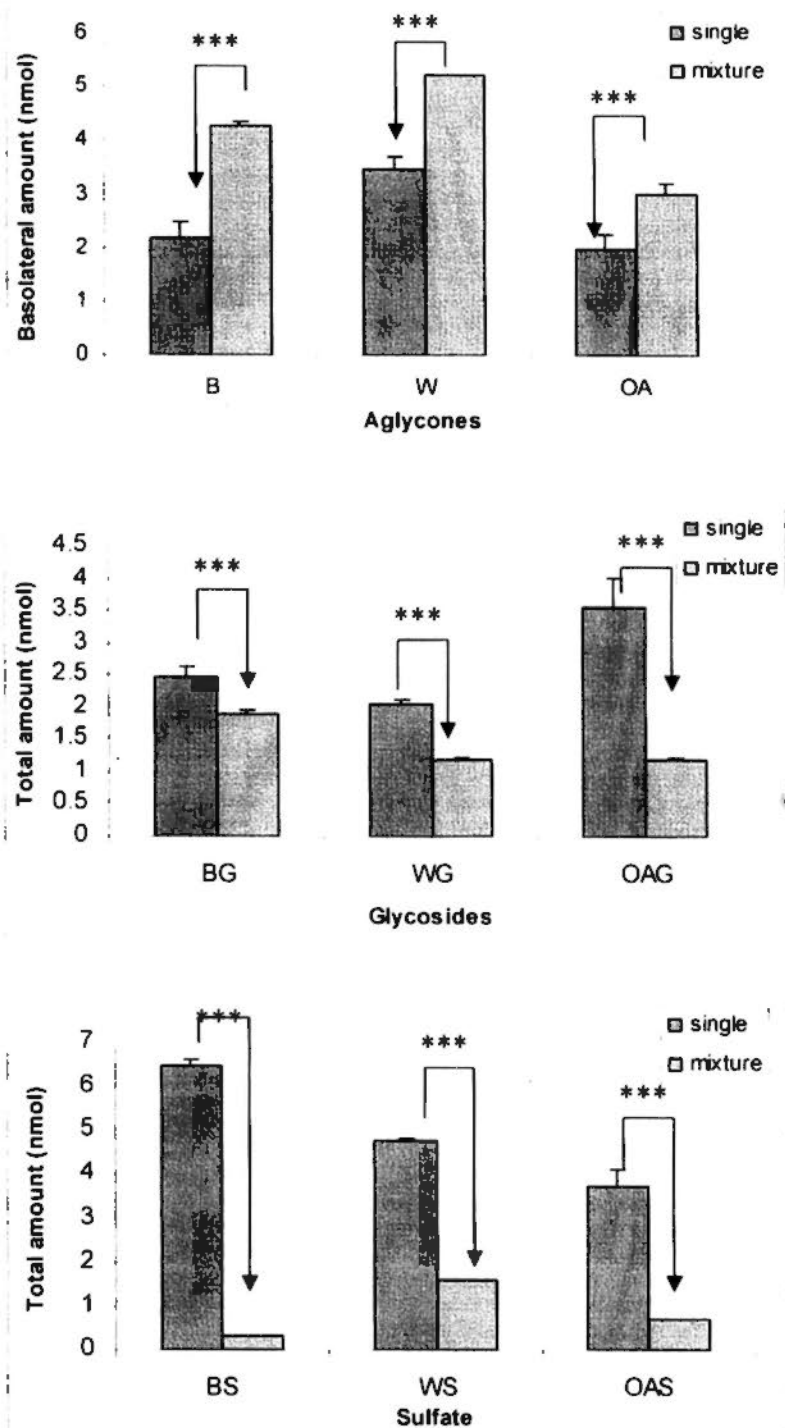
Fig. 6.1 Comparison of cumulative amount of B, W and OA at receiver side and total amount of their intracellularly formed metabolites between single compound group and compound mixture group at the ratio of 1: 1: 1, *w/w/w*
***: *p*< 0.001

Table 6.1   Comparison of apical to basolateral permeability of B, W and OA between single compound group and compound mixture group in Caco-2 cell monolayer model

Mixture ratio	P_{app} ($\times 10^{-6}$ cm/sec)					
	B		W		OA	
	Single	Mixture	Single	Mixture	Single	Mixture
1:1:1	5.40±0.85	10.66±0.98 **	11.68±1.51	14.94±0.21 *	10.28±2.48	12.11±1.03

** : $p < 0.01$, * : $p < 0.05$

6.4.2   Intestinal absorption interaction among B, W and OA in rat *in situ* single-pass intestinal perfusion model

The interaction among three bioactive flavones during their intestinal absorption and disposition was also investigated on the rat *in situ* single-pass intestinal perfusion model. The compound mixture of B, W and OA was perfused at the ratio of 1: 1: 1 (50 μM, each). The representative HPLC/UV chromatograms of perfusate samples and mesenteric plasma samples were shown in Fig. 6.2 and Fig. 6.3, respectively. For all the studied flavones, the cumulative amount of their glucuronides in perfusate and mesenteric blood as well as the absorbed parent flavones into the mesenteric blood increased linearly with the perfusion time (Fig. 6.4a to c).
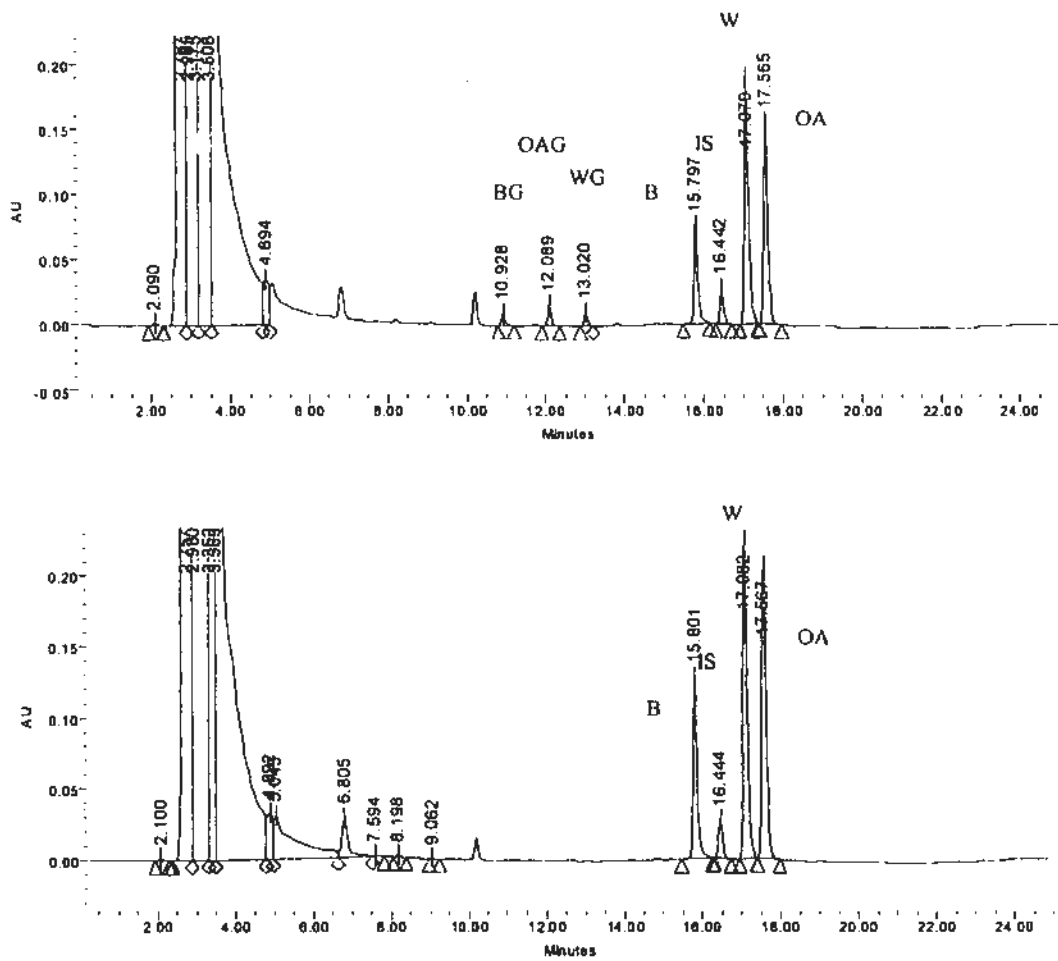
Fig. 6.2   Representative HPLC/UV chromatograms of perfusate samples obtained after (upper) and before (lower) perfusing 50 µM of compound mixture of B, W and OA (1:1:1, w/w/w) into rat small intestine

B: baicalein, BG: baicalin, W: wogonin, WG: wogonoside,

OA: oroxylin A, OAG: oroxylin A-7-O-glucuronide, IS: internal standard
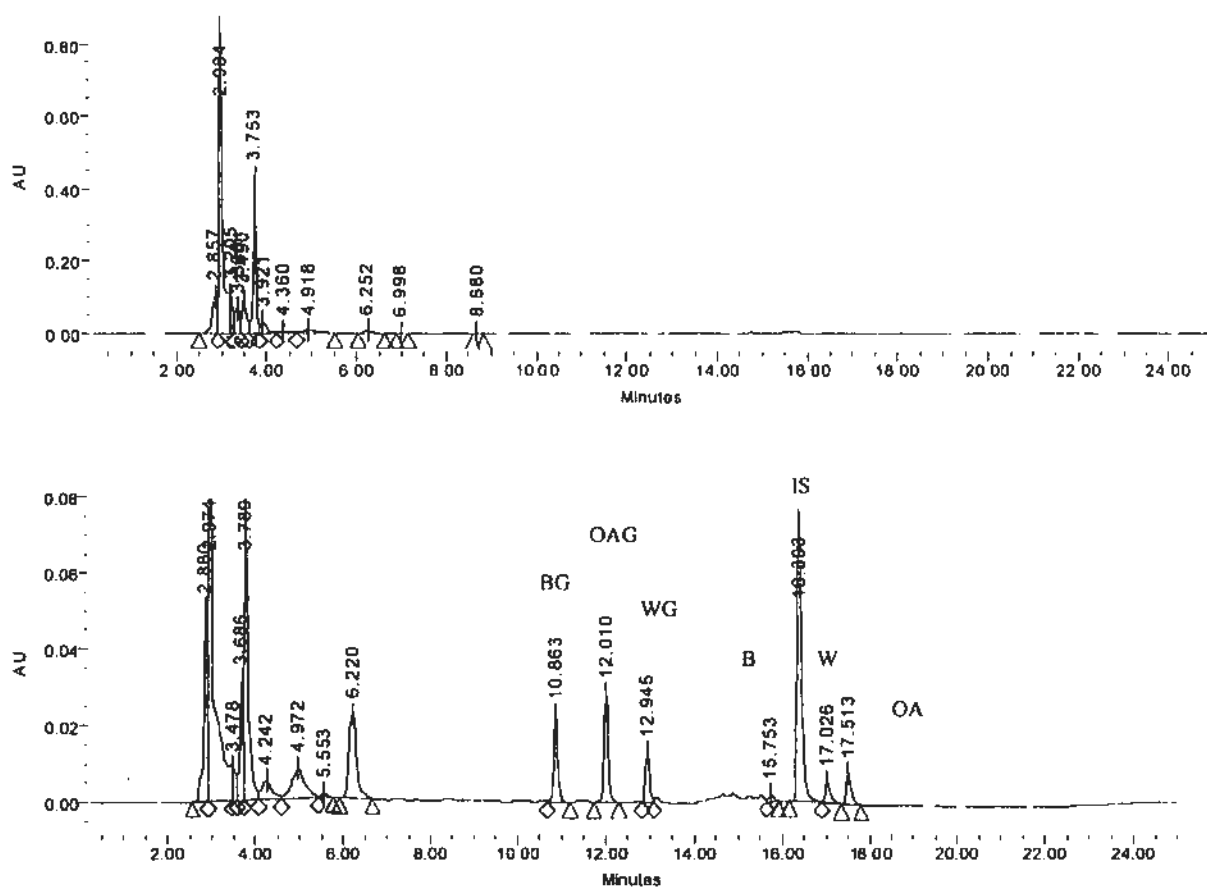
Fig. 6.3   Representative HPLC/UV chromatograms of blank plasma (upper);
and mesenteric plasma samples obtained after rat *in situ* single-pass
intestinal perfusion of compound mixture of B, W and OA (1:1:1,
w/w/w) (lower)

B: baicalein, BG: baicalin, W: wogonin, WG: wogonoside,
OA: oroxylin A, OAG: oroxylin A-7-*O*-glucuronide, IS: internal
standard
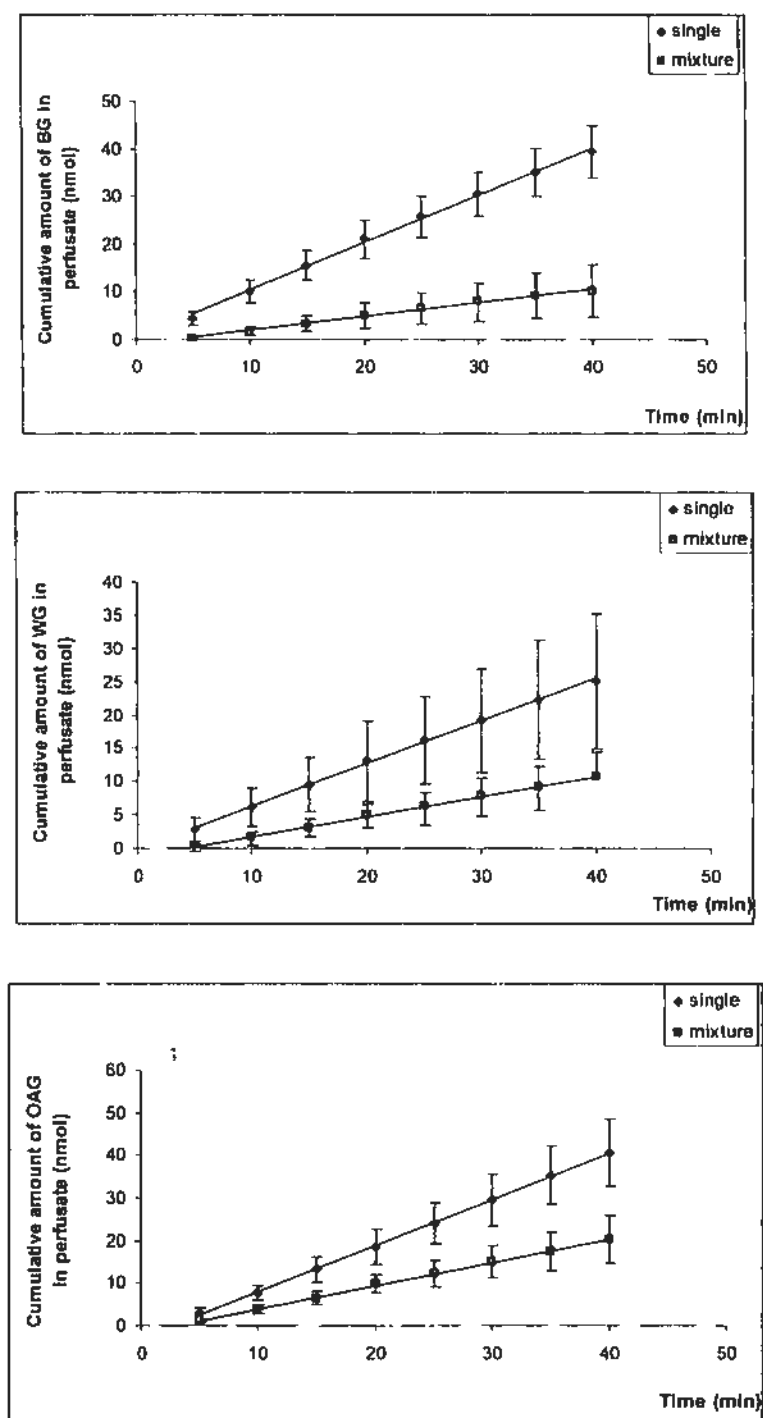
Fig. 6.4a   Cumulative amount of corresponding glucuronides appearing in the
             perfusate over time after perfusing 50 μM of B (upper), W (middle),
             OA (lower) into rat small intestine
             B: baicalein, W: wogonin, OA: oroxylin A
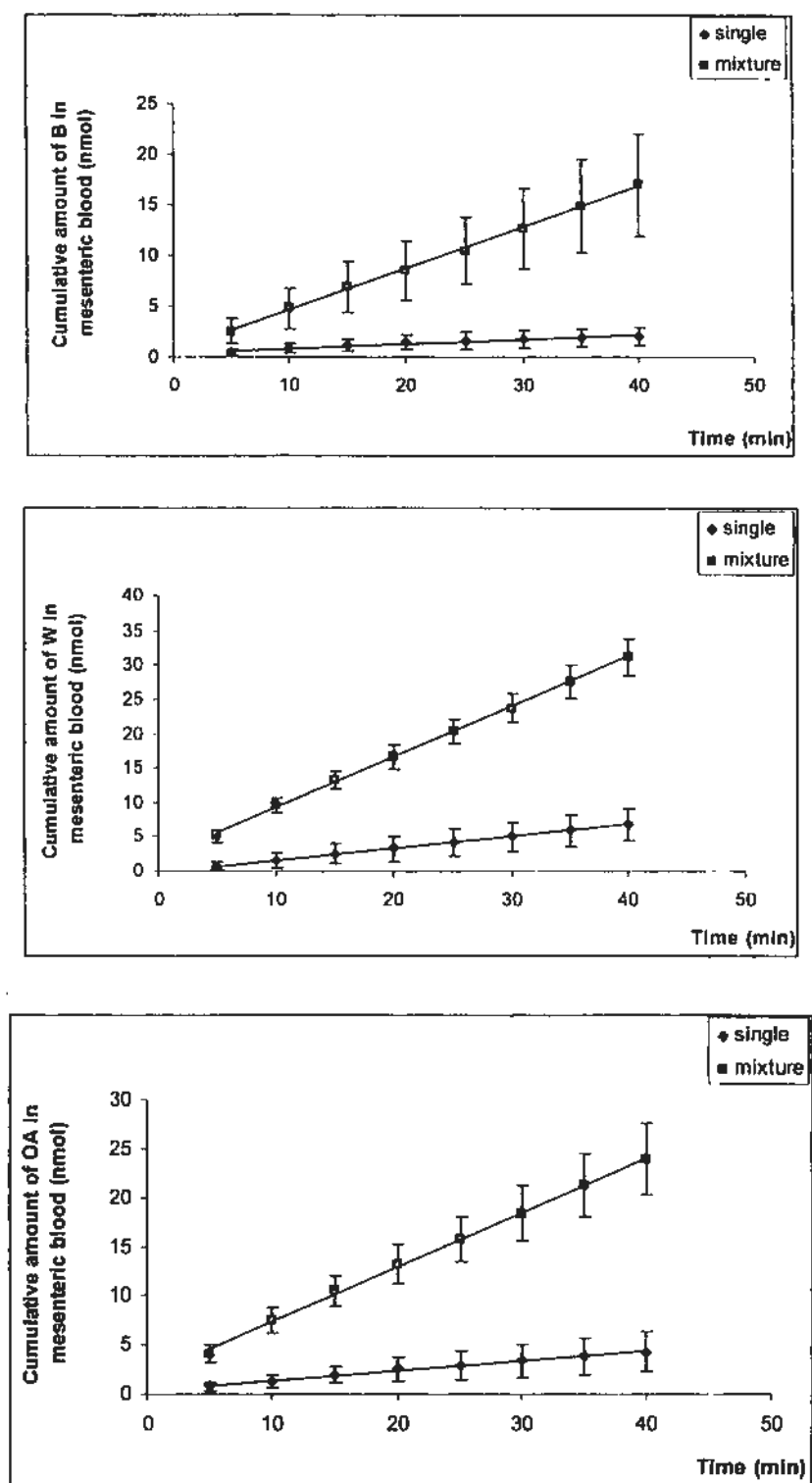
Fig. 6.4b   Cumulative amount of parent drugs appearing in the mesenteric blood over time after perfusing 50 μM of B (upper), W (middle), OA (lower) into rat small intestine

B: baicalein, W: wogonin, OA: oroxylin A
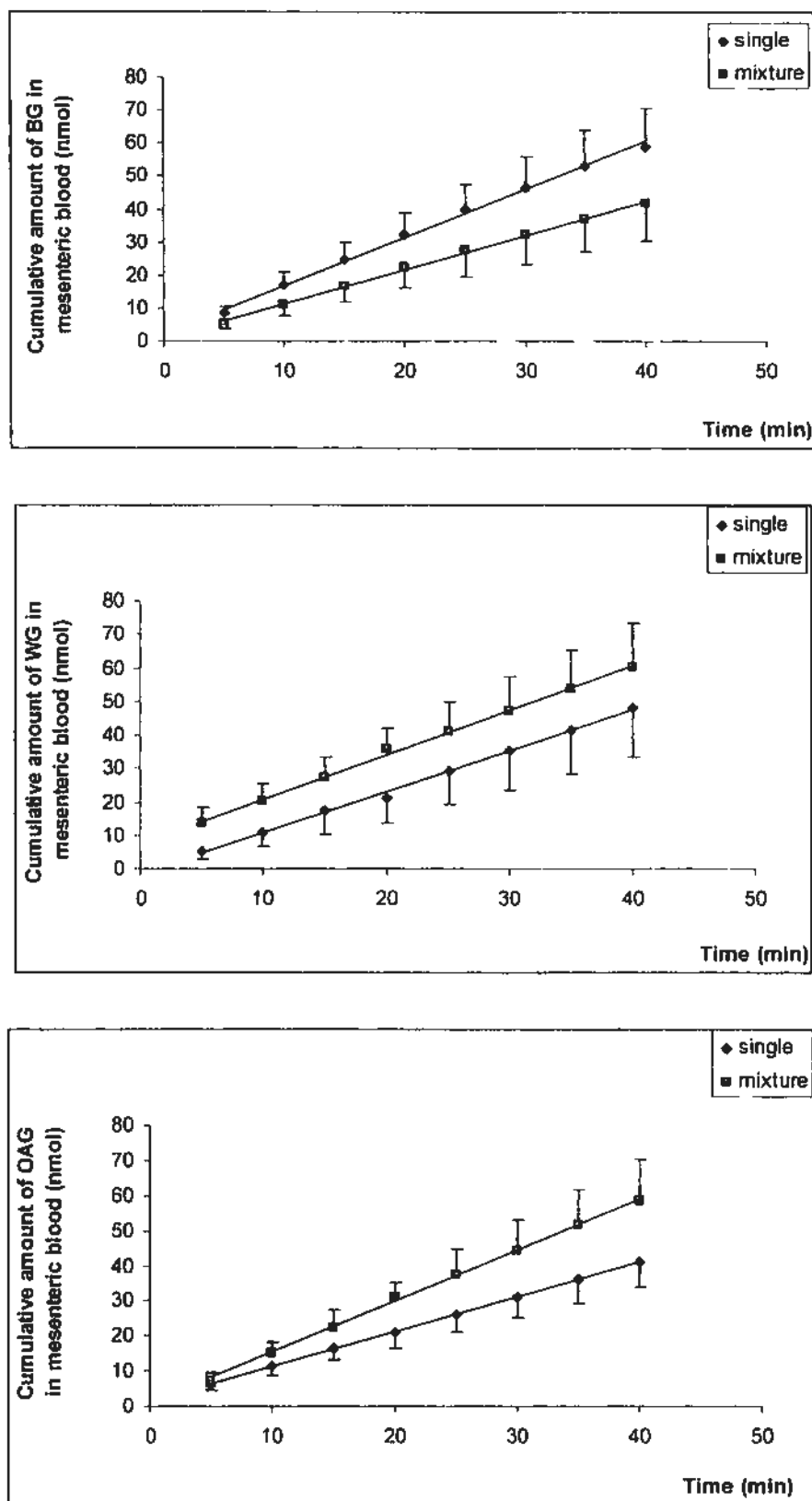
Fig. 6.4c Cumulative amount of corresponding glucuronides appearing in the mesenteric blood over time after perfusing 50 μM of B (upper), W (middle), OA (lower) into rat small intestine

B: baicalein, W: wogonin, OA: oroxylin A

Permeability coefficients of parent drugs were calculated based on both the appearance of the compounds in the mesenteric blood (P_{blood}) and the disappearance of the compound in the perfusate (P_{lumen}). The permeability coefficient (P_{blood}) of B, W and OA were $28.79 \pm 8.15 \times 10^{-6}$ cm/sec, $23.61 \pm 6.66 \times 10^{-6}$ cm/sec and $18.80 \pm 5.94 \times 10^{-6}$ cm/sec in the compound mixture group (Table 6.2). Nevertheless, after perfusing three flavones together, the P_{lumen} of B, W and OA did not change significantly in the compound mixture group. This might be due to the high background concentration of these compounds in perfusate, which may not allow sensitive detection of the relative minor changes in concentrations. On the contrary, comparing with the single compound group, the P_{blood} values were all significantly increased in the compound mixture group by 20-fold, 5-fold and 6-fold for B, W and OA, respectively (Table 6.2).

Table 6.3 summarized the cumulative amount of parent drug and glucuronides, Cummins's extraction ratio of B, W and OA in the compound mixture group were calculated and compared with those in single compound group. A significant increase in the absorbed parent drugs in mesenteric blood was observed after three flavones were administered together. The corresponding glucuronides of B, W and OA were detected in both mesenteric blood and perfusate samples. The cumulative amounts of glucuronides at both sides were plotted in Fig. 6.5. Compared with the single compound group, the cumulative amount of glucuronides of B, W and OA in perfusate were significantly decreased in the compound mixture group, whereas the cumulative amount of these glucuronides in mesenteric blood showed no significant difference between the two groups. Since the cumulative amount of glucuronides in mesenteric blood was much

higher than that in the perfusate, the decreased formation of glucuronides in mesenteric blood after perfusing three flavones together might not be sensitive enough to be detected due to the high concentration background of glucuronides in perfusate. Besides, the Cummins's extraction ratio (ER) was compared between the single compound group and compound mixture group to estimate the effect on metabolisms. It was found that the ER of all the three flavones was significantly decreased after perfusing them together. It was suggested that the increase in the amount of parent flavones in mesenteric blood might be due to the metabolic competition between three flavones during their intestinal absorption.

Table 6.2 **Comparison of permeability coefficients of B, W and OA in perfusate buffer and mesenteric blood between single compound group and compound mixture group (n=6)**

Flavones	P_{lumen} ($\times 10^{-4}$ cm/sec)		P_{blood} ($\times 10^{-6}$ cm/sec)	
	Single	Mixture	Single	Mixture
B	1.52±0.56	3.07±2.16	1.44±0.57	28.79±8.15 ***
W	2.27±1.26	2.24±1.39	4.48±1.86	23.61±6.66 ***
OA	3.50±1.46	2.72±1.02	3.00±1.51	18.80±5.94 ***

***, $p < 0.001$ (significant difference between single compound group and compound mixture group)

Table 6.3 Comparison of transport and metabolism of bioactive flavones between single compound group and compound mixture group in rat *in situ* single-pass intestinal perfusion (n=6)

Flavones	Cumulative amount for single compound group (nmol)				Cumulative amount for compound mixture group (nmol)			
	Glucuronide in blood	Glucuronide in perfusate	Parent flavone in blood	ER	Glucuronide in blood	Glucuronide in perfusate	Parent flavone in blood	ER
B	58.90±11.84	39.53±5.52	2.02±0.88	0.98±0.01	41.52±11.38	10.20±5.50	14.17±8.31	0.80±0.11[***]
W	47.87±14.33	25.07±10.21	6.80±2.33	0.91±0.03	60.34±13.30	10.72±3.64	31.20±2.59	0.69±0.06[***]
OA	41.11±7.39	40.61±7.79	4.29±1.99	0.95±0.02	58.73±11.49	20.18±5.47	23.69±3.66	0.76±0.05[***]

ER: extraction ratio; [***]: $p<0.001$
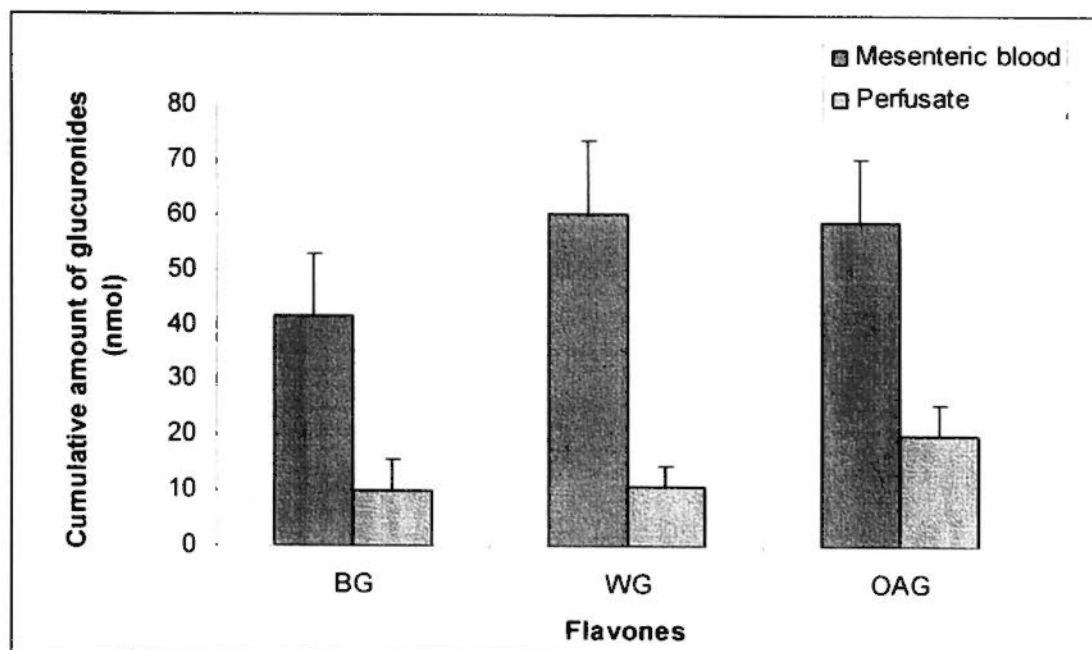
Fig. 6.5   Cumulative amount of BG, WG and OAG in mesenteric blood and perfusate after perfusing compound mixture of B, W and OA (1:1:1, *w/w/w*) (n=6)

6.4.3 Competition in glucuronidation of B, W and OA in sub-cellular fractions and UGTs

The metabolic competition of liver and intestine glucuronidation among B, W and OA were investigated. Human and rat liver microsomes as well as UGT 1A9 were chosen to study the competition in liver; the intestinal competition were investigated in human intestinal microsome, rat intestinal S9 fraction as well as UGT 1A8. The representative chromatograms of samples from different sub-cellular fractions and UGT isozymes for the compound mixture of B, W and OA are shown in Fig. 6.6.
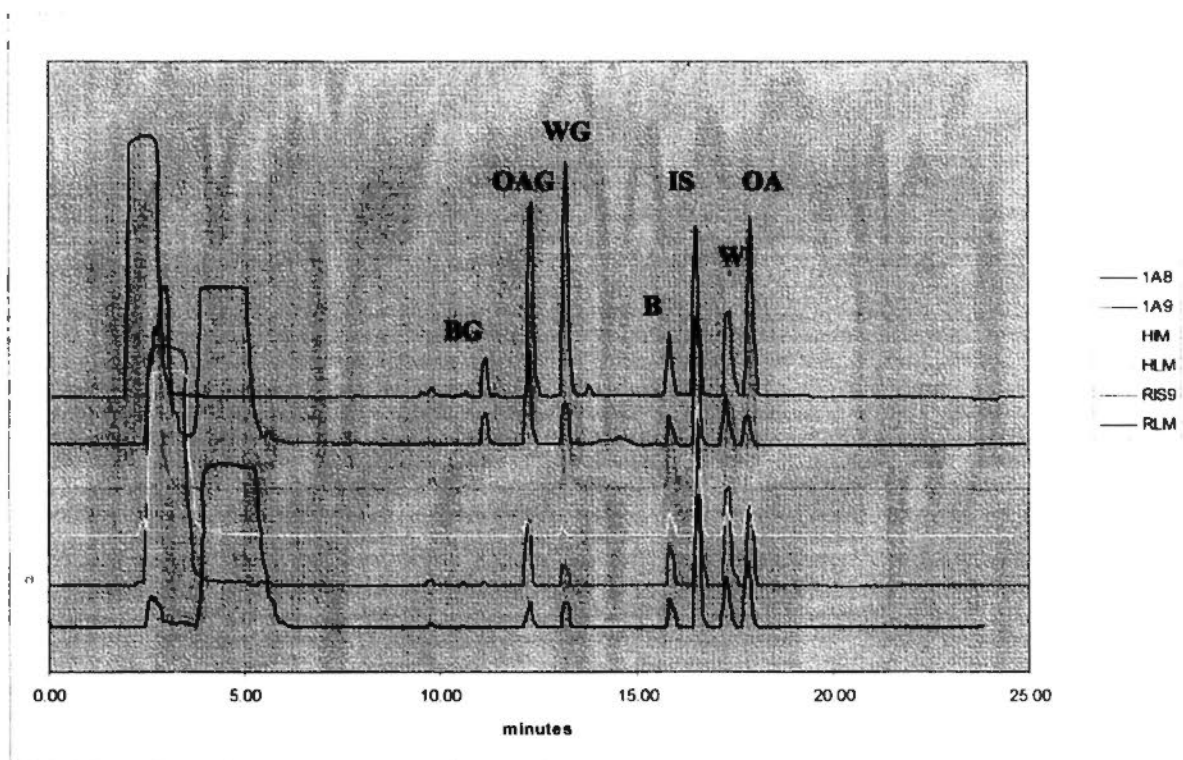
Fig. 6.6   **Representative HPLC/UV chromatograms of samples from *in vitro* glucuronidation kinetic study of compound mixture of B, W and OA in various sub-cellular fractions and UGT isozymes HLM: human liver microsome; HIM: human intestine microsome; RLM: rat liver microsome; RIS9: rat intestine S9 fraction**

The generated enzymatic kinetic parameters were listed in Table 6.4a to c. After three flavones were loaded together, the concentrations of formed glucuronides were decreased. Furthermore, the V_{max} and K_m for B, W and OA had dramatically decreased in compound mixture group comparing with those in single compound group. In the compound mixture group, OA still showed the highest intrinsic clearance among the three studied flavones. The results indicated that three flavones competed with each other to form their corresponding glucuronides. The reduced metabolism might increase the amount of parent drugs remaining, which might prolong their circulation *in vivo* and increase their bioavailability. Such assumption needs further *in vivo* study to verify if the co-administration of B, W and OA will increase their systemic exposure.

Table 6.4a   Comparison of enzyme kinetic parameters of glucuronidation of B between single compound group and compound mixture group (n=3)

Sub-cellular fraction /isozyme	Single compound group			Mixture group		
	V_{max} (nmol/min/mg)	K_m (μM)	Cl_{int} (μl/min/mg)	V_{max} (nmol/min/mg)	K_m (μM)	Cl_{int} (μl/min/mg)
HLM	11.57±0.65	90.73±9.08	127	1.32±0.15	4.30±1.59	306
RLM	39.79±6.20	148.10±34.83	268	2.33±0.14	6.66±1.29	349
HIM	3.14±1.80	24.99±29.56	125	N.A.	N.A.	N.A.
RIS9	6.15±0.85	46.69±10.22	131	0.57±0.06	3.33±1.13	171
UGT 1A8	3.17±0.27	19.46±4.80	162	N.A.	N.A.	N.A.
UGT 1A9	7.82±0.52	18.25±3.66	428	N.A.	N.A.	71*

*Cl$_{int}$ was calculated based on the slope of the initial linear portion of the metabolite formation rate versus substrate concentrations plot

Table 6.4b   Comparison of enzyme kinetic parameters of glucuronidation of W between single compound group and compound mixture group (n=3)

Sub-cellular fraction /isozyme	Single compound group			Mixture group		
	V_{max} (nmol/min/mg)	K_m (μM)	Cl_{int} (μl/min/mg)	V_{max} (nmol/min/mg)	K_m (μM)	Cl_{int} (μl/min/mg)
HLM	20.53±1.80	23.59±4.08	870	8.30±0.32	8.44±0.87	967
HIM	5.13±0.16	1.23±0.17	4170	1.46±0.05	0.34±0.08	4294
RLM	51.16±5.16	44.31±7.09	1154	16.47±1.77	17.25±4.24	954
RIS9	8.05±0.56	44.04±4.85	182	0.73±0.05	2.18±0.56	334
UGT 1A8	8.86±0.54	9.37±1.54	945	2.37±0.22	2.96±0.99	800
UGT 1A9	9.22±0.42	7.26±0.95	1269	N.A.	N.A.	360*

*Cl$_{int}$ was calculated based on the slope of the initial linear portion of the metabolite formation rate versus substrate concentrations plot

Table 6.4c Comparison of enzyme kinetic parameters of glucuronidation of OA between single compound group and compound mixture group (n=3)

Fraction /isozyme	Single compound group			Mixture group		
	V_{max} (nmol/min/mg)	K_m (μM)	Cl_{int} (μl/min/mg)	V_{max} (nmol/min/mg)	K_m (μM)	Cl_{int} (μl/min/mg)
HLM	13.69±0.94	8.76±1.67	1562	5.87±0.41	2.51±0.66	2338
HIM	5.24±0.24	1.04±0.23	5038	2.42±0.10	0.60±0.13	4033
RLM	34.83±2.97	19.25±3.49	1809	10.08±0.83	4.51±1.33	2235
RIS9	3.87±0.14	9.95±0.96	388	2.28±0.15	4.35±0.89	524
UGT 1A8	7.37±0.31	3.24±0.48	2274	2.07±0.17	1.62±0.57	1277
UGT 1A9	7.29±0.33	4.81±0.68	1515	3.00±0.12	1.29±0.23	2325

6.4.4 Pharmacokinetics of major bioactive components in RS and their pharmacokinetic interactions after oral administration

6.4.4.1 Identification of metabolites of each flavone after oral administration of single compound and compound mixture of B, W and OA to rats

After the oral administration of single compounds to SD rats, only the glucuronides of B, W and OA rather than their corresponding aglycones were found in the plasma. The representative HPLC/UV chromatograms of the plasma samples are shown in Fig. 6.7. Interestingly, in addition to WG, there was a new peak appearing at the HPLC/UV chromatogram after oral administration of W. Similar LC-MS/MS identification was conducted as described in section 3.2.2.2 of Chapter Three was carried. Considering the chemical structure of WG, the new metabolite was proposed to be the glucuronic acid conjugate at 5-OH of W. With respect to B and OA, there was only one metabolite detected in rat plasma samples.

Compared to metabolism studies on W and OA, the metabolism of B to BG was well investigated in urine, bile and systemic circulation. Several studies reported the metabolites of BG in human, but the identified metabolites were quite different from each report. Muto et al. found that baicalein 7-O-glucuronide and baicalein 6-O-sulfate were predominant metabolites after the administration of "Sho-saiko-to" in human (Muto et al., 1998). After oral administration of Radix Scutellariae commercial powder to human, the glucuronides and sulfate of baicalein and wogonin were identified in urine samples (Lai et al., 2003). Nevertheless, after oral administration of BG to human, three metabolites
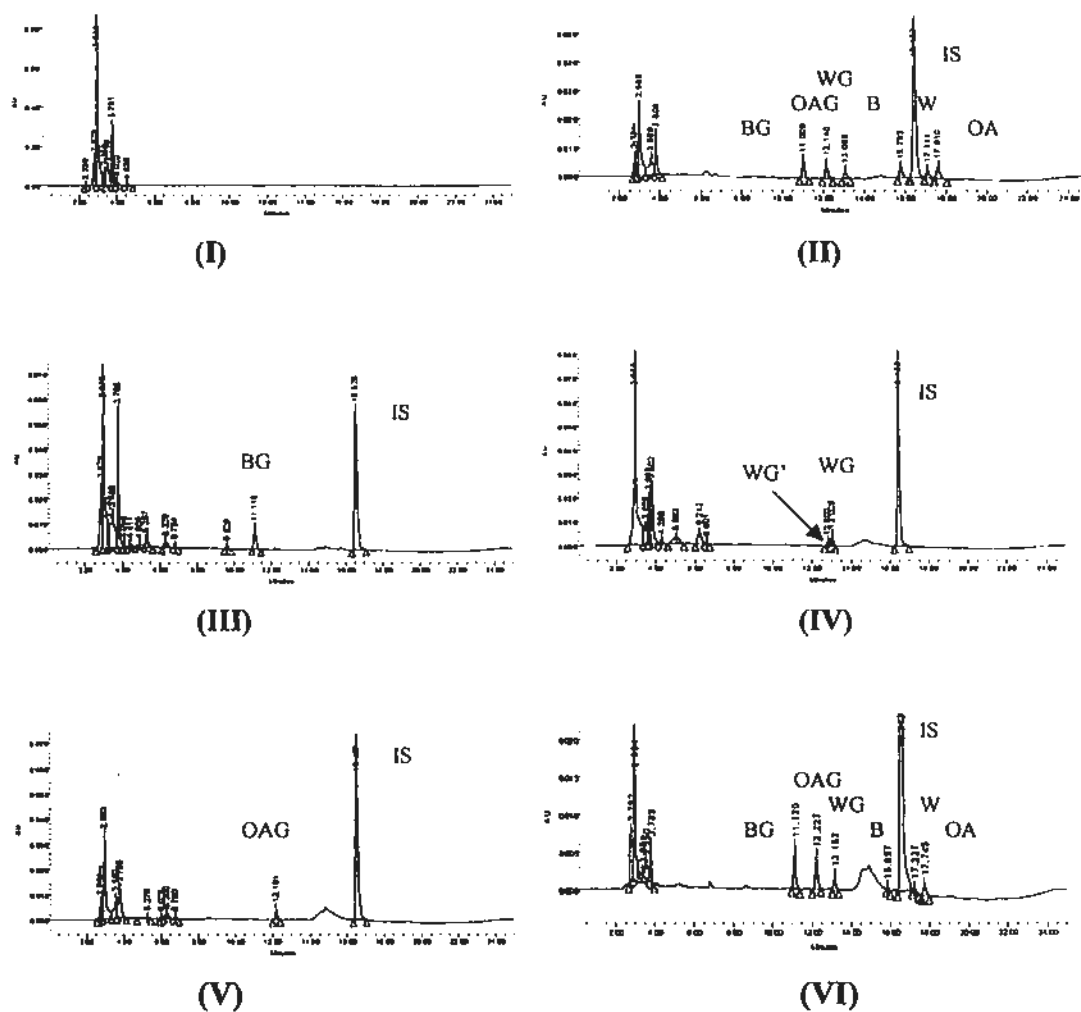
Fig. 6.7   Representative HPLC/UV chromatograms of rat blank plasma (I) and blank plasma spiked with standard solution at the concentration of 1 μg/ml (II); plasma sample obtained 10 min after oral administration of B at 5mg/kg (III); W at 5mg/kg (IV); OA at 5mg/kg (V); compound mixture of B, W and OA (5mg/kg each) (VI)

were identified in the urine samples. They were baicalin, isoform of baicalin with glucuronic acid conjugated at 6-OH and oroxylin A-7-*O*-glucuronide without sulfate conjugate of B identified (Che et al., 2001). For the pharmacokinetic studies in rats, baicalin was found to be the predominant form in system circulation after intravenous or oral administration of baicalein (Wakui et al., 1992). Five metabolites were identified in rat bile samples after oral administration of baicalin (Abe et al., 1990). Nevertheless, most of the studies treated the plasma samples by hydrolysis with β-glucuronidase/sulfatase and the amount of conjugates was quantified by the difference between hydrolyzed sample and unhydrolyzed sample (Xing et al., 2005, Lai et al., 2002). As a result, such hydrolysis treatment method could not differentiate glucuronide from sulfates. Besides, the number of glucuronic acid or sulfate conjugated to the parent compound cannot be clarified by this method either.

6.4.4.2 Pharmacokinetic profiles and interactions of bioactive flavones in RS after oral administration

Theoretically, the administration dose on animal model should be calculated based on the human equivalent dose. However, in clinical application, there is no pure form of B, W and OA employed and RS is often used in the form of herbal extract. The components of such extract are complicated and the content of each component may vary a lot among different products. As a result, it is difficult to calculate an animal dose based on the traditional human equivalent dose. Since the main focus of the current study is to investigate the pharmacokinetic profiles and the interaction among B, W and OA, we expected to be able to monitor both the parent flavones and their metabolite in rat plasma.

Based on the solubility capabilities of the three tested compounds, the highest concentration that could be produced is 1.25 mg/ml each in solvent mixture of PEG 400 and 20% Solutol $^®$ HS 15 when B, W and OA were mixed. Considering the maximum concentration (1.25 mg/ml) and the maximum volume of solution allowed for rat oral delivery (1 ml), the dose of 5 mg/kg each was chosen for the mixture of B, W and OA. Besides, the choice of the dose was also supported by the study from Chen et al,. in which W was orally administrated to Wistar rat at a dose of 5 mg/kg (Chen et al., 2002).

The plasma concentrations of three glucuronides after oral administration of B, W and OA as well as their compound mixture were plotted versus time, respectively (Fig. 6.8). After oral administration, there was no parent drug of B, W and OA detected in the plasma samples for the single compound group. All the pharmacokinetic parameters were calculated based on the plasma concentrations of corresponding glucuronides versus time profiles (Table 6.5). BG, WG and OAG exhibited a short T_{max} (average 5 min), indicating that the parent drug was quickly absorbed followed by a fast Phase II metabolism occurring. This finding complied with our results on Caco-2 cell monolayer model and the rat *in situ* single-pass intestinal perfusion model in Chapter Four. However, in the latter two models, the parent drugs could still be detectable in the receiver chamber or in the mesenteric blood, whereas the parent compound was barely found in plasma *in vivo*. That was because the loading concentration of drugs was rather higher in the *in vitro* and *in situ* models in the first place. Moreover, parent drugs did not undergo hepatic metabolism on these two models. Since the *in vitro* enzymatic kinetic study demonstrated that hepatic metabolism also contributes a lot to the disposition of the parent flavones, it

should not be surprised that no parent compound was detectable in the rat plasma samples *in vivo*. Nevertheless, in the study by Chen et al., wogonin was detectable in 24h after oral administration of W to Wistar rats at a dose of 5 mg/kg (Chen et al., 2002). Such difference in findings may be caused by two reasons. On one hand, our plasma assay method might not be sensitive enough to quantify the parent flavones, but we could not exclude the possibility that there might be some difference between SD rat and Wistar rat on the pharmacokinetic of these flavones.
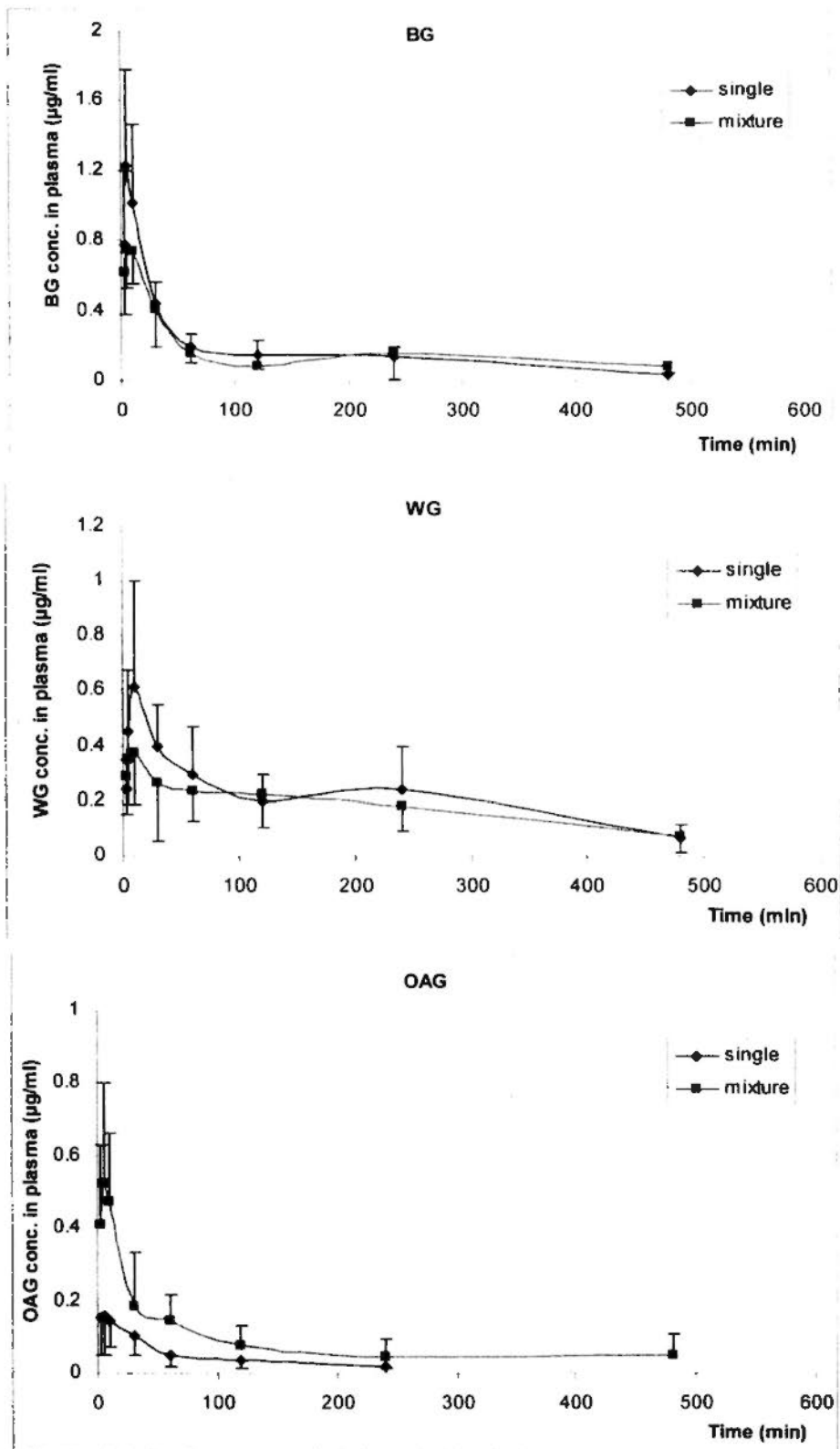
Fig. 6.8 Plasma concentration versus time profiles of BG, WG and OAG after oral administration of single compound as well as the compound mixture of B, W and OA to rats (n=6)

Table 6.5 Pharmacokinetic parameters of corresponding glucuronides after oral administration of single compound of B, W and OA and their compound mixture to rats (n=6)

Parameters	BG		WG		OAG	
	Single	Mixture	Single	Mixture	Single	Mixture
T_{max} (min)	5.00±0.00	8±2.74*	12±10.37	9±2.24	4.33±1.15	6.25±2.50
C_{max} (µg/ml)	1.10±0.49	0.77±0.24	0.57±0.14	0.44±0.16	0.24±0.08	0.58±0.28
$AUC_{0 \to t}$ (µg*min/ml)	54.98±9.93	41.75±11.26	68.32±18.33	60.44±13.10	9.47±0.93	25.55±9.22*
$t_{1/2\lambda z}$ (min)	155.25±43.99	161.37±31.81	102.31±35.93	194.50±111.21	38.75±12.74	47.38±35.59

*: $p < 0.05$ (significant difference between single compound group and compound mixture group)

To compare the pharmacokinetic characteristics among BG, WG and OAG in their single compound group, after administrated at the same dose of 5 mg/kg of their corresponding flavones, OAG exhibited a much lower AUC than that of BG and WG. Since the permeability of OA was comparable to that of B and W as demonstrated in absorption models both *in vitro* and *in situ*, such lower $AUC_{0 \to t}$ of OAG might be caused by the fast elimination and distribution of OAG rather than the poor absorption of OA.

The pharmacokinetic parameters were compared between single compound group and compound mixture group for each flavone. The proposed mechanism of pharmacokinetic interactions among B, W and OA were summarized in Fig. 6.9. T_{max} of BG was longer in mixture group. $AUC_{0 \to t}$ of OAG was significantly enhanced in mixture group than the single compound group. Such findings in rats were different from what were observed *in vitro* and *in situ*. Since the results on Caco-2 cell monolayer model and rat *in situ* single-pass perfusion model suggested that the co-administration of three flavones can increase their intestinal absorption. Further results by *in vitro* enzymatic kinetic study indicated that such increase might resulte from the competition among three flavones for the Phase II metabolism. As a result, it was expected that the AUCs of parent compounds would be increased after co-administration of three flavones together in rat. However, due to much more extensive metabolism *in vivo*, only the pharmacokinetic profiles of metabolites rather than the parent flavones could be obtained *in vivo*. As shown in Fig. 6.7, although the parent flavones of B, W and OA were still detectable after oral administration of the compound mixture in the plasma samples at T_{max}, their pharmacokinetic profiles could not be obtained due to insufficient data points. However, comparing with what was

observed from single compound administration, such detectable parent flavones could serve as evidence for the enhanced absorption of B, W and OA after their co-administration. The *in vivo* results of the detected metabolites demonstrated that only the difference in the AUC of OAG was observed rather than BG and WG. The possible explanations for the *in vivo* findings could be explained from three aspects: 1): As shown from the results in the Caco-2 cell monolayer model and rat *in situ* single-pass intestinal perfusion model, the increased absorption of B, W and OA might be due to their metabolism competitions. As a result, strong formation of OAG *in vivo* might resulte from the metabolism competition among three flavones during their intestinal absorption and hepatic disposition. 2): As discussed in Chapter Five of *in vitro* enzymatic kinetic study, the Cl_{int} of OA was much higher than B and W, indicating that the formation of OAG was much more extensive than BG and WG. 3): B and OA are very similar in chemical structure with only difference in 6-C. The hydroxyl group at 6-C of B is methylated in OA. Although our above findings on single compound proposed that the glucuronidation is the major metabolic pathway after oral administration of each single compound, we could not exclude the other metabolic pathways *in vivo*. As shown in previous study, 97% of quercetin was excreted in urine as 3'-*O*-methylquercetin after intraperitoneal administration (Zhu et al., 1994). Our previous study on B in rat liver cytosol in the presence of S-adenosyl-L-methionine (data not shown here) confirmed the possible methylation of B to OA *in vitro*. When three flavones are administrated together, their competition on metabolism could firstly result in the increased amount of parent flavones retained. However, the chance of B to undergo other metabolic pathways such

as methylation could be enhanced, which may further contribute to the increased amount of OAG, the methylated BG at 6-OH.

6.5   Conclusion

After oral administration, the parent flavones of B, W and OA underwent extensive first pass metabolism to form their corresponding glucuronic acid conjugates at intestine and liver. Due to the increased polarity and hydrophilicity, these Phase II conjugates metabolites were quickly eliminated with relatively short $t_{1/2\lambda z}$. Co-administration of B, W and OA together resulted in significant increase of absorbed parent drugs in Caco-2 cell monolayer model and rat *in situ* single-pass intestinal perfusion model due to the competition in their glucuronidation metabolism. However, after oral administration of three flavones together in rat, only the metabolites were found in plasma. In comparison to that obtained from single compound administration, only the AUC of OAG increased.
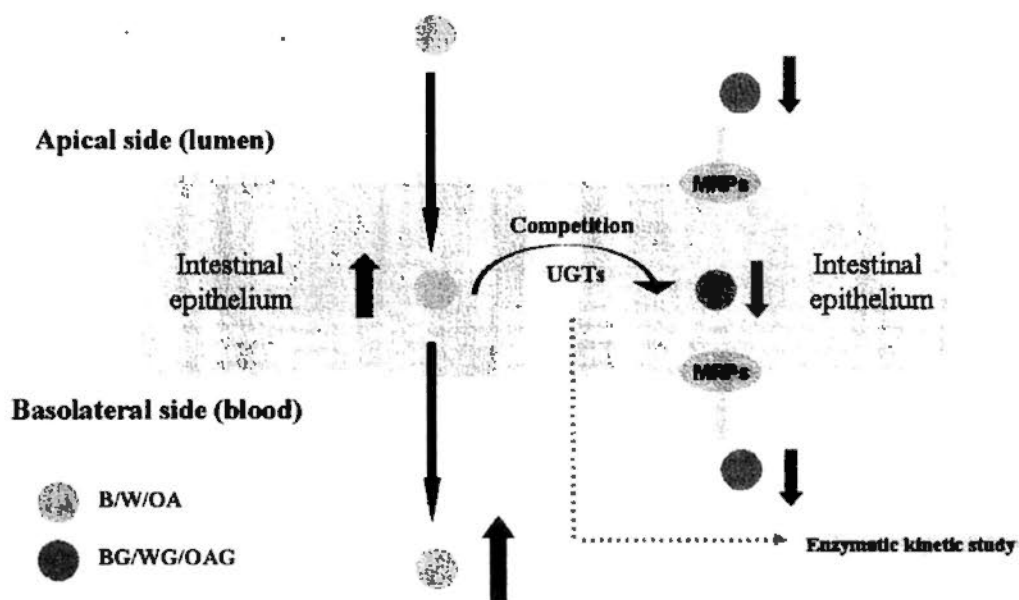
Fig. 6.9   Mechanistic explanation of pharmacokinetic interactions among B, W and OA

Chapter Seven

Overall conclusion

In order to investigate the biopharmaceutic and pharmacokinetic interactions among the major bioactive flavones in RS, the current project firstly quantified the content of major bioactive flavones in the reference herb and proprietary Traditional Chinese medicinal products of *Radix Scutellariae*. Subsequently, the potential mechanism of the intestinal absorption, intestinal and hepatic metabolism and disposition as well as the biopharmaceutic and pharmacokinetic interactions of three major bioactive flavones were investigated using a series of *in vitro*, *in situ* and *in vivo* models.

In practice, baicalin was usually employed as a compound marker for the quality control of the crude raw material of *Radix Scutellariae*. However, our content analysis by HPLC/UV found that in addition to baicalin (BG), wogonoside (WG) and oroxylin A-7-*O*-glucuronide (OAG) as well as the corresponding aglycones including baicalein (B), wogonin (W) and oroxylin A (OA) also exist in relatively high amount in *Radix Scutellariae*. Considering their pharmacological activities as well as sufficient amount existed in raw herb of *Radix Scutellariae*, it was suggested that all the six bioactive flavones should be involved for the quality control of raw herbs and preparatory traditional Chinese medicinal products of *Radix Scutellariae*.

Investigations on W and OA, the two less commonly studied flavones, revealed that they did share similar biopharmaceutics characteristics as that of B. Although favorable permeability of W and OA were observed in both Caco-2 cell monolayer model and rat *in situ* single-pass intestinal perfusion model, they also underwent extensive intestinal first-pass metabolism. For both W and OA, their extent of metabolism was even higher than 90% on Caco-2 model at low loading concentration. The Cummins's extraction ratio of B, W and OA were all above 0.9 when 50 μM of them were perfused through a segment of small intestine. Therefore, it was suggested that the low bioavailability of the flavones including B, W and OA might be caused by their extensive first-pass metabolism. Similar to B, the formed glucuronides of W and OA could be detected at both the apical side (lumen side) and basolateral side (mesenteric blood side). Such efflux transport of intracellularly formed glucuronides was also found to be mediated by multidrug-resistance associated proteins.

Further *in vitro* enzymatic kinetic studies of W and OA demonstrated that they underwent both extensive hepatic and intestinal glucuronidation in rat and human. It was found that their hepatic glucuronidation was mainly catalyzed by UGT 1A9, whereas UGT 1A8 and UGT 1A10 were responsible for their intestinal glucuronidation. Compared to glucuronidation, the extent of sulfation of W and OA was low in human and rat liver cytosol with no sulfate conjugates detected in rat intestinal S9 fraction. In addition, the hepatic glucuronidation and sulfation of W and OA showed no species difference. Among the three tested flavones in RS, OA demonstrated the highest glucuronidation rate.

The pharmacokinetic profiles of B, W and OA were investigated in male Sprague-Dawley rats. Similar to B, after oral administration, the parent flavones of W and OA were found to undergo more extensive first pass metabolism than what we observed *in vitro* and *in situ* with no parent flavones detectable in blood samples. The pharmacokinetic parameters were calculated based on the profile of plasma concentration of their corresponding glucuronide versus time. Due to the increased polarity and hydrophilicity, the phase II metabolites were quickly eliminated with relatively short $t_{1/2\lambda z}$.

In addition to the characterization of individual flavones, the biopharmaceutic and pharmacokinetic interaction among B, W and OA was finally investigated at *in vitro*, *in situ* and *in vivo* levels. After co-administration of B, W and OA, the formed glucuronides decreased whereas the absorbed parent flavones increased in Caco-2 cell monolayer model and rat *in situ* single-pass intestinal perfusion model. Besides, the *in vitro* enzymatic kinetic study demonstrated that the B, W and OA competed with each other to form corresponding glucuronides. Due to extensive metabolic competition *in vivo*, co-administration of three flavones only led to increased AUC of OAG.

In summary, three major bioactive flavones in *Radix Scutellariae* were found to be well absorbed but subjected to extensive intestinal and hepatic metabolism to form glucuronic acid and/or sulfate conjugates, which could be further effluxed by MRPs. Co-administration of three flavones together would result in metabolic competition and lead to enhancement of parent flavones absorbed.

In addition to generating scientific evidence, the present study successfully established the first assay method to quantify the major bioactive flavones in *Radix Scutellariae*, which provided better quality control of the proprietary traditional Chinese medicine products containing *Radix Scutellariae*. Furthermore the mechanistic study on the intestinal absorption and disposition, hepatic metabolism and the pharmacokinetics characteristics of W and OA filled up the blanks in the research of W and OA. The interactions study among the bioactive flavones in *Radix Scutellariae* will provide useful guidance in the clinical application of herbal extract.

Nevertheless, there is further work need to be done. For example, the inhibitors used in the identification of potential membrane transporters of WG and OAG in Chapter Four are not specific enough. Although MDCK cell lines transfected with human gene of specific transporters were further employed, there were only three human transporters transfected cell lines available in our lab. In the future, more sensitive and specific approaches will be used such as the membrane APTase assay or vesicular transport studies utilizing membranes from Sf9 cells overexpressing specific transporters. Besides, the drug efficacy and toxicity depend on its concentration. Thus, the change in pharmacokinetics will ultimately influence the pharmacodynamic effectss. Further experiments will be conducted to investigate whether the pharmacokinetic interactions will result in the changes in their pharmacodynamic effects.

References

Abe K, Inoue O, Yumioka E. Biliary excretion of metabolites of baicalin and baicalein in rats. *Chem Pharm Bull* (Tokyo). 1990, 38: 209-211

Ahn HC, Lee SY, Kim JW, Son WS, Shin CG, Lee BJ. Binding aspects of baicalein to HIV-1 integrase. *Mol Cells*. 2001, 12:127-130

Akao T, Kawabata K, Yanagisawa E, Ishihara K, Mizuhara Y, Wakui Y, Sakashita Y, Kobashi K. Baicalin, the predominant flavone glucuronide of Scutellariae Radix, is absorbed from the rat gastrointestinal tract as the aglycone and restored to its original form. *J Pharm Pharmacol*. 2000, 52: 1563-1568

Akao T, Skashita Y, Hanada M, Goto H, Shimada Y, Terasawa K. Enteric excretion of baicalein, a flavone of Scutellariae Radix, via glucuronidation in rat: involvement of multidrug resistance-associated protein 2. *Pharm Res*. 2004, 21: 2120-2126

Amidon GL, Leesman GD and Elliott RL. Improving intesitnalabsorption of water-insoluble compounds: a membrane metabolism strategy. *J Pharm Sci*. 1980, 69: 1363-1368

Artersson P and Karlsson J. Correlation between oral drug absorption in humans and apparent drug permeability coefficients in human intestinal epithelial (Caco-2) cells. *Biochem Biophys Res Commun.* 1991, 175: 880-885

Artursson P, Borchardt R. Intestinal drug absorption and metabolism in cell cultures: Caco-2 and beyond. *Pharm Res.* 1997, 14: 1655-1658

Artursson P, Palm K, Luthman K. Caco-2 monolayers in experimental and theoretical predictions of drug transport. *Adv Drug Deliv Rev.* 2001, 46: 27-43

Bansal T, Mishra G, Jaggi M, Khar RK, Talegaonkr S. Effect of P-glycoprotein inhibitor, verapamil, on oral bioavailability and pharmacokinetics of irinotecan in rats. *Eur J Pharm Sci.* 2009, 36: 580-590

Barthe L, Woodley J and Houin G. Gastrointestinal absorption of drugs: methods and studies. *Fundam Clin Pharmacol.* 1999, 13: 154-168

Barthomeuf C, Grassi J, Demeule M, Fournier C, Boivin D, Béliveau R. Inhibition of P-lgycoprotein transport function and reversion of MDR1 multidrug resistance by cnidiadin. *Cancer Chemother Pharmacol.* 2005, 56: 173-181

Bochořáková H, Paulavá H, Slanina J, Musil P, Táborská E. Main flavonoids in the root of *Scutellaria baicalensis* cultivated in Europe and their comparative antiradical properties. *Phytother Res.* 2003, 17:640-644

Boisset M, Botham RP, Haegele KD, Lenfant B, Pachot JI. Absorption of angiotensin II antagonists in Ussing chambers, Caco-2, perfused jejunum loop and in vivo: inportance of drug ionisation in the in vitro prediction of in vivo absorption. *Eur J Pharm Sci.* 2000, 10: 215-224

Bonham M, Posakony J, Coleman I, Montgomery B, Simon J, Nelson PS. Characterization of chemical constituents in Scutellaria baicalensis with antiandrogenic and growth-inhibitory activities toward prostate carcinoma. *Clin Cancer Res.* 2005, 11: 3 905-3914

Bousquet L, Pruvost A, Didier N, Farinotti R, Mabondzo A. Emtricitabine: inhibitor and substrate of multidrug resistance associated protein. *Eur J Pharm Sci.* 2008, 35: 247-256

Brand W, Schutte ME, Williamson G, van Zanden JJ, Cnubben NH, Groten JP, van Bladeren PJ, Rietjens IM. Flavonoid-mediated inhibition of intestina lABC transporters may affect the oral bioavailability of drugs, food-borne toxic compounds and bioactive ingredients. *Biomed Pharmacother.* 2006, 60: 508-519

Bruno M, Piozzi F, Maggio AM, Simmonds MS. Antifeedant activity of neoclerodane diterpenoids from two Sicilian species of Scutellaria. *Biochem Syst Ecol.* 2002, 30: 793-799

Cao Y, Wang L, Yu X, Ye J. Development of the chromatographic fingerprint of herbal preparations Shuang-Huang-Lian oral liquid. *J Pharm Biomed Anal*. 2006, 41: 845-856

Campbell SD, de Morais SM, Xu JJ. Inhibition of human organic anion transporting polypeptide OATP 1B1 as a mechanism of drug-induced hyperbilirubinemia. *Chem Biol Interact*. 2004, 150: 179-187

Chang CP, Huang WT, Cheng BC, Hsu CC, Lin MT. The flavonoid baicalin protects against cerebrovascular dysfunction and brain inflammation in experimental heatstroke. *Neuropharmacology*. 2007, 52:1024-1033

Chang JS, Wang KC, Liu HW, Chen MC, Chiang LC, Lin CC. Sho-Saiko-Ko (Xiao-Chai-Hu-Tang) and crude saikosaponins inhibit hepatitis B virus in a stable HBV-producing cell line. Am J Chin Med. 2007, 35: 341-351

Chang Q, Zuo Z, Ho WK, Chow MS. Comparison of the pharmacokinetics of hawthorn phenolics in extract versus individual pure compound. *J Clin Pharmacol*. 2005, 45: 106-112

Che QM, Huang XL, Mei LY, Zhang K, Akao T, Hattori M. Studies on metabolites of baicalin in human urine. *Zhongguo Zhong Yao Za Zhi*. 2001, 26: 768-769

Chen CS, Chen NJ, Lin LW, Hsieh CC, Chen GW, Hsieh MT. Effects of Scutellariae Radix on gene expression in HEK 293 cells using cDNA microarray. *J Ethnopharmacol.* 2006, 105: 346-351

Chen G, Zhang H, Ye J. Determination of baicalein, baicalin and quercetin in Scutellariae Radix and its preparations by capillary electrophoresis with electrochemical detection. *Talanta.* 2000, 53: 471-479

Chen X, Wang H, Du Y, Zhong D. Quantitation of the flavonoid wogonin and its major metabolite wogonin-7β-D-glucuronide in rat plasma by liquid chromatography-tandem mass spectrometry. *J Chromatogr B.* 2002, 775: 169-178

Chen Y, Yang L, Lee TJ. Oroxylin A inhibition of lipopolysaccharide-induced iNOS and COX-2 gene expression via suppression of nuclear factor-κB activation. *Biochem Pharmacol.* 2000, 59:1445-1457

Chen Y, Xie S, Chen S, Zeng S. Glucuronidation of flavonoids by recombinant UGT 1A3 and UGT 1A9. *Biochem Pharmacol.* 2008, 76: 416-425

Cheng, Z, Radominska-Pandya, A and Tephly, TR. Cloning and expression of human UDP-glucuronosyltransferase (UGT) 1A8. *Arch Biochem Biophys.* 1998, 356: 301-305

Chi YS, Cheon BS and Kim HP. Effect of wogonin, a plant flavone from Scutellaria radix, on the suppression of cyclooxygenase-2 and the induction of inducible nitric oxide synthase in lipopolysaccharide-treated RAW 264.7 cells. *Biochem. Pharmacol.* 2001, 61:1195-1203

Choi J, Conrad CC, Malakowsky CA, Talent JM, Yuan CS, Gracy RW. Flavones from Scutellaria baicalensis Georgi attenuate apoptosis and protein oxidation in neuronal cell limes. *Biochim Biophys Acta.* 2002, 1571: 201-210

Cho J and Lee HK. Wogonin inhibits excitotoxic and oxidative neuronal damage in primary cultured rat cortical cells. *Eur J Pharmacol.* 2004, 485:105-110

Chu M, Chu ZY and Wang DD. The extract of comound Radix Scutellariae on mRNA replication and IFN expression of influenza virus in mice. *Zhong Yao Cai.* 2007, 30: 63-65

Chung HL, Yue G, To KF Su YL, Huang Y, Ko WH. Effect of *Scutellariae Radix* extract on experimental dextran-sulfate sodium-induced colitis in rats. *World J Gastroenterol.* 2007, 13: 5605-5611

Ciesielska E, Gwardys A and Metodiewa D. Anticancer, antiradical and antioxidative actions of novel Antoksyd S and its major components, baicalin and baicalein. *Anticancer Res.* 2002, 22: 2885-2891

Cook TJ and Shenoy SS. Intestinal permeability of chlorpyrifos using the single-pass intestinal perfusion method in the rat. *Toxicology*. 2003, 84: 125-133

Copeland RA. In: Enzymes: A practical introduction to structure , mechanism, and data analysis. 2nd ed. Chapter Five. Wiley-VCH, Inc., 2000: 137-138

Cui L, Gu HX, Lu JX, Lin HB, Lin JQ, Lin JQ. The analysis of the germplasm resources and cultivation of Scutellaria baicalensis Georgi. *Acta Chinese Medicine and Pharmacology*. 2010, 38: 69-72

Cummins CL, Salphati L, Reid MJ, Benet LZ. In vivo modulation of intestinal CYP3A metabolism by P-glycoprotein: studies using the rat single-pass intestinal perfusion model. *J Pharmacol Exp Ther*. 2003, 305: 306-314

Dai JY, Yang JL and Li C. Tranport and metabolism of flavonoids from Chinese herbal remedy Xiaochaihu-tang across human intestinal Caco-2 cell monolayers. *Acta Pharmacol Sin*. 2008, 29: 1086-1093

Darnell M, Karlsson JE, Owen A, Hidalgo IJ, Li J, Zhang W, Andersson TB. Investigation of the involvement of P-glycoprotein and multidrug resistance-associated protein 2 in the efflux of ximelagatran and its metabolites by using short hairpin RNA knockdown in Caco-2 cells. *Drug Metab Dispos*. 2010, 38: 491-497

Day AJ, Canada FJ, Diaz J, Kroon PA, McLauchlan R, Faulds CB, Plumb GW, Morgan MR, Williamson G. Dietary flavonoid and isoflavone glycosides are hydrolysed by the lactase site of lactase phlorizin hydrolase. *FEBS Lett*. 2000, 468: 166-170

Day AJ, Gee JM, DuPont MS, Johnson IT, Williamson G. Absorption of quercetin-3-glucoside and quercetin-4'-glycoside in the rat small intestine: The role of lactase phlorizin hydrolase and the sodium-dependent glucose transporter. *Biochem Pharmacol*. 2003, 65: 1199-1206

Di B, Feng NP and Liu WY. Pharmacokinetic comparisons of Shuang-Huang-Lian with the different combinations of its constitutional herbs. *J Ethnopharmacol*. 2006, 107: 401-405

Evers DL, Chao CF, Wang X, Zhang Z, Huong SM, Huang ES. Human cytomegalovirus-inhibitory flavonoids: Studies on antiviral activity and mechanism of action. *Antiviral Res*. 2005, 68: 124-134

Fagerholm U, Johansson M, Lennernäs H. Comparison between permeability coefficients in rat and human jejunum. *Pharm Res*. 1996, 13: 1336-1342

FDA. Guidance for Industry: Bioanalytical Method Validation. Rockville. 2001

Fugh-Berman A. Herb-drug interactions. *Lancet*. 2000, 355:134-138

Fukutake M, Yokota S, Kawamura H, Iizuka A, Amagaya S, Fukuda K, Komatsu Y. Inhibition effect of Coptidis Rhizoma and Scutellariae Radix on Azoxymethane-induced Aberrant Crypt Foci formation in rat colon. *Bio Pharm Bull*. 1998, 21: 814-817

Gao Z, Huang K, Yang X, Xu H. Free radical scavenging and antioxidant activities of flavonoids extracted from the radix of Scutellaria baicalensis Georgi. *Biochim Biophys Acta*. 1999, 1472:634-650

Ge QF, Hu X, Ma ZQ, Liu JR, Zhang WP, Chen Z, Wei EQ. Baicalin attenuates oxygen-glucose deprivation-induced injury via inhibiting NMDA receptor-mediated 5-lipoxygenase activation in rat cortical neurons. *Pharmacol Res*. 2007, 55: 148-157

Giri N, Agarwal S, Shik N, Pan G, Chen Y, Elmquist WF. Substrate-dependent breast cancer resistance protein (Bcrp1/Abcg2)-mediated interactions: consideration of multiple biding sites in in vitro assay design. *Drug Metab Dispos*. 2009, 37: 560-570

Gläßer G, Graefe EU, Struck F, Veit M, Gebhardt R. Comparison of antioxidative capacities and inhibitory effects on cholesterol biosynthesis of quercetin and potential metabolites. *Phytomedicine*. 2002, 9: 33-40

Grès MC, Julian B, Bourrié M, Meunier V, Roques C, Berger M, Boulenc X, Berger Y, Fabre G. Correlation between oral drug absorption in humans, and apparent drug

permeability in TC-7 cells, a human epithelial intestinal cell line: comparison with the parental Caco-2 cell line. *Pharm Res.* 1998, 15: 726-733

Guo Q, Zhao L, You Q, Yang Y, Gu H, Song G, Lu N, Xin J. Anti-hepatitis B virus activity of wogonin in vitro and in vivo. *Antiviral Res.* 2007, 74: 16-24

Guo Y, Wang H and Zhang C. Establishment of rat precision-cut fibrotic liver slice technique and its application in verapamil metabolism. *Clin Exp Pharmacol Physiol.* 2007, 34: 406-413

Guo ZJ, Zhang Y, Tang X, Li H, Sun QS. Pharmacokinetic Interaction between Tanshinones and Polyphenolic Extracts of Salvia miltinorrhiza BUNGE after Intravenous Administration in Rats. *Biol Pharm Bull.* 2008, 31: 1469-1474

Hagenbuch B. Cellular entry of thyroid hormones by organic anion transporting polypeptides. *Best Pract Res Clin Endocrinol Metab.* 2007, 21: 209-221

Hamada H, Hiramatsu M, Edamatsu R, Mori A. Free radical scavenging action of baicalein. *Arch Biochem Biophys.* 1993, 306: 261-266

Hämäläinen MD and Frostell-Karlsson A. Prediction the intestinal absorption potential of hits and leads. *Drug Discov today: Technologies.* 2004, 1: 397-405

Han FM, Li Y, Li LJ, Chen Y. Simultaneous determination of geniposide, baicalin and berberine hydrochloride in Angong Niuhuang pill by RP-HPLC. *Zhongguo Zhong Yao Za Zhi*. 2007, 32: 1406-1408

Herzlinger DA, Easton TG and Ojakian GK. The MDCK epithelial cell line expresses a cell surface antigen of the kidney distal tubule. *J Cell Biol*. 1982, 93: 269-277

Himeji M, Ohtsuki T, Fukazawa H, Tanaka M, Yazaki S, Nishio K, Yamamoto H, Tasaka K, Mimura A. Difference of growth-inhibitory effect of *Scutellaria baicalensis*-producing flavonoid wogonin among human cancer cells and normal diploid cell. *Cancer Lett*. 2007, 245: 269-274

Hirano M, Maeda K, Shitara Y, Suyiyama Y. Drug-drug interaction between pitavastatin and various drugs via OATP 1B1. *Drug Metab Dispos*. 2006, 34: 1229-1236

Hirohashi T, Suzuki H, Chu XY, Tamai I, Tsuji A, Sugiyama Y. Function and expression of multidrug resistance-associated protein family in human colon adenocarcinoma cells (Caco-2). *J Pharmacol Exp Ther*. 2000, 292: 265-270

Horvath CR, Martos PA, Saxena PK. Identification and quantification of eight flavones in root and shoot tissues of the medicinal plant Huang-qin (Scutellaria baicalensis Georgi) using high-performance liquid chromatography with diode array and mass spectrometric detection. *J Chromatogr A*. 2005, 1062:199-207

Hu M, Chen J amd Lin H. Metabolism of flavonoids via enteric recycling: mechanistic studies of disposition of apigenin in the Caco-2 cell culture model. *J Pharmacol Exp Ther*. 2003, 307: 314-321

Hu Y, Yang Y, You QD, Liu W, Gu HY, Zhao L, Zhang K, Wang W, Wang XT, Guo QL. Oroxylin A induced apoptosis of human hepatocellular carcinoma cell line HepG2 was involved in its antitumor activity. *Biochem Biophys Res Commun*. 2006, 351:521-527

Huen MS, Leung JW, Ng W, Lui WS, Chan MN, Wong JT, Xue H. 5,7-dihydroxy-6-methoxyflavone, a benzodiazepine site ligand isolated from Scutellaria baicalensis Georgi, with selective antagonistic properties. *Biochem Pharmacol*. 2003, 66: 125-132

Hunter J, Jepson MA, Tsuruo T, Simmons NL, Hirst BH. Functional expression of P-glycoprotein in apical membranes of human intestinal Caco-2 cells. *J Biol Chem*. 1993, 268: 14991-14997

Ishimaru K, Nishikawa K, Omoto T, Asai I, Yoshihira K, Shimomura K. Two flavone 2'-glucosides from Scutellaria Baicalensis. *Phytochemistry*. 1995, 40: 279-281

Ikemoto S, Sugimura K, Yoshida N, Yasumoto R, Wada S, Yamamoto K, Kishimoto T. Antitumor effects of Scutellariae radix and its components baicalein, beicalin and wogoin on bladder cancer cell lines. *Urology*. 2000, 55: 951-955

Ikemoto S, Sugimura K, Kuratukuri K, Nakatani T. Antitumor effects of lipoxygenase inhibitors on murine bladder cancer cells line (MBT-2). *Anticancer Res*. 2004, 24: 733-736

Irvine J, Takahashi L, Lockhart K, Cheong J, Tolan JW, Selick HE, Grove JR. MDCK (Madin-Darby Canine Kidney) cells: a tool for membrane permeability screening. *J Pharm Sci*. 1999, 88: 28-33

Jedlitschky G, Cassiday AJ, Sales M, Pratt N, Burchell B. Cloning and characterization of a novel human olfactory UDP glucuronosyltransferase. *Biochem J*. 1999, 340: 837–843.

Jonhson BM, Chen WQ, Borchardt RT, Charman WN, Porter CH. Akinetic evaluation of the absorption, efflux and metabolism of verapamil in the qutoperfused rat jejunum. *J Pharmacol Exp Ther*. 2003, 305: 151-158

Kang H, Choi TW, Ahn KS, Lee JY, Han IH, Choi HY, Shim ES, Sohn NW. Upregulation of interferon and interleukin-4, Th cell-derived cytokines by So-Shi-Ho-

Tang (Sho-Saiko-To) occurs at the level of antigen presenting cells, but not CD4 T cells. *J Ethnopharmacol.* 2009, 123: 6-14

Kang K, Oh YK, Choue R, Kang SJ. Scutellariae radix extracts suppress ethanol-induced caspase-11 expression and cell death in N_2a cells. *Mol Brain Res.* 2005, 142:139-145

Kansy M, Senner E, Gubernator K. Physicochemical high throughput screening: parallel artificial membrane permeation assay in the description of passive absorption processes. *J Med Chem.* 1998, 41: 1007-1010

Kiang TK, Ensom MH, Chang TK. UDP-lgucuronosyltransferases and clinical drug-drug interactions. *Pharmacol Ther.* 2005, 106: 97-132

Kim DH, Jeon SJ, Son KH, Jung JW, Lee S, Yoon BH, Choi JW, Cheong JH, Ko KH, Ryu JH. Effect of the flavonoid, oroxylin A, on transient cerebral hypoperfusion-induced memory impairment in mice. *Pharmacol Biochem Behav.* 2006, 85:658-668

Kim DH, Jeon SJ, Son KH, Jung JW, Lee S, Yoon BH, Lee JJ, Cho YW, Cheong JH, Ko KH, Ryu JH. The ameliorating effect of oroxylin A on scopolamine-induced memory impairment in mice. *Neurobiol Learn Mem.* 2007, 87: 536-546

Kim HK, Cheon BS, Kim YH, Kim SY, Kim HP. Effects of naturally occurring flavonoids on nitric oxide production in the macrophage cell Line RAW 264.7 and their structure–activity relationships. *Biochem Pharmacol*. 1999, 58: 759-765

Kim YH, Jeong DW, Paek IB, Ji HY, Kim YC, Sohn DH, Lee HS. Liquid chromatography with tandem mass spectrometry for the simultaneous determination of baicalein, baicalin, oroxylin A and wogonin in rat plasma. *J Chromatogr B*. 2006, 844: 261-267

Kim YH, Jeong DW, Kim YC, Sohn DH, Park ES, Lee HS. Pharmacokinetics of baicalein, baicalin and wogonin after oral administration of a standardized extract of *Scutellaria baicalensis*, PF-2405 in rats. *Arch Pharm Res*. 2007, 30: 260-265

Kitamura K, Honda M, Yoshizaki H, Yamamoto S, Nakane H, Fukushima M, Ono K, Tokunaga T. Baicalin, and inhibitor of HIV-1 production in vitro. *Antiviral Res*. 1998, 37: 131-140

Kobayashi D, Nozawa T, Imai K, Nezu J, Tsuju A, Tamai I. Involvement of human organic anion transporting polypeptide OATP-B (SLC21A9) in pH-dependent transport across intestinal apical membrane. *J Pharmacol Exp Ther*. 2003, 306: 703-708

Lai MY, Hsui SL, Tsai SY, Hou YC, Lee Chao PD. Comparison of metabolic pharmacokinetics of baicalin and baicalein in rats. *J Pharm Pharmacol*. 2003, 55: 205-209

Lai MY, Hsiu SL, Chen CC, Hou YC, Lee Chao PD. Urinary pharmacokinetics of baicalein, wogonin and their glycosides after oral administration of *Scutellariae* Radix in humans. *Biol Pharm Bull*. 2003, 26: 79-83

Lai MY, Hsiu SL, Hou YC, Tsai SY, Chao PD. Significant decrease of cyclosporine bioavailability in rats caused by a decoction of the roots of Scutellaria baicalensis. *Planta Med*. 2004, 70: 132-137

Lambert JD, Sang S, Lu AY, Yang CS. Metabolism of dietary polyphenols and possible interactions with drugs. *Curr Drug Metab*. 2007, 8: 499-507

Lapchak PA, Maher P, Schubert D, Zivin JA. Baicalein, an antioxidant 12/15-lipoxygenase inhibitor improves clinical rating scores following multiple infarct embolic strokes. *Neuroscience*. 2007, 150: 585-591

Lee HZ, Leung HW, Lai MY, Wu CH. Baicalein induced cell cycle arrest and apoptosis in human lung squamous carcinoma CH27 cells. *Anticancer Res*. 2005, 25: 959-964

Lee WR, Shen SC, Lin HY, Hou WC, Yang LL, Chen YC. Wogonin and fisetin induce apoptosis in human promyeloleukemic cells, accompanied by a decrease of reactive oxygen species, and activation of caspase 3 and Ca(2+)-dependent endonuclease. *Biochem Pharmacol*. 2002, 63: 225-236

Leslie EM, Deeley RG, Cole SP. Multidrug resistance proteins: role of P-glycoprotein, MRP1, MRP2, and BCRP (ABCG2) in tissue defense. *Toxicol Appl Pharmacol*. 2005, 204: 216-217

Li BQ, Fu T, Gong WH, Dunlop N, Kung H, Yan Y, Kang J, Wang JM. The flavonoid baicalin exhibits anti-inflammatory activity by binding to chemokines. *Immunopharmacology*. 2000, 49: 295-306

Li BL, Chen ZL, Jiang SP. HPLC determination of baicalin in compound Puqin tablets. *Clin J Pharm Anal*. 2010, 30: 703-705

Li CR, Zhou LM, Lin G, Zuo Z. Contents of major bioactie flavones in proprietary traditional Chinese medicine products and reference herb of *Radix Scutellariae*. *J Pharm Biomed Anal*. 2009, 50: 298-306

Li CY, Hou YC, Chao PD, Shia CS, Hsu IC, Fang SH. Potential *ex vivo* immunomodulatory effects of San-Huang-Xie-Xin-Tang and its component herbs on mice and humans. *J Ethnopharmacol*. 2010, 127: 292-298

Li HB and Chen F. Isolation and purification of baicalein, wogonin and oroxylin A from the medicinal plant Scutellaria baicalensis by high-speed counter-current chromatography. *J Chromatogr A*. 2005, 1074:107-110

Li HN, Nie FF, Liu W, Dai QS, Lu N, Qi Q, Li ZY, You QD, Guo QL. Apoptosis induction of oroxylin A in human cervical cancer HeLa cell line in vitro and in vivo. *Toxicology*. 2009, 257: 80-85

Li JR, Zuo F, Zhang L, Nakamura N, Hattori M. Study on the metabolism of the precipitation of Xiexin decoction in rats. *Zhangguo Zhong Yao Za Zhi*. 2005, 30: 1673-1676

Li KL and Sheu SJ. Determination of flavonoids and alkaloids in the scute-coptis herb couple by capillary electrophoresis. *Anal Chim Acta*. 1995, 313:113-120

Li Y, Wu T, Zhu J, Wan L, Yu Q, Li X, Cheng Z, Guo C. Combinative method using HPLC fingerprint and quantitative analyses for quality consistency evaluation of an herbal medicinal preparation produced by different manufacturers. *J Pharm Biomed Anal*. 2010, 52 597-602

Liang X, Zhang L, Zhang X, Dai W, Li H, Hu L, Liu H, Su J, Zhang W. Qualitative and quantitative analysis of traditional Chinese medicine Niu Huang Jie Du Pill using ultra

performance liquid chromatography coupled with tunable UV detector and rapid resolution chromatography coupled with time-of-flight tandem mass spectrometry. *J Pharm Biomed Anal.* 2010, 51: 565-571

Lin MC, Tsai MJ and Wen KC. Supercritical fluid extraction of flavonoids from *Scutellariae Radix. J Chromatogr A.* 1999, 830:387-395

Lin SJ, Tseng HH, Wen KC, Suen TT. Determination of gentiopicroside, mangiferin, palmatine, berberine, baicalin, wogonin and glycyrrhizin in the traditional Chinese medicinal preparation Sann-Joong-Kuey-Jian-Tang by high-performance liquid chromatography. *J Chromatogr A.* 1996, 730: 17-23

Liu W, Mu R, Nie FF, Yang Y, Wang J, Dai QS, Lu N, Qi Q, Rong JJ, Hu R, Wang XT, You QD, Guo QL. MAC related mitochondrial pathway in oroxylin A induces apoptosis in human hepatocellular carcinoma HepG2 cells. *Cancer Lett.* 2009, 284: 198-207

Liu Y, Deng SW, Yuan WP, Ma SC. Determination of three flavones in Scutellaria baicalensis Georgi by RP-HPLC. *Chinese Traditional and Herbal Drugs.* 2005, 36: 1247-1248

Liu QC, Zhao JN, Yan LC, Yi JH, Song J. Simultaneous determination of five active constituents in Xiaochaihu Tang by HPLC. *Zhongguo Zhong Yao Za Zhi.* 2010, 35: 708-710

Liu TM, Jiang XH. Studies on the absorption kinetics of baicalin and baicalein in rats' stomachs and intestines. *Zhongguo Zhong Yao Za Zhi*. 2006, 31: 999-1001

Liu CH, Jiang ZZ, Huang X, Wang CF, Duan WG, Yao JC, Liu J, Wu XD, Zhang LY. Cellular absorption of emodin influcenced by anthraquinones in human intestinal Caco-2 cells. *Chinese journal of natural medicines*. 2008, 6: 298-301

Liu C, Sugita K, Nihei K, Yoneyama K, Tanaka H. Absorption of hydroxyproline-containing peptides in vascularly perfused rat small intestine in situ. *Biosci Biotechnol Biochem*. 2009, 73:1741-1747

Liu ML, Yang LX, Wan YH, Zuo F. Determination of Baicalin and wogonoside in seven species of Radix scutellariae by RP-HPLC. *Chinese Journal of Pharmaceutical Analysis*. 2002, 22: 99-102

Liu Y and Hu M. Absorption and metabolism of flavonoids in the Caco-2 cell culture model and a perused rat intestinal model. *Drug Metab Dispos*. 2002, 30:370-377

Lu T, Song J, Huang F, Deng Y, Xie L, Wang G, Liu X. Comparative pharmacokinetics of baicalin after oral administration of pure baicalin, Radix scutellariae extract and Huang-Lian-Jie-Du-Tang to rats. *J Ethnopharmacol*. 2007, 110: 412-418

Luo F, Paranjpe P, Guo A, Rubin E, Sinko P. Intestinal transport of irinotecan in Caco-2 cells and MDCK II cells overexpressing efflux transporters PGP, CMOAT, and MRP1. *Drug Metab Dispos.* 2002, 30: 763-770

Ma SC, Du J, But PP, Deng XL, Zhang YW, Ooi VE, Xu HX, Lee SH, Lee SF. Antiviral Chinese medicinal herbs against respiratory syncytial virus. *J Ethnopharmacol.* 2002, 79: 205-211

Mahringer A, Delzer J, Fricker G. A fluorescence-based in vitro assay for drug interactions with breast cancer resistance protein (BCRP, ABCG2). *Eur J Pharma Biopharm.* 2009, 72: 605-613

Marques MR, Stüker C, Kichik N, Tarragó T, Giralt E, Morel AF, Dalcol II. Flavonoids with prolyl oligopeptidase inhibitory activity isolated from Scutellaria racemosa Pers. *Fitoterapia.* 2010, 81: 552-556

Mathews JM, Etheridge AS, Valentine JL, Black SR, Coleman DP, Patel P, So J, Burka LT. Pharmacokinetics and disposition of the kavalactone kawain: interaction with dava extract and kavalactones in vivo and in vitro. *Drug Metab Dispos.* 2005, 33: 1555-1563

Maurel P. The use of adult human hepatocytes in primary culture and other in vitro systems to investigate drug metabolism in man. *Adv Drug Deliv Rev.* 1996, 22: 105-132

Miller LL. Technique of isolated rat liver perfusion. In "Isolated Liver Perfusion and Its Applications" (Bartosek I, Guaitani A, and Miller LL, eds.), Raven Press, New York, 1973: 11-52.

Morris ME and Zhang SZ. Flavonoid-drug interactions: effects of flavonoids on ABC transporters. *Life Sci.* 2006, 78: 2116-2130

Muto R, Motozuka T, Nakano M, Tatsuma Y, Sakamoto F, Kosaka N. The chemical structure of new substance as the metabolite of baicalin and time profiles for the plasma concentration after oral administration of sho-saiko-to in human. *Yakugaku Zasshi.* 1998, 118: 79-87

Nishikawa K, Furukawa H, Fujioka T, Fujii H, Mihashi K, Shimomura K, Ishimaru K. Flavone production in transformed root cultures of Scutellaria baicalensis Georgi. *Phytochemistry.* 1999, 52: 885-890

Ohno S and Nakajin S. Determination of mRNA expression of human UDP-glucuronosyltransferases and application for localization in various human tissures by real-time reverse transcriptase-polymerase chain reaction. *Drug Metab Dispos.* 2009, 37: 32-40

Okudaira N, Tatebayashi T, Speirs GC, Komiya I, Sugiyama Y. A study of the intestinal absorption of an ester-type prodrug ME3229, in rats: active efflux transport as a casue of poor bioavailability of the active drug. *J Pharmacol Exp Ther*. 2000, 294: 580-587

Ong ES, Len SM, Lee AC. Differential protein expression of the inhibitory effects of a standardized extract from *Scutellariae radix* in liver cancer cell lines using liquid chromatography and tandem mass spectrometry. *J Agric Food Chem*. 2005, 53: 8-16

Otake Y, Hsieh F, Walle T. Glucuronidation versus oxidation of the flavonoid galangin by human live microsomes and hepatocyes. *Drug Metab Dispos*. 2002, 30:576-581

Paine MF, Fisher MB. Immunochemical identification of UGT isoforms in human small bowel and in Caco-2 cell monolayers. *Biochem Biophys Res Commun*. 2000, 273: 1053-1057

Park BK, Heo MY, Park H, Kim HP. Inhibition of TPA-induced cyclooxygenase-2 expression and skin inflammation in mice by wogonin, a plant flavone from Scutellaria radix. *Eur J Pharmacol*. 2001, 425: 153-157

Park HG, Yoon SY, Choi JY, Lee GS, Choi JH, Shin CY, Son KH, Lee YS, Kim WK, Ryu JH, Ko KH, Cheong JH. Anticonvulsant effect of wogonin isolated from Scutellaria baicalensis. *Eur J Pharmacol*. 2007, 574: 112-119

Peng J, Qi Q, You Q, Hu R, Liu W, Feng F, Wang G, Guo Q. Subchronic toxicity and plasma pharmacokinetic studies on wogonin, a natural flavonoid, in Beagle dogs. *J Ethnopharmacol.* 2009, 124: 257-262

Peterson MD and Mooseker MS. Characterization of the enterocyte-like brush border cytoskeleton of the $C2_{BBe}$ clones of the human intestinal cell line, Caco-2. *J Cell Sci.* 1992, 102: 581-600

Qu H, Ma Y, Yu K, Cheng Y. Simultaneous determination of eight active components in Chinese medicine 'YIQING' capsule using high-performance liquid chromatography. *J Pharm Biomed Anal.* 2007, 43: 66-72

Ranaldi G, Islam K, Smbuy Y. Epithelial cells in culture as a model for the intestinal transport of antimicrobial agents. *Antimicrob Agents Chemother.* 1992, 36: 1374-1381

Ranaldi G, Seneci P, Guba W, Islam K, Sambuy Y. Transport of antibacterial agent Oxazolidin-2-One and dirivatives across intetinal (Caco-2) and renal (MDCK) epithelial cell lines. *Antimicrob Agents Chemother.* 1996, 40: 652-658

Ren Y, Houghton PJ, Hider RC, Howes MJ. Novel diterpenoid acetylcholinesterase inhibitors from *Salvia miltiorrhiza. Planta Med.* 2004, 70: 201-204

Romero MR, Efferth T, Serrano MA, Castaño B, Macias RJ, Briz O, Marin JJ. Effect of artemisinin/artesunate as inhibitors of hepatitis B virus production in an "in vitro" replicative system. *Antiviral Res*. 2005, 68: 75-83

Rosenberg MF, Bikadi Z, Chan J, Liu X, Ni Z, Cai X, Ford RC, Mao Q. The human breast cancer resistance protein (BCRP/ABCG2) shows conformational changes with mitoxantrone. *Structure*. 2010, 18: 482-493

Schinella GR, Tournier HA, Prieto JM, Mordujovich de Buschiazzo P, Ríos JL. Antioxidant activity of anti-inflammatory plant extracts. *Life Sci*. 2002, 70: 1023-1033

Shah P, Jogani V, Bagchi T, Misra A. Role of Caco-2 cell monolayers in prediction of intestinal drug absorption. *Biotechnol Prog*. 2006, 22:186-198

Shang X, He X, He X, Li M, Zhang R, Fan P, Zhang Q, Jia Z. The genus Scutellaria an ethnopharmacological and phytochemical review. *J Ethnopharmacol*. 2010, 128: 279-313

Shao ZH, Li CQ, Vanden Hoek TL, Becker LB, Schumacker PT, Wu JA, Attele AS, Yuan CS. Extract from Scutellaria baicalensis Georgi attenuates oxidant stress in cardiomyocytes. *J Mol Cell Cardiol*. 1999, 31: 1885-1895

Shen SC, Lee WR, Lin HY, Huang HC, Ko CH, Yang LL, Chen YC. In vitro and in vivo inhibitory activities of rutin, wogonin and quercetin on lipopolysaccharide-induced nitric oxide and prostaglandin E2 production. *Eur J Pharmacol*. 2002, 446: 187-194

Siissalo S, Laine L, Tolonen A, Kaukonen AM, Finel M, Hirvonen J. Caco-2 cell monolayers as a tool to study simultaneous phase II metabolism and metabolite efflux of indomethacin, paracetamol and 1-naphthol. *Int J Pharm*. 2010, 383: 24-29

Siissalo S, Zhang H, Stilgenbauer E, Kaukonen AM, Hirvonen, J, Finel M. The expression of most UDP-Glucuronosyltransferases (UGTs) is increased significantly during Caco-2 Cell differentiation, whereas UGT1A6 is highly expressed also in undifferentiated cells. *Drug Metab Dispos*. 2008, 36: 2331-2336

So FV, Guthrie N, Chambers AF, Moussa M, Carroll KK. Inhibition of human breast cancer cell proliferation and delay of mammary tumorigenesis by flavonoids and citrus juices. *Nutr Cancer*. 1996, 26: 167-181

Son D, Lee P, Lee J, Kim H, Kim SY. Neuroprotective effect of wogonin in hippocampal slice culture exposed to oxygen and glucose deprivation. *Eur J Pharmacology*. 2004, 493: 99-102

Song M, Hang TJ, Zhang Z, Chen HY. Effects of the coexisting diterpenoid tanshinones on the pharmacokinetics of cryptotanshinone and tanshinone IIA in rat. *Eur J Pharm Sci*. 2007, 32: 247-253

Song SH, Zhang Y and Wang ZZ. Determination of the flavonoids contents in Scutellaria baicalensis Georgi from different areas by HPLC. *Zhongguo Zhong Yao Za Zhi*. 2006, 31: 598-600

Souza J, Benet L, Huang Y and Storpirtis S. Comparison of bidirectional lamivudine and zidovudine transport using MDCK, MDCK-MDR1, and Caco-2 cell monolayers. *J Pharm Sci*. 2009, 98: 4413-4419

Strassburg CP, Oldhafer K, Manns MP, Tukey RH. Differential expression of the UGT1A locus in human liver, biliary, and gastric tissue: identification of UGT1A7 and UGT1A10 transcripts in extrahepatic tissues. *Mol Pharmacol*. 1997, 52: 212–220

Suh KS, Nam YH, Ahn YM, Kim NJ, Park CY, Koh G, Oh S, Woo JT, Kim SW, Kim JW, Kim YS. Effect of Scutellariae Radix extract on the high glucose-induced apoptosis in cultured vascular endothelial cells. *Biol Pharm Bull*. 2003, 26: 1629-1632

Suk K, Lee H, Kang SS, Cho GJ, Choi WS. Flavonoid baicalein attenuates antivation-induced cell death of brain microglia. *J Phamacol Exp Ther*. 2003, 305: 638-645

Sun D, Lennernas H, Welage LS, Barnett JL, Landowski CP, Foster D, Fleisher D, Lee KD, Amidon GL. Comparison of human duodenum and Caco-2 gene expression profiles for 12,000 gene sequences tags and correlation with permeability of 26 drugs. *Pharm Res*. 2002, 19: 1400-1416

Sun GX, Hu YS, Bi KS. Evaluating the quality of Niuhuangjiedu tablets by the systematic quantified fingerprint method. *Yao Xue Xue Bao*. 2009, 44: 401-105

Suresh Babu K, Hari Babu T, Srinivas PV, Sastry BS, Hara Kishore K, Murty US, Madhusudana Rao J. Synthesis and in vitro study of novel 7-O-acyl derivatives of Oroxylin A as antibacterial agents. *Bioorg Med Chem Lett*. 2005, 15: 3953-3956

Tang W, Sun X, Fang JS, Zhang M, Sucher NJ. Flavonoids from *Radix Scutellariae* as potential stroke therapeutic agents by targeting the second postsynaptic density 95 (PSD-95)/disc large/ zonula occludens-1 (PDZ) domain of PSD-95. *Phytomedicine*. 2004, 11: 277-284

Taub ME, Kristensen L, Frokjaer S. Optimized conditions for MDCK permeability and terbidimetric solubility studies using compounds representative of BCS classes I-IV. *Eur J Pharm Sci*. 2002, 15: 331-340

The Pharmacopeia Commission of P. R. China. 2005. Pharmacopeia of the People's Republic of China Version 2005. Vol.1. Beijing Chemical Industry Press: Beijing/ pp. 211

Tiwari AK, Sodani K, Wang SR, Kuang YH, Ashby CR Jr, Chen X, Chen ZS. Nilotinib (AMN107, Tasigna®) reverses multidrug resistance by inhibiting the activity of the ABCB1/Pgp and ABCG2/BCRP/MXR transporters. *Biochem Pharmacol*. 2009, 78: 153-161

Van Zanden JJ, Wortelboer HM, Bijlsma S, Punt A, Usta M, Bladeren PJ, Rietjens IM, Cnubben NH. Quantitative structure activity relationship studies on the flavonoid mediated inhibition of multidrug resistance proteins 1 and 2. *Biochem Pharmacol.* 2005, 69: 699-708

Venkataramanan R, Komoroski B and Strom S. In vitro and in vivo assessment of herb drug interactions. *Life Sci.* 2006, 78: 2105-2115

Videmann B, Tep J, Cavret S, Lecoeur S. Epithelial transport of deoxynivalenol: involvement of human P-glycoprotein (ABCB1) and multidrug resistance-associated protein 2 (ABCC2). *Food Chem Toxicol.* 2007, 45: 1938-1947

Wakabayashi I. Inhibitory effects of baicalein and wogonin on lipopolysaccharide-induced nitric oxide production in macrophages. *Pharmacol Toxicaol.* 1999, 84: 288-291

Wakui Y, Yanagisawa E, Ishibashi E, Matsuzaki Y, Takeda S, Sasaki H, Aburada M, Oyama T. Determination of baicalin and baicalein in rat plasma by high-performance liquid chromatography with electrochemical detection. *J Chromatogr.* 1992, 13: 131-136

Wang HH, Liao JF, Chen CF. Anticonvulsant effect of water extract of *Scutellariae radix* in mice. *J Ethnopharmacol.* 2000, 73: 182-190

Wang HZ, Yu CH, Gao J, Zhao GR. Effects of processing and extracting methods on active components in Radix Scutellariae by HPLC analysis. *Zhongguo Zhong Yao Za Zhi*. 2007, 32: 1637-1640

Wang JC, Liu XY, Lu WL, Chang A, Zhang Q, Goh BC, Lee HS. Pharmacokinetics of intravenously administered stealth liposomal doxorubicin modulated with verapamil in rats. *Eur J Pharm Biopharm*. 2006, 62: 44-51

Wang Q, Strab R, Kardos P, Ferguson C, Li J, Owen A, Hidalgo IJ. Application and limitation of inhibitors in drug-transporter interactions studies. *Int J Pharm*. 2008, 356: 12-18

Wang YF, Aun R and Tse F. Absorption of D-glucose in the rat studied using in situ intestinal perfusion: a permeability-index approach. *Pharma Res*. 1997, 14: 1563-1567

Woo KJ, Lim JH, Suh SI, Kwon YK, Shin SW, Kim SC, Choi YH, Park JW, Kwon TK. Differential inhibitory effects of baicalein and baicalin on LPS-induced cyclooxygenase-2 expression through inhibition of C/EBPβ DNA-binding activity. *Immunobiology*. 2006, 211: 359-368

Wortelboer H, Balvers M, Usta M, Bladeren P, Cnubben N. Glutathione-dependent interaction of heavy metal compounds with multidrug resistance proteins MRP1 and MRP2. *Environ Toxicol Pharmacol*. 2008, 26: 102-108

Wu H, Zhu Z, Zhang G, Zhao L, Zhang H, Zhu D, Chai Y. Comparative pharmacokinetic study of paeoniflorin after oral administration of pure paeoniflorin, extract of Cortex Moutan and Shuang-Dan prescription to rats. *J Ethnopharmacol*. 2009, 125: 444-449

Wu S, Sun A and Liu R. Separation and purification of baicalin and wogonoside from the Chinese medicinal plant Scutellaria baicalensis Georgi by high-speed counter-current chromatography. *J Chromatogr A*. 2005, 1066:243-247

Xie SG, Chen YK, Zhang W, Chen SQ, Zeng S. QSMR studies on glucuronidation of flavonoids catalyzed by human UGT 1A3. *Chin Pharm J*. 2007, 42: 1505-1508

Xing J, Chen X and Zhong D. Absorption and enterohepatic circulation of baicalin in rats. *Life Sci*. 2005, 78: 140-146

Xu M, Wang G, Xie H, Huang Q, Wang W, Jia Y. Pharmacokinetic comparisons of schizandrin after oral administration of schizandrin monomer, Fructus Schisandrae aqueous extract and Sheng-Mai-San to rats. *J Ethnopharmacol*. 2008, 115: 483-488

Yan JC, Lu ZM, Wang TM, Shi R, Ma YM. Pharmacokinetics of flavonoids from Xiexin decoction in rats. *Yao Xue Xue Bao*. 2007, 42: 722-729

Yang LX, Liu D, Feng XF, Cui SL, Yang JY, Tang XJ, He XR, Liu JF, Hu SL. Determination of flavone for Scutellaria baicalensis from different areas by HPLC. *Zhongguo Zhong Yao Za Zhi.* 2002, 27: 166-170

Yee S. In vitro permeability across Caco-2 cells (colonic) can predict in vivo (small intestinal) absorption in man- fact or myth. *Pharm Res.* 1997, 14: 763-766

Yoon SB, Lee YJ, Park SK, Kim HC, Bae H, Kim HM, Ko SG, Choi HY, Oh MS, Park W. Anti-inflammatory effects of *Scutellaria baicalensis* water extract on LPS-activated RAW 264.7 macrophages. *J Ethnopharmacol.* 2009, 125: 286-290

You JY, Zhang HR, Ding L, Xiao TT, Zhang HQ, Song DQ. Dynamic microwave-assisted extraction of flavonoids from Radix Scutellariae. *Chem Res Chines U.* 2007, 23: 148-153

You J, Gao S, Jin H, Li W, Zhang H, Yu A. On-line continuous flow ultrasonic extraction coupled with high performance liquid chromatographic separation for determination of the flavonoids from root of *Scutellaria baicalensis* Georgi. *J Chromatogr A.* 2010, 1217: 1875-1881

Yu K, Gong Y, Lin Z, Cheng Y. Quantitative analysis and chromatographic fingerprinting for the quality evaluation of Scutellaria baicalensis Georgi using capillary electrophoresis. *J Pharm Biomed Anal.* 2007, 43: 540-548

Wu YJ, Hong CY, Lin SJ, Wu P, Shiao MS. Increase of vitamin E content in LDL and reduction of atherosclerosis in cholesterol-fed rabbits by a water-soluble antioxidatnt rich fraction of Salviaa miltiorrhiza. *Arterioscler Thromb Vasc Biol.* 1998, 18: 481-486

Zaman N, Tam YK, Jewell LD, Coutts RT. Effects of taurine supplementation in parenteral nutrition-associated hepatosteatosis and lidocaine metabolism. *Drug Metab Dispos.* 1996, 24: 534-541

Zgórka G and Hajnos A. The application of solid-phase extraction and reversed phase high-performance liquid chromatography for simultaneous isolation and determination of plant flavonoids and phenolic acids. *Chromatographia Supplement.* 2003, 57: 77-80

Zhang H, Tian K, Tang J, Qi S, Chen H, Chen X, Hu Z. Analysis of baicalein, baicalin and wogonin in Scutellariae radix and its preparation by microemulsion electrokinetic chromatography with 1-butyl-3-methylimizolium tetrafluoborate ionic liquid as additive. *J Chromotogr A.* 2006, 1129: 304-307

Zhang J, Xiao LH and Li FM. Content determination of five active components in four sources of Scutellaria baicalensis by RP-HPLC. *Journal of Chinese Medicinal Materials.* 2005, 28: 389-391

Zhang L, Lin G, Zuo Z. High-performance liquid chromatographic method for simultaneous determination of baicalein and baicalein 7-glucuronide in rat plasma. *J Pharm Biomed Anal*. 2004, 36: 637-641

Zhang L, Lin G, Chang Q, Zuo Z. Role of intestinal first-pass metabolism of baicalein in its absorption process. *Pharma Res*. 2005, 22: 1050-1058

Zhang L, Lin G, Kovács B, Jani M, Krajcsi P, Zuo Z. Mechanistic study on the intestinal absorption and disposition of baicalein. *Eur J Pharm Sci*. 2007a, 31: 221-231

Zhang L, Lin G, Zuo Z. Involvement of UDP-glucuronosyltransferases in the extensive liver and intestinal first-pass metabolism of flavonoids baicalein. *Pharma Res*. 2007b, 24: 81-89

Zhang, L., Zheng, Y., Chow, M., Zuo, Z., 2004. Investigation of intestinal absorption and disposition of green tea catechins by Caco-2 monolayer model. *Int J Pharm*. 2004, 287: 1-12

Zhang L, Xing D, Wang W, Wang R, Du L. Kinetic difference of baicalin in rat blood and cerebral nuclei after intravenous administration of *Scutellariae* Radix extract. *J Ethnopharmacol*. 2006, 103:120-125

Zhang S, Yang X, Coburn RA, Morris ME. Structure activity relationships and quantitative structure activity relationships for the flavonoid-mediated inhibition of breast cancer resistance protein. *Biochem Pharmacol*. 2005, 70: 627-639

Zhang YY, Guo YZ, Onda M, Hashimoto K, Ikeya Y, Okada M, Maruno M. Four flavonoids from Scutellaria baicalensis. *Phytochemistry*. 1994, 35: 511-514

Zhang YY, Guo YZ, Ageta H. A new flavone C-glycoside from Scutellaria baicalensis. *J Chinese Pharm Sci*. 1997, 6: 182-186

Zhang YY, Don HY, Guo YZ, Ageta H, Harigaya Y, Onda M, Hashimoto K, Ikeya Y, Okada M, Maruno M. Comparative study of *Scutellaria Planipes* and *Scutellaria Baicalensis*. *Biomed Chromatogr*. 1998, 12: 31-33

Zhao J, Wang D, Duan S, Wang J, Bai J, Li W. Analysis of Fuzhisan and quantitation of baicalin and ginsenoside Rb1 by HPLC-DAD-ELSD. *Arch Pharm Res*. 2009, 32: 989-996

Zhou XN and Yang B. Determination of contents of the effective ingredients in root of Scutellaria baicalensis by HPLC-ECD. *Zhongguo Zhong Yao Za Zhi*. 2006, 31: 47-50

Zhu BT, Ezell EL, Liehr JG. Catechol-*O*-methyltransferase-catalyzed rapid *O*-methylation of mutagenic flavonoids. *J Biol Chem*. 1994, 269: 292-299

Zuo F, Zhou ZM, Zhang Q, Mao D, Xiong YL, Wang YL, Yan MZ, Liu ML. Pharmacokinetic study on the multi-constituents of Huangqin-Tang decoction in rats. *Bio Pharm Bull*. 2003, 26: 911-919

Zhou XN and Yang B. Determination of contents of the effective ingredients in root of Scutellaria baicalensis by HPLC-ECD. *Zhongguo Zhongyao Za Zhi*. 2006, 31: 47-50